

Dynamics of large sessile seabed fauna, important for structural fisheries habitat and biodiversity of marine ecosystems – and use of these habitats by key finfish species

Project No. 97/205

CSIRO Marine Research

C. R. Pitcher

T. J. Wassenberg

G. P. Smith

M. Austin

S. R. Gordon

R. H. Bustamante

C. H. Moeseneder

Australian Institute of Marine Science

M. C. Cappo

P. J. Speare

P. J. Doherty

Queensland Museum

J. A. Kennedy

J. N. A. Hooper



CSIRO
MARINE RESEARCH



Australian Government
Fisheries Research and
Development Corporation



AUSTRALIAN INSTITUTE
OF MARINE SCIENCE



museum

August 2004

**DYNAMICS OF LARGE SESSILE SEABED
FAUNA, IMPORTANT FOR STRUCTURAL
FISHERIES HABITAT AND BIODIVERSITY OF
MARINE ECOSYSTEMS – AND USE OF THESE
HABITATS BY KEY FINFISH SPECIES**

**C.R. Pitcher¹, T.J. Wassenberg¹, M.C. Cappo²,
G.P. Smith¹, M. Austin¹, S.R. Gordon¹, R.H.
Bustamante¹, C.H. Moeseneder¹, P.J. Speare²,
J.A. Kennedy³, P.J. Doherty², J.N.A. Hooper³**

1



2



3



PROJECT No. 97/205

ISBN 1 876 996 77 3

National Library of Australia Cataloguing-in-Publication entry:

Dynamics of large sessile seabed fauna, important for structural fisheries habitat and biodiversity of marine ecosystems — and use of these habitats by key finfish species.

ISBN 1 876996 77 3.

1. Fishery management - Australia. 2. Fish habitat improvement - Australia. 3. Marine sciences - Australia. 4. Marine ecology - Australia. 5. Marine fauna. I. Pitcher, C. R. (Clifford Roland). II. CSIRO Marine Research. III. Fisheries Research & Development Corporation (Australia).

333.9560994

This Report should be cited as:

Pitcher, C.R., Wassenberg, T.J., Cappo, M.C., Smith, G.P., Austin, M., Gordon, S.R., Bustamante, R.H., Moeseneder, C.H., Speare, P.J., Kennedy, J.A., Doherty, P.J., Hooper, J.N.A. (2004). Dynamics of large sessile seabed fauna, important for structural fisheries habitat and biodiversity of marine ecosystems — and use of these habitats by key finfish species. Final report to Fisheries Research & Development Corporation. CSIRO Marine Research. Pp. 304

Copyright Fisheries Research and Development Corporation and CSIRO Marine Research 2004

This work is copyright. Except as permitted under the Copyright Act 1968 (Cth), no part of this publication may be reproduced by any process, electronic or otherwise, without the specific written permission of the copyright owners. Neither may information be stored electronically in any form whatsoever without such permission.

The Fisheries Research and Development Corporation plans, invests in and manages fisheries research and development throughout Australia. It is a federal statutory authority jointly funded by the Australian Government and the fishing industry.

Table of Contents

Acknowledgements	iv
1 Non-technical summary:	1-1
2 Background	2-5
3 Need	3-6
4 Objectives	4-8
5 The initial survey to find suitable study sites	5-9
5.1 Introduction	5-11
5.2 Methods	5-12
5.3 Results	5-23
5.4 Discussion	5-38
5.5 Appendix	5-43
6 Dynamics of tagged megabenthos	6-57
6.1 Introduction	6-59
6.2 Methods	6-60
6.3 Results	6-68
6.4 Discussion	6-97
6.5 Appendices	6-102
7 Modeling the dynamics of sessile megabenthos	7-105
7.1 Introduction	7-108
7.2 Methods	7-109
7.3 Results	7-117
7.4 Discussion	7-129
7.5 Appendices	7-136
8 The ecological usage of epibenthic habitat by key commercial finfish species	8-176
8.1 Introduction	8-179
8.2 Methods	8-181
8.3 Results	8-190
8.4 Discussion	8-212
8.5 Appendices	8-219
9 Acoustic techniques for surveying tropical demersal finfish resources	9-224
9.1 Introduction	9-226
9.2 Desktop approach	9-227
9.3 Field survey approach	9-231
9.4 Discussion	9-265
9.5 Appendix	9-269
10 Benefits	10-271
11 Further development	11-273
12 Planned outcomes	12-277
13 Conclusions	13-279
13.1 Objective 1. Determine the dynamics of megabenthos.	13-279
13.2 Objective 2. Model the dynamics of megabenthos.	13-280
13.3 Objective 3. Document the use of megabenthos by key fish species.	13-282
13.4 Objective 4. Assess methods for surveying fish abundance.	13-283
14 References	14-286
15 Appendices	15-299
15.1 Intellectual Property	15-299
15.2 Staff	15-300

Acknowledgements

This project was a collaboration between CSIRO Marine Research, the Australian Institute of Marine Science and the Queensland Museum. The project was funded by Fisheries Research and Development Corporation and the research agencies. We are indebted to many people who helped us to obtain a successful conclusion to this project. Don Battersby and Marc Lennard, (Crew of the James Kirby). Paula Tomkin (then of the Queensland Museum) contributed her expertise to the initial epibenthos field survey and Gary Fry (CSIRO) sorted many of the epibenthos samples. Sue Cheers and Anthea Koutsoukos did much of the video analysis. Dr Christie Adams and Steve Cook (Queensland Museum) identified many of the specimens collected. Darren Dennis (CSIRO) was a helped with many of the dives to measure the megabenthos animals. Louise Bell designed the report covers. FRDC's anonymous reviewers provided helpful comments on the draft report. Toni Cannard co-ordinated and collated the revisions by multiple co-authors, and corrected our typographic, formatting and cross-referencing errors and inconsistencies.

97/205 Dynamics of large sessile seabed fauna, important for structural fisheries habitat and biodiversity of marine ecosystems — and use of these habitats by key finfish species

Principal Investigator:

Dr C.R. Pitcher

Address:

CSIRO Marine Research

PO Box 120

Cleveland, Qld 4163

Telephone: 07 3826 7250

Fax: 07 3826 7222

Objectives:

1. To determine the dynamics (recruitment, growth, mortality, and reproduction) of structurally dominant large seabed habitat organisms (ie. megabenthos = sponges, gorgonians, and alcyonarians and corals etc) important for demersal fisheries habitat and biodiversity of the seabed environment, in a tropical region.
2. To model the dynamics of seabed habitat organisms and predict the potential of trawled megabenthos to recover and contribute as fisheries habitat.
3. To document the ecological usage of living epibenthic habitat by key commercial finfish species, in terms of species micro-distribution, shelter requirements, and food chain links.
4. To assess three fishery-independent and “environmentally-friendly” techniques for surveying tropical finfish resource abundance in inter-reefal areas, including fish-traps, remote (baited) video stations and quantitative acoustics.

1 Non-technical summary:

OUTCOMES ACHIEVED

This project has delivered outputs in relation to each objective that have contributed to a high priority area for research identified previously by the FRDC (i.e. habitat dynamics and processes), and will contribute to a range of outcomes as they are adopted by management, industry and the wider community.

The project’s results have contributed to increased understanding of the nature and importance of deeper water habitats, provided fishery-independent tools for monitoring tropical finfish resources that have little or no environmental impact, and will be useful for planning management strategies for sustainable fisheries, planning habitat protection areas, refuges, and marine protected areas, and consideration of the feasibility of habitat restoration activities. The results will be used in a “trawl-scenario-model” that enables managers to examine alternative management strategies that have less impact on habitat, preserve critical habitat in refuges, reduce conflict between commercial extractive activities and conservation needs, and may lead to increased productivity among commercial species. These results and approaches have become increasingly important as fisheries, particularly tropical trawl fisheries, respond to and implement changes to meet the sustainability and ecological assessment requirements of contemporary legislation. For example, the results are now being taken up in developing ecological risk assessments for Commonwealth and Queensland fisheries, and for Environmental Strategic Assessments. The scope and importance of these outcomes will increase as other new and ongoing projects deliver additional information needed for fisheries sustainability evaluations. The ultimate outcomes of these activities are ecologically sustainable fisheries and an objective balance between commercial fishing and national biodiversity conservation goals.

NEED FOR THE RESEARCH

Assemblages of sponges, sea-fans and whips (megabenthos) that provide structural complexity to the seabed are an important component of fisheries habitats, and also contribute to the biodiversity of the marine environment. These assemblages can be impacted by trawling; however, management is now required to achieve ecological sustainability of such fisheries. To evaluate management strategies to achieve these goals, information is needed on the population dynamics of megabenthos and their use by other species, including fish species that may move between trawled areas and habitat. This project focused on these information needs in the Great Barrier Reef region near Townsville.

Also needed by fisheries managers are methods for monitoring tropical finfish resources. To assist this need, we have also examined environmentally-friendly, fishery-independent techniques for estimating finfish abundance, including remote (baited) video stations and acoustics. Information on fish-habitat associations is needed to develop habitat proxies for estimating the spatial distribution of deeper water fish stocks.

SUMMARY OF RESULTS AND CONCLUSIONS

1.1 Objective 1. Determine the dynamics of megabenthos.

The population dynamics parameters (growth, mortality, recruitment, and reproduction) of nine species of structurally dominant large seabed habitat organisms (megabenthos), including sponges, gorgonians, and corals, were successfully estimated in a tropical region — the Great Barrier Reef, off Townsville.

This objective was preceded by an initial survey primarily to locate suitable study sites but also to document habitat distribution and benthic biodiversity. The survey covered substrata ranging from muddy sand in with rocky remnants of palaeo-reefs. Areas with harder and rocky substrata supported most of the megabenthos assemblages (gardens) and the occurrence and abundance of these gardens correlated positively with higher current velocity and negatively with muddy and sandy substrata.

Megabenthos recruitment, growth, mortality and reproduction were measured during repeated visits to tagged animals at sites near the Palm Islands. Relatively few new recruits were observed. The growth of individual animals within a species was highly variable, as some individuals were observed to grow and shrink in size over the study period. The average linear growth rates were about 1 – 7 cm yr⁻¹, ranging up to a maximum of 4 – 25 cm yr⁻¹. Animals could also shrink as much as -2 – -20 cm yr⁻¹. Natural mortality was an unpredictable process averaging about 14% yr⁻¹ across all species but varied widely (typically 8–23% yr⁻¹) under normal conditions. Little evidence of reproduction was found, perhaps due to the limited (bi-annual) sampling possible during the study and further work is required to yield data for impact and recovery modeling. Two cyclones occurred during the study and had a significant effect: reducing recruitment, causing damage or killing megabenthos — the additional observed mortality averaged 8–9%. However, many new soft corals appeared several months after the cyclones passed.

1.2 Objective 2. Model the dynamics of megabenthos.

The dynamics of nine species of seabed habitat megabenthos fauna were modeled based on analyses of the data collected. These models showed that variations in recruitment, growth, survival or other perturbations or impacts caused megabenthos populations to have unstable size-distributions and abundance states. Model growth showed that some megabenthos could achieve about half maximum size in 3–9 years post-recruitment, contrasting with the expectations of slow growth for these species. Nevertheless, highly variable growth meant some individuals may never grow large and size is a poor indicator of age. Mortality rates were relatively low, between 5–30% per annum, similar to the range observed for corals.

Modeled impacts showed that a cyclone would typically cause an additional mortality of about 6% and may restructure megabenthos size-distributions. The additional mortality caused by the pass of a single trawl averaged about twice that caused by a cyclone.

Modeled recovery after cyclones or trawling could be lengthy and was more dependent on recruitment rates, rather than growth rates — higher recruitment lead to faster recovery. Estimates of full recovery times were imprecise because model recovery slowed near ‘carrying capacity’. Time to half-recovery was typically half to two decades. Thus, megabenthos may take several to many decades to fully recover or re-establish where they have been significantly impacted or removed.

This study is the first to estimate the dynamics of off-reef tropical megabenthos and for nine species we have succeeded in measuring growth-rates adequately, especially considering the mixed benefit due to the impact of the cyclones. Mortality was less precisely described, because relatively few deaths occurred, but also due to the cyclones. However, recruitment remains the most uncertain, yet critical, parameter. This uncertainty is crucial, given the long recovery times are critically dependent on rates of recruitment. Further, the rates of actual recruitment that we measured were typically half that required to maintain the observed resident densities. Given the sensitivity of recovery rates to recruitment, this emphasizes the need for further work to obtain additional data on rates of recruitment, as well as mortality and growth, for these megabenthos.

The fauna studied here represent a range of vulnerability to trawling (the combination of removal and recovery rates) from medium-low to very high. The more vulnerable species, especially, need to be considered when evaluating management strategies aiming to achieve environmental sustainability.

1.3 Objective 3. Document the use of megabenthos by key fish species.

The use of living megabenthos habitat by fish species, particularly those of key commercial interest, was assessed by examining fish distributions with respect to megabenthos habitat, and by fish stomach contents for evidence of food chain links.

Baited and un-baited video cameras were used to observe the fish assemblages associated with megabenthos habitat. Cross-shelf position of habitats was a prime determinant of the observed patterns in fish assemblages, as previous studies have shown. Within the strong cross-shelf pattern, different fish assemblages were observed in areas with megabenthos compared with areas without. A number of non-commercial species were common in megabenthos areas but not elsewhere.

Of commercially important species, we observed that juvenile *L. sebae* were most commonly observed in habitats dominated by megabenthos, though their numbers were moderate. They appear to be an important component of the fish assemblage associated with megabenthos, but we cannot be certain whether they are restricted to such habitats. With respect to adults of commercially important species, there was no indication of a dependency of adult “redfish” (*Lutjanus sebae*, *L. malabaricus*, *L. erythropterus*) on megabenthos habitats. Occurrences of these adults were restricted to coarse carbonate sediments and sand/Halimeda habitats in deep gutters.

Further work would require high resolution mapping of megabenthos habitat patches, so that observations and sampling of fish in different habitats could be conducted accurately.

The stomach contents of 108 fish sampled on and off megabenthos habitats were examined, but few (15) contained food other than the bait provided to attract them into the traps. None of the prey items found could be related solely to megabenthos habitats.

1.4 Objective 4. Assess methods for surveying fish abundance.

Three fishery-independent and “environmentally-friendly” techniques for surveying tropical finfish resource abundance in inter-reefal areas were assessed, including: fish-traps, remote (baited) video stations and quantitative acoustics.

Fish traps proved to be very poor sampling tools, because few (14%) fish observed around traps entered traps – and only 21% of fish that entered were actually retained and caught by the traps. A few species were “trap happy”, but some important families of fish never entered the traps. This gave a very limited picture of the fish biodiversity in different habitat types. Traps do have the advantage of providing specimens for ageing and dietary studies, which are important for assessment purposes, and they can be used overnight for nocturnal species.

Remote baited and unbaited video cameras, set in replicate strings, proved a powerful tool for daytime collection of information on fish biodiversity and relative abundance. In the case of baited cameras, the action of the bait plume increased the accumulation of fish species compared with unbaited, and there was no evidence that any species was deterred from attending the video stations. Video stations have the advantage of being non-extractive, though species identification can sometimes be difficult. Accurate and precise measurements of fish length in situ is possible if calibrated paired camera systems are deployed. However, video stations, like traps, provide only estimates of relative abundance, not absolute abundance as both are dependent on the attraction to the bait plume and other fish behaviour. In the case of video stations, fish abundance can be extracted only as the largest number of individuals of a given species seen on the video at any instant (MaxN), and so does not reflect actual numbers around the video. Thus it is difficult to estimate absolute abundance from video stations, as is the case with traps.

Acoustics was found to be a useful fishery independent and environmentally friendly technique to assist assessment of tropical finfish resources. This result was in spite of characteristics of these fish that make acoustic abundance assessments difficult; that is, they inhabit areas close to rough seabeds, posing problems for detection due to the acoustic dead zone, they occur in low abundance, and in complex multi-species assemblages so it is not possible to separate individual species within multi species schools. The acoustic technique had the advantage of improved precision of fish biomass estimates because of the larger amount of acoustic data available for an entire vessel track through a survey area, not just at sampled sites. Other advantages of acoustic techniques include: a much larger area can be sampled, operation through turbid water, non-extractive (or environmentally friendly) and can sample over rough ground. Acoustic systems are easy to deploy, though they do require technical expertise to operate correctly and data analysis may be time consuming. Nevertheless, other methods have similar post-survey time demands, such as sorting trawled samples or scoring video tapes, and technological advancements in acoustic hardware and software will facilitate post-analysis. The results achieved suggest that further development is warranted. In particular, the best results are likely to be achieved when acoustic methods are integrated with other direct sampling methods such as video, baited traps or other catch data. The acoustics would provide additional information useful for improving precision and/or for guiding the deployment (stratification) of the other sampling techniques.

Keywords:

megabenthos, sponges, gorgonians, corals, assemblage, biodiversity, distribution, population dynamics, growth, mortality, recruitment, leslie matrix modeling, cyclone impact, trawl impact, recovery, sustainability, fish habitat associations, fish abundance, fish trap, baited video, acoustic biomass assessment, Great Barrier Reef.

2 Background

Loss of habitat is not only a significant cause of reduced production in Australian fisheries, it threatens the very sustainability of these resources (Sainsbury *et al.* 1987, 1993, 1997). Many fishers have noticed such links between the level of fishery production and the status of the habitat, and some links have been demonstrated by research surveys and experiments. For example, on the Northwest Shelf, surveys by overseas agencies and more recent CSIRO research have shown that as seabed (benthic) habitat has been lost, fishery production has also declined in terms of quantity and quality (Sainsbury *et al.* 1987, 1993, 1997). Their long-term research indicates the cause of this decline is the relationship between high value commercial fish stocks (snappers and emperors) and the structure provided by large sessile epibenthic organisms (megabenthos such as sponges, gorgonians, alcyonarians and corals) on the seabed.

Assemblages of large sessile epibenthic organisms that provide structural complexity to the seabed are not only an important component of fisheries habitats, but also contribute to the biodiversity of the marine environment. Further, they form the basis of “biodiscovery” programs that screen specimens for natural products of pharmaceutical promise. However, megabenthos assemblages are vulnerable to damage by fishing, sedimentation, and dredging (Jones, 1992; Dayton *et al.* 1995; Watling and Norse, 1998; Hall 1999). Of these impacts, bottom trawling for tropical finfish and prawns has the highest public profile. The CSIRO/QDPI Project “Effects of Trawling on the GBR” has recently demonstrated the significance of impacts of prawn trawling on seabed habitat (Poiner *et al.* 1998). Because of these impacts, management for ecological sustainability of fisheries that exploit stocks associated with megabenthos assemblages will need to preserve the seabed habitats by establishing representative refuge areas (spatial management) and/or by fishing in ways that do not affect the critical habitat (gear management). Identifying direct effects of fishing gear on habitats and determining acceptable levels of impact from fishing gear have been identified by AFMA as key research areas to maintain healthy marine ecosystems.

3 Need

Predicting the response of megabenthos to the establishment of refuge/replenishment areas and acquiring an understanding of the ecological interactions between trawled and refuge areas are both essential steps in the effective design of refuges for fisheries habitat and the stocks they support. This key knowledge is also necessary for the development of alternative fishing strategies or management practices that will minimize or remove the impact on habitat. To achieve these goals, it will be necessary first to obtain information on the recovery rates of species that comprise such habitats and then the processes that link trawled areas and refuges. For that, this project focused on the simultaneous assessment of finfish species and the dynamics of coexisting sessile benthic species of sponges, corals, seafans, seawhips, and soft corals, whose physical associations form benthic structural complexity and are considered here as habitat-organisms.

We have investigated the population dynamics (recruitment, growth, mortality, reproduction) of structurally dominant megabenthos habitat-organisms and documented the relationship between benthic habitat and ecological usage by important commercial finfish species. These issues — habitat dynamics and processes — were identified at FRDC habitat workshops as high priority areas for research. Also identified as high priority, especially by managers of tropical finfishes, is the need for finfish resource monitoring. To this end, we have also examined environmentally-friendly, fishery-independent techniques for measuring finfish abundance, including remote (baited) video stations and acoustics. Documentation of fish-habitat (e.g. megabenthos) associations is the first step toward mapping the spatial distribution of snapper and emperor grounds on the basis of key habitat proxies, a process that began with the development of the Interim Marine and Coastal Regionalisation of Australia. Regionalisation and mapping of major habitats is a significant task that is continuing under processes such as Regional Marine Planning lead by the National Oceans Office.

Alternative fishing strategies, which have less impact on habitat and lead to increased productivity among commercial species will, by preserving critical habitat in refuges, in turn will help to reduce conflict between commercial extractive activities and conservation. It may also improve the public perception of trawling. Some possible alternative strategies may include: changing from fish-trawl to non-trawl methods; changing trawling strategies to

corridor trawling or rotational practices; or avoiding trawling over habitats that are not resilient to impact. Such strategies may allow former trawling grounds to recover and resume their role as fisheries habitat supplying stock to trawled areas, whilst maintaining or even enhancing catch rates. In each case, the recovery time frames for the seabed habitat — and hence fisheries resources — are important, because they will influence the feasibility of switching to alternative fishing strategies.

The results of this study will become increasingly important as the requirement for ecologically sustainable fisheries management is implemented in trawl fisheries from the temperate zone to the tropics. The lessons learned from this study in the form of knowledge of habitat dynamics, and methods for monitoring habitats and commercial stocks will contribute objective information to allow managers to achieve balance between ecologically sustainable fishing, biodiversity and conservation when ESD related management changes are implemented in those Australian fisheries dependent on seabed habitat.

4 Objectives

1. To determine the dynamics (recruitment, growth, mortality, and reproduction) of structurally dominant large seabed habitat organisms (ie. megabenthos = sponges, gorgonians, and alcyonarians and corals etc) important for demersal fisheries habitat and biodiversity of the seabed environment, in a tropical region (ie. GBR).
2. To model the dynamics of seabed habitat organisms and predict the potential of trawled megabenthos to recover and contribute as fisheries habitat.
3. To document the ecological usage of living epibenthic habitat by key commercial finfish species, in terms of species micro-distribution, shelter requirements, and food chain links.
4. To assess three fishery-independent and “environmentally-friendly” techniques for surveying tropical finfish resource abundance in inter-reefal areas, including fish-traps, remote (baited) video stations and quantitative acoustics.

5 The initial survey to find suitable study sites

To conduct stratified benthic surveys of three areas of seabed to locate sites suitable for intensive study of sessile megabenthos dynamics. In each area, characterise and map seabed habitat and benthos assemblages.

Contents

5	The initial survey to find suitable study sites	5-9
5.1	Introduction	5-11
5.1.1	The study area	5-11
5.2	Methods	5-12
5.2.1	Selecting a suitable study area using current stress models	5-12
5.2.2	Grab sampling	5-13
5.2.3	Towed video	5-14
5.2.4	Naturalist's dredge	5-15
5.2.5	Data analysis	5-20
5.2.6	Assemblage analyses	5-21
5.3	Results	5-23
5.3.1	Selecting a suitable study area using current stress models	5-23
5.3.2	Grab sampling	5-25
5.3.3	Towed video	5-25
5.3.4	Naturalist's dredge	5-29
5.3.5	Assemblage analyses	5-31
5.4	Discussion	5-38
5.4.1	Prior studies of inter-reefal fauna in the Great Barrier Reef	5-38
5.4.2	This study of the benthic fauna in the central Great Barrier Reef	5-41
5.5	Appendix	5-43

Tables

Table 5-1.	Proportions of sediment fractions estimated from each sediment sample taken with the Smith-McIntyre grab.	5-14
Table 5-2a.	Eigenvalues, percentages and correlation values for the first six axis of the CCA ordination of taxa and station scores.	5-34
Table 5-2b.	Weighted correlation coefficients of the environmental variables for the first two axes of the CCA ordination. Degrees of Freedom = ((no. stations - no of variables) -1).	5-34
Appendix 5.5-1.	List of species (taxa) in decreasing order of occurrence collected by naturalist dredge from four areas off Townsville.	5-43

Figures

Figure 5-1.	Map of the Queensland coastline showing offshore islands and reefs	5-12
Figure 5-2.	Image showing the simple video drop-camera, in water proof housing, suspended from a wire above a heavy weight and a fin to keep the camera facing in the direction of travel. Also shown are the sediment grab and video cable to the surface.	5-15
Figure 5-3a.	Bare substratum – code 1 – in this instance with many crinoids	5-16
Figure 5-3b.	Bare substratum with rubble – code 2.	5-16
Figure 5-3c.	Substratum of sand with large patches of algae – code 3 (mostly <i>Caulerpa</i> sp).	5-17
Figure 5-3d.	Substratum with beds of <i>Pinctada</i> shells in depressions – code 4.	5-17

Figure 5–3e. Small garden with gorgonians on rubble substratum – code 5.....	5-18
Figure 5–3f. Larger garden with gorgonians and fan sponges (<i>Ianthella</i> sp) – code 6.	5-18
Figure 5–3g. Garden of gorgonians, sponges and hard corals (often <i>Turbinaria</i> sp.) –code 7.....	5-19
Figure 5–3h. Rough ground with a rock ledge – code 8.....	5-19
Figure 5–4. Map of the Queensland coastline showing the location of the sampling sites for the video camera, dredge and grabs.....	5-23
Figure 5–5. Depth at all the sites in each of four areas east of Townsville.....	5-24
Figure 5–6. Current speed at the sites in each of four areas east of Townsville.	5-24
Figure 5–7. Current speed at depth at the sites in each of three areas east of Townsville.	5-24
Figure 5–8. Sedimentary fractions obtained from all the sites in each of four areas east of Townsville. Codes for sedimentary fractions are: S= Sand; (g)mS= Little Gravely Muddy Sand; gmS= Gravely Muddy Sand; gS= Gravely Sand; mS= Muddy Sand; sM= Sandy Mud; mG= Muddy Gravel; sG= Sandy Gravel; G= Gravel; R= Rock.....	5-25
Figure 5–9a. Relative proportions of habitat types in the Kelso Reef area derived from towed video sled observations (Pie diagrams) overlaid on current speed (knots x 0.1). Substrata are mostly sand or rubble-sand with deep reefs (dark purple) in proximity to the base of surface reefs (grey).....	5-26
Figure 5–9b. Relative proportions of habitat types in the Broadhurst-Davies Reef area derived from towed video sled observations (Pie diagrams) overlaid on current speed (knots x 0.1). Substrata are mostly sand or rubble-sand with deep reefs (dark purple) in proximity to the base of surface reefs (grey).	5-27
Figure 5–9c. Relative proportions of habitat types in the Flinders-Old Reef area derived from towed video sled observations (Pie diagrams) overlaid on current speed (knots x 0.1). Substrata are mostly sand or rubble-sand with megabenthos (pink) between surface reefs (grey) or rock (black) in proximity to the base of surface reefs.....	5-28
Figure 5–10. Average number of species (a) and biomass per dredge sample (b) at the four study areas. The vertical bars equals one standard deviation. n = number of sites sampled.....	5-29
Figure 5–11. Average (a) diversity and (b) evenness of species per dredge sample at the four study areas. The vertical bars equals one standard deviation. n = number of sites sampled.....	5-30
Figure 5–12. Species area curves based on the contribution of the number of new observed and predicted species, and species that occurs in a single sample or singletons, ($\pm 1SD$) for the surveyed areas.....	5-31
Figure 5–13. Results of the cluster analysis of biomass of animals collected in a naturalist dredge showing groupings of species assemblages.	5-32
Figure 5–14. Results of the cluster analysis of biomass of animals collected in a naturalist dredge showing groupings of stations based on species assemblages.	5-33
Figure 5–15. Map of station groups obtained from the cluster analysis of dredge biomass	5-35
Figure 5–16. The results of the multivariate ordination CCA where the position of the taxa (circles) are plotted along the first two axis of the ordination in relation to the major environmental variables (arrows)	5-36
Figure 5–17. The results of the multivariate ordination CCA where the position of the stations are plotted along the first two axis of the ordination in relation to the major environmental variables	5-37

5.1 Introduction

Assemblages of large sessile epibenthic organisms that provide structural complexity to the seabed are not only an important component of marine biodiversity of the marine environment, but also form a structural component of the seabed habitat used by fish. Some of these fish species are the basis of important fisheries. Most of the large sessile megabenthos animals are filter-feeders and as such may be expected to be in areas of greatest current speed and water turnover. Consequently, benthic assemblages found in areas of high energy and water movement have proven to be the most diverse and yield the highest diversity and biomass, compared with more sheltered benthic environments (McQuaid, *et al.* 1985; Leigh *et al.*, 1987; Denny, 1988).

In this section of the report we use existing current speed information (King and Wolanski, 1996) to help locate study sites where dense and representative patches of megabenthos are likely to occur. We then use a number of sampling methods (video, acoustics, epi-benthic dredge and grab) to map the seabed of these sites. In addition to locating study sites for the remainder of the Project, the mapping results of this study are presented in full as they are valuable and can contribute to a number of spatial management issues. These include: trawling strategies, the reduction of conflicts between trawl fisheries and line and trap fisheries, and conservation (appropriate uses and marine protected areas). Some of these issues revolve around the impact of trawling on seabed habitat and associated stocks.

5.1.1 The study area

The central region of the Great Barrier Reef lies on the Queensland shelf off Townsville at latitudes 18°00' S to 20°00' S and 146°00'E to 149°00'E (Figure 5–1). The continental shelf is about 100 km wide, with reefs around the nearshore continental islands (eg. Palm Is), then a 40 km wide lagoon with few reefs. Further offshore, to the north-east are the mid-shelf reefs that reach sea surface, irregularly clustered and separated by deep broad passages. In the north are the Kelso and Slashers Reefs, to the southeast – Broadhurst and Davies Reefs, and a third group further southeast – Flinders and Old Reefs.

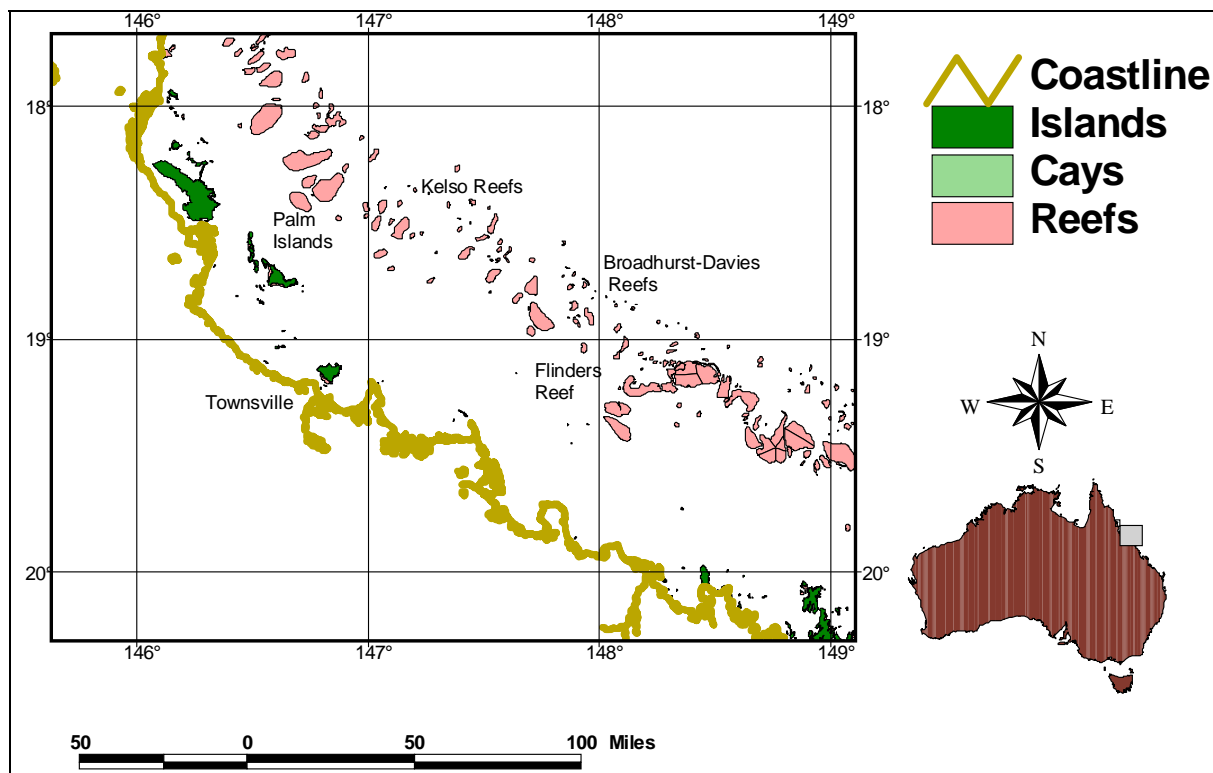


Figure 5–1. Map of the Queensland coastline showing offshore islands and reefs

The following climate and oceanographic details are derived from Scoffin and Tudhope (1985). Southeast trade winds dominate the area in winter (April-September) and the north-west monsoon affects the region during summer (January-March). These winds have a modal range of about 11 to 20 km h⁻¹ with trade winds up to 40 km h⁻¹. In summer, the area may be impacted by cyclones and associated with heavy rainfall. The water on the shelf is a mixture of oceanic waters from the northeast and terrestrial from the southwest. Water temperature ranges from 21°C in winter to 27°C in summer and salinities vary seasonally with rainfall, ranging from 32‰ to 26 ‰. Tides are basically diurnal and have a range of up to 3 m.

5.2 Methods

5.2.1 Selecting a suitable study area using current stress models

Current speed information for the region off Townsville was provided from circulation models by Brian King, then of the Australian Institute of Marine Science (AIMS). King and Wolanski (1996) used tidal data from the literature and from the field to make a two-

dimensional (depth averaged) model to simulate the dominant semi-diurnal tidal hydrodynamics of the central Great Barrier Reef continental shelf. The individual mesh dimensions of the numerical scheme were set at about $2 \text{ km} \times 2 \text{ km}$ which was sufficient resolution to incorporate the topography of each reef within the matrix.

We used the data provided and constructed the thematic current speed maps interpolated from an irregular sample point data set of current speeds geo-referenced by latitude and longitude (AGD66 Datum). We chose three potential study areas (Figure 5–1: The Kelso Reefs, Broadhurst-Davies Reefs and the Flinders Reefs), which were likely to have a range of benthic habitats based on the current speeds provided. For each of those three areas, the frequency of each current speed was tabulated. As the areas of greatest current speed are more likely to have megabenthos, they received highest priority for sampling. In order to sample the areas of different current speeds systematically, the frequency of greatest current speed locations were allocated to 2×2 nautical miles (n.mile) grids, intermediate current speed data on 4×4 n.mile grids and low current speed data on 8×8 n.mile grids. By dividing the frequency of each current speed by the respective areas we were able to derive a number of potential stations to sample in each of the three regions. The number of stations derived was adjusted downwards, based on what was practical to achieve in the ship time available. Again priority was given to sites with greater current speed.

5.2.2 Grab sampling

At each site, a Smith-McIntyre grab ($\sim 0.1 \text{ m}^2$) was deployed to collect a sample of sediment. From each sample, about 100 ml was placed into a plastic bag and frozen for quantitative analysis. Before the sample was frozen it was qualitatively characterized based on the sediment scale derived in Folk (1968) and according to perceived proportions of sediment type (Table 5–1) and histograms of the various fractions were plotted for each of the four areas. The remainder of the sediment sample was placed into a sieve-set of 2 mm^2 over 1 mm^2 and washed through both sieves. The sieved samples were placed in formaldehyde/rose bengal solution and retained for future infauna analysis. The sediment data was incorporated as an environmental parameter in the analysis of the benthos dredge data.

Table 5–1. Proportions of sediment fractions estimated from each sediment sample taken with the Smith-McIntyre grab.

Substratum Type	Mud	Sand	Gravel	Rock
S= Sand	0	1	0	0
(g)mS= Little Gravely Muddy Sand	0.25	0.65	0.1	0
gmS= Gravely Muddy Sand	0.25	0.5	0.25	0
gS= Gravely Sand	0	0.75	0.25	0
mS= Muddy Sand	0.25	0.75	0	0
sM= Sandy Mud	0.75	0.25	0	0
mG= Muddy Gravel	0.25	0	0.75	0
sG= Sandy Gravel	0	0.25	0.75	0
G= Gravel	0	0	1	0
R= Rock	0	0	0	1

5.2.3 Towed video

At each site, we surveyed a 500 m long transect of seabed with a towed video camera (Figure 5–2) suspended about 0.5 m above the seabed. At the same time, we acquired acoustic and depth data. Position was logged into a database and on both the video and acoustic tracks by recording the output of a Differential GPS. Semi-quantitative descriptions of the epibenthos and substratum at each site were made from the video, using the same protocol as for previous surveys in Torres Strait and on the GBR (Skewes *et al.* 1996; Long *et al.* 1997; Poiner *et al.* 1998).

Additionally, the habitats along the video transects were coded every second in real time using a classification system based on a range of epibenthos and substratum descriptions. The simple code used ranged from one to nine (Figures 5–3a-h); 1 = Sand, 2 = Rubble, 3 = Flora, 4 = Pinctada shell beds, 5 = Whips and Gorgonians, 6 = 5 + Sponges, 7 = 6 + Hard Corals, 8 = Rock and 9 = Reef. The composition of the seabed substratum, particularly the relative amounts of reef, rock, rubble, sand and mud were estimated and the proportion of each habitat type (code) was then calculated for each transect. The proportion of each habitat code for each site was included as environmental parameters in the benthic assemblage analysis.



Figure 5–2. Image showing the simple video drop-camera, in water proof housing, suspended from a wire above a heavy weight and a fin to keep the camera facing in the direction of travel. Also shown are the 0.1m² Smith-McIntyre sediment grab and video cable to the surface.

5.2.4 Naturalist's dredge

A small naturalist's dredge was towed, at the same time as the video camera was deployed, for up to 300 m, depending on the nature of the substratum and the density of fauna observed on the video monitor. The naturalist dredge (about 60 cm wide × 25 cm high) with a cod-end made of prawn trawl material (mesh size about 40 mm stretched) was deployed on a trawl wire. After each tow, the sample was placed onto a sorting table with trays of varying sieve sizes ranging from 100 mm², 50 mm² to 2 mm². The animals in each tray were sorted from the substratum and sorted into phyla or classes and either frozen or preserved in alcohol for further sorting and identification. A record was taken of the weight and numbers of each major group of animals collected and of the substratum material discarded. In some cases (6), a species was sub-sampled where there were very large numbers — a proportion of the catch was weighed and counted and the total weight was recorded to give total numbers. The bivalves and gastropods were identified at the Queensland Museum and only numbers of each species collected were obtained. Biomass (g) was recorded for all other taxonomic groups.



Figure 5-3a. Bare substratum – code 1 – in this instance with many crinoids

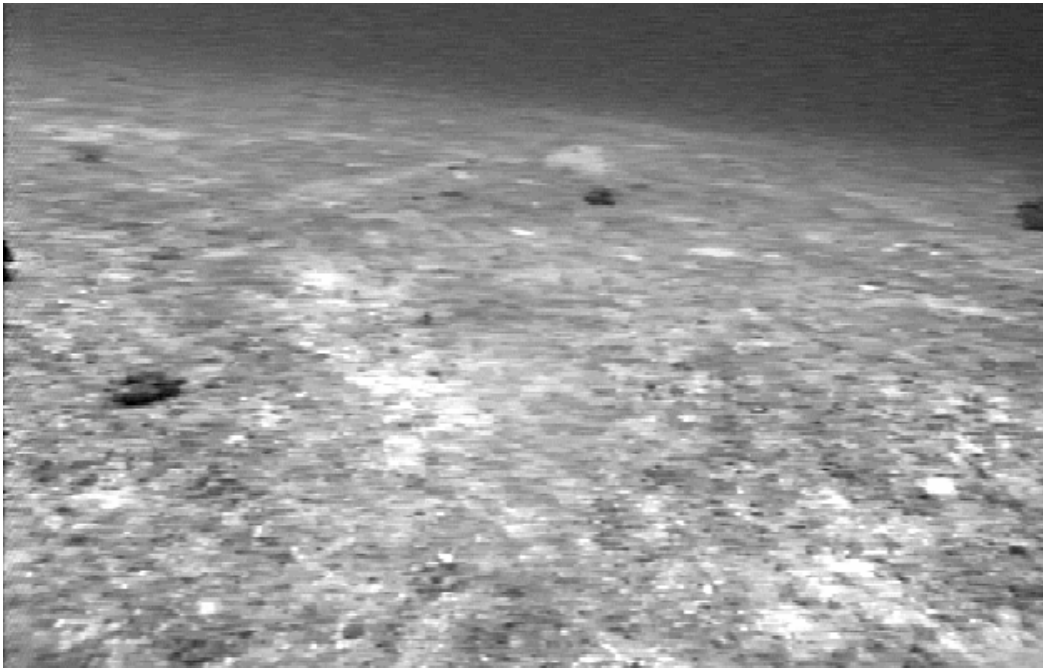


Figure 5-3b. Bare substratum with rubble – code 2.



Figure 5-3c. Substratum of sand with large patches of algae – code 3 (mostly *Caulerpa* sp).



Figure 5-3d. Substratum with beds of *Pinctada* shells in depressions – code 4.



Figure 5-3e. Small garden with gorgonians on rubble substrate – code 5.



Figure 5-3f. Larger garden with gorgonians and fan sponges (*Ianthella* sp) – code 6.

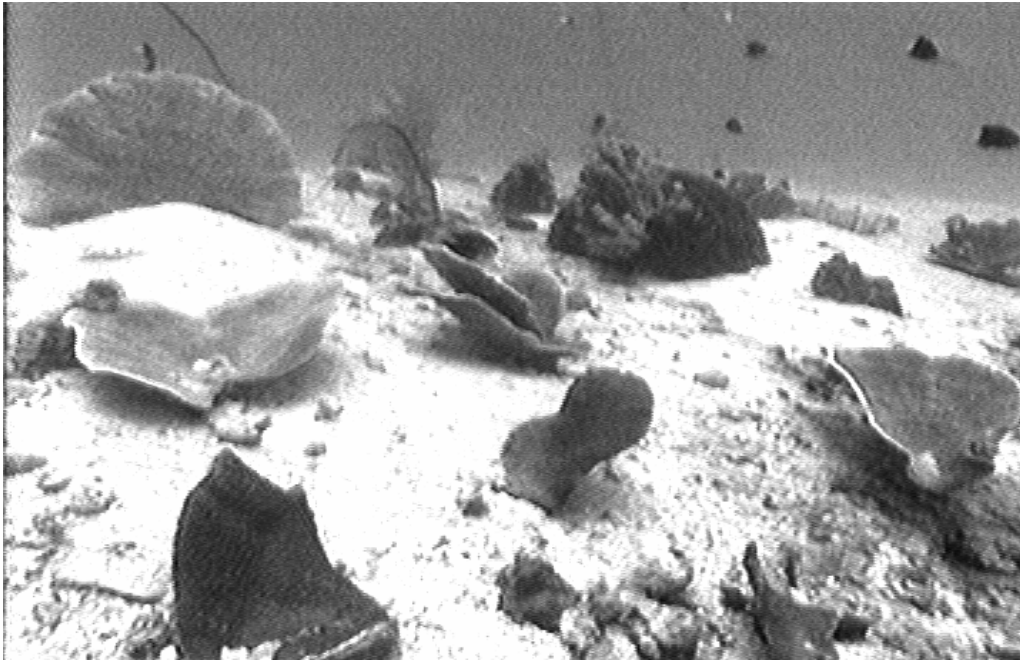


Figure 5-3g. Garden of gorgonians, sponges and hard corals (often *Turbinaria* sp.) –code 7.

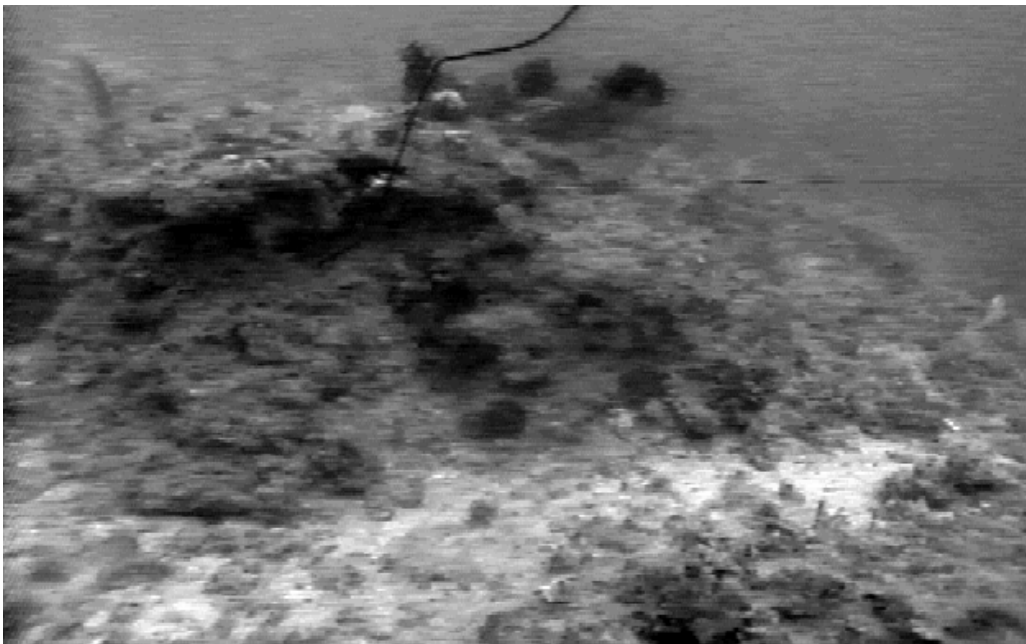


Figure 5-3h. Rough ground with a rock ledge – code 8.

5.2.5 Data analysis

A total of 606 algae and invertebrate taxa were recorded at all four localities (see Figure 5–4) collected from a total of 105 dredge stations (Appendix 5.5–1). The different taxa that represented 23 major taxonomic groups included identified species as well as unknown and unidentified specimens that were classified on higher taxonomic levels with common denominations (see Appendix 5.5–1). It must be recognized that sampling by naturalist's dredge will fail to detect many of the less abundant, highly mobile and/or burrowing or cryptic species, but it will well represent the presence and abundance of the great majority of species exposed to benthic trawling. For the total of 606 species recorded, 444 were registered by their wet biomass and 471 by the number of individuals in each dredge. Basic ecological descriptors of species alpha diversity (richness and evenness) were used for species and grouped by locality based on their biomass by species. For the biomass and multivariate analyses, all taxa that contributed >1 gram were included. Nevertheless, the assemblage biomass data used comprises nearly all species recorded during the surveys. In the biomass analyses, dredge samples from 90 sites were included of a total of 105. Overall, the contribution of the different species to the assemblage biomass varied by five orders of magnitude (from 1 g to ca. 98,000 g). Consequently, in the multivariate analyses the biomass data were standardized and logarithmically transformed [$\log_{10}(x+1)$]. The ordinal environmental variables (sediment type, habitat type, water current, and depth) were entered as continuous variables.

Exploratory and descriptive data analyses for regressions and univariate and factorial analyses of variance (ANOVA) with a-posteriori mean comparisons of main effects (Tuckey t-test) were performed for the comparison of biomass, diversity, richness and evenness within localities. All ANOVAs and regressions were performed using Generalized Linear Models, GLM (SPSS, 1999).

Because sampling effort was proportional to the area covered in the surveys, we examine the species accumulation (or species-areas) curves as an indicator of whether our sampling was capturing the local species richness. We used the "Estimates" software (Colwell, 1997) that computes randomized species accumulation curves, statistical estimators of species richness (S), and a statistical estimators of the number of species shared between pairs of samples, based on species-by-sample (or sample-by-species) incidence or abundance matrices. As the

samples accumulate, more and more information is included in the analysis and the local (or regional) species richness estimates generally become more accurate. The curves should reach an asymptote as the total number of species present in the areas is approached as sampling increases. By adding all new species encountered in sequential samples, a species area curve could be constructed by randomizing the selection of samples, say 50 times, to eliminate the potential bias of sample order. The mean species number (± 1 SD) of the randomizations were then plotted against the number of samples. Rarity and low incidence of species were also assessed by plotting species that occur in only one sample (singletons). An incidence-based estimator of species richness (Chao 1984, 1978) was used to predict the minimum number of species that the surveyed areas must contain to account for the observed 606 species encountered. The full bias-corrected formula is:

$$S_{Chao2} = S_{obs} + \frac{Q_1^2}{2(Q_2 + 1)} - \frac{Q_1 Q_2}{2(Q_2 + 1)^2} \quad (\text{eq. 1})$$

where S_{Chao2} is the predicted species richness, S_{obs} is the total observed species, Q_1 is the frequency of unique (singletons) and Q_2 is the frequency of duplicates species (doubletons) (Colwell, 1997).

5.2.6 Assemblage analyses

Multivariate assemblage analyses were performed in order to identify spatial or ecological assemblage differentiation among taxa and dredging stations in the log-transformed biomass data set. To be able to identify clear patterns of assemblage agglomeration, the 444 taxa identified in all dredges were collapsed into 23 major higher taxa. Then, a dredge taxa-matrix was constructed and a classification analysis using an agglomerative hierarchical method was performed to divide the objects of the study (whether taxa or dredging stations) into discrete groups or clusters. The distance between the resulting groups is the distance between the centroids. The centroid itself can be described as the average point of the cluster. It is calculated by taking the mean value of the coordinates on each axis for all the points in the cluster. These groups are based on the similarity (or dissimilarity) of the objects and it is expected that the clusters have spatial ecological significance. Each group that resulted from the classification was calculated using the Spearman Coefficient (equation 2). In equation 2, i and j represent two rows (dredge stations) of the data matrix, k represents the column (taxa), and therefore x_{ik} would be the datum in the k th column of row i and n is the total number of

variables:

$$SCC_{ij} = 1 - \frac{6 \sum_{k=1}^n (R_{ik} - R_{jk})^2}{n^3 - n} \quad (\text{eq.2})$$

where: R = rank order of element in variable.

To explore the joint relationship between the biomass of benthic species assemblages and the selected environmental variables, a multivariate (ordination) direct gradient analysis was performed. Canonical Correspondence Analysis (CCA) was used to relate the benthic assemblage with the abiotic variables (ter Braak 1986; Palmer 1993). Direct gradient analysis was carried out using the average biomass per major taxonomic groups at each dredge site. The environmental variables used in the analyses were: the depth (in metres), water speed or bottom stress (in knots), habitat type (9 levels), and sediment type (4 levels). The computer package MVSP v.3.11f (Kovach Computing Services, 2000) was used to perform CCA (ter Braak and Prentice 1988).

Canonical correspondence analysis (CCA; ter Braak, 1986, 1987) is a multivariate direct gradient analysis method that has become very widely used in ecology. This method is derived from correspondence analysis, but has been modified to incorporate environmental data in the analysis. It is calculated using the reciprocal averaging form of correspondence analysis. However, at each cycle of the averaging process, a multiple regression is performed of the stations scores on the environmental variables. New scores are calculated based on this regression, and then the process is repeated, continuing until the scores stabilize. The result is that the axes of the final ordination, rather than simply reflecting the dimensions of the greatest variability in, in this case the dredge taxa data, are restricted (constrained) to be linear combinations of the environmental variables and the stations data. In this way these two sets – i.e. the biomass per station and the environmental values per stations, of data are then directly related. The results of CCA are presented in scatter diagrams containing the environmental variables plotted as arrows or vectors emanating from the center of the graph, along with points (and names and numbers) for the station and taxa. The relationships between the stations and taxa are displayed in that way that each sample point lies at the centroid of the points for taxa that occur in those stations. The arrows representing the environmental variables indicate the direction of maximum change of that variable across the diagram.

5.3 Results

5.3.1 Selecting a suitable study area using current stress models

Based on the stratification by current speed data and the logistics of completing the field-trip 101 sites were selected — 25 sites in the Kelso Reefs area, 31 in the Broadhurst-Davies Reefs and 45 in the Flinders Reef areas (Figure 5–4). Three extra sites (Robbery Shoal) were identified east of Palm Islands based on local knowledge of a seabed feature fished by anglers. Not all selected sites could be sampled and in some areas extra sites were sampled with the video sled to find megabenthos. At some sites, due to the roughness or presence of rock shelves, the dredge or grab could not be deployed or failed to sample properly.

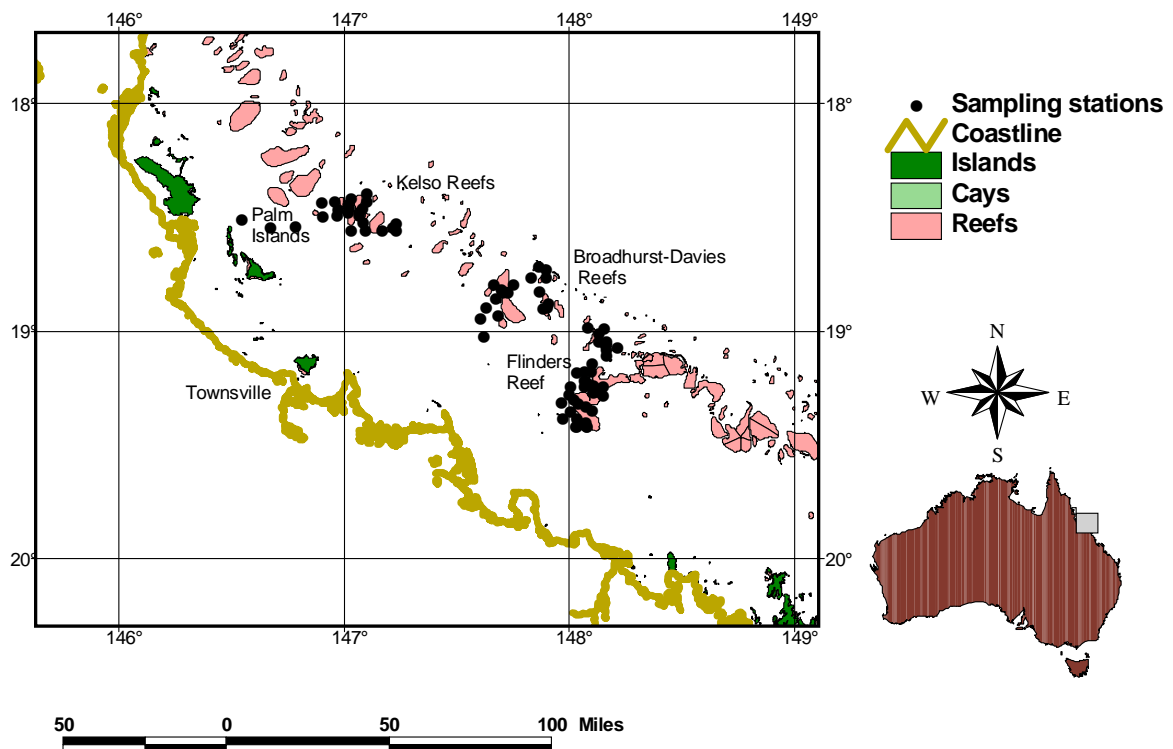


Figure 5–4. Map of the Queensland coastline showing the location of the sampling sites for the video camera, dredge and grabs.

The depth range was similar in the three major sampling areas and ranged from about 35–78 m (Figure 5–5), though the deepest sites were in the Broadhurst area. There was a noticeable trend in current speed among sampling sites in the three areas. Current speed (from modeled data) ranged from 0.1 knot to 0.6 knot in the Kelso area, 0.2 knot to 0.7 knot in the Broadhurst area and from 0.2 to 1.3 knot in the Flinders area (Figure 5–6), with three channel sites (Figure 5–9c) having particularly high current speed. There was no significant relationship between current speed and depth (Figure 5–7) at the three sampling areas, but the mud fraction decreased significantly with increasing current speed ($p=0.001$).

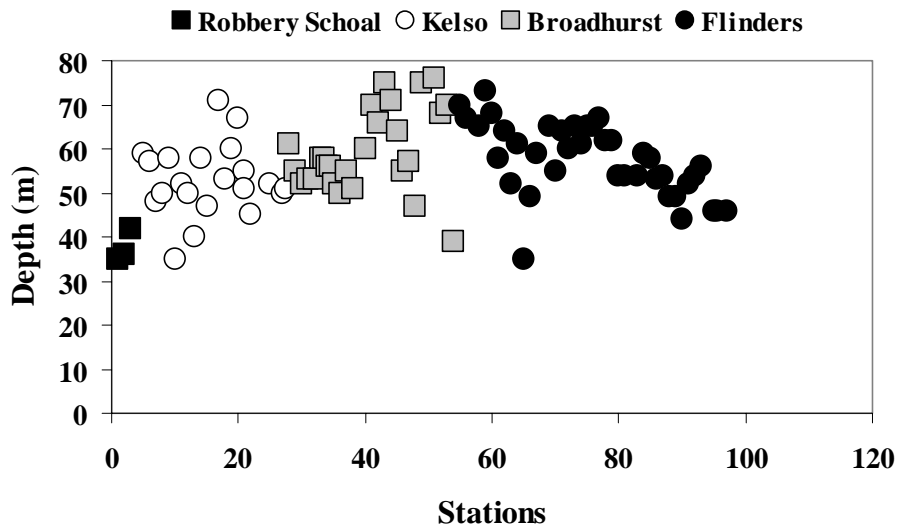


Figure 5–5. Depth at all the sites in each of four areas east of Townsville.

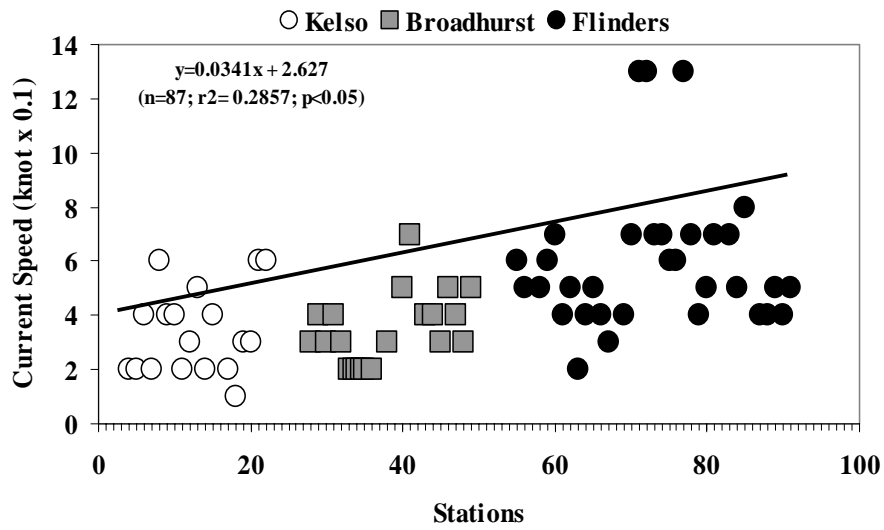


Figure 5–6. Current speed at the sites in each of four areas east of Townsville. Three channel sites are outliers.

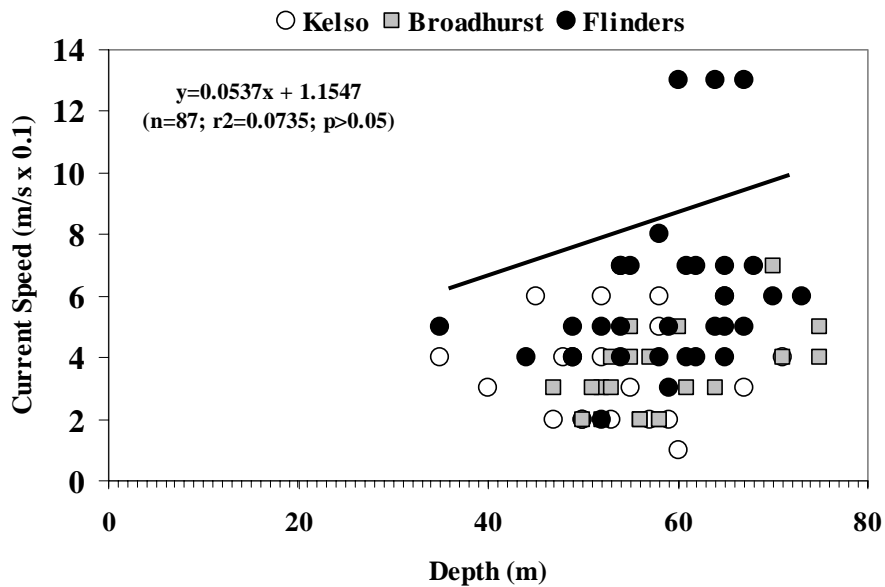


Figure 5–7. Current speed at depth at the sites in each of three areas east of Townsville.

5.3.2 Grab sampling

Sediment data was obtained from 90 stations. A histogram of the relative proportions of sediment composition for the study areas is given in Figure 5–8. The lagoonal stations (Robbery Shoal) are predominantly muddy-sand (~65%) and sandy-mud (35%). The composition of sediment at the Kelso region are gravelly-sand (~30%), muddy-sand (25%), sandy-mud (~15%) with small amounts of sand (<5%) or rock. Compared with the Kelso region, sand increased to 22% at the Broadhurst area and muddy sand decreases to ~19%. This change becomes more marked at the Flinders area where sand was over 40%, gravelly-sand was ~25% and muddy-sand was <10% of the sediment composition. Rock was about 10% at Kelso but decreases to < 5% at the Flinders area.

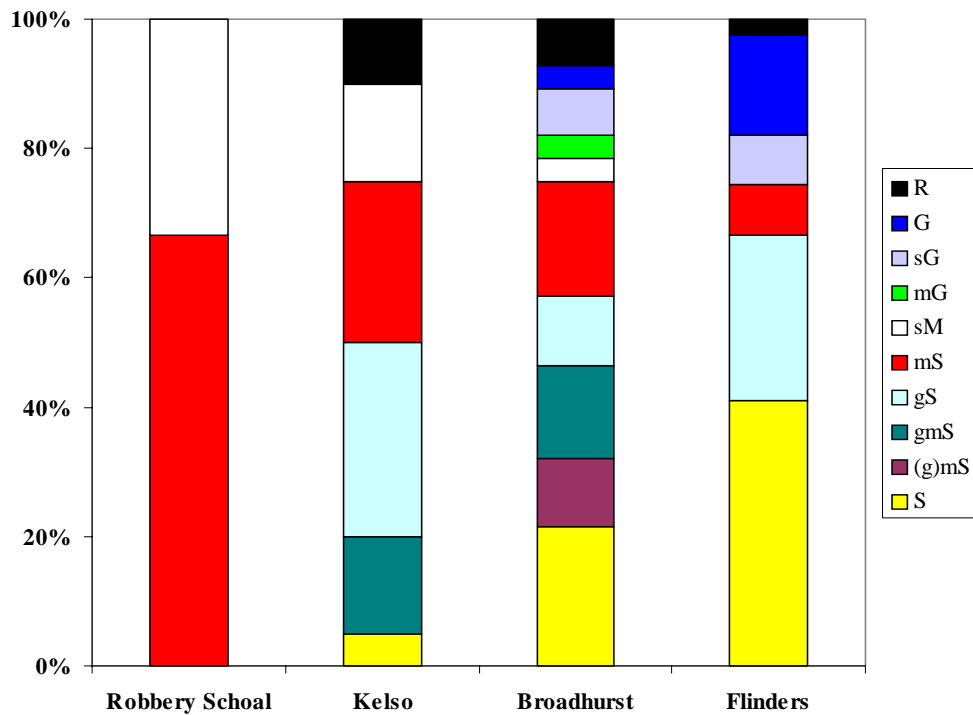


Figure 5–8. Sedimentary fractions obtained from all the sites in each of four areas east of Townsville. Codes for sedimentary fractions are: S= Sand; (g)mS= Little Gravelly Muddy Sand; gmS= Gravelly Muddy Sand; gS= Gravelly Sand; mS= Muddy Sand; sM= Sandy Mud; mG= Muddy Gravel; sG= Sandy Gravel; G= Gravel; R= Rock.

5.3.3 Towed video

The substratum at a total of 106 sites (Kelso, Broadhurst-Davies and Old reefs were sampled with a video camera (Figures 5–9a-c). The substratum in most sites was bare sand (62%, over all transects) or sand with coral rubble (20%). Few megabenthos sites were found in areas of

high current speed (the pink or red regions). Old coral reefs (black – indicating rock – 8%) with no organisms visible on it were found around platforms from which extant coral reefs (silver-grey) arise. Only three sites were found that had significant amounts of flora (algae – *Halimeda* sp.) (2%) – these were in the Broadhurst-Davies Reefs area. Most of the sites with some megabenthos (1%) were in close proximity to the base of extant reefs. Deep coral reefs (6%) were also found close to extant reefs.

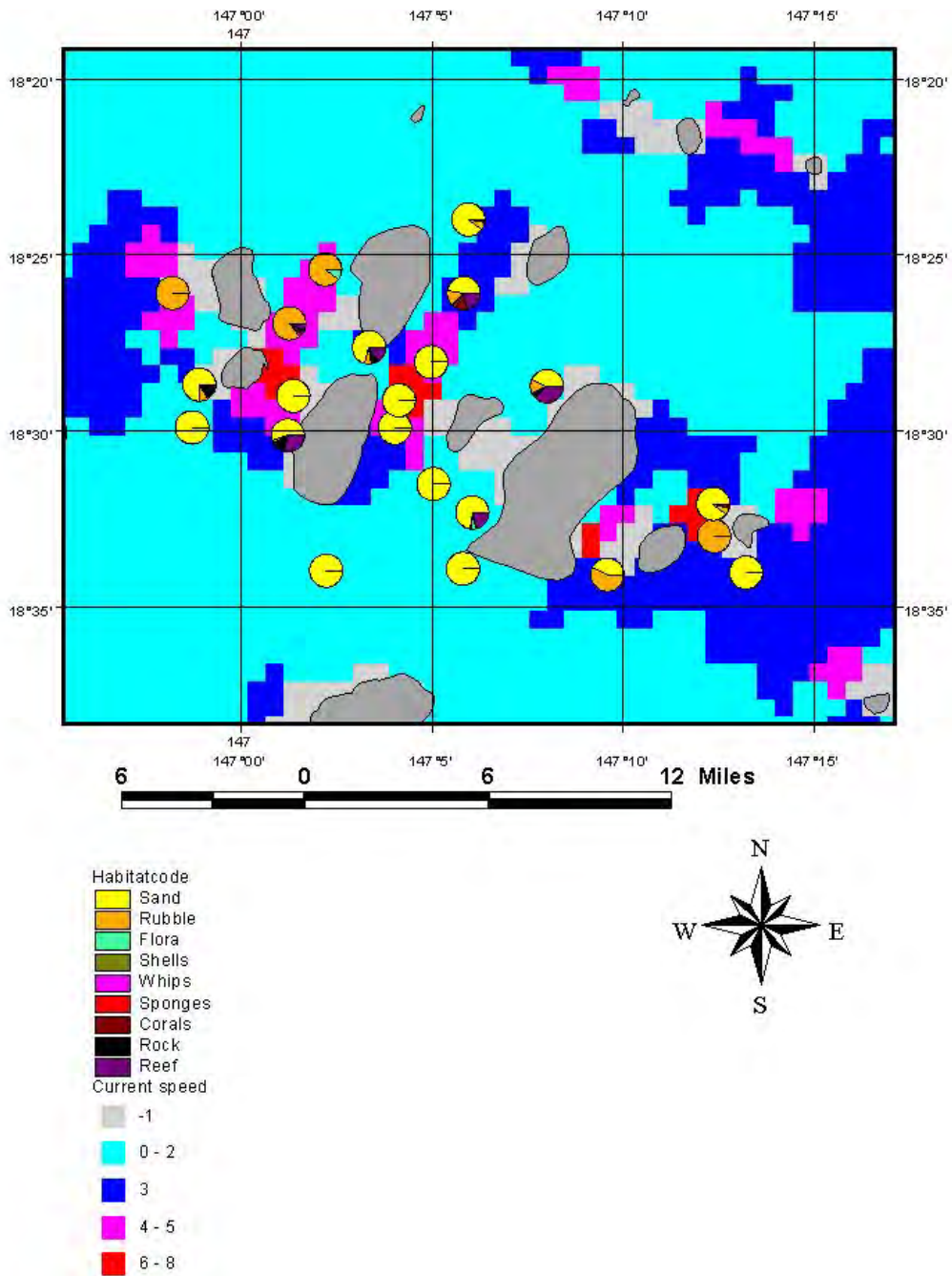


Figure 5–9a. Relative proportions of habitat types in the Kelso Reef area derived from towed video sled observations (Pie diagrams) overlaid on current speed (knots x 0.1). Substrata are mostly sand or rubble-sand with deep reefs (dark purple) in proximity to the base of surface reefs (grey).

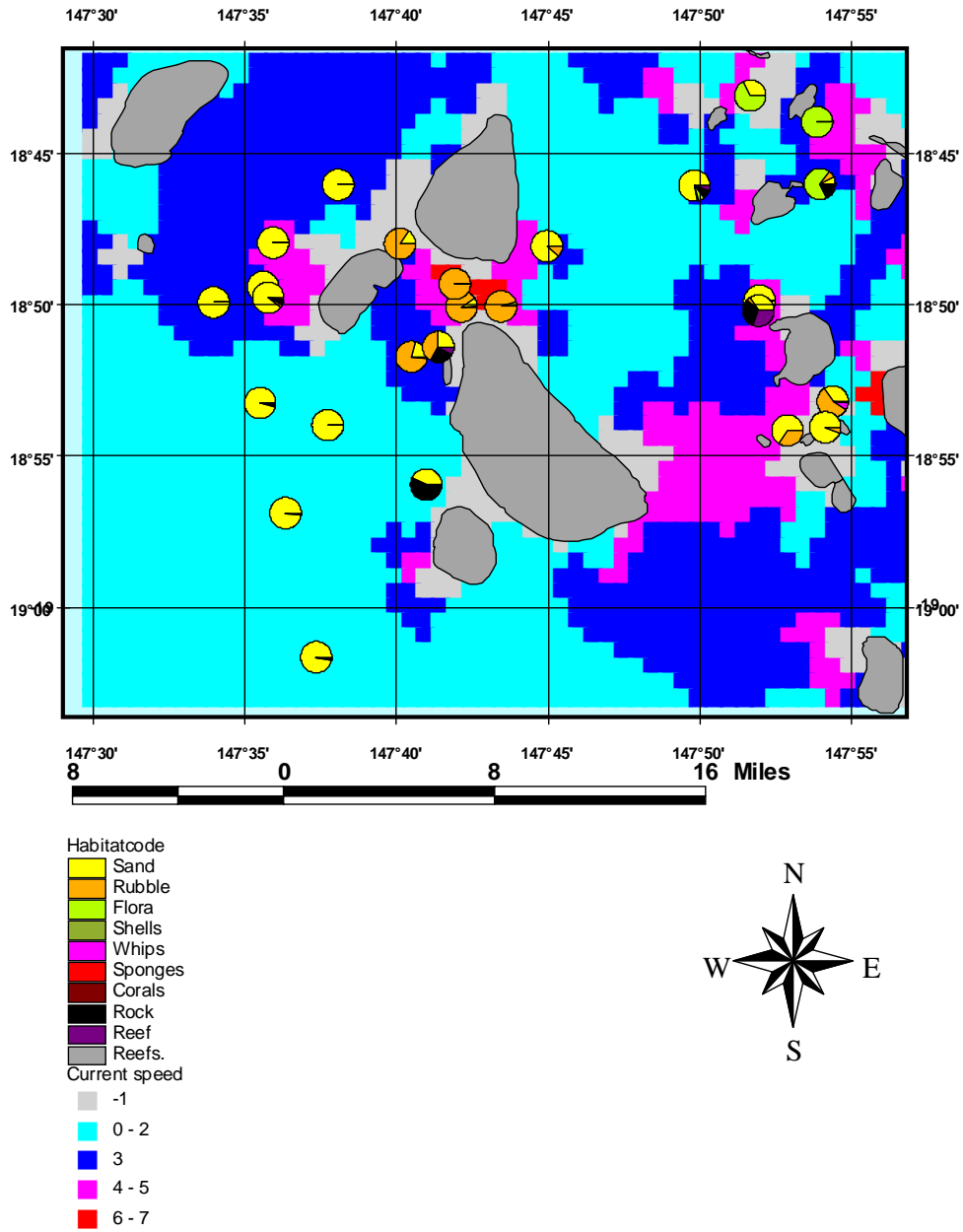


Figure 5-9b. Relative proportions of habitat types in the Broadhurst-Davies Reef area derived from towed video sled observations (Pie diagrams) overlaid on current speed (knots x 0.1). Substrata are mostly sand or rubble-sand with deep reefs (dark purple) in proximity to the base of surface reefs (grey).

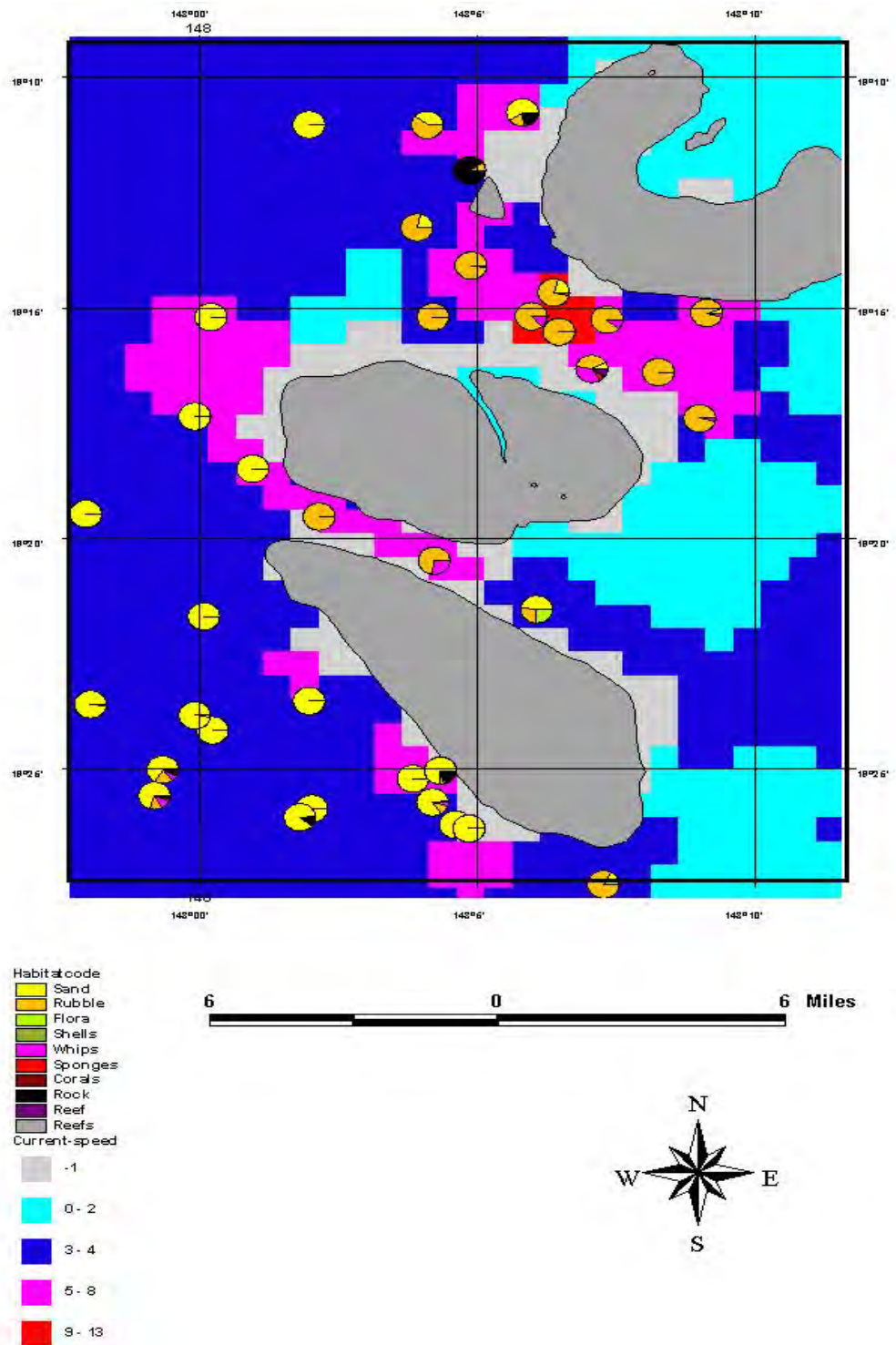


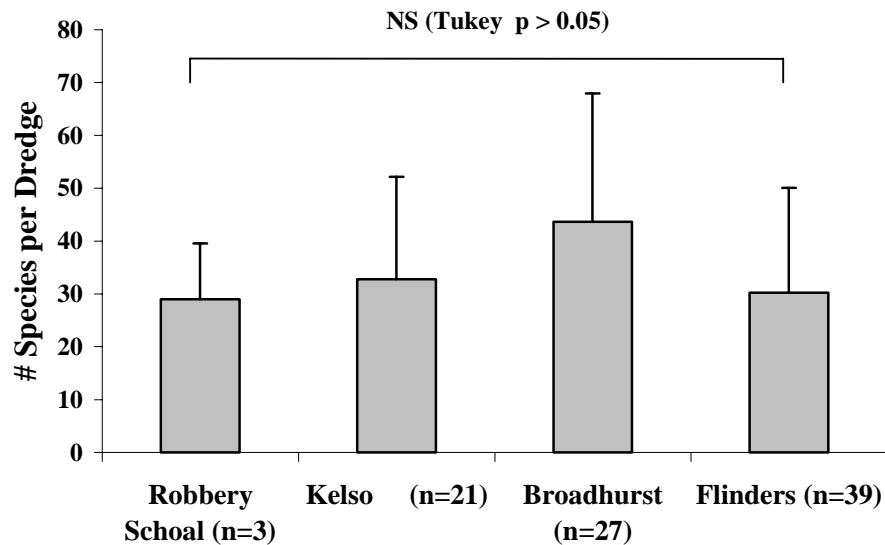
Figure 5–9c. Relative proportions of habitat types in the Flinders–Old Reef area derived from towed video sled observations (Pie diagrams) overlaid on current speed (knots x 0.1). Substrata are mostly sand or rubble-sand with megabenthos (pink) between surface reefs (grey) or rock (black) in proximity to the base of surface reefs.

5.3.4 Naturalist's dredge

A total of 90 sites were sampled with the naturalist's dredge (3 at Robbery Shoal, 21 at Kelso Reefs, 27 at Broadhurst-Davies reefs and 39 at Flinders Reefs). A full listing of the taxa collected, ordered by occurrence, is given in Appendix 5.1.

The average number of species and the average biomass per dredge was not significantly different ($p > 0.05$) between the four sampling areas (Figure 5–10 a,b). However, the mean number of species and their biomass were greater in the Broadhurst-Davies Reef area with about 45 species represented in a tow and weighing just over 2 kg. Biomass was lowest in the Flinders Reef area with about 0.9 kg per tow. Biomass of bivalves and gastropods were not available.

(a)



(b)

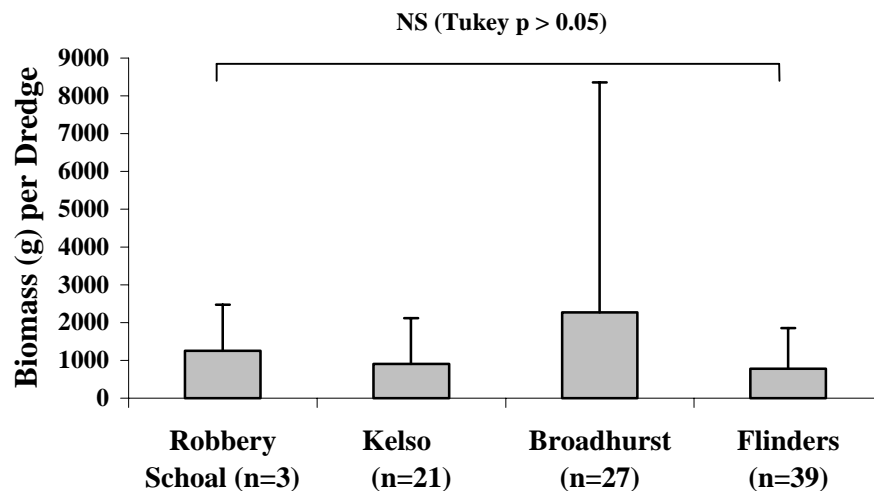
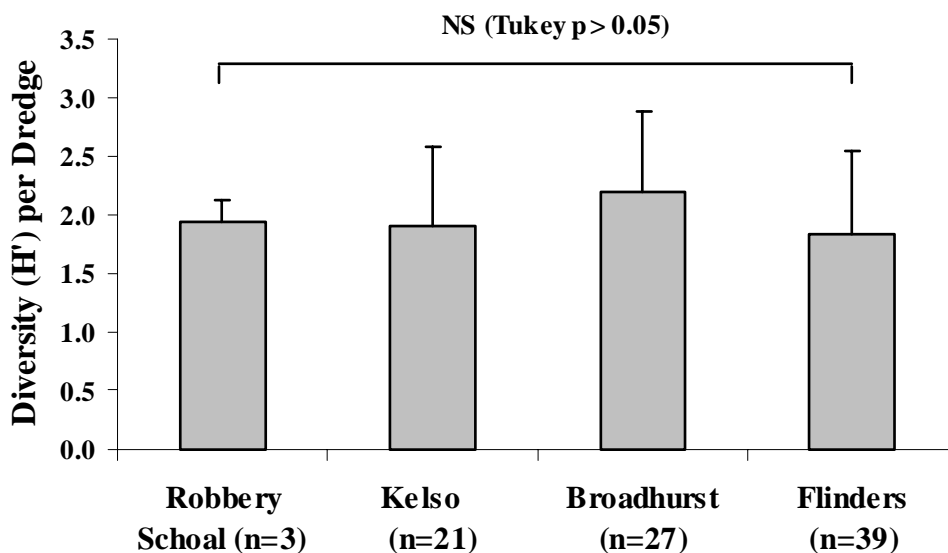


Figure 5–10. Average number of species (a) and biomass per dredge sample (b) at the four study areas. The vertical bars are \pm one standard deviation. n = number of sites sampled.

The average species diversity (H') and evenness per dredge were not significantly different ($p > 0.05$) between the four areas (Figure 5–11 a,b). The Broadhurst-Davies Reef area had the greatest average species diversity. Robbery Shoal, with only three dredge samples was as diverse as the other areas sampled.

(a)



(b)

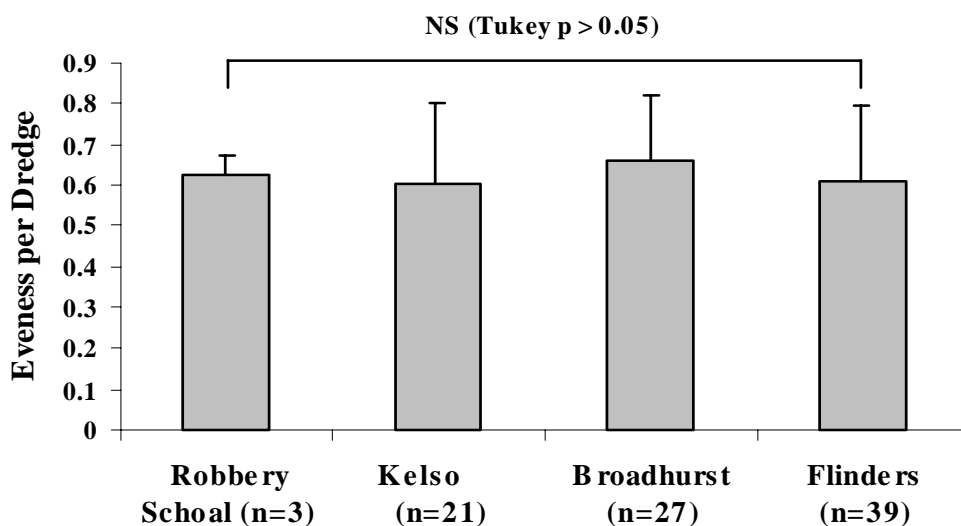


Figure 5–11. Average (a) diversity and (b) evenness of species per dredge sample at the four study areas. The vertical bars are \pm one standard deviation. n = number of sites sampled.

The species accumulation curve (Figure 5–12), based on random addition of samples, allowed us to evaluate the effectiveness of our survey to sample the species richness of the benthic biota. The curves represent the observed number of species without the bias of sample order.

The curve steadily increases as additional samples continue to bring in more new species and does not reach an asymptote, indicating that the sampling was insufficient to capture the entire local species richness (Figure 5–12). This result also showed that almost 50% of the observed species, in the 90 samples analysed, occurred in only a single sample (singletons) (Figure 5–12). The predicted species richness curve, based on the incidence of species in each sample, also did not reach an asymptote and suggests that more than 1,000 species must be present in the surveyed areas to account for the observed richness.

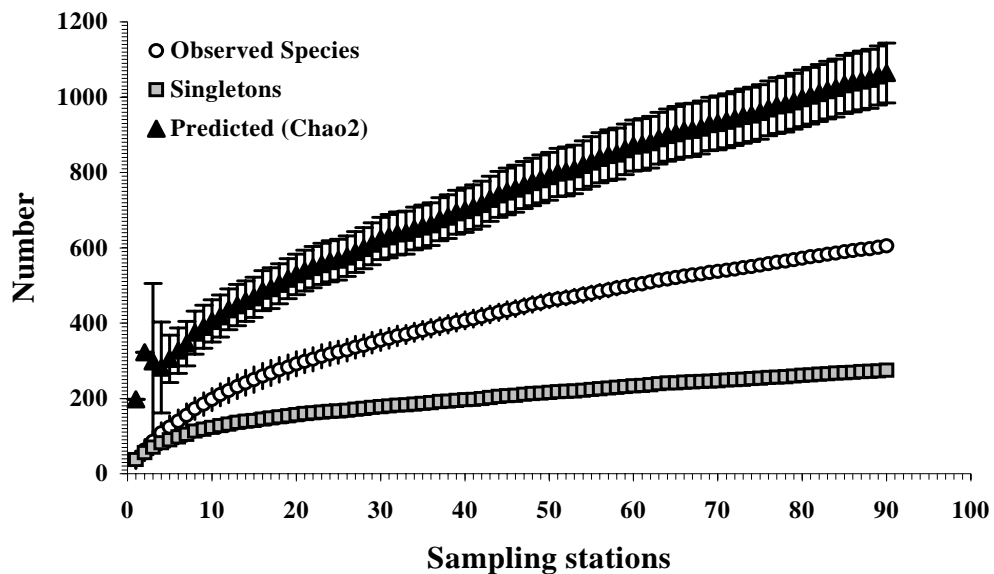


Figure 5–12. Species area curves based on the contribution of the number of new observed and predicted species, and species that occurs in a single sample or singletons, ($\pm 1SD$) for the surveyed areas.

5.3.5 Assemblage analyses

The cluster analyses for the biomass data showed that there are discrete groups for different taxa and dredge stations (Figures 5–13 and 5–14 respectively). The results of these analyses confirmed that clusters of different combinations of dredge taxa and stations represent different species assemblages, being separated by the differential biomass contribution of each taxa.

Four major clusters of taxa were found and these were separated from each other by values of the Spearman Coefficient of similarity (SC) that ranged from to $SC = 0$ to -0.1 (Figure 5–13). Cluster I comprised the taxa seagrasses (Hydrocharitacea), green algae (Chlorophyta), and sea slugs (Opisthobranchia) species. Cluster II comprised most mobile taxa like sea stars

(Asteroidea), brittle star (Ophiuroidea), sea urchins (Echinoidea), prawns (Penaeioidea), crabs (Anomura and Brachyura) and sessile species like brown algae (Phaeophyta) and Zoanthidea) species (Figure 5–13). Cluster III comprised almost entirely of sessile deposit and filter feeder species that include sponges, (Porifera), sea squirts (Ascidiacea), bryozoa (Bryozoa), hydroids (Hydrozoa), soft corals (Alcyonacea), sea fans (Gorgonacea), and brown algae (Phaeophyta) species (Figure 5–13). Cluster IV was made up of a mixture of sessile and mobile species, including corals, (Scleractinia), sea cucumbers (Holothuridea), polychaete worms (Polychaeta) and shrimp (Caridea) species.

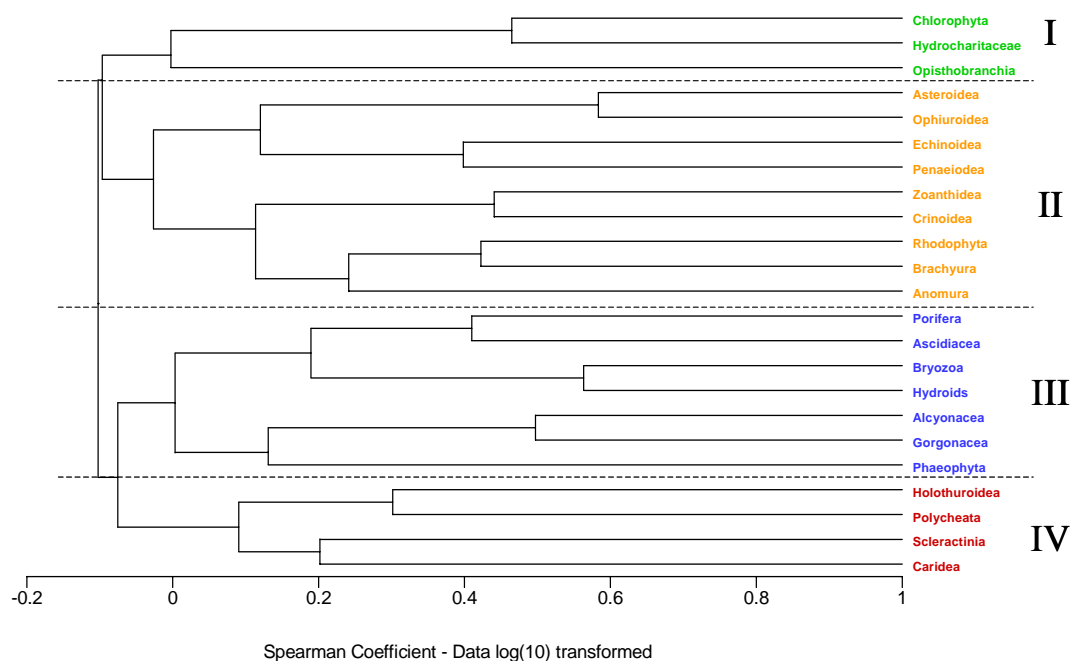


Figure 5–13. Results of the cluster analysis of biomass of animals collected in a naturalist dredge showing groupings of species assemblages.

The dredge stations clustered into groups based on their species biomass composition (Figure 5–14). They did not separate into discrete spatial entities, instead they showed a mosaic of different assemblages and species assemblages throughout the sampling areas (Figure 5–15). Groups 1 (green circles) and 3 (blue circles), composed mainly of floral species assemblages and associated animals and sessile and deposit feeders respectively, appeared equally common in the Kelso, Broadhurst-Davies Reefs areas and Flinders Reef areas. Station groups 2 (yellow circles) and 4 (red circles) appeared to be more common in the Kelso and Broadhurst-Davies Reefs areas than in the Flinders Reef area.

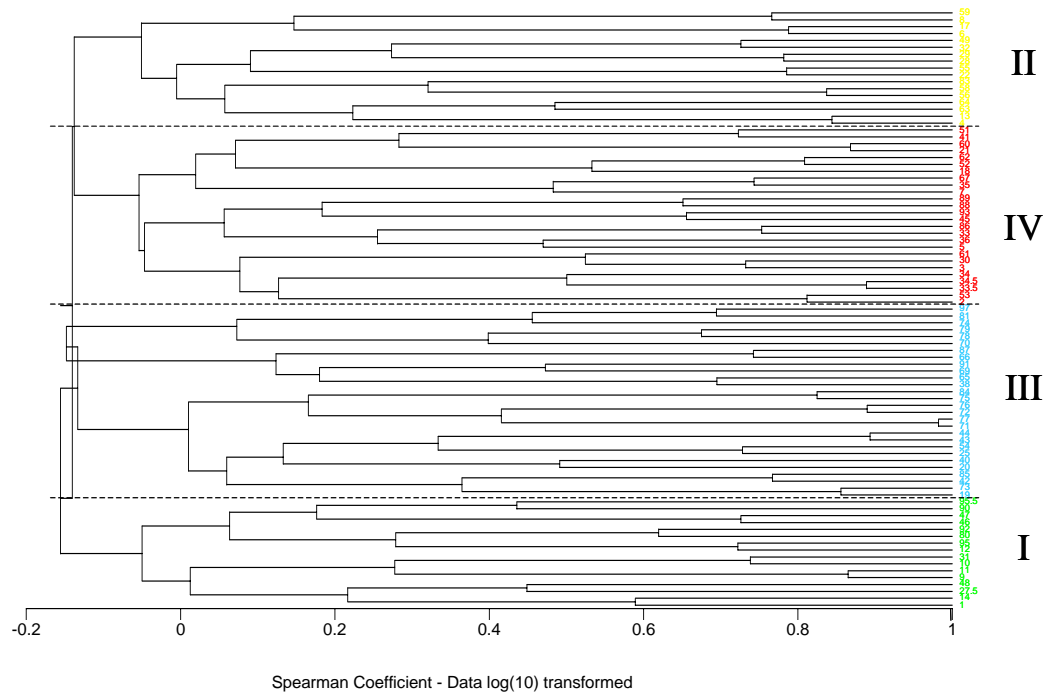


Figure 5–14. Results of the cluster analysis of biomass of animals collected in a naturalist dredge showing groupings of stations based on species assemblages.

In addition to the classification analyses, the results of the multivariate ordination CCA are presented in Figures 5–16 and 5–17, where the position of the variables (taxa) and cases (stations) are plotted along the first two axis of the ordination in relation to the major environmental variable or vectors. In each figure, the circles represent the position of the taxa (named circles in Figure 5–16) or dredge station (numbered circles in Figure 5–17) in relation to each environmental variable, depicted as vectors (arrows). All vectors are displayed orthogonally to the two major ordination axes and the length expresses its importance or weight in the overall explanation of the variances of the biomass data matrix. The position of each taxa or station, whether close or away from the end of the arrow, indicates that a given taxa or station is positively or negatively correlated to that environmental variable, respectively. Thus, most of the variance of the data set is largely explained by the first two axis of the ordination, both accounting for more than the 63% of the constrained variance of the data and showing the higher correlation values between the taxa and the environmental variables (Table 5–2a). Axis 1 was positively and significantly correlated with current speed, rubble, depth and sparse and mid density gardens, and negatively correlated with the amount of sandy or muddy bottom (Table 5–2b). Axis 2 was positively and significantly correlated with only the presence of algae beds and negatively correlated with the amount of mud and depth (Table 5–2b). In summary, the results indicate that the water current or bottom stress (expressed in knots) was the single most important variable in explaining the variation of the

biomass data along the horizontal axis for both taxa and stations. Other important environmental variables that are significantly correlated with the biomass of most taxa were some types of bottom habitat, in particular the presence of rubble, sand and mud.

Table 5–2a. Eigenvalues, percentages and correlation values for the first six axis of the CCA ordination of taxa and station scores.

Axes	Eigenvalues	Cumulative	
		Variance (%)	Taxa-env. correlations
Axis 1	0.086	37.75	0.771
Axis 2	0.058	63.33	0.681
Axis 3	0.021	72.45	0.550
Axis 4	0.016	79.63	0.517
Axis 5	0.013	85.35	0.430
Axis 6	0.010	89.82	0.574

Table 5–2b. Weighted correlation coefficients of the environmental variables for the first two axes of the CCA ordination. Degrees of Freedom = ((87 stations - 12 variables) - 1) = 74

Environmental variables			Environmental variables		
	Axis 1	<i>p</i>		Axis 2	<i>p</i>
Current	0.599	<0.01	Algae	0.347	<0.01
Rubble	0.551	<0.01	Depth	-0.469	<0.01
Sparse Garden	0.426	<0.01	Mud	-0.297	<0.01
Depth	0.243	<0.05	Rock Ledges	0.204	>0.05
Mid Garden	0.267	<0.05	Sandy	-0.043	>0.01
Sandy	-0.276	<0.01	Current	-0.005	>0.01
Mud	-0.288	<0.01	<i>Pinctada</i> shells	-0.027	>0.01
Algae	-0.112	>0.01	Mid Garden	0.063	>0.01
<i>Pinctada</i> shells	-0.079	>0.01	Dense Garden	0.116	>0.01
Rock Ledges	0.083	>0.01	Coral Garden	0.040	>0.01
Coral Garden	0.099	>0.01	Rubble	-0.077	>0.01
Dense Garden	0.000	>0.01	Sparse Garden	-0.072	>0.01

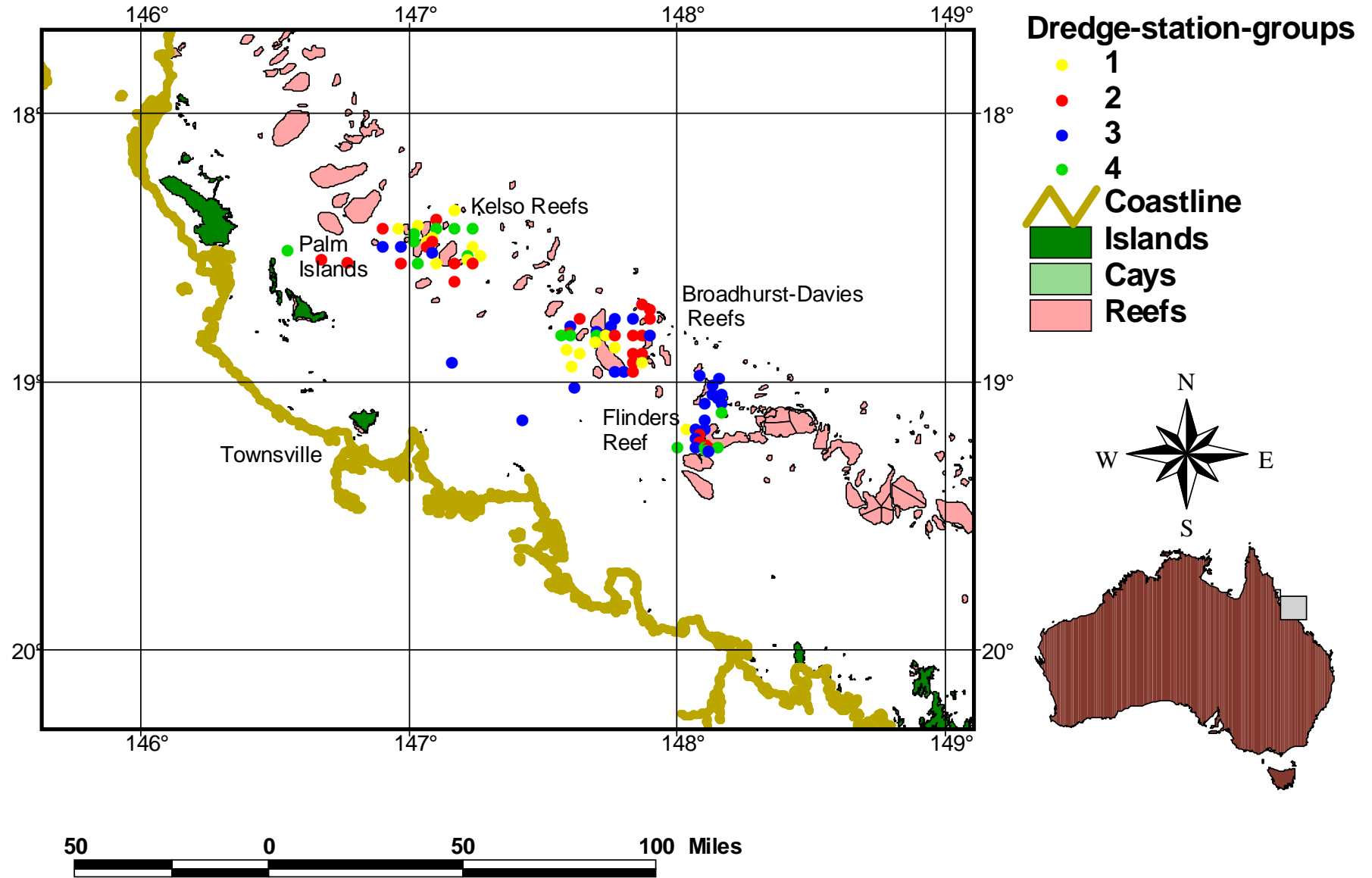


Figure 5-15. Map of station groups obtained from the cluster analysis of dredge biomass content during 1997.

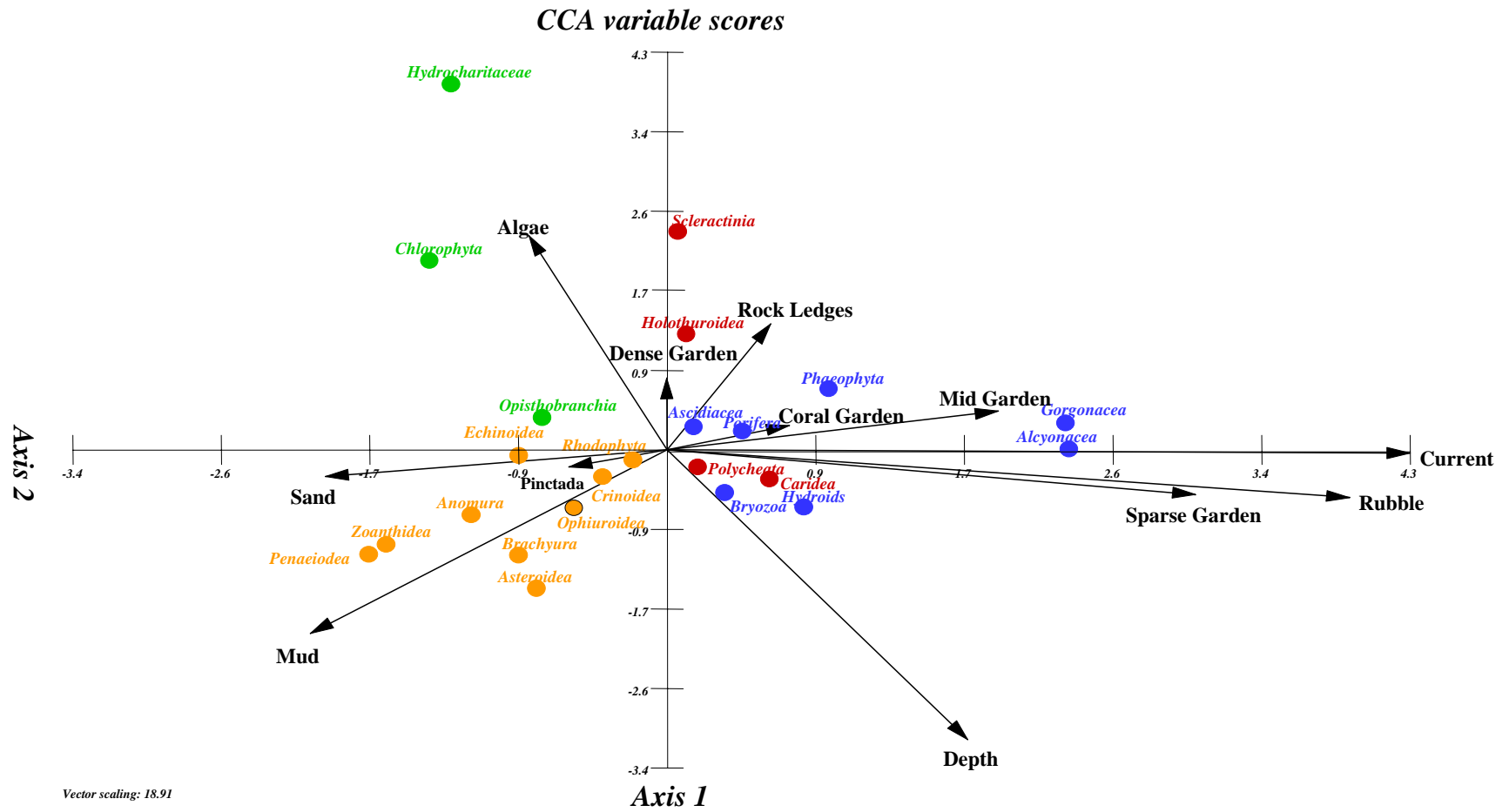


Figure 5-16. The results of the multivariate ordination CCA where the position of the taxa (circles) are plotted along the first two axis of the ordination in relation to the major environmental variables (arrows)

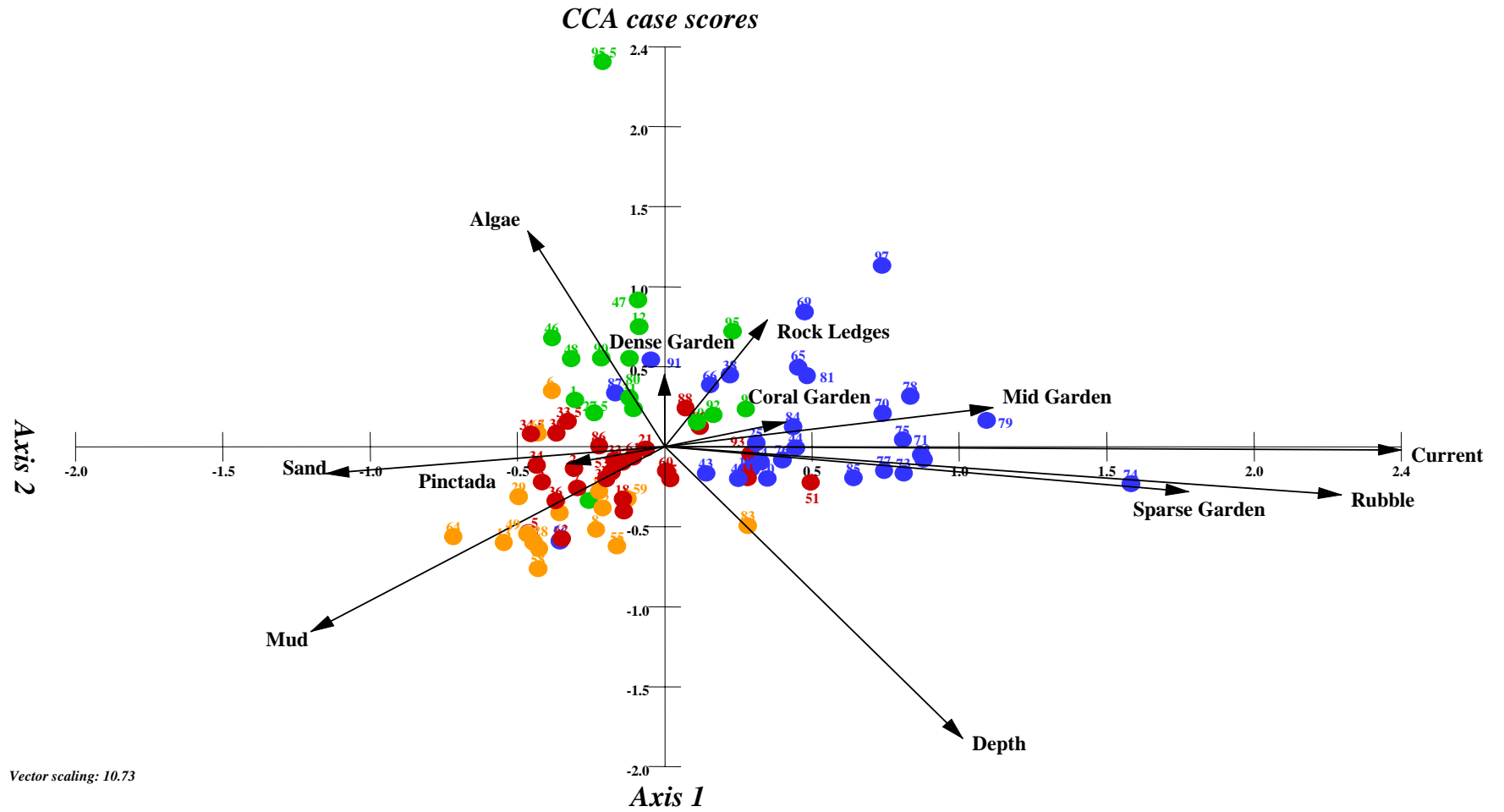


Figure 5–17. The results of the multivariate ordination CCA where the position of the stations (circles) are plotted along the first two axis of the ordination in relation to the major environmental variables (arrows).

5.4 Discussion

Previous studies of the seabed in Great Barrier Reef Marine Park (GBRMP) have dealt mainly with the central section of the Great Barrier Reef and most of these studies have been on a limited scale. The most relevant comparable reports are those of Birtles and Arnold (1983, 1988), Cannon *et al.* (1987), Jones and Derbyshire (1987), Watson and Goeden (1989), Watson *et al.* (1990) and Coles *et al.* (1996) who studied various sections of the Great Barrier Reef. These studies are briefly reviewed here as background context, followed by comparative discussion with our results.

5.4.1 Prior studies of inter-reefal fauna in the Great Barrier Reef

Birtles and Arnold (1983 & 1988) used a 1.6 m epibenthic dredge to sample inter-reefal epibenthos during a series of integrated studies at up to ~90 sites, on a roughly 8 n.mile grid off Townsville, at various intensities between 1977 and 1983. Most sites were in the GBR lagoon area, between the coast and the reef-matrix, although a few sites were sampled on the outer half of the shelf, amongst the reefs. Multivariate assemblage analyses clearly showed cross-shelf zonation in fauna. There was a shallower (<20 m) inshore zone, to about 30 n.miles offshore characterised by resuspended terrigenous muddy deposits, with low species richness of carnivorous and deposit feeding echinoderms, molluscs, crustaceans, fish, bryozoans and algae, and low species evenness. Further offshore, from ~30 n.miles to the mid-shelf reef-matrix at ~80 n.miles, the main lagoon zone was characterised by deeper water (20-50 m) and less muddy sediments dominated by coarse sand and rubble, primarily of biological origin, with higher species richness of all faunal groups. In part, this increased diversity was due to increased habitat heterogeneity in terms of patches of harder substratum that allowed a wide variety of suspension feeders, such as sponges, ascidians, crinoids, holothurians, and bryozoans, to gain a foothold in addition to the deposit feeders in the sediments between the patches. On the outer half of the shelf (> ~80 n.miles), in the offshore inter-reef zone the fauna changed again, with less fine sediment, more harder patches, and greater depth. A time series of six years was available for echinoderms at selected sites. For these fauna, patterns of distribution and abundance remained essentially stable over the period. Greatest variability was apparent in the nearshore sites, due to physical instability of the sediments caused by wind generated waves.

Cannon, Goeden and Campbell (1987) conducted classification and ordination analyses of trawl bycatch (fishes and macro & mega benthos) from two of a series of seven exploratory trawl surveys from three main areas of the GBR. Samples were collected primarily with 2 m try-shot nets at about 230 sites between 1979 and 1982. Although providing significant latitudinal coverage, most sampling was unstructured, with the objective of identifying new commercial prawning grounds. However, one survey in particular (series V), provided replicated cross-shelf samples off Cairns. Trawl series I covered $\sim 6^\circ$ of latitude, from $\sim 12^\circ\text{S}$ to 18°S , but cross-shelf effects were not controlled for and data could only be analysed in binary form (presence or absence). Analysis of series I at several taxonomic levels generally separated the sites into three main groups, but the groupings did not correspond to any clear geographic pattern, except that sites from Princess Charlotte Bay usually were separated. There appeared to be no major latitudinal differences, the patterns were interpreted as weak cline, or continuum — however, the authors treated this result with caution given the uncontrolled nature of the sampling. Trawl series V off Cairns was more rigorously conducted, with three replicate cross-shelf transects ~ 20 n.miles apart with five representative and quantitatively sampled sites along each transect, from the inshore, lagoon and offshore inter-reef zones. The samples and the classification and ordination were dominated, not surprisingly given the sampling method, by fishes. Nevertheless, the results were qualitatively similar to those of Birtles and Arnold (1983 & 1988): the sites split into three main groups, inshore and offshore inter-reef with a transition zone in the lagoon between. The inshore zone was much less diverse than the offshore inter-reef zone. These patterns in the distribution of benthos were correlated with and may be influenced by physical factors changing from inshore to offshore, ie. increasing depth and sediment type from fine terrigenous to coarser carbonate sediments Cannon *et al.* (1987).

Watson and Goeden (1989) used commercial prawn trawl gear to sample fauna at monthly intervals in 20 sites distributed from the inshore, across the lagoon, into the offshore inter-reef matrix, over a $\sim 1^\circ \times 1^\circ$ region off Townsville in 1985. Classification analysis showed very consistent group membership of sites, despite seasonal variation — the faunal composition of the samples consistently grouped the sites into three distinct assemblages of inshore, lagoonal and offshore inter-reef zones similar to that of Birtles and Arnold (1983 & 1988). However, species richness appeared to be greater inshore than offshore, with 82% of the 200 species analysed present in the coastal zone, 80% in the inshore zone and 70% in the offshore. As with the other studies, these patterns were correlated with the physical factors depth, sediment

grain size and carbonate content. Watson and Goeden (1989) did not sample the offshore (outer lagoon) region.

Coles, Lee-Long and co-workers (1996) conducted a video survey over $\sim 4^\circ$ of latitude north of Cairns, primarily for broad scale mapping of seagrass, but sediment, algae and epibenthic megafauna were also recorded. The sampling strategy for the survey was to divide the region into 15-minute-of-latitudinal blocks and select a cross-shelf transect at random from each block; each transect was divided into 1 n.mile segments and a randomly placed video transect ~ 100 - 300 m long was conducted in each segment. The patterns observed concurred with patterns documented by others: most megafauna were observed offshore on harder substratum. Algal beds (*Caulerpa* & *Halimeda*) and solitary corals were also more abundant offshore.

In a 5 year study of the effects of trawling on seabed assemblages in the inter-reef areas in the Far Northern Section of the Great Barrier Reef (Green Zone), Poiner *et al.* (1998) found that most of the seabed is relatively bare soft substratum with patches of epibenthos. These patches comprised a diversity of sessile megabenthos invertebrates including sponges, hard and soft corals and gorgonians, with a rich associated fauna of echinoderms, crustaceans and fish. The benthic assemblage composition showed a strong cross-shelf (east-west) change. In the soft substratum, there was a decline in the number of species caught per dredge, from 49 species per 15 min tow in the muddier inshore lagoon to 30 in the sandier outer lagoon, but the total number of species offshore was higher as more species accumulated with additional samples offshore than inshore. Within this area there was also a corresponding strong gradient in the physical environment (sediment and topography) as well as the biological “communities”. Poiner *et al.* (1998) found that the Green Zone could be divided into five cross-shelf strata on a physical basis. This differed from the central GBR, which is usually regarded as having three strata.

The above studies showed that the least diverse areas had muddier sediments, where the dominant animals were deposit feeders. Sandier and harder areas tended to be more diverse, at least partly because of the greater range of physical habitats. The fauna of harder areas were also more abundant, and the dominant animals were filter feeders, scavengers or carnivores. The megabenthic epifauna, which form living structural habitat attached to the seabed, generally were restricted to rubbly or rocky patches, or areas where the bedrock or coarse substrata were exposed by fast currents. Such patterns are also typical of other regions (eg.

Torres Strait: Pitcher *et al.* 1992; Gulf of Carpentaria: Long and Poiner, 1994, Long *et al.* 1995).

These various studies have shown that there is a distinct cross-shelf zonation of benthic fauna in the GBR. This zonation is a consequence of the physical habitat requirements of the fauna and is a reflection of the change from terrigenous muddy sediments of the inshore lagoon through to coarse calcareous sediments of the offshore inter-reef. Typically, multivariate analyses separated the fauna into three main groups: inshore lagoon, offshore inter-reef, and a mid-shelf lagoon transition area. This zonation was apparent in all the GBR studies, although the composition of the species groups among the different studies has not been examined for consistency. Only one of the studies (Cannon *et al.* 1987) compared samples from a range of latitudes (~12°S to ~18°S) and showed an overlapping continuum rather than discrete groupings of (prawn trawl bycatch) faunal variation. However, the authors treated this result with caution due to their unstructured sampling strategy.

5.4.2 This study of the benthic fauna in the central Great Barrier Reef

Our study was largely within the offshore inter-reef-matrix areas offshore from Townsville and was thus a more detailed latitudinal study of this region. We also included habitat attributes from video and current speed data, thus extending the knowledge of these areas. The sediment collected from the four areas within the region consisted of a variety of mixes and ranged from a muddy sand at the lagoonal stations (Robbery Shoal) to sand and gravelly sand in the Flinders Reef region with sections of rock shelf interspersed among the sites as remnants of old reefs. The benthic assemblages reflected this mix of substrata with a mosaic of different species assemblages. Despite the design and focused effort of sampling, we were unable to provide a full assessment of the local species richness. A steady increase of new species was found as more samples were taken. Consequentially, substantially more sampling effort is required to approach the local species richness of the inter-reefal benthic assemblages. The limited variability among sites for species richness and abundance suggest that the surveyed sites share the same species pool, and the addition of new species are a product of sampling more complex habitats. Like the results of prior studies we found that algae, mobile invertebrates, and deposit feeders dominated the muddier and sandy areas.

Again, like of prior studies, the harder and rocky substratum areas contained most of the suspension and filter feeders and coral and gorgonian assemblages (gardens). These sites

tended to be located on deep extinct coral reefs that formed platforms on which extant coral reefs were founded. Other than these extinct reefs, the occurrence and abundance of gardens correlated positively with regions of higher current velocity and negatively with muddy and sandy substrata. In the highest current-speed channels, between Stanley and Old Reefs, the gorgonians and other fauna appeared stunted. The megabenthos in these gardens tended to be sparse and had a dissimilar composition to that typically observed in the Poiner *et al.* (1998) far northern section effects of trawling study. A few potential sites suitable for the study of megabenthos dynamics were identified in each of the three areas, particularly near the Kelso-Slashers Reefs, however, most were highly exposed which became a problem for subsequent access. On the return to Townsville, the video camera was used to investigate some of the channels among the Palm Islands Group and a number of more suitable, less exposed sites were found (see Chapter 6) and these were chosen as study sites for measuring the dynamics of the megabenthos.

This part of the study documented species composition and abundances and how they relate to some physical parameters, all of which are important to implement environmentally based management of the marine biodiversity of the region. Australia's Ocean Policy and Commonwealth environmental legislation (Environmental Protection and Biodiversity Conservation Act 1999 and Wildlife Protection (Regulation of Exports and Imports) Acts 1982) require ecosystem level approaches to managing our marine living resources. There is also a commitment by the Commonwealth Government to creating a National Representative System of Marine Protected Areas (NRSMPA) throughout Australia's marine environment. These Marine Protected Areas (MPA's) are intended to protect representative portions of all major ecological regions and the plant and animal assemblages within them. Fundamental to these management objectives is knowledge of the biodiversity, composition of the assemblage and distribution of the species. The video, sediment-grab and naturalists dredge data that was gathered for this part of the project can form part of a broader study to map the species distribution and "community" composition of the seabed in the Great Barrier Reef region for these purposes.

5.5 Appendix

Appendix 5.5–1. List of species (taxa) in decreasing order of occurrence collected by naturalist dredge from four areas off Townsville.

#	Taxa Name	Sites				Total Occurrence
		Broadhurst	Flinders	Kelso	Lagoon	
1	Hydroid 9	19	22	15	3	59
2	Hydroid 8	20	18	17	1	56
3	Bryozoan 23	18	20	13	2	53
4	Bryozoan 1	19	21	10		50
5	<i>Halimeda opuntia</i>	15	18	10		43
6	<i>Retiflustra cornea</i>	15	13	10	1	39
7	<i>Sphaenopus marsupialis</i>	13	14	9	2	38
8	<i>Hypnea cervicornis</i>	11	14	12		37
9	<i>Tudivasum armigerum</i>	12	14	10	1	37
10	<i>Halimeda tuna</i>	12	15	7	1	35
11	<i>Scrupocellaria</i> sp.	13	14	7	1	35
12	Brittle star 5	12	13	7	1	33
13	Sponge: Porifera	14	11	7	1	33
14	Didemnid 2	13	9	10		32
15	<i>Polycarpa ovata</i>	14	7	10	1	32
16	<i>Udotea</i> sp. 3	13	11	6	2	32
17	Bryozoan 25	10	14	7		31
18	Bryozoan 3	12	16	3		31
19	Bryozoan 26	15	8	6	1	30
20	<i>Chicoreus banksii</i>	10	15	5		30
21	<i>Udotea glutinata</i>	13	13	3	1	30
22	Crinoid 2	13	10	5		28
23	<i>Laganum</i> sp. 4	9	8	11		28
24	Bryozoa	8	13	6		27
25	Bryozoan 2	13	7	6	1	27
26	<i>Stellaster equestris</i>	8	6	11	2	27
27	Bryozoan 18	7	13	5	1	26
28	Algae E	6	14	5		25
29	Bryozoan 8	13	8	2	2	25
30	<i>Dilophus intermedius</i>	3	13	9		25
31	<i>Lenormandiopsis lorentzii</i>	5	14	6		25
32	<i>Microcosmus exasperatus</i>	7	9	7	2	25
33	<i>Strombus dilitatus</i>	8	8	8		24
34	Alcyonarian 1	6	11	6		23
35	<i>Astropecten</i> sp. 3	7	7	8	1	23
36	<i>Fusinus colus</i>	10	8	5		23
37	Hydroid 5	6	12	5		23
38	Gorgonian 4	6	13	2		21
39	<i>Metrodira subulata</i>	8	6	5	1	20
40	Gorgonian 15	2	15	2		19
41	Sponge 8	7	8	4		19
42	Algae A	6	8	4		18
43	Crinoid 17	10	2	5	1	18
44	<i>Metapenaeopsis</i> sp.	8	3	5	2	18
45	<i>Murex queenslandica</i>	5	3	9		17
46	<i>Padina sanctaerucis</i>	5	9	3		17
47	<i>Polycarpa chinensis</i>	8	6	2	1	17

#	Taxa Name	Broadhurst	Flinders	Kelso	Lagoon	Occurrence
48	<i>Portunus argentatus</i>	5	4	7	1	17
49	<i>Xenophora solariooides</i>	7		9	1	17
50	Ascidacea	5	6	4	1	16
51	<i>Polycarpa fungiformis</i>	4	6	4	2	16
52	Alcyonarian 11	4	6	5		15
53	<i>Halophila spinulosa</i>	4	6	4	1	15
54	Alcyonarian 15	4	9	1		14
55	Crinoid 1	7	7			14
56	Algae C	2	7	3	1	13
57	<i>Dardanus imbricata</i>	7	2	4		13
58	Sea urchin 11	5	6	2		13
59	Sea urchin 3	7	4	2		13
60	<i>Spatangoida</i> sp.	6	2	3	2	13
61	Ascidacea J	6	2	3	1	12
62	Brittle star 11	5	5	2		12
63	<i>Chicoreus territus</i>	4	4	4		12
64	<i>Condominium</i> sp.	7	4		1	12
65	Crinoid 11	7	4		1	12
66	Didemnid 18	4	7	1		12
67	Hydroid 4	1	11			12
68	<i>Ircinia</i> sp.	7	3	1	1	12
69	Bryozoan 22	5	5	1		11
70	Bryozoan 33	4	6	1		11
71	<i>Caulerpa prolifera</i>	5	2	2	2	11
72	Didemnid 16	5	3	2	1	11
73	<i>Glycymeris fringilla</i>	4	6	1		11
74	Gorgonacea D	1	7	3		11
75	<i>Portunus granulatus</i>	5	3	3		11
76	Sea urchin 14	7	3	1		11
77	Solitary coral 2	2	6	3		11
78	<i>Spondylus wrightianus</i>	7	2	2		11
79	Brittle star 41	6	2	2		10
80	Bryozoa A	4	4	2		10
81	Bryozoan 36	5	3	2		10
82	<i>Cymbiola pulchra</i>	3	6	1		10
83	Holothurian 3	4	5	1		10
84	Hydroid 7	2	8			10
85	Polychaete tubes empty	3	4	3		10
86	Sea urchin 6	5	3	2		10
87	Sponge 10	4	4	2		10
88	Alcyonarian 10	3	4	2		9
89	Alcyonarian 4	2	6	1		9
90	<i>Aplidium</i> sp. 1	2	4	2	1	9
91	<i>Aplidium</i> sp. 4	5	1	3		9
92	Bryozoa K	2	7			9
93	<i>Callyspongia</i> sp. 553	5		4		9
94	<i>Caulerpa racemosa</i>	3	1	5		9
95	Gorgonacea B	4	2	3		9
96	Gorgonian 17	1	6	2		9
97	<i>Halophila ovalis</i>	2	3	3	1	9
98	<i>Iconaster longimanus</i>	2	6	1		9
99	<i>Notocorbula tunicata</i>	2	7			9
100	<i>Prionocidaris</i> sp. 1	4	3	2		9

#	Taxa Name	Broadhurst	Flinders	Kelso	Lagoon	Occurrence
101	<i>Spiropagurus</i> sp. 4	4	3	2		9
102	Alcyonarian 22	2	4	2		8
103	<i>Amusium pleuronectes</i>	3	3	2		8
104	<i>Antigonia lamellaris</i>	2	6			8
105	Asteroid 30	4	3	1		8
106	Crinoid 35	6	1	1		8
107	Crinoid 4	3	4		1	8
108	<i>Dictyopteris</i> sp	4	4			8
109	<i>Fungia</i> sp. 5	6	1	1		8
110	<i>Fusinus salisburyi</i>	3	2	3		8
111	Gorgonian 7	3	5			8
112	<i>Lima lima vulgaris</i>	4	4			8
113	<i>Myra mammillaris</i>	3	2	2	1	8
114	<i>Pentaceraster</i> sp.	5	2	1		8
115	Sponge 191	4	1	2	1	8
116	Sponge 227	3	3	1	1	8
117	Ascidacea O	1	3	3		7
118	Basket star 1	1	5	1		7
119	Brittle star 28	4		2	1	7
120	<i>Cardita preissii</i>	2	3	1	1	7
121	Crinoid 15	3	2	1	1	7
122	Crinoid 3	2	4	1		7
123	<i>Dosinia juvenilis</i>	2	5			7
124	<i>Filograna</i> sp.	3	3	1		7
125	<i>Fungia</i> sp. 1	1	5	1		7
126	Gorgonian 2	2	4	1		7
127	Hard coral	2	2	3		7
128	<i>Laganum</i> sp. 3	2	2	2	1	7
129	<i>Melaxinia vitrea</i>	2	2	1	2	7
130	<i>Plicatula muricata</i>	2	4	1		7
131	<i>Rhopalaea crassa</i>	1	1	4	1	7
132	<i>Xenophora cera</i>	4	2	1		7
133	Zoanthinaria	3	2	1	1	7
134	Alcyonarian 19	2	3	1		6
135	Alcyonarian 2	2	3	1		6
136	<i>Anadara crebricostata</i>	3		2	1	6
137	Ascidacea D	3	1	2		6
138	<i>Bolma aureola</i>	3	3			6
139	Caridea: Carid	3	1	2		6
140	<i>Circe scripta</i>	3	3			6
141	Crinoid 24	4	1	1		6
142	<i>Ctenocardia virgo</i>	5		1		6
143	Didemnid 13	4		2		6
144	<i>Flabellum</i> sp.	2	1	2	1	6
145	<i>Fungia</i> sp. 3		4	2		6
146	<i>Monia timida</i>	2	2	2		6
147	<i>Pseudovertagus phylarchus</i>	1	5			6
148	Sponge 14	2	3	1		6
149	<i>Thalamita</i> sp.	2	3	1		6
150	<i>Arca navicularis</i>	1	3	1		5
151	Bryozoan 20	3	2			5
152	Crinoid 12	4		1		5
153	Crinoid 19	1	4			5

#	Taxa Name	Broadhurst	Flinders	Kelso	Lagoon	Occurrence
154	<i>Dentalium grahami</i>	3	1	1		5
155	Gorgonacea I	1	3	1		5
156	<i>Granicorum indutum</i>	2	3			5
157	<i>Haustellum tweedianum</i>	3	2			5
158	<i>Laevicardium biradiatum</i>	2	2	1		5
159	<i>Leucosia</i> sp. 2	1		3	1	5
160	<i>Mimachlamys gloriosa</i>	3		1	1	5
161	<i>Oreophorus reticulatus</i>	4	1			5
162	<i>Phalangipes longipes</i>	1	2	2		5
163	Polycheata	3	1		1	5
164	Sponge 166		3	2		5
165	Sponge 49	2	2	1		5
166	<i>Thaconophrys longispinus</i>	2	2	1		5
167	Alcyonarian 3	2	1	1		4
168	Algae I	1	2	1		4
169	Algae K		2	2		4
170	<i>Annachlamys kuhnoltzi</i>	2		2		4
171	Asciacea C	1	1	2		4
172	Asciacea E	2	2			4
173	Brittle star 27	4				4
174	Brittle star 38	2	1	1		4
175	Bryozoa H	2	2			4
176	Bryozoan 11	3		1		4
177	<i>Bursa rana</i>	1		2	1	4
178	<i>Clathrya vulpina</i>	1	1	2		4
179	Crinoid 27	1	2	1		4
180	<i>Cypraea subviridis</i>	1	2	1		4
181	<i>Engyprosopon grandisquama</i>	2	1	1		4
182	<i>Inimicus didactylus</i>		2	2		4
183	<i>Latirus paetelianus</i>	1	3			4
184	<i>Malleus malleus</i>		3	1		4
185	<i>Monilea morti</i>	3	1			4
186	<i>Murex rectirostris</i>	3		1		4
187	Paguroidea: Paguridae	3	1			4
188	<i>Parthenope longimanus</i>	3		1		4
189	<i>Phos roseatus</i>	1		3		4
190	<i>Portunus tenuipes</i>	1	1	2		4
191	<i>Scyllarus demani</i>	2	1	1		4
192	Sea pen 7	1		3		4
193	Sepioidae	1	2	1		4
194	Sponge 208	1	2	1		4
195	Sponge 23	3	1			4
196	Sponge 55	1	2		1	4
197	<i>Stichopus variegatus</i>	1	1	1	1	4
198	<i>Udotea</i> sp. 2	3	1			4
199	<i>Xenophora indica</i>	2	1	1		4
200	<i>Acrosterigma transcendens</i>	1		2		3
201	Alcyonacea	1	1	1		3
202	Alcyonarian 17		3			3
203	Alcyonarian 18	1	2			3
204	Algae M		3			3
205	<i>Anadara passa</i>	1		2		3
206	Asciacea Q	2	1			3

#	Taxa Name	Broadhurst	Flinders	Kelso	Lagoon	Occurrence
207	Brittle star 45	2		1		3
208	Brown algae 10		3			3
209	Bryozoa C	1	1	1		3
210	Bryozoa G		3			3
211	Bryozoa M		3			3
212	<i>Calappa gallus</i>	2		1		3
213	<i>Caulerpa cupressoides</i>		3			3
214	<i>Chama lazarus</i>	2		1		3
215	<i>Codium galeatum</i>	1		2		3
216	Crinoid 13	1	2			3
217	Crinoid 31	2		1		3
218	Crinoid 34	1	2			3
219	Crinoid 37	2		1		3
220	<i>Cymatium caudatum</i>	3				3
221	<i>Cymatium pfeifferianum</i>			3		3
222	Didemnid 26		3			3
223	<i>Distorsio reticularis</i>	1	1	1		3
224	<i>Dolicholatirus angustus</i>	2	1			3
225	<i>Fragum retusum</i>	3				3
226	<i>Globivenus capricornea</i>	2	1			3
227	Gorgonacea H	1	2			3
228	Gorgonia 24	3				3
229	Gorgonian 11	1	2			3
230	<i>Hyastenus</i> sp. 1	2		1		3
231	<i>Hyatella intestinalis</i>	2		1		3
232	<i>Limopsis multistriatus</i>		1	2		3
233	<i>Luidia maculata</i>	1	2			3
234	<i>Lupocyclus tugelae</i>	1	1	1		3
235	<i>Palicoides longimanus</i>	1		2		3
236	<i>Parthenope harpax</i>	1		2		3
237	Pilumnidae	1	2			3
238	<i>Polycarpa papillata</i>	1		1	1	3
239	<i>Richardsonichthys leucogaster</i>	2		1		3
240	<i>Sarcophyta</i> sp		3			3
241	<i>Sorsogona tuberculata</i>	1	2			3
242	Sponge 123	3				3
243	Sponge 167	2	1			3
244	Sponge 179	3				3
245	Sponge: Porifera D	1		2		3
246	Stelleroidea: Asteroidea	2	1			3
247	<i>Talabrica</i> sp	3				3
248	<i>Turris crispa</i>	1	1		1	3
249	<i>Vexillum takakuwai</i>		1	2		3
250	<i>Actaea</i> sp.	1	1			2
251	Alpheidae		1	1		2
252	<i>Amoria guttata</i>			2		2
253	<i>Anadara trapezia</i>		1	1		2
254	<i>Anadara vellicata</i>			1	1	2
255	Antennariidae			2		2
256	<i>Arcania</i> sp.			2		2
257	Ascidacea L			2		2
258	Asteroid 26	1	1			2
259	Asteroid 28	1	1			2

#	Taxa Name	Broadhurst	Flinders	Kelso	Lagoon	Occurrence
260	Asteroid 29	1		1		2
261	Asteroidea	2				2
262	<i>Bathypilumnus pugilator</i>	1		1		2
263	Brittle star 21	1	1			2
264	Brittle star 31	1			1	2
265	Brittle star 40	1		1		2
266	Bryozoa B	2				2
267	Bryozoa D		2			2
268	Bryozoa F		2			2
269	Bryozoan 10	1	1			2
270	<i>Calliostoma similarae</i>	1	1			2
271	<i>Chama fibula</i>	1		1		2
272	<i>Charybdis jaubertensis</i>		2			2
273	<i>Circe personata</i>	1		1		2
274	<i>Complichlamys wardiana</i>	1		1		2
275	<i>Conus neilsenae</i>	1	1			2
276	Crinoid 10	2				2
277	Crinoid 16	1	1			2
278	Crinoid 21		2			2
279	Crinoid 5	2				2
280	Crinoidea B	1	1			2
281	Crinoidea D		2			2
282	<i>Cymatium cynocephalum</i>	1	1			2
283	<i>Cymatium exaratum</i>	1	1			2
284	Didemnid 14	1	1			2
285	Didemnid 17	1	1			2
286	Didemnid 21	2				2
287	<i>Didemnum molle</i>	1	1			2
288	<i>Euretaster insignis</i>			2		2
289	<i>Fungia</i> sp. 4		1	1		2
290	Galatheid sp. 4			1	1	2
291	<i>Globovenus embrithes</i>	1	1			2
292	<i>Glycymeris queenslandica</i>	1		1		2
293	Gorgonacea		2			2
294	Gorgonacea E		1	1		2
295	Gorgonacea J		2			2
296	Gorgonacea K		2			2
297	Gorgonacea L		1	1		2
298	Gorgonian 10		1	1		2
299	Gorgonian 13		2			2
300	<i>Hippospongia elastica</i>			1	1	2
301	Holothurian 39	1	1			2
302	Holothuriidae E	2				2
303	<i>Hypodistoma deerratum</i>	1	1			2
304	<i>Laganum</i> sp. 2	2				2
305	<i>Leptoclinide</i> sp.	1		1		2
306	Leucosidae		1	1		2
307	<i>Lioconcha</i> sp	1	1			2
308	<i>Malleus albus</i>	2				2
309	<i>Myra biconica</i>	1		1		2
310	<i>Myrodes eudactylus</i>			2		2
311	<i>Naxoides tenuirostris</i>		1	1		2
312	<i>Nemocardium bechei</i>			2		2

#	Taxa Name	Broadhurst	Flinders	Kelso	Lagoon	Occurrence
313	<i>Odontodactylus</i> sp.	1	1			2
314	<i>Parthenope longispinus</i>		2			2
315	<i>Pentacta anceps</i>		2			2
316	<i>Phos senticosus</i>	1	1			2
317	<i>Placamen tiara</i>		2			2
318	<i>Pteria breviaalata</i>		2			2
319	Scleractinia N		2			2
320	Sea pen 1		2			2
321	Sepia 91A	1	1			2
322	<i>Sicyonia cristata</i>	2				2
323	<i>Siphamia argyrogaster</i>	1	1			2
324	Sponge 197	2				2
325	Sponge 204	2				2
326	Sponge 42	1		1		2
327	Stelleroidea: Asteroidea B	1		1		2
328	<i>Strombus erythrinus</i>	1	1			2
329	<i>Tucetona</i> sp	1	1			2
330	<i>Tutufa oyamai</i>		1	1		2
331	<i>Acrosterigma</i> sp	1				1
332	<i>Aipysurus duboisii</i>			1		1
333	Alcyonacea B		1			1
334	Alcyonarian 7		1			1
335	<i>Alertigorgia orientalis</i>	1				1
336	Algae coralline red	1				1
337	Algae G	1				1
338	Algae N		1			1
339	Alpheid sp. 2		1			1
340	<i>Amoria maculata</i>		1			1
341	<i>Amygdalum beddomei</i>			1		1
342	<i>Anadara antiquata</i>		1			1
343	<i>Anadara gubernaculum</i>	1				1
344	<i>Annachlamys flabellata</i>		1			1
345	<i>Antennarius pictus</i>			1		1
346	<i>Antipathes</i> sp	1				1
347	<i>Aplysia</i> sp	1				1
348	<i>Arca ventricosa</i>		1			1
349	<i>Arnoglossus waitei</i>		1			1
350	Ascidacea 1901	1				1
351	Ascidacea A	1				1
352	Ascidacea B			1		1
353	Ascidacea F		1			1
354	Ascidacea G	1				1
355	Ascidacea I	1				1
356	Ascidacea K			1		1
357	Ascidacea R		1			1
358	Ascidacea S	1				1
359	Asteroid 14	1				1
360	Asteroid 18	1				1
361	Asteroid 24	1				1
362	Asteroid 8	1				1
363	Asteroid sp. 25	1				1
364	Asteroidea: <i>Fromia monilis</i>	1				1
365	<i>Atysp</i> sp	1				1

#	Taxa Name	Broadhurst	Flinders	Kelso	Lagoon	Occurrence
366	Balistidae	1				1
367	<i>Barbatia bistrigata</i>	1				1
368	<i>Barbatia foliata</i>			1		1
369	<i>Barbatia iota</i>		1			1
370	<i>Biemna</i> sp.	1				1
371	Bivalvia	1				1
372	<i>Bohadschia marmorata</i>		1			1
373	Brittle star 42		1			1
374	Brittle star 43				1	1
375	Brittle star 44	1				1
376	Bryozoa E				1	1
377	Bryozoa I		1			1
378	Bryozoa J		1			1
379	Bryozoa L		1			1
380	Bryozoa N		1			1
381	Bryozoa P			1		1
382	Bryozoan 107		1			1
383	Bryozoan 34		1			1
384	Bryozoan 35	1				1
385	<i>Callionymus japonicus</i>	1				1
386	<i>Canthigaster rivulata</i>			1		1
387	<i>Capulus violaceus</i>		1			1
388	<i>Carinosquilla multicaudata</i>		1			1
389	<i>Caulerpa sertularioides</i>			1		1
390	<i>Ceratoplax</i> sp. 1	1				1
391	<i>Cerithium</i> sp	1				1
392	<i>Chaetoderma penicilligera</i>			1		1
393	<i>Chaetodiadema granulatum</i>		1			1
394	<i>Chicireus territus</i>		1			1
395	<i>Chicoreus strigatus</i>	1				1
396	<i>Chlamys senatoria</i>	1				1
397	<i>Clanculus unedo</i>		1			1
398	<i>Colpospira congelata</i>		1			1
399	Conidae		1			1
400	<i>Conus aculeiformis</i>	1				1
401	<i>Conus ammiralis</i>		1			1
402	<i>Conus ferrugineus</i>		1			1
403	<i>Conus generalis</i>	1				1
404	<i>Conus lynceus</i>		1			1
405	<i>Cribochalina olemda</i>	1				1
406	Crinoid 22		1			1
407	Crinoid 26		1			1
408	Crinoid 30	1				1
409	Crinoid 36	1				1
410	Crinoidea A				1	1
411	Crinoidea C		1			1
412	Crinoidea E		1			1
413	<i>Cryptopecten bullatus</i>	1				1
414	<i>Cucullaea labiata</i>		1			1
415	<i>Cuspidaria elegans</i>	1				1
416	<i>Cyclichthys orbicularis</i>		1			1
417	<i>Cymatium comptum</i>	1				1
418	<i>Cypraea</i> sp	1				1

#	Taxa Name	Broadhurst	Flinders	Kelso	Lagoon	Occurrence
419	<i>Dardanus asperus</i>			1		1
420	<i>Dardanus pedunculatus</i>			1		1
421	<i>Dardanus</i> sp. 1			1		1
422	<i>Decatopecten strangei</i>				1	1
423	<i>Didemnid</i> 19		1			1
424	<i>Didemnid</i> 20		1			1
425	<i>Didemnid</i> 23		1			1
426	<i>Didemnid</i> 28	1				1
427	<i>Dolicholatirus acus</i>		1			1
428	<i>Dosinia</i> sp			1		1
429	<i>Dysidea</i> sp.	1				1
430	<i>Enantiocladia robinsonii</i>		1			1
431	<i>Erosa erosa</i>		1			1
432	<i>Eurytrochus strangei</i>			1		1
433	<i>Gazameda declivis</i>	1				1
434	<i>Gelloides</i> sp1	1				1
435	<i>Gemmula graeffei</i>	1				1
436	<i>Globivenus toreuma</i>	1				1
437	<i>Glossus moltkiana</i>		1			1
438	<i>Glycymeris</i> sp		1			1
439	Gobiidae		1			1
440	<i>Gonodactylus graphurus</i>		1			1
441	Gorgonacea A	1				1
442	Gorgonacea C	1				1
443	Gorgonacea F		1			1
444	Gorgonia 26		1			1
445	Gorgonian 3	1				1
446	<i>Grammatobothus polyophthalmus</i>	1				1
447	<i>Grandeliacus moretonsenae</i>	1				1
448	<i>Gymnothorax</i> sp.		1			1
449	<i>Gyrineum bituberculare</i>	1				1
450	<i>Halimeda monile</i>			1		1
451	Hard coral 4		1			1
452	<i>Hippocampus kuda</i>	1				1
453	<i>Holothuria edulus</i>		1			1
454	Holothurian 106	1				1
455	Holothurian 50				1	1
456	Holothurian 52	1				1
457	Holothurian 54		1			1
458	Holothuriidae		1			1
459	Holothuriidae A	1				1
460	Holothuriidae B				1	1
461	Holothuriidae C	1				1
462	Holothuriidae F	1				1
463	Holothuriidae G	1				1
464	<i>Hyastenus aries</i>	1				1
465	Hydroid 24	1				1
466	Hydroid 25	1				1
467	Hydroid: Hydrozoa		1			1
468	<i>Hypocolpus punctatus</i>	1				1
469	<i>Ianthella flabelliformis</i>		1			1
470	<i>Jania</i> sp			1		1
471	<i>Junceella fragilis</i>	1				1

#	Taxa Name	Broadhurst	Flinders	Kelso	Lagoon	Occurrence
472	<i>Laevicardium attenuatum</i>		1			1
473	<i>Leucosia anatum</i>	1				1
474	<i>Limaria fragilis</i>			1		1
475	<i>Limopsis woodwardi</i>			1		1
476	<i>Liochoncha</i> sp.	1				1
477	<i>Lioconcha ornata</i>	1				1
478	<i>Lioconcha polita</i>	1				1
479	<i>Lobophyllia</i> sp.			1		1
480	<i>Lobophyta</i> sp.		1			1
481	<i>Lophiotoma acuta</i>	1				1
482	<i>Lupocyclus rotundatus</i>	1				1
483	<i>Lutraria australis</i>	1				1
484	<i>Mactra artensis</i>		1			1
485	<i>Malleus anatinus</i>			1		1
486	<i>Modiolus auriculatus</i>	1				1
487	<i>Modiolus micropterus</i>		1			1
488	<i>Modiolus proclivis</i>			1		1
489	<i>Murex kerslakae</i>	1				1
490	<i>Musculus cummingianus</i>	1				1
491	<i>Myochama strangei</i>		1			1
492	<i>Nassarius conoidalis</i>				1	1
493	<i>Nassarius splendidulus</i>	1				1
494	<i>Neomerinthe megalepis</i>			1		1
495	<i>Nidalia</i>			1		1
496	<i>Niphates</i> sp.			1		1
497	Nudibranchia A	1				1
498	Nudibranchia B	1				1
499	Nudibranchia C		1			1
500	Nudibranchia D			1		1
501	<i>Onigocia spinosa</i>			1		1
502	Ophichthidae		1			1
503	Ophiuroidea			1		1
504	Ophiuroidea A	1				1
505	Ophiuroidea B		1			1
506	Ophiuroidea C	1				1
507	<i>Pagurid</i> sp4		1			1
508	<i>Paraetis globosus</i>	1				1
509	<i>Parapeneopsis</i> sp.			1		1
510	<i>Penaeus esculentus</i>				1	1
511	<i>Phyllidia</i> sp. 1212	1				1
512	<i>Pilumnus</i> sp. X		1			1
513	<i>Pinctada maxima</i>	1				1
514	<i>Plicatula philippinarum</i>			1		1
515	Pomacentridae	1				1
516	<i>Pomacentrus nagasakiensis</i>		1			1
517	<i>Pontocaris orientalis</i>	1				1
518	<i>Porites</i> 3		1			1
519	<i>Portunus gracilimanus</i>		1			1
520	<i>Portunus rugosus</i>	1				1
521	<i>Portunus</i> sp. 1			1		1
522	<i>Pristotis jerdoni</i>		1			1
523	<i>Pseudochromis quinqueidentatus</i>	1				1
524	<i>Pteria bernhardi</i>		1			1

#	Taxa Name	Broadhurst	Flinders	Kelso	Lagoon	Occurrence
525	<i>Pterynotus patagiatus</i>			1		1
526	<i>Pupa solidula</i>			1		1
527	Pycnogonid			1		1
528	<i>Pyrene</i> sp	1				1
529	<i>Rapana rapiformis</i>	1				1
530	<i>Rogadius asper</i>			1		1
531	<i>Samaris cristatus</i>		1			1
532	<i>Scintilla cuvieri</i>		1			1
533	Scleractinia A	1				1
534	Scleractinia B	1				1
535	Scleractinia C	1				1
536	Scleractinia D	1				1
537	Scleractinia E			1		1
538	Scleractinia F			1		1
539	Scleractinia G		1			1
540	Scleractinia H		1			1
541	Scleractinia K		1			1
542	Scleractinia L		1			1
543	Scleractinia M		1			1
544	Scorpaenidae	1				1
545	<i>Scutus granulatus</i>			1		1
546	<i>Semicassis angasi</i>			1		1
547	<i>Semipallium tigris</i>	1				1
548	Sipuncula	1				1
549	Sipuncula A		1			1
550	Sipuncula B			1		1
551	<i>Solenocaulon</i> sp			1		1
552	<i>Solenocera</i> sp.	1				1
553	<i>Spiropagurus</i> sp. 1			1		1
554	<i>Spondylus sinensis</i>		1			1
555	<i>Spondylus</i> sp	1				1
556	Sponge 121	1				1
557	Sponge 161	1				1
558	Sponge 228	1				1
559	Sponge 235	1				1
560	Sponge 25	1				1
561	Sponge 43			1		1
562	Sponge 53	1				1
563	Sponge 61			1		1
564	Sponge 69			1		1
565	Sponge: Porifera A			1		1
566	Sponge: Porifera C	1				1
567	Sponge: Porifera E	1				1
568	Sponge: Porifera G	1				1
569	Sponge: Porifera H			1		1
570	Sponge: Porifera I			1		1
571	Sponge: Porifera J				1	1
572	Sponge: Porifera N		1			1
573	Sponge: Porifera O		1			1
574	Sponge: Porifera Q	1				1
575	<i>Stavelia subditorta</i>		1			1
576	Stelleroidea: Asteroidea A	1				1
577	Stelleroidea: Asteroidea D		1			1

#	Taxa Name	Broadhurst	Flinders	Kelso	Lagoon	Occurrence
578	Stelleroidea: Asteroidea F		1			1
579	<i>Strombus sinuatus</i>		1			1
580	<i>Strombus vittatus</i>			1		1
581	<i>Stueroites sp</i>			1		1
582	<i>Subergorgia reticulata</i>	1				1
583	<i>Subergorgia suberosa</i>	1				1
584	<i>Sycozoa sp.</i>	1				1
585	Syngnathidae			1		1
586	<i>Synodus sageneus</i>		1			1
587	<i>Terebellum terebellum</i>	1				1
588	<i>Terebra textilis</i>	1				1
589	<i>Teuthoidea</i>				1	1
590	<i>Thalamita intermedia</i>		1			1
591	<i>Thelonota anax</i>		1			1
592	<i>Tonna variegata</i>			1		1
593	<i>Trachinocephalus myops</i>			1		1
594	<i>Trachypenaeus sp.</i>	1				1
595	<i>Trichomya hirsutus</i>		1			1
596	<i>Trizopagurus strigatus</i>			1		1
597	<i>Turris specabilis</i>		1			1
598	<i>Ulna australiensis</i>	1				1
599	<i>Vexillum obeliscus</i>	1				1
600	<i>Volutidae</i>		1			1
601	<i>Volva volva</i>	1				1
602	<i>Xenophora mekranensis</i>			1		1
603	<i>Xenophora peroniana</i>		1			1
604	<i>Zebrias craticula</i>		1			1
605	<i>Zoanthiniaria B</i>			1		1
Occurrence		1179	1179	689	87	3134
Number of species		396	351	276	74	605

6 Dynamics of tagged megabenthos

To determine the dynamics (recruitment, growth, mortality, and reproduction) of structurally dominant large seabed habitat organisms (ie. megabenthos = sponges, gorgonians, and alcyonarians and corals etc) important for demersal fisheries habitat and biodiversity of the seabed environment, in a tropical region.

Contents

6	Dynamics of tagged megabenthos	6-57
6.1	Introduction	6-59
6.2	Methods	6-60
6.2.1	Logistics of the tagging & measurement	6-63
6.2.2	Megabenthos dynamics	6-65
6.2.2.1	Recruitment	6-65
6.2.2.2	Growth	6-65
6.2.2.3	Mortality	6-67
6.2.3	Reproduction	6-67
6.3	Results	6-68
6.3.1	Megabenthos dynamics	6-70
6.3.1.1	Recruitment	6-70
6.3.1.2	Growth	6-73
6.3.1.3	Mortality	6-94
6.3.2	Reproduction	6-97
6.4	Discussion	6-97
6.4.1	Recruitment	6-98
6.4.2	Growth	6-99
6.4.3	Mortality	6-100
6.4.4	Reproduction	6-101
6.5	Appendices	6-102

Tables

Table 6–1.	The number of each species of megabenthos counted in haphazardly-thrown 1 m quadrats at four locations in the Palm Islands during the last field-trip. (A= Alcyonacea, As = Ascidian, C = Scleractinia, G = Gorgonacea, S = Porifera). (* = species tagged for dynamics study).....	6-69
Table 6–2.	Resident density summary of tagged species in haphazardly thrown quadrats at four sites in the Palm Islands.....	6-70
Table 6–3.	The species initially tagged at the four study sites around Curacoa Island, listed alphabetically, and the number of recruits of each species found in the quadrats on subsequent field-trips. (A= Alcyonacea, C = Scleractinia, G = Gorgonacea, S = Porifera). No new recruits were found on the fifth survey (MBD0200). 6-71	
Table 6–4.	Mortality summary of tagged species in the Palm Island study sites	6-95
Table 6–5.	Density of tagged species in the Palm Islands study sites contrasted with density (estimated from inverse nearest neighbour distances NND averaged for each of 32 ROV sites) in megabenthos garden patches in the far northern section of the Great Barrier Reef (GZ). (G = gorgonian, S = sponge, C = coral) 6-98	
Appendix 6.5–1.	Record of the number of species collected from various locations and lodged with the Queensland Museum	6-102
Appendix 6.5–2.	Photographs of specimens of tagged species, collected and lodged with the Queensland Museum (including QM specimen reference number)	6-104

Figures

- Figure 6–1. Map of the study sites around Curacao Island in the Palm Island group showing two sites in the Calliope Channel and two sites on the north side of the island in the Curacao Channel.6-60
- Figure 6–2. Schematic diagram showing the method of mooring a 20 m vessel over the study sites and deployment of the ROV and diver.6-64
- Figure 6–3. System diagram showing integration of components necessary for automated tracking of the ROV and synchronous logging of position, tracking, tag numbers and video data, to facilitate post-analysis and measurement of sessile benthic fauna. DGPS: differential global positioning system, VCR: video recorder, PC: logging computer, SCU: surface control unit for ROV, TXD: tracking system transducers.6-64
- Figure 6–4. Display of computer screen demonstrating software to compare video image sequences and data matching individual tagged animals to check integrity of measurements. The white dashed lines indicate the measurements made by operators. In the case of this gorgonian (*Ctenocella pectinata*), width was the most suitable parameter, as the tips often dropped off.6-66
- Figure 6–5. Average height of animals measured in quadrats at the four study sites.6-70
- Figure 6–6. The number of living tagged individuals of a species followed through time from the beginning of the experiment.6-72
- Figure 6–7. The number of individuals of a species recruited (first cohort) to quadrats since the first field-trip followed through time.6-72
- Figure 6–8. The number of individuals of a species recruited (second cohort) to quadrats since the second field-trip, followed through time.6-73
- Figure 6–9. The number of individuals of a species recruited (third cohort) to quadrats since the third field-trip, followed through time.6-73
- Figure 6–10. (a) Video still of *Ctenocella pectinata* (red dots are lasers 100 mm apart). (b) The sizes of 22 individual *Ctenocella pectinata* followed through time (32 months) from four locations around Curacao Island (1998-2000).6-77
- Figure 6–11. Walford-plots of *Ctenocella pectinata* width data for pre (a) and post (b) cyclone periods.6-78
- Figure 6–12. (a) Video still of *Subergorgia suberosa*. (b) The sizes of 19 individual *Subergorgia suberosa* followed through time (32 months) from four locations around Curacao Island.6-79
- Figure 6–13. Walford-plots of *Subergorgia suberosa* height data for pre (a) and post (b) cyclone periods.6-80
- Figure 6–14. (a) Video still of *Junceella divergens*. (b) The sizes of 18 individual *Junceella divergens* followed through time (32 months) from four locations around Curacao Island.6-81
- Figure 6–15. Walford-plots of *Junceella divergens* height data for pre (a) and post (b) cyclone periods.6-82
- Figure 6–16. (a) Video still of *Semperina brunei*. (b) The sizes of 15 individual *Semperina brunei* followed through time (32 months) from four locations around Curacao Island.6-83
- Figure 6–17. Walford-plots for *Semperina brunei* height data for pre (a) and post (b) cyclone periods.6-84
- Figure 6–18. (a) Video still of *Subergorgia reticulata*. (b) The sizes of 7 individual *Subergorgia reticulata* followed through time (32 months) from four locations around Curacao Island.6-85
- Figure 6–19. Walford-plots of *Subergorgia reticulata* height data for pre (a) and post (b) cyclone periods.6-86
- Figure 6–20. (a) Video still of *Xestospongia testudinaria*. (b) The sizes of 14 individual *Xestospongia testudinaria* followed through time (32 months) from four locations around Curacao Island.6-87
- Figure 6–21. Walford-plots of *Xestospongia testudinaria* height for pre (a) and post (b) cyclone periods.6-88
- Figure 6–22. (a) Video still of *Cymbastella coralliophila*. (b) The sizes of 14 individual *Cymbastella coralliophila* followed through time (32 months) from four locations around Curacao Island.6-89
- Figure 6–23. Walford-plots of *Cymbastella coralliophila* area data for pre (a) and post (b) cyclone data.6-90
- Figure 6–24. (a) Video still of *Ianthella basta*. (b) The sizes of 12 individual *Ianthella basta* followed through time (32 months) from four locations around Curacao Island.6-91
- Figure 6–25. Walford-plots of *Ianthella basta* height data for pre (a) and post (b) cyclone periods.6-92
- Figure 6–26. (a) Video still of *Turbinaria* sp. (b) The sizes of 15 individual *Turbinaria* sp followed through time (32 months) from four locations around Curacao Island.6-93
- Figure 6–27. Walford-plots of *Turbinaria* sp area data for pre (a) and post (b) cyclone periods.6-94
- Figure 6–28. Temporal patterns of mortality of nine megabenthos species over four sampling intervals — two separate cyclones affected the third and fourth intervals.6-95
- Figure 6–28. Image of *Ctenocella pectinata* (tag no. 1591) taken during (a) March 1999 (note the background - many live gorgonians); (b) March 2000 (note the changes in the background - after the first cyclone impact); (c) Oct/Nov 2000 (dead, note the algae in the background - after the second cyclone impact). ..6-96

6.1 Introduction

Assemblages of large sessile epibenthic species, or megabenthos, such as invertebrates or seaweeds, provide structural complexity to the seabed — an important component of habitat for a myriad of other species — and also contribute to the maintenance of biodiversity of marine environments (Van Dolah *et al.* 1987; Hutchings, 1990; Pitcher, 1997). Many different taxa comprise these megabenthos assemblages, and these include for example large brown macrophytes or kelp forests in temperate regions (Dayton, 1984; Dayton and Tegner, 1984), mussel beds in exposed intertidal rocky shores (Payne, 1974; Lewis, 1964), and sponges, gorgonians, alcyonarians and corals in tropical regions. Further, they form the basis of ‘bioprospecting’ to discover natural products of pharmaceutical promise (Hooper *et al.* 1998). However, megabenthos assemblages are vulnerable to damage by sedimentation, dredging and extensive disruption of the seabed such as benthic trawling (Collie, 1998, Pitcher *et al.* 1997; Rogers *et al.* 1998; Sainsbury *et al.* 1997). In a recently completed project in north-eastern Queensland Poiner *et al.* (1998) demonstrated the significance of impacts of prawn trawling on tropical seabed habitats. One possible method of managing or mitigating these impacts for ecological sustainability is spatial closures, both temporal and permanent (Sainsbury *et al.* 1997) — ie. establishing large, replicated refuge areas to preserve representative seabed habitats. Predicting the response of megabenthos to the establishment of these refuge areas, and acquiring an understanding of the ecological interactions between trawled and refuge areas, are both essential steps in the design of effective refuges for fisheries habitat and the stocks and biodiversity they support. To achieve these goals, it is first necessary to gain an understanding of the dynamics and recovery rates of megabenthos species and their habitat including the processes that link trawled areas and refuges.

Estimation of recovery rates requires information on population dynamics, which is virtually unknown for most large sessile epibenthic fauna (Hutchings, 1990). Here we are investigating the fundamental population dynamics parameters like recruitment, growth, mortality, and reproduction of structurally dominant megabenthos habitat fauna. The results presented in this chapter are key requirements for estimating the likely recovery rates and modelling the dynamics of key megabenthos species (Chapter 7) and documenting the relationship between benthic habitat and ecological usage by some commercially important finfish species (Chapter 8).

6.2 Methods

Initially fieldwork began in March 1998 at sites previously identified in the Kelso-Slashers Reefs area (Chapter 5). However, after an initial few days of ideal weather conditions, high winds set-in and more sheltered sites had to be identified urgently. Subsequently, four sites were selected in a more inshore area around the Palm Islands (18.7°S, 146.5°E) (Figure 6–1), in depths ranging from 18 m (shallow) to 30 m (deep). Each site was chosen to contain benthos habitat with species representative of those found on the types of seabed that are trawled for prawns or finfishes. In fact, the megabenthos habitat found in the Palm Islands area was more extensive and richer than the offshore sites — and more similar to those benthic assemblages observed in the far northern GBR and Torres Strait. Table 6–1 shows the list of the main representative megabenthos species that were included in this work.

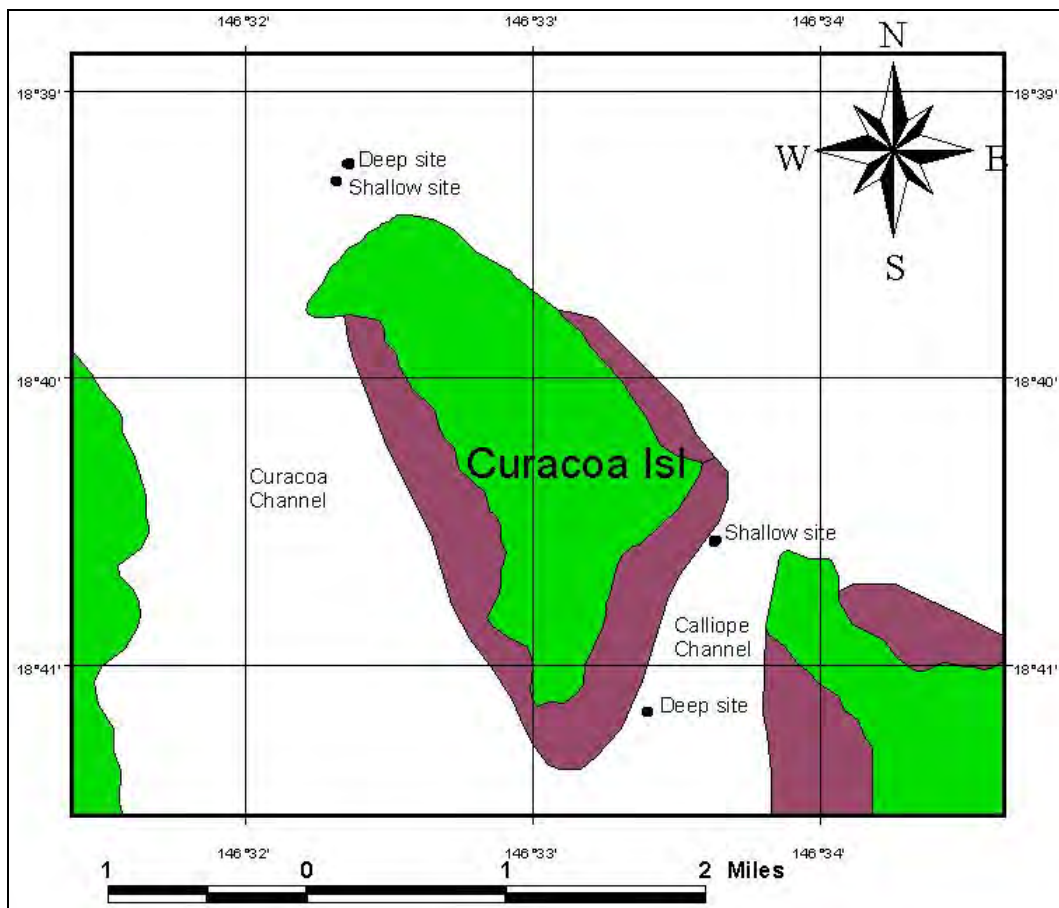


Figure 6–1. Map of the study sites around Curacaoa Island in the Palm Island group showing two sites in the Calliope Channel and two sites on the north side of the island in the Curacaoa Channel.

The megabenthos animals that were tagged at the Kelso sites, unfortunately, could not be re-measured due to the occurrence of poor weather conditions on each subsequent field trip. The

ROV-based megabenthos work at these deep (45-55 m) and relatively exposed sites required both wind conditions <18 knots and neap tide cycles. Other work (Chapter 8) was less restricted and did proceed at the Kelso sites. Those sites previously identified (Chapter 5) at the more distant and even more exposed areas of Broadhurst/Davies Reefs and Flinders/Old Reefs were not attempted so that remaining valuable field time could be focussed at the more assured Palm Islands sites.

The population dynamics of sessile megabenthos fauna that provide structural habitat was assessed by following five basic steps:

1. mapping the dominant fauna at each site.
2. tagging several individuals of dominant species of sponges, gorgonians, and alcyonarians to identify and perform repetitive measures to same individuals,
3. making video measurements of individual growth and mortality rates through time,
4. observing the occurrence of new small individuals in quadrats for measurement of recruitment, and
5. taking samples to confirm taxonomy; and histological examination in the laboratory to determine reproductive strategies.

At each of the four Palm Islands sites, a 4×3 m quadrat was established to measure growth, mortality and recruitment. Initially, all individuals of all species of sessile fauna within each quadrat were tagged so that the appearance of new individuals could be detected, mapped and tagged. Typically, 10-20 individuals of megabenthos species were present and tagged in or near the quadrats. The settlement of any new individuals on 0.25m² concrete marker blocks placed at one corner of each quadrat was also recorded.

To estimate lifetime growth curves in three years, we tagged across the full size-range of individuals of several species common in the area, and for the next three years we measured tagged individuals about every six months (except in 1999 there was a 12 month gap, so that other components of the study could proceed — Chapter 8). The dominant species included sponges (*Xestospongia testudinaria*, *Ianthella basta*, *Cymbastella coraliophylla*), gorgonians (*Ctenocella pectinata*, *Junceella divergens*, *Semperina brunei*, *Subergorgia suberosa*, *Subergorgia reticulata*) and the hard coral *Turbinaria* sp. We attempted to cover the size range of each dominant species available at each site by tagging 3-5 individuals in each size-class, from small, medium-small, medium-large and large. The absolute size range depended

on the species present. After tagging individuals in the recruitment quadrat, the size range was completed by choosing animals within a 20-30m radius of the quadrat. Typically 35-50 individuals were tagged at each of the four sites. Large and/or old sessile fauna may have grown very slowly and, in a three-year study, their growth may not have been measured as precisely as small or young fauna. To counter this, benthos were measured as accurately as possible, using laser scaling equipment and video image capture and analysis techniques.

The latitude/longitude position on the seabed of each tagged individual was recorded with a specialist navigation system and mapped so they could be found again on subsequent occasions, for repeated measurement. Growth of tagged individuals was estimated by measuring increments in linear and/or area dimensions over time. Mortality was estimated by the observed death or disappearance of tagged individuals in consecutive surveys. Mortality, when not directly observed from skeletal or decayed remains, was separated from tag loss by cross-checking any apparent losses with accurate position information and the photographic record.

During each field trip, separate specimens of the target suite of species were collected for histological studies to determine reproductive condition. The taxonomy, identification and reproductive studies of the sessile fauna were undertaken at the Queensland Museum. We have concentrated on relatively few species of structurally dominant fauna and we were able to separate different species and determine which different forms belong to the same species. On the last field-trip, in order to estimate the local population structure of the tagged species, divers repeatedly placed a one-metre square quadrat haphazardly, to estimate the relative density and size distributions of megabenthos animals in the vicinity of the study sites.

Two tropical cyclones passed over the study sites before and after the fourth field-trip in March-April 2000. These storms impacted the study sites with rough seas, influxes of terrestrial grasses and probably freshwater, and by shifting large amounts of substratum. These impacts appeared to affect severely the survival and growth of a number of tagged animals. Consequently, the demographic data were separated into pre- and post-cyclone groups. The pre-cyclone data included comparisons between measurements made on field-trips 1-2-3, and the post cyclone data included comparisons between field-trips 3-4-5. This was a mixed benefit, on one hand providing insight to the impact of cyclones, but at the same time reducing the sample size in each group for the analyses of demographic data.

6.2.1 Logistics of the tagging & measurement

Tagging in the marine environment is typically troubled by fouling and grazing by fish, which leads to difficulties with tag reading and tag loss and associated ambiguities. To minimise these problems and facilitate identification, the tags used in the study were radio-frequency identification tags in 23×4 mm glass capsule form (Texas Instruments RI-TRP-RRHP), that were read automatically by an induction transceiver (Texas Instruments TIRIS Series 2000 module) mounted in an underwater housing. The tags were attached to sessile epifauna by cable-ties, or inserted into sponges with a large needle, or moulded into epoxy pucks placed at the base of the target animal.

Initially a small remotely operated vehicle (ROV — Hydrovision ‘Offshore HYBALL’) was used to conduct most of the underwater tasks. Divers assisted to a maximum depth of 30 m, by setting up quadrats, tagging benthos in shallow sites and in later field trips to video the animals during ROV downtime. Navigation using an acoustic underwater tracking system and differential GPS enabled accurate (± 1 m) latitude/longitude position fixing and re-location of tagged fauna for measurement at each sampling time. The ROV telemetry link also allowed data such as tag numbers to be automatically acquired in real time, displayed, logged to database along with corresponding position, video frame numbers and captured image filenames. A pair of parallel lasers fitted in the ROV provide a 100 mm scale on the video images of megabenthos for measurements.

Deployment of the ROV or divers involved anchoring the vessel precisely close to the study sites with a 800kg weight as a temporary mooring on a 25mm plaited nylon rope that absorbed up to 30% rise and fall of the vessel on the waves (Figure 6–2). The ROV umbilical was clipped onto the rope to minimize the drag due to currents. This method is simple and effectively enables repeated, accurate positioning of the vessel over the study sites.

Integrated data acquisition, storage and retrieval were central to the logistics of the field operations and analysis. Custom software controlled the integration of data for vessel position and orientation, ROV tracking, video frame, and tag numbers (Figure 6–3). It also provided a navigation system that gave accurate co-ordinate positions of the vehicle, which were overlaid on the video tape record and displayed as an ROV track on a plotter window. The positions of

tagged fauna were presented as waypoints to facilitate their re-location. When a tagged animal was detected, previous images of that individual were displayed for confirmation and to enable the same image orientation and perspective to be captured.

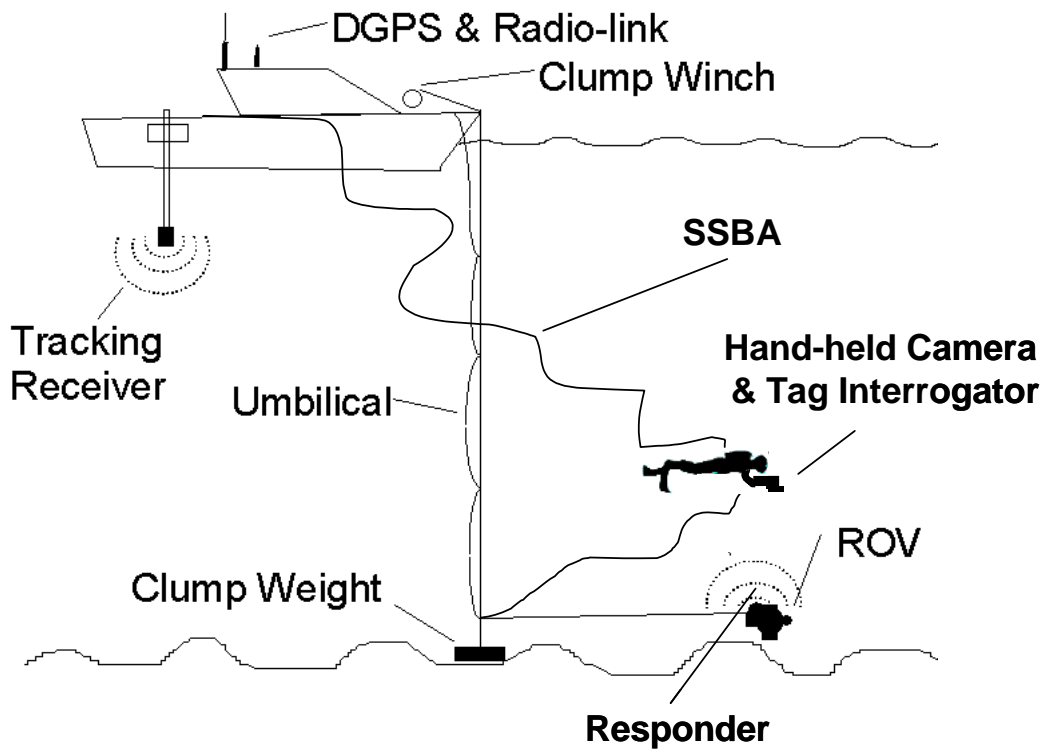


Figure 6–2. Schematic diagram showing the method of mooring a 20 m vessel over the study sites and deployment of the ROV and diver.

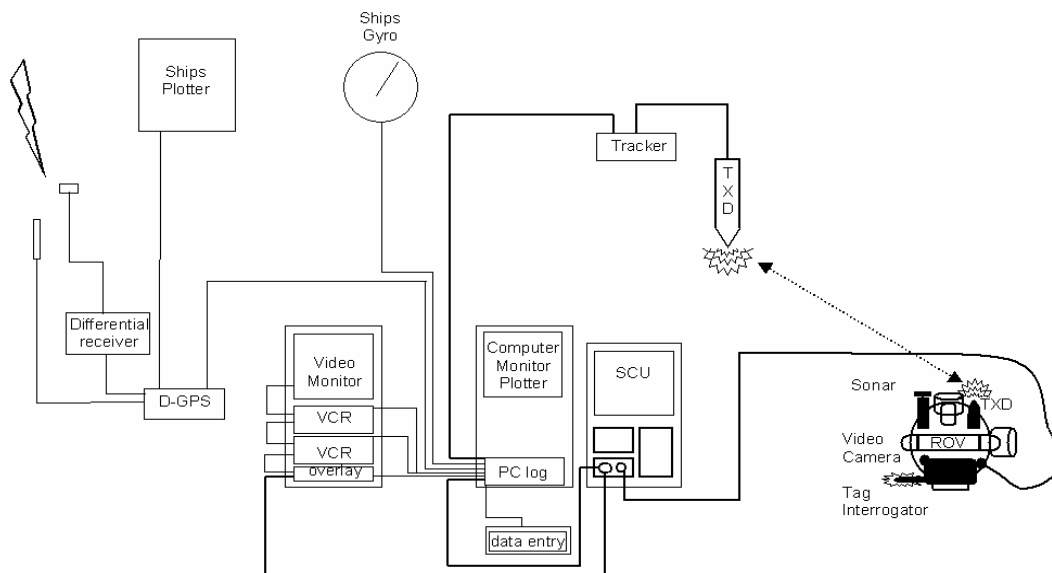


Figure 6–3. System diagram showing integration of components necessary for automated tracking of the ROV and synchronous logging of position, tracking, tag numbers and video data, to facilitate post-analysis and measurement of sessile benthic fauna. DGPS: differential global positioning system, VCR: video recorder, PC: logging computer, SCU: surface control unit for ROV, TXD: tracking system transducers.

The laser scaled images of fauna recorded from the ROV's video camera were captured live or from tape. The lasers were calibrated by projecting onto scaled grids to check accuracy and precision of measurements of size through time. Image analyses were achieved efficiently by using custom software to control, link and synchronise the field databases (of tracking, positioning, and tag numbers) with the video images and execute macros within the Optimas® image analysis software. Image measurement involved an operator digitising the the laser points (100 mm scale), and height, width, and area of profile of the animal as appropriate for the growth form — then choosing species and condition information from a select list. The software transferred the measurement data to a database along with the image filename and corresponding field data. This provided a semi-automated method for extracting the required quantitative data in the form of site, tag-number, species, date/time, position, morphometrics and condition. A software package was also developed that enabled the image sequence for each tagged individual over the five field-trips to be compared simultaneously together with the corresponding data. This enabled a visual verification of tagged individuals with the data (Figure 6–4).

6.2.2 Megabenthos dynamics

6.2.2.1 Recruitment

Recruitment was recorded as the appearance of any new, usually small, animals within each of the quadrats (4 m × 3 m) set up at each of the four sites. Any new animals located were tagged (except on the final field-trip) and identified and recorded on video for subsequent measurement. The total number of new and small individuals per species detected and tagged at each site, on each survey, were considered as recruits and these formed cohorts. Each tagged recruit and cohort of each species was followed through time.

6.2.2.2 Growth

Growth was estimated by plotting the height, width and area for individual animals over time. Height was chosen as the most appropriate parameter for recording growth of the gorgonians (except for *Ctenocella pectinata* where width was used), and the sponges *Xestospongia testudinaria* and *Ianthella basta*. Area was used to measure growth of the sponge *Cymbastella coralliophila* and the coral *Turbinaria* sp. The assessment of the growth of individuals was treated separately for *pre-cyclone* and *post-cyclone* conditions.

MegabenthosCruiseHist

TAGNO: 23061575 Status: OK 0198 MEAS 1 files \\Forty2-cv\vcse_video\Projects\Megal 0298 MEAS 1 files \\Forty2-cv\vcse_video\Projects\Megal

Error type:

Status Comments:

Animal name:

Site:

Tag History:

COMMENT TAGID no ABC:

benthosdata

TAGID:	BenthosID:	CRUISELONG:	TableName:	Final_Width_CM:	Final_Height_CM:	Final_Area_CM:	BenthosLaserX1U
23061575	1998040223325423061575	mbd199801	mbd0198	95.8	57.2	2658.1	
23061575	1998121105140823061575	mbd199802	mbd0298	99.6	39.8	2351.7	
23061575	1999042022303223061575	mbd199901	mbd0199	112.8	55.1	2997.5	
23061575	2000032422405123061575	mbd200001	mbd0100	130.3	63.5	3629.4	

0199 MEAS 1 files \\Forty2-cv\vcse_video\Projects\Megal 0100 MEAS 1 files \\Forty2-cv\vcse_video\Projects\Megal 0200 MEAS 2 files \\Forty2-cv\vcse_video\Projects\Megal

Record: 1 of 234

Figure 6-4. Display of computer screen demonstrating software to compare video image sequences and data matching individual tagged animals to check integrity of measurements. The white dashed lines indicate the measurements made by operators. In the case of this gorgonian (*Ctenocella pectinata*), width was the most suitable parameter, as the tips often dropped off.

To account for the different time intervals between sampling field-trips, the increment in the growth, whether height, width or area, for each individual in a species, between sampling field-trips, was standardised to six months intervals by dividing their overall increment by the time interval between field-trips (months) and multiplying by 6 and adding the result to the initial parameter. Growth for these six months intervals was represented by Ford-Walford type plots of size at time t versus size at time $t + 1$. For animals with determinate growth, such as fish, the slope of the Ford-Walford regression gives the parameters of the von Bertalanffy growth model, but this is not appropriate for megabenthos.

6.2.2.3 Mortality

Tagged individuals were tracked for their status: live or dead. Deaths were determined when tagged individuals were found either dead, or missing on all subsequent occasions after thorough search of their recorded location and reference to previous images. Some tagged individuals were not found at every occasion, but were found subsequently — these were not included as deaths. For each observation survey, total mortality for each species was estimated by the number of deaths compared with the total number alive in each immediately preceding survey.

6.2.3 Reproduction

Specimens of sessile megabenthos (mostly sponges, gorgonians, alcyonarians and ascidians) were collected by ROV or divers. Each voucher specimen was assigned a Queensland Museum registration number and field notes were recorded of live specimen characteristics. Photographs of individual specimens along side their registration number tags were taken as visual records of fresh material. Some specimens were also photographed in situ, prior to collection, with a numbered tag to enable matching of image and registration number (Appendix 6.5–2). Specimens were then frozen and later transferred to 70% ethanol upon return to the Queensland Museum. These specimens have been stored and maintained in the permanent collections of the Queensland Museum, Brisbane.

Morphology and histological preparations were used to determine the taxonomic identity of specimens. Histological preparations of materials were made according the methods of

Hooper (1996) for sponges, and of Alderslade (1998) for alcyonarians (but prepared for light microscope rather than SEM).

Taxonomic identifications were made to genus and species morphotype levels and assigned species names where possible. However, most sessile marine megabenthos invertebrate species remain undescribed in the scientific literature or cannot be reconciled with published descriptions, which are inadequate and based on preserved museum specimens which bear little resemblance to living material. Species unrecognized with published species names were given Queensland Museum species numbers (e.g. sp. 2518), which authenticates each distinct species morphotype, catalogued within the Sessile Marine Invertebrates Section of the Queensland Museum.

Reproductive status of specimens was investigated through dissection of specimens and examination of histological slide preparations in search of gonads, gametes and larvae. The exact nature of these examinations varied with the type of organism. Specimens were also investigated for signs of asexual budding.

6.3 Results

Five field-trips, over a 32-month period, were conducted to measure the demographic parameters of the tagged megabenthos. The initial field-trip was conducted during March/April 1998; the second field-trip during October/November 1998; the third field-trip during April 1999; the fourth field-trip during March/April 2000 and the fifth field-trip during October/November 2000.

The taxonomic identifications of collected specimens are shown in Appendix 6.5–1.

The relative abundances and sizes of the megabenthos counted (Table 6–1) and measured (Figure 6–5) in the haphazardly placed 1 m quadrats, by divers during the final field-trip, provide information to characterise the study sites. The species *Ctenocella pectinata*, *Junceella divergens*, *Subergorgia suberosa* and *Cirrhopathes* sp (whips) were the most common species present. Density in random quadrats is summarized (Table 6–2) for those tagged species for which observations of growth and deaths were most numerous.

Height data are presented only for the common species, most of which were tagged for the growth studies. The *Cirrhopathes* sp were the tallest with some individuals extending over 1 meter in height, but as these are thin and very elongate they are not measurable with the video-based system and were not tagged. The average size of the common gorgonians and sponges (*Ctenocella pectinata*, *Junceella divergens*, *Subergorgia suberosa*, *Semperina brunei*, *Xestospongia testudinaria*, *Ianthella basta*) ranged between 20 and 40 cm in height. The less common (not tagged) soft corals (*Lemnalina* sp and *Lobophytum* sp) and sponges (*Coscinoderma mathewsi*) were smaller than 10 cm.

Table 6–1. The number of each species of megabenthos counted in haphazardly-thrown 1 m quadrats at four locations in the Palm Islands during the last field-trip. (A= Alcyonacea, As = Ascidian, C = Scleractinia, G = Gorgonacea, S = Porifera). (* = species tagged for dynamics study).

Species	Taxa	Calliope deep n=9	Calliope shallow n=11	Curacoa deep n=11	Curacoa shallow n=11	Total
<i>Ctenocella pectinata</i> *	G	14	5	12	9	40
<i>Cirrhopathes</i> sp	G	9		21	7	37
<i>Lamnalina</i> sp	A		1	24		25
<i>Subergorgia suberosa</i> *	G	5	18		1	24
<i>Junceella divergens</i> *	G	1	7	6	6	20
<i>Iotrochota</i> sp	S			9	3	12
<i>Coscinoderma mathewsi</i>	S	2	3	3	2	10
<i>Ianthella basta</i> *	S		1	2	1	4
<i>Junceella fragilis</i>	G				4	4
<i>Lobophytum</i> sp	A		1	1	2	4
<i>Semperina brunei</i> *	G			2	2	4
<i>Muricella</i> sp	G	1			1	2
<i>Plexaura</i> sp	G		2			2
<i>Xestospongia pacifica</i>	S	2				2
<i>Xestospongia testudinaria</i> *	S	1		1		2
<i>Aplidium protectans</i>	As				1	1
<i>Aplysina</i> sp	S		1			1
<i>Callyspongia</i> sp	S		1			1
<i>Clathria vulpina</i>	S			1		1
<i>Dendronephthya</i> sp	A	1				1
<i>Echinogorgia</i> sp	G				1	1
<i>Gelloides fibulatus</i>	S			1		1
<i>Halichondria</i> sp	S				1	1
<i>Hippospongia elastica</i>	S			1		1
<i>Jaspis</i> sp	G				1	1
<i>Nephthya</i> sp	A	1				1
<i>Oceanapia</i> sp	S			1		1
<i>Pericharax</i> sp	S			1		1
<i>Phakellia flabellata</i>	S		1			1
<i>Raspalia</i> sp	S			1		1
<i>Sarcophyton</i>	A				1	1
<i>Turbinaria</i> sp*	C		1			1
Unidentified sp		1				1
Total		38	42	87	43	210

Table 6–2. Resident density summary of tagged species in haphazardly thrown quadrats at four sites in the Palm Islands.

Species	Total residents in 42m ²	Resident density /10 m ²	SD	SE mean	95%CI	Lower	Upper
<i>Ctenocella pectinata</i>	40	9.52	3.73	1.86	5.93	3.59	15.46
<i>Subergorgia suberosa</i>	24	5.71	7.89	3.95	12.56	-6.84	18.27
<i>Junceella divergens</i>	20	4.76	2.58	1.29	4.10	0.66	8.87
<i>Xestospongia testudinaria</i>	4	0.95	0.55	0.27	0.87	0.08	1.83
<i>Semperina brunei</i>	4	0.95	1.10	0.55	1.75	-0.80	2.70
<i>Ianthella basta</i>	4	0.95	0.78	0.39	1.24	-0.28	2.19
<i>Turbinaria</i> sp	1	0.24	0.48	0.24	0.76	-0.52	1.00
<i>Cymbastella coralliophila</i>	0						
<i>Subergorgia reticulata</i>	0						

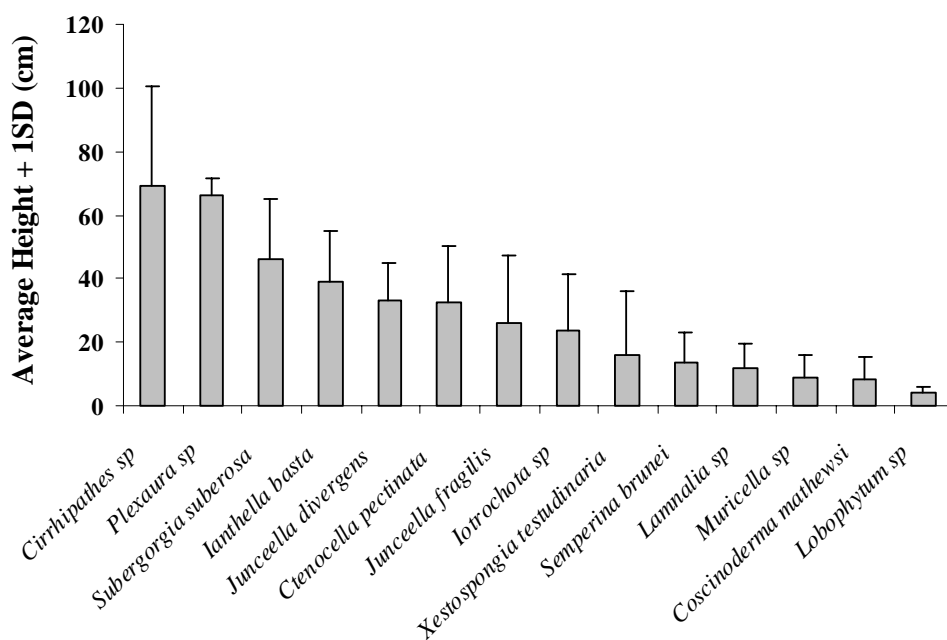


Figure 6–5. Average height of animals measured in quadrats at the four study sites.

6.3.1 Megabenthos dynamics

6.3.1.1 Recruitment

Recruits to the four study sites were recorded from within fixed quadrats (total 48 m²). In total, 32 new individuals were detected over the experimental period (Table 6–3). In the second survey, 14 new recruits were found (Table 6–3), consisting of 13 gorgonians (0.27 m²) and one hard coral (0.02 m²). On the third survey, 12 recruits were located and these consisted of eight gorgonians (0.17 m²) and two corals (0.04 m²). On the fourth survey, only six recruits were found; four sponges (0.08 m²), one coral (0.02 m²) and one soft coral (0.02

m²). No new recruits were found on the last survey, possibly due to the impact of the cyclones before and after the fourth survey.

Table 6–3. The species initially tagged at the four study sites around Curacao Island, listed alphabetically, and the number of recruits of each species found in the quadrats on subsequent field-trips. (A= Alcyonacea, C = Scleractinia, G = Gorgonacea, S = Porifera). No new recruits were found on the fifth survey (MBD0200).

Species	Taxa	Initial Nos.		Recruits		Total
		MBD0198	MBD0298	MBD0199	MBD0100	
<i>Ctenocella pectinata</i>	G	26	4	1		31
<i>Subergorgia suberosa</i>	G	22	5	1		28
<i>Junceella divergens</i>	G	20		2		22
<i>Xestospongia testudinaria</i>	S	19			2	21
<i>Turbinaria</i> sp	C	16		2		18
<i>Semperina brunei</i>	G	16		1		17
<i>Cymbastella coralliophila</i>	S	13				13
<i>Ianthella basta</i>	S	13				13
<i>Gorgonia</i> sp	G	5	4	3		12
<i>Subergorgia reticulata</i>	G	7				7
<i>Hemiasterella</i> sp	S	6				6
Coral	C	1	1	2	1	5
<i>Sarcophyton</i> sp	A	4			1	5
<i>Mopsella</i> sp	G	4				4
<i>Muricella</i> sp	G	4				4
<i>Menella</i> sp	G	3				3
Sponge A	S	2				2
<i>Astrogorgia</i> sp	G	1				1
<i>Ciaocalypta</i> sp	S	0			1	1
<i>Coscinoderma mathewsi</i>	S	1				1
<i>Halichondria</i> sp	S	1				1
<i>Iotrochota</i> sp	S	1				1
<i>Ircinia</i> sp	S	1				1
<i>Melithaea</i> sp	G	1				1
<i>Niphates</i> sp	S	0			1	1
<i>Raphidotethya enigmatica</i>	S	1				1
Total		188	14	12	6	220

The number of individuals of each species cohort of newly tagged individuals decreased over subsequent field-trips (Figures 6–6 to 6–8). Of the six species of recruits found after the first field-trip, at least four species *Subergorgia suberosa*, *Ctenocella pectinata*, *Turbinaria* sp and *Gorgonia* sp steadily declined in numbers (Figure 6–7). Four of the eight species recruited after the second field-trip (Figure 6–8) (*Xestospongia testudinaria*, *Turbinaria* sp, Coral and

gorgonia sp) and three of the six species recruited after the third field-trip (Figure 6–9) (*Xestospongia testudinaria*, *Turbinaria* sp and *Ciaocalypta* sp) declined in numbers.

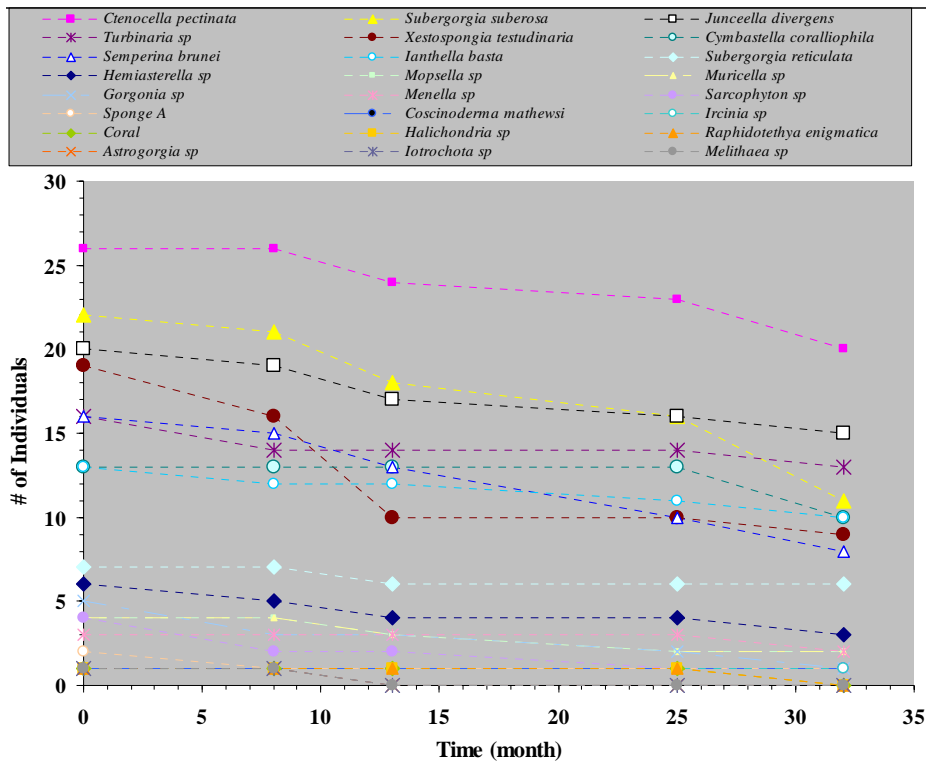


Figure 6–6. The number of living tagged individuals of a species followed through time from the beginning of the experiment.

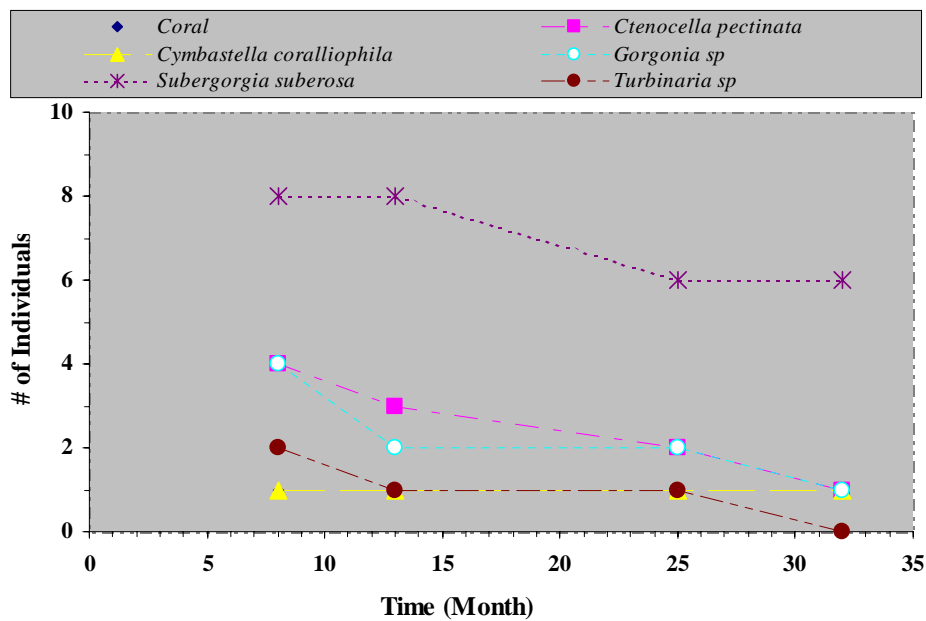


Figure 6–7. The number of individuals of a species recruited (first cohort) to quadrats since the first field-trip followed through time.

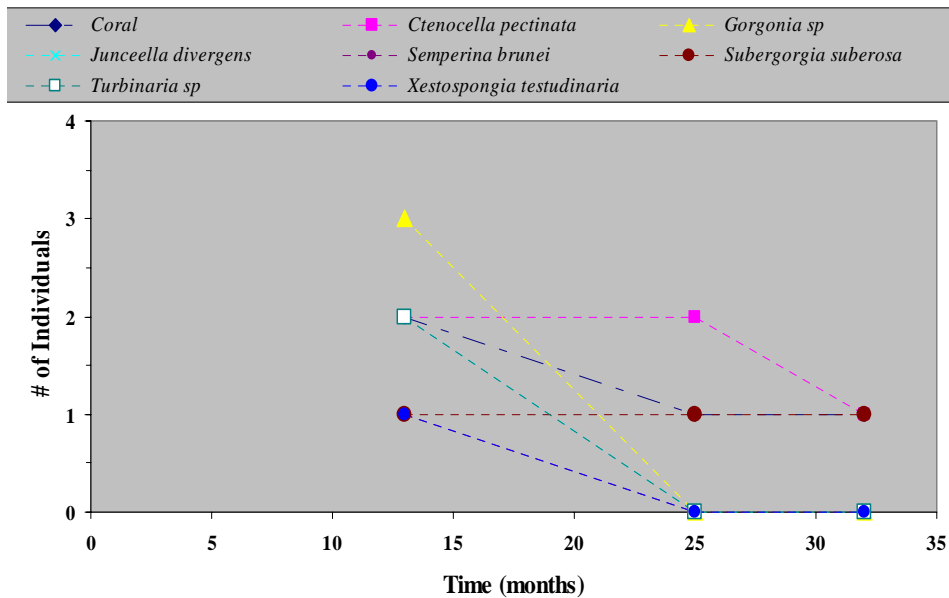


Figure 6-8. The number of individuals of a species recruited (second cohort) to quadrats since the second field-trip, followed through time.

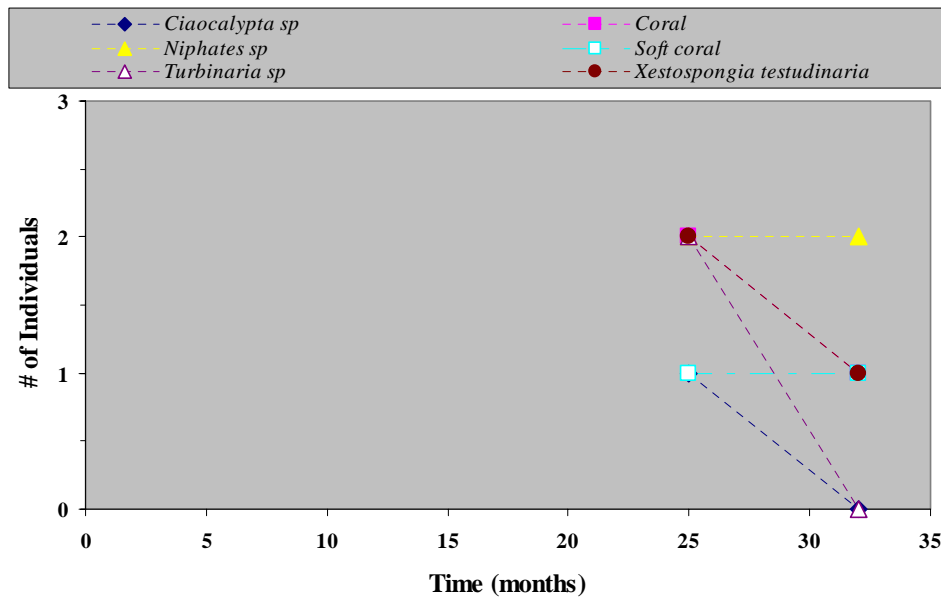


Figure 6-9. The number of individuals of a species recruited (third cohort) to quadrats since the third field-trip, followed through time.

6.3.1.2 Growth

Growth of individual animals was recorded over five sampling field-trips (32 months) for gorgonians, sponges and corals. Only five species of gorgonians; *Ctenocella pectinata*, *Junceella divergens*, *Subergorgia suberosa*, *Semperina brunei*, *Subergorgia reticulata*), three species sponges (*Xestospongia testudinaria*, *Ianthella basta*, *Cymbastella coralliophila*) and

one species hard coral (*Turbinaria* sp) survived to the end of the investigation in sufficient numbers for analysis. As groups, each of these species did not show any remarkable growth rates, but some individuals did grow very quickly — and some shrank.

For *Ctenocella pectinata* (Figure 6–10a), the maximum width was the most suitable parameter measured. The initial width range recorded varied from about 18 cm to 100 cm. The widths of some individuals fluctuated over time, while others showed a steady increase over the first three sampling periods and then declined (Figure 6–10b). The fastest growth was recorded for one large individual that increased in width by almost 40% (Figure 6–10b). The average growth rate over one year (1998-1999) was 0.82 cm y^{-1} with a range of -19 cm to 19 cm y^{-1} . The mean growth increment for *Ctenocella pectinata* after the cyclones ($\text{mean} = 0.55 \text{ cm}$, $\text{s.d.} = 11.11 \text{ cm}$, $n=32$) and before the cyclones ($\text{mean} = 0.11 \text{ cm}$, $\text{s.d.} = 8.81 \text{ cm}$, $n= 46$) was not significantly different ($P > 0.05$) (Figures 6–11a,b).

For *Subergorgia suberosa* (Figure 6–12a) the maximum vertical height was growth parameter analysed. For the tagged individuals, height initially ranged from 10 cm to 40 cm. Only one individual grew up to 60 cm over the 32 months (Figure 6–12b) while the majority remained around 20 cm in height or declined in height to about 10 cm (Figure 6–12b). Five of the 28 tagged individuals exhibit a marked decline in height prior to the fourth field-trip, but three of these then increased in height (Figure 6–12b). The average growth rate over one year (1998-1999) was 1.5 cm y^{-1} with a range of -21 cm to 13 cm y^{-1} . The mean growth increment of *Subergorgia suberosa* (Figure 6–13a,b) prior to the cyclones ($\text{mean} = -0.04 \text{ cm}$, $\text{s.d.} = 7.24 \text{ cm}$, $n=28$), and under post cyclone conditions ($\text{mean} = -0.25 \text{ cm}$, $\text{s.d.} = 6.53 \text{ cm}$, $n=11$) was not significantly different ($P > 0.05$). However, the growth increment after the cyclones came from few individuals and one animal had remarkable growth after the cyclones.

For tagged *Junceella divergens* individuals (Figure 6–14a), the initial height ranged (Figure 6–14b) from about 8 cm to 48 cm. In general, very small changes in vertical height were detected, despite one individual increasing from about 48 cm to 62 cm during the first sampling period, but was then not found again. Most individuals either remained at about the same height or increased slightly, and of those alive after the second cyclone most declined (Figure 6–14b). One individual increased from about 8 cm to 40 cm over 4 sampling periods (25 month) and then declined to about 20 cm. The mean increment (Figure 6–15a,b) before ($\text{mean} = 1.36 \text{ cm}$, $\text{s.d.} = 6.34 \text{ cm}$, $n=29$) and after ($\text{mean} = 0.55 \text{ cm}$, $\text{s.d.} = 8.81 \text{ cm}$, $n=33$) the

cyclones was not significantly different ($P > 0.05$). The average growth rate over one year (1998 to 1999) was 0.25 cm y^{-1} with a range of -13 cm to 25 cm y^{-1} .

Semperina brunei (Figure 6–16a) initially ranged from 9 cm to 70 cm high (Figure 6–16b). Many *Semperina brunei*, both tagged and untagged, disappeared from the study sites after the second sampling field-trip. At least four animals decreased in size over the first two sampling periods and then vanished. Not all individuals were found on all sampling periods, they are represented by gaps in some of the lines for individuals. The mean growth increment during the pre-cyclone period ($\text{mean} = -1.275 \text{ cm}$, $\text{s.d.} = 11.64 \text{ cm}$, $n=19$), was not significantly different ($P > 0.05$) from the post cyclone period ($\text{mean} = -1.25 \text{ cm}$, $\text{s.d.} = 7.09 \text{ cm}$, $n=7$), though the sample size for the latter is small. The average growth rate over one year (1998 to 1999) was 3.0 cm y^{-1} with a range of -19 cm to 25 cm y^{-1} .

Individuals of *Subergorgia reticulata* (Figure 6–18a) ranged from 21 to over 90 cm high (Figure 6–18b). Only 7 individuals were observed and 6 remained for the full 32 months of the experiment (Figure 6–18b). The height of one individual varied considerably while the rest showed relatively similar heights (Figure 6–18b). The post cyclone period appeared to affect the two largest individuals most, reducing their final size (Figure 6–18b). The mean growth increments for *Subergorgia reticulata* were not significantly different ($P > 0.05$) under pre-cyclone ($\text{mean} = -3.41 \text{ cm}$, $\text{s.d.} = 15.25 \text{ cm}$, $n=11$) or post-cyclone ($\text{mean} = -3.27 \text{ cm}$, $\text{s.d.} = 15.59 \text{ cm}$, $n=12$) conditions (Figure 6–19a,b).

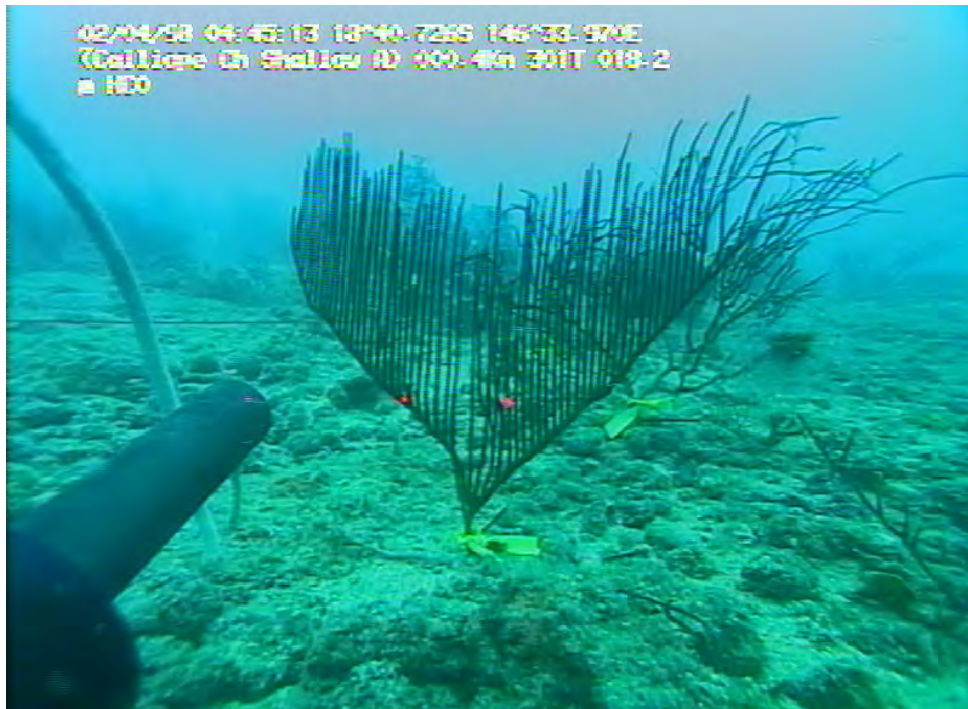
For the sponge *Xestospongia testudinaria* (Figure 6–20a), initial height ranged from 5 to 35 cm (Figure 6–20b). The largest individuals grew to nearly 50 cm in height while the average was about 25 cm. All individuals were relatively steady in height over the first three sampling periods, with the exception of three individuals that showed a slight decrease (Figure 6–20b). One of those three died between the second and third field-trip. The average growth rate over one year (1998 to 1999) was 2.0 cm y^{-1} with a range of -2 cm to 7 cm y^{-1} . However, the most dramatic changes in height occurred after the first cyclone (fourth survey, Figure 6–20b), with most survivors increasing in size, then after the second cyclone most reduced in height. The mean growth increment of *Xestospongia testudinaria* under pre-cyclone conditions ($\text{mean} = 0.09 \text{ cm}$, $\text{s.d.} = 3.96 \text{ cm}$, $n=22$) was not significantly different ($P > 0.05$) from post-cyclone conditions ($\text{mean} = -0.18 \text{ cm}$, $\text{s.d.} = 4.22 \text{ cm}$, $n=16$) (Figure 6–21a,b).

The sponge *Cymbastella coralliophila* (Figure 6–22a) were viewed from above, as their morphology is a flat irregular disc, and area was the parameter used for estimates of its growth (Figure 6–22b). Initially, area ranged from 100 to 1500 cm² (Figure 6–22b). The average growth rate over one year (1998 to 1999) was 62.6 cm² y⁻¹ with a range of –177 cm² to 187 cm² y⁻¹. For *C. coralliophila*, there was no significant difference ($P > 0.05$) in the mean growth increment under pre cyclonic ($mean = 54.26 \text{ cm}^2$, $s.d. = 124.5 \text{ cm}^2$, $n=22$) and post cyclonic ($mean = 4.68 \text{ cm}^2$, $s.d. = 47.52 \text{ cm}^2$, $n=19$) conditions (Figure 6–23a,b).

The vertical height for the irregular sponge *Ianthella basta* (Figure 6–24a) initially ranged from 18 cm to 40 cm in height (Figure 6–24b), but grew up to 65 cm high. All tagged individuals increased in height over the 32 months (Figure 6–24b), and one individual grew from 40 cm to 65 cm height over 13 months. The average growth rate over one year (1998 to 1999) was 8.2 cm y⁻¹ with a range of 2 cm to 6 cm y⁻¹. *Ianthella basta* mean growth increment was not significantly different ($P > 0.05$) under pre-cyclone ($mean = 3.85 \text{ cm}$, $s.d. = 6.35 \text{ cm}$, $n = 20$) or post-cyclone ($mean = 0.83 \text{ cm}$, $s.d. = 3.30 \text{ cm}$, $n = 16$) conditions (Figure 6–25a,b), although the sample size for the post cyclone period is small and of a restricted size range.

The coral *Turbinaria* sp (Figure 6–26a) were also viewed from above and growth was estimated from measurement of area, despite the fact that some individuals were inverted cone-shaped rather than a flat disc. Their areas ranged from about 100 cm² to 1400 cm² (Figure 6–26b). These corals showed very little change in size during the study period, except for one individual that grew very rapidly from 500 cm² to 3000 cm² over the study period. The average growth rate over one year (1998 to 1999) was 326.9 cm² y⁻¹ with a range of –92 cm² to 2247 cm² y⁻¹. Their mean growth increments under pre and post cyclone conditions (Figure 6–27ab) were not significantly different ($P > 0.05$; pre cyclone: $mean = 160.51 \text{ cm}^2$, $s.d. = 438.76 \text{ cm}^2$, $n = 23$; post cyclone: $mean = 12.42 \text{ cm}^2$, $s.d. = 125.93 \text{ cm}^2$, $n = 16$).

(a)



(b)

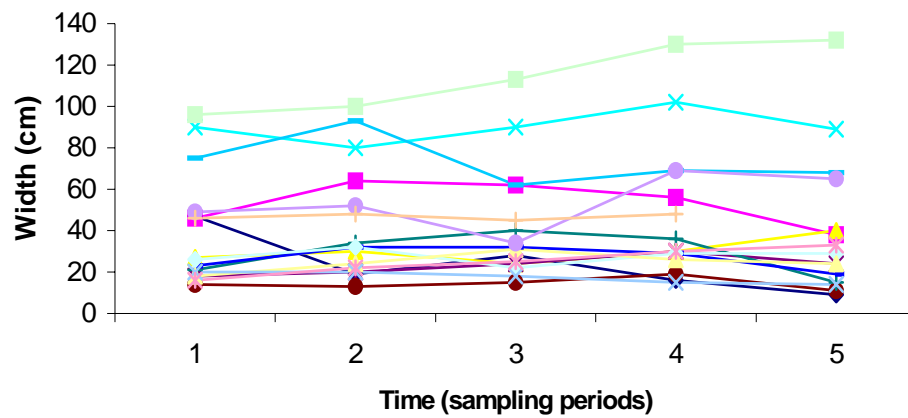


Figure 6-10. (a) Video still of *Ctenocella pectinata* (red dots are lasers 100 mm apart). (b) The sizes of 22 individual *Ctenocella pectinata* followed through time (32 months) from four locations around Curacao Island (1998-2000).

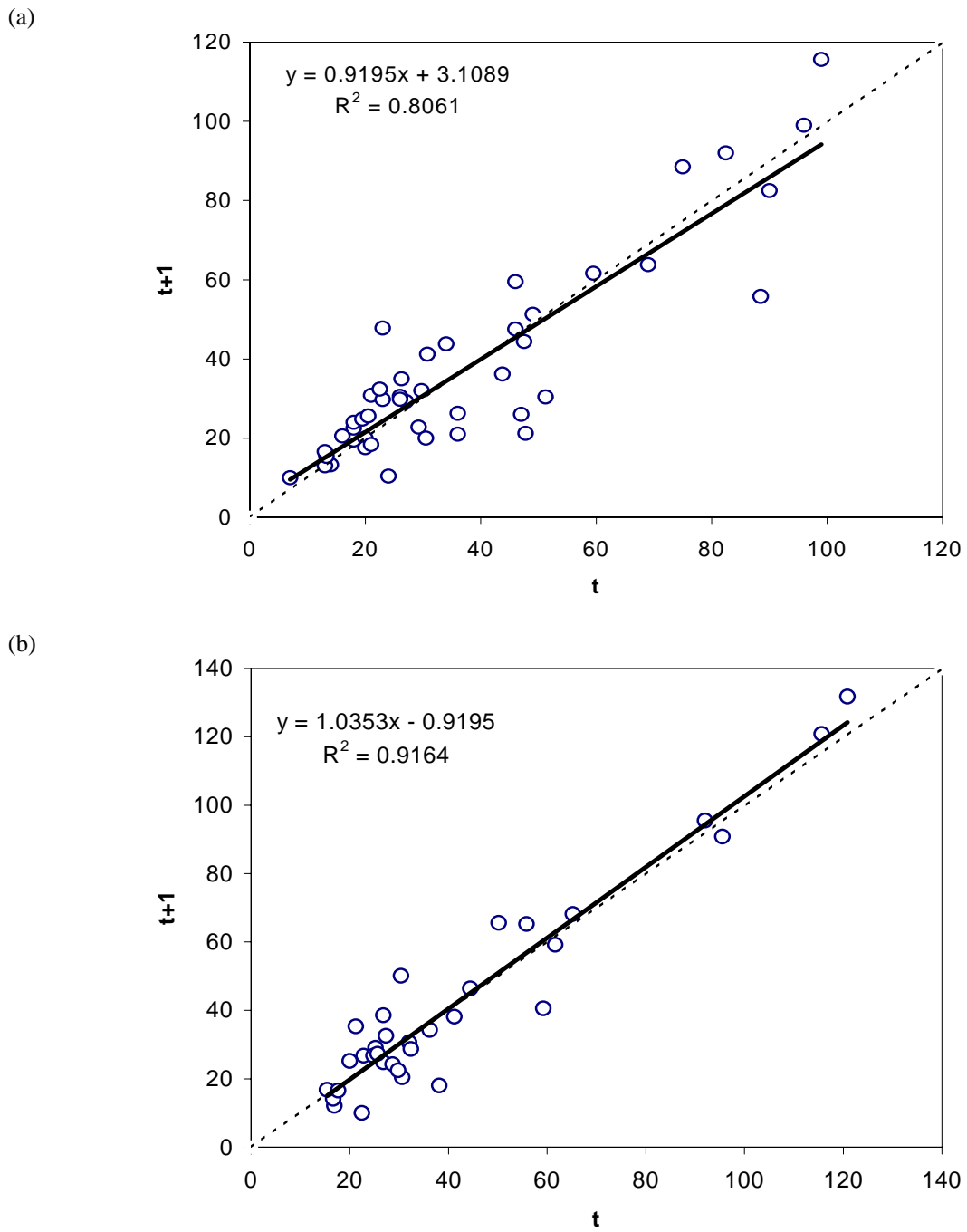


Figure 6–11. Walford-plots of *Ctenocella pectinata* width data for pre (a) and post (b) cyclone periods.

(a)



(b)

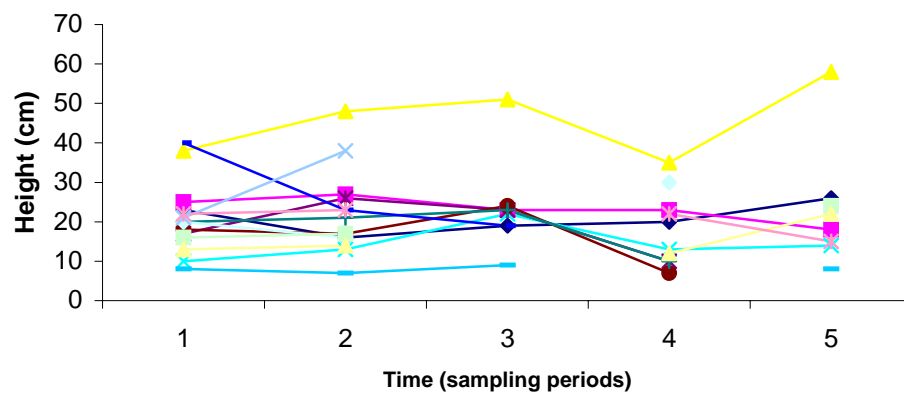


Figure 6-12. (a) Video still of *Subergorgia suberosa* (red dots are lasers 100 mm apart). (b) The sizes of 19 individual *Subergorgia suberosa* followed through time (32 months) from four locations around Curacao Island (1998-2000).

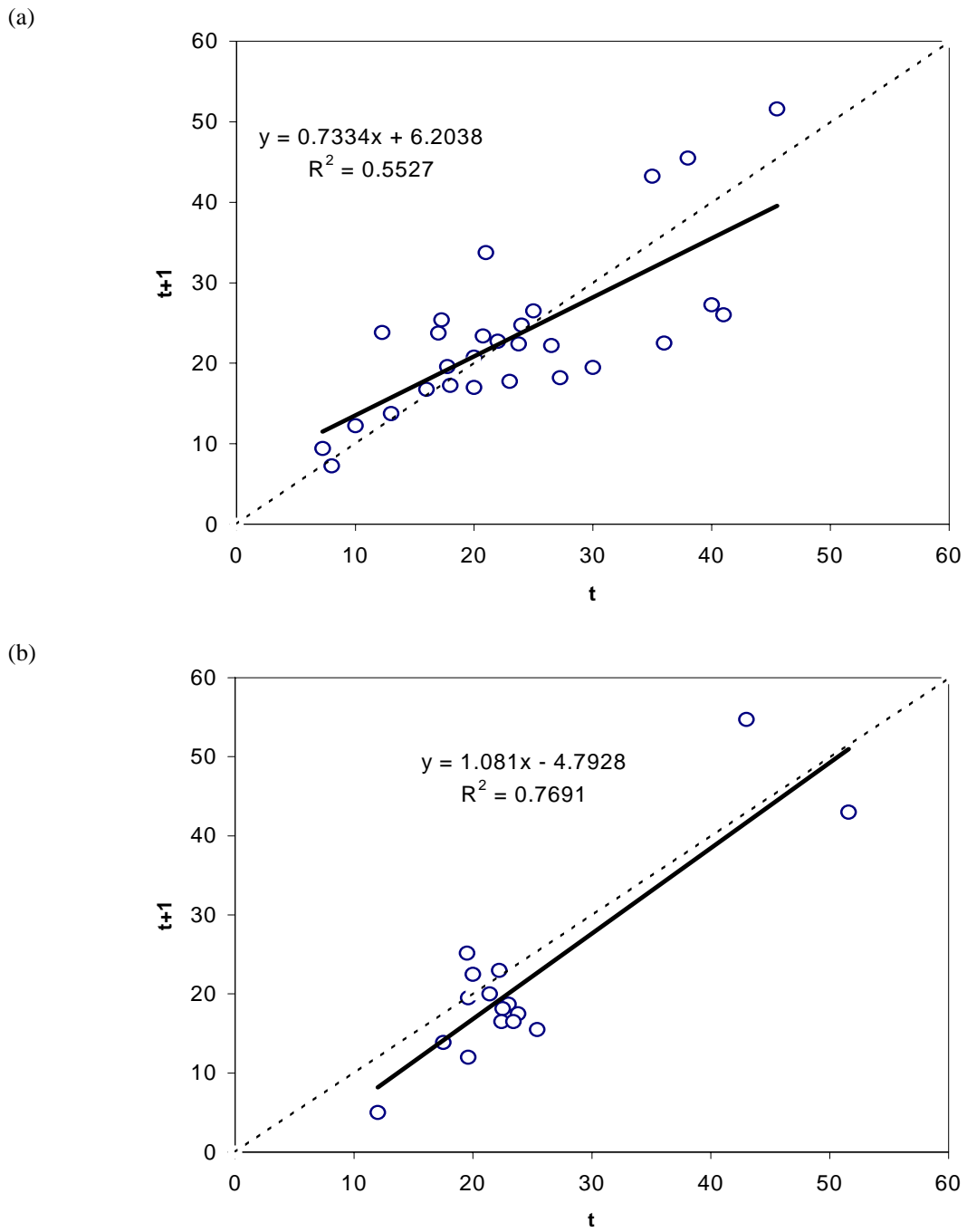


Figure 6–13. Walford-plots of *Subergorgia suberosa* height data for pre (a) and post (b) cyclone periods.

(a)



(b)

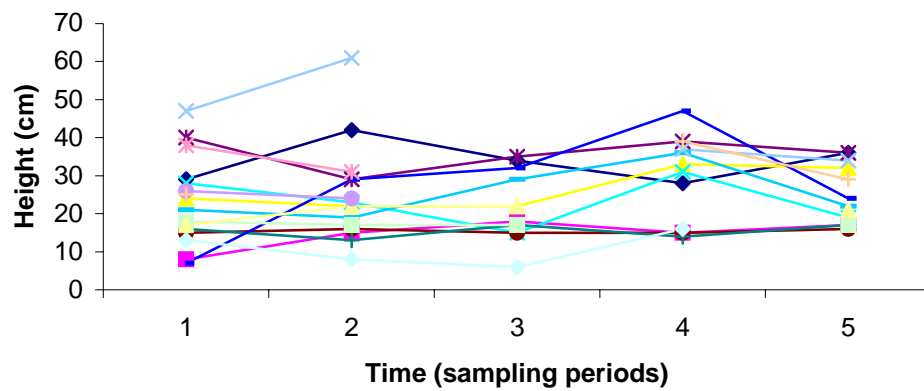


Figure 6-14. (a) Video still of *Junceella divergens* (red dots are lasers 100 mm apart). (b) The sizes of 18 individual *Junceella divergens* followed through time (32 months) from four locations around Curacao Island (1998-2000).

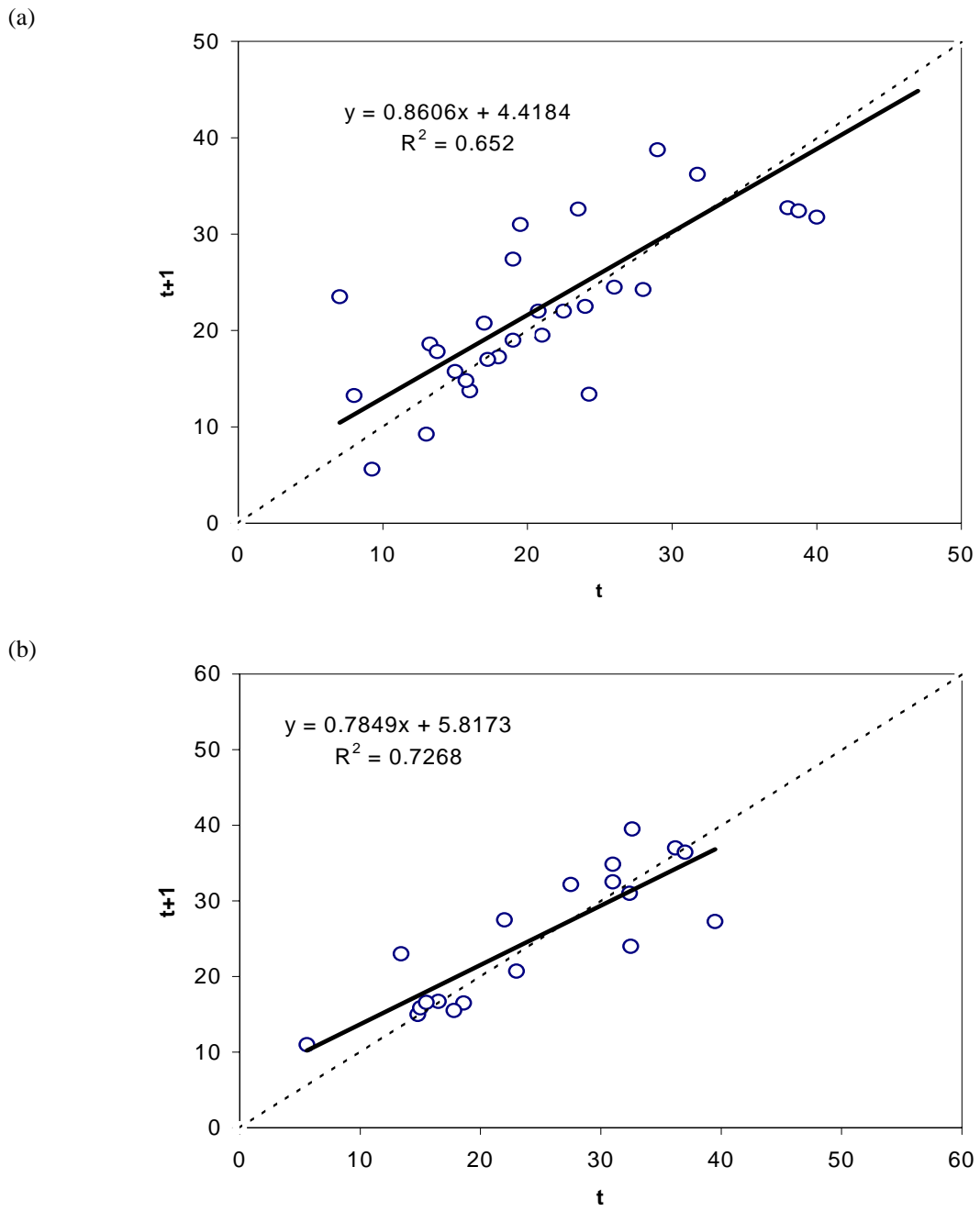


Figure 6-15. Walford-plots of *Junceella divergens* height data for pre (a) and post (b) cyclone periods.

(a)



(b)

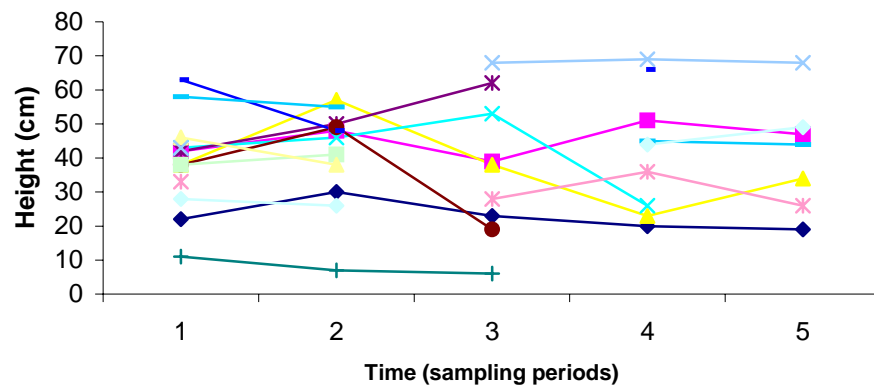


Figure 6-16. (a) Video still of *Semperina brunei* (red dots are lasers 100 mm apart). (b) The sizes of 15 individual *Semperina brunei* followed through time (32 months) from four locations around Curacao Island (1998-2000).

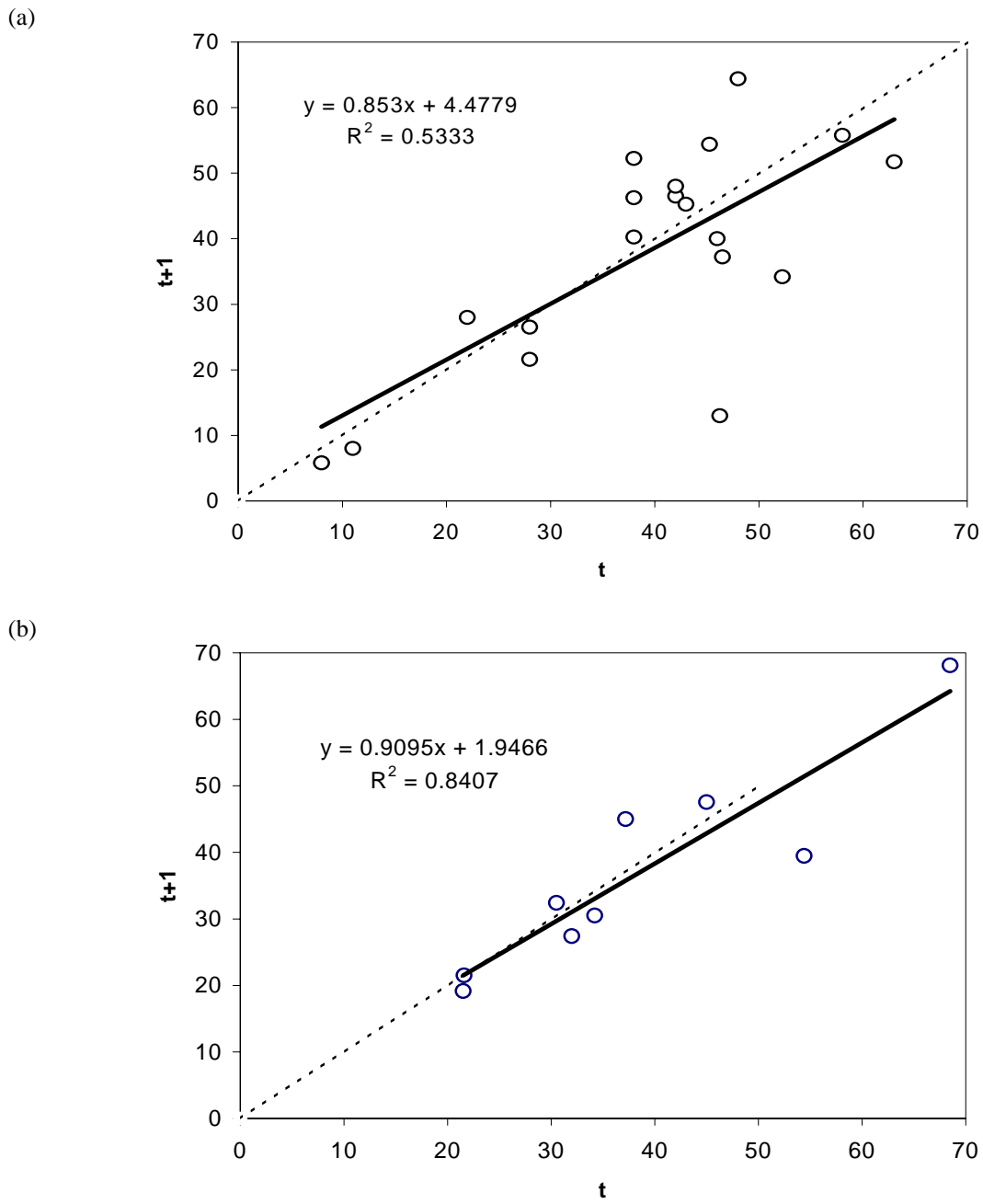
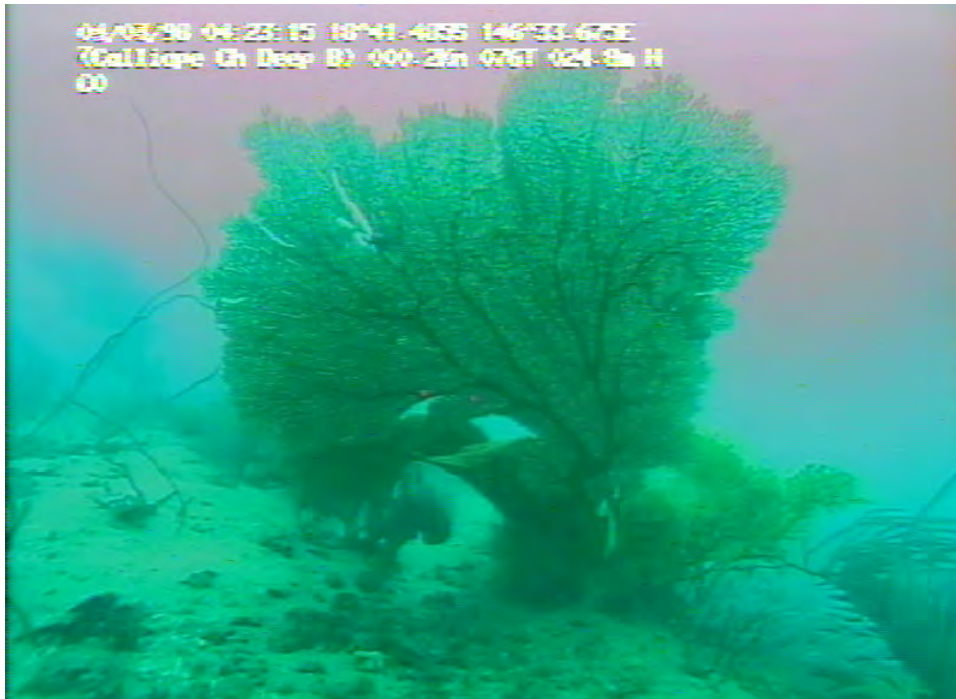


Figure 6–17. Walford-plots for *Semperina brunei* height data for pre (a) and post (b) cyclone periods.

(a)



(b)

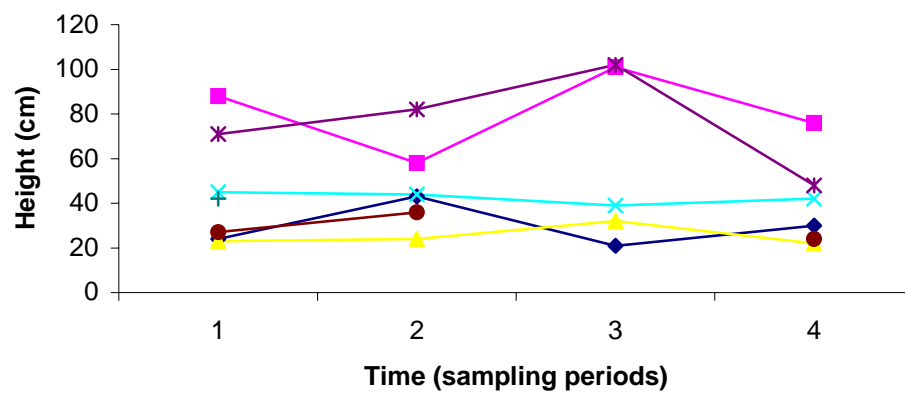


Figure 6-18. (a) Video still of *Subergorgia reticulata* (red dots are lasers 100 mm apart). (b) The sizes of 7 individual *Subergorgia reticulata* followed through time (32 months) from four locations around Curacao Island (1998-2000).

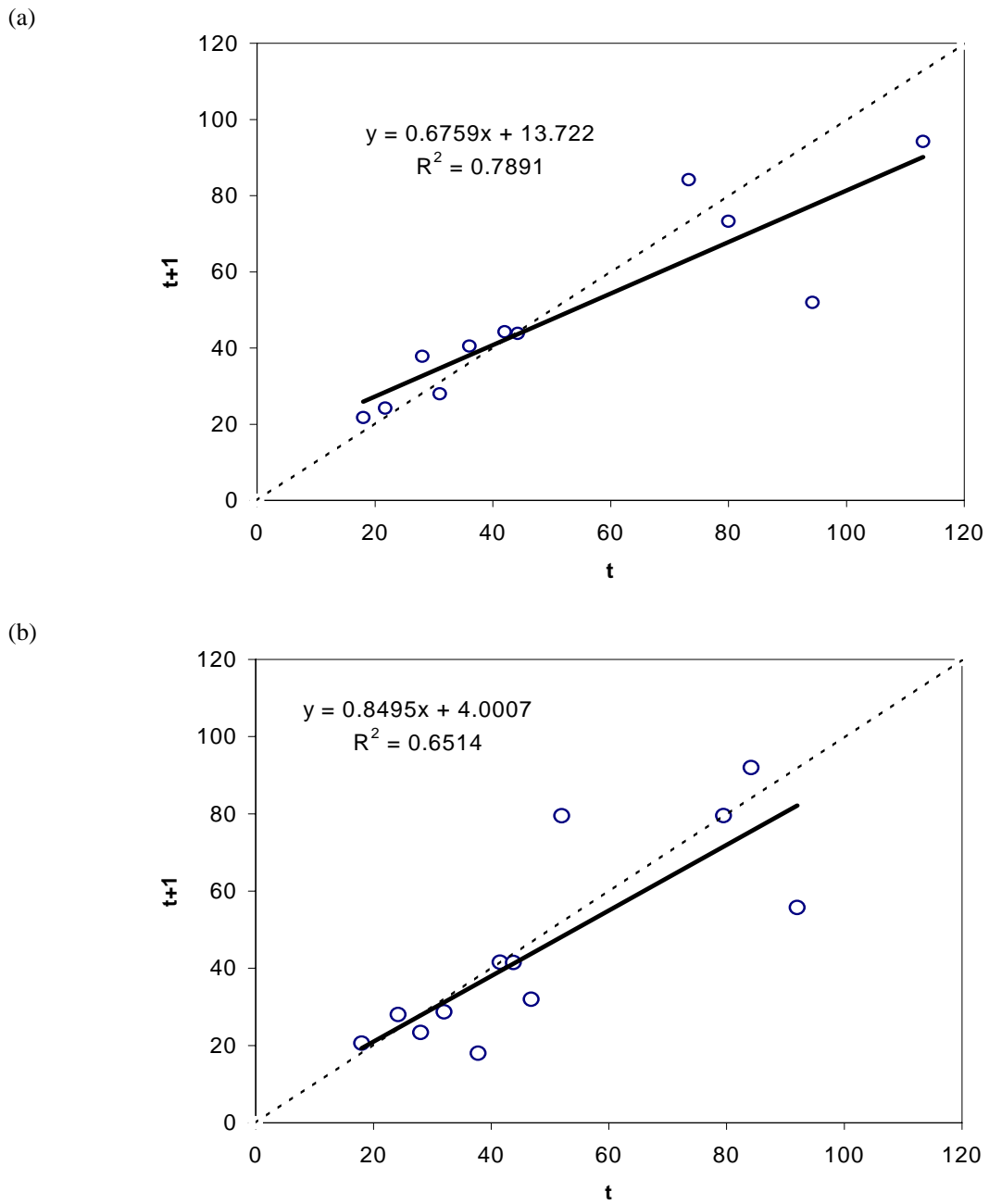
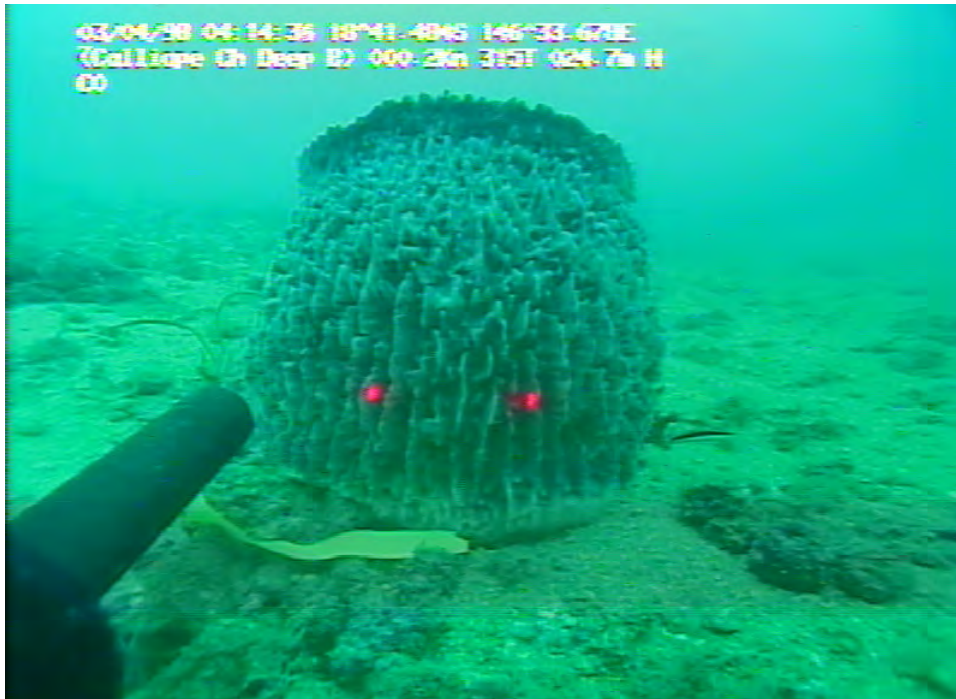


Figure 6–19. Walford-plots of *Subergorgia reticulata* height data for pre (a) and post (b) cyclone periods.

(a)



(b)

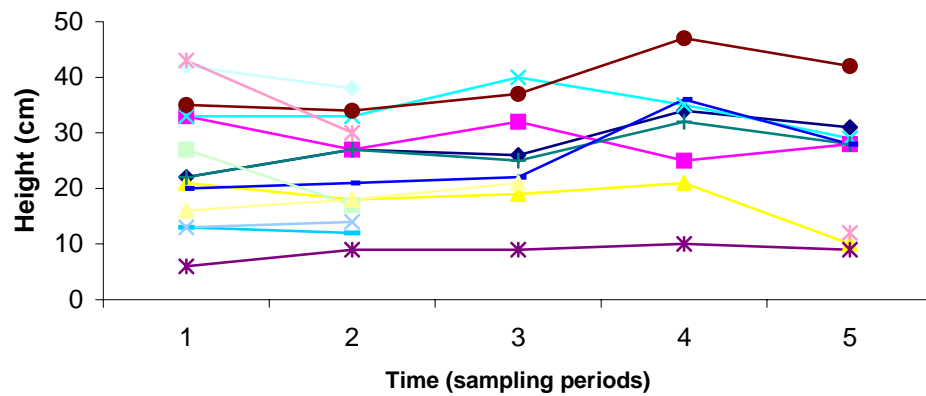


Figure 6–20. (a) Video still of *Xestospongia testudinaria* (red dots are lasers 100 mm apart). (b) The sizes of 14 individual *Xestospongia testudinaria* followed through time (32 months) from four locations around Curacao Island (1998-2000).

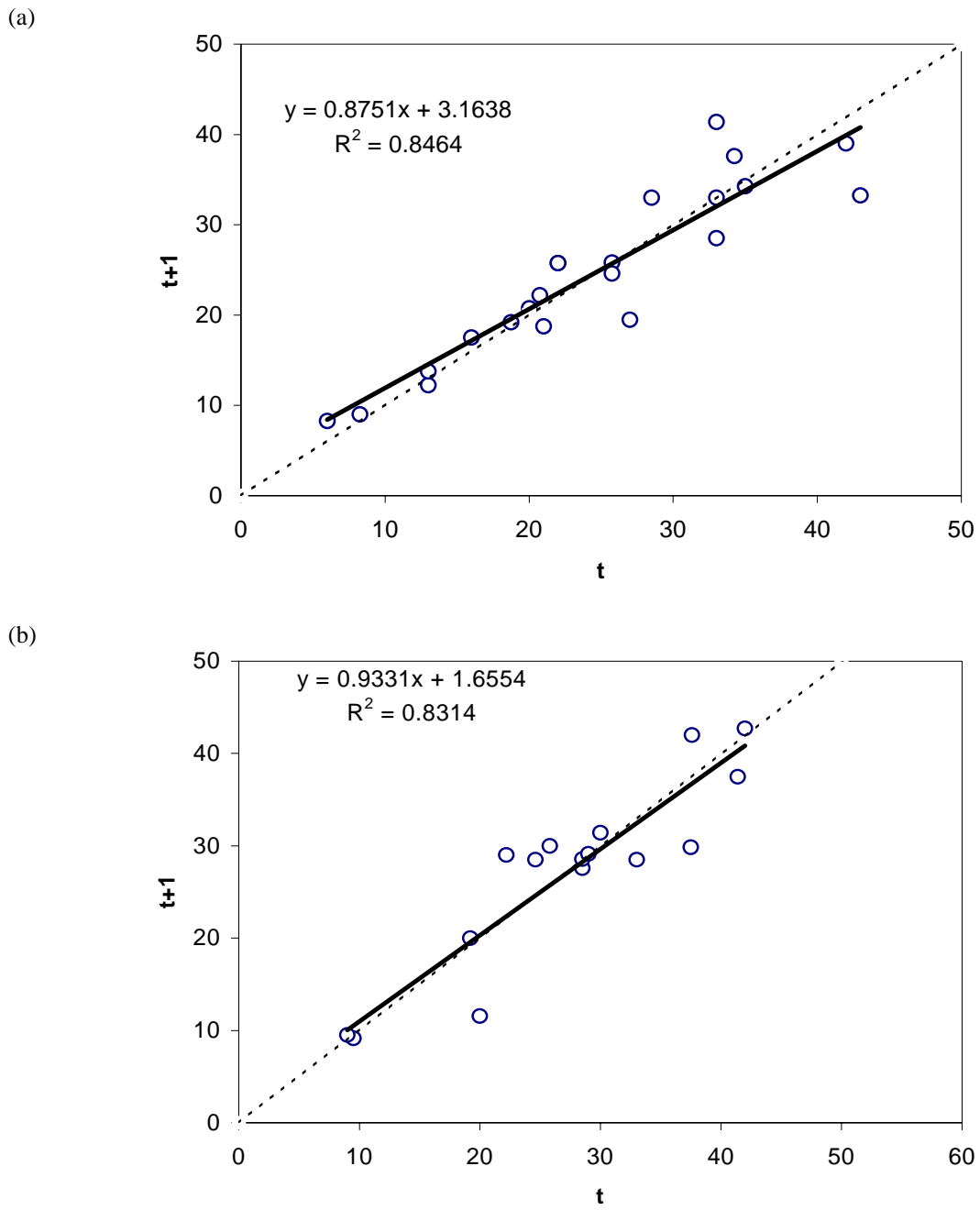
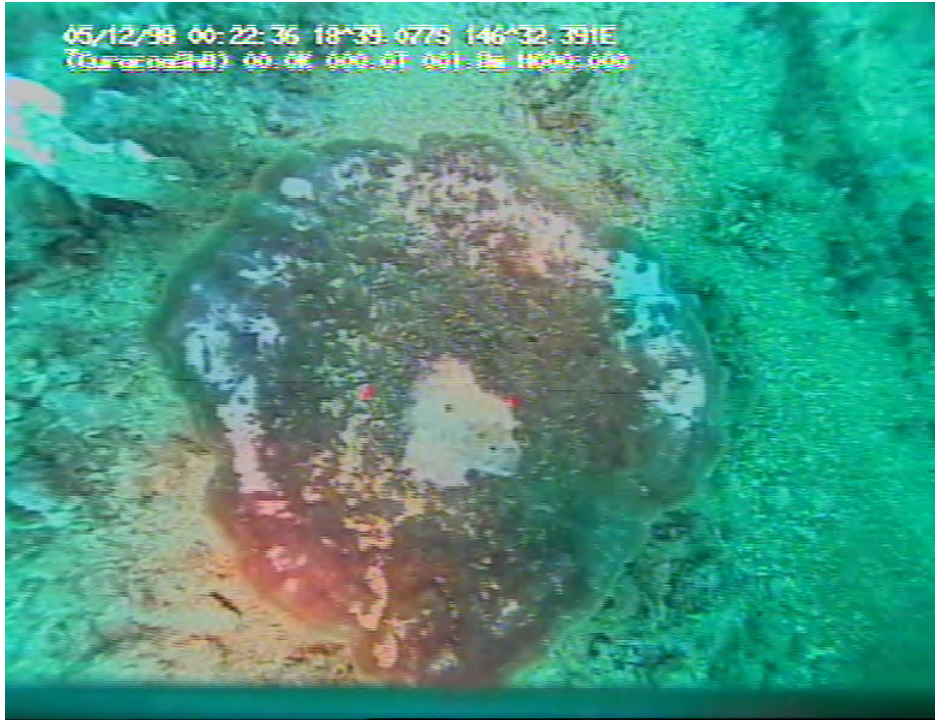


Figure 6–21. Walford-plots of *Xestospongia testudinaria* height data for pre (a) and post (b) cyclone periods.

(a)



(b)

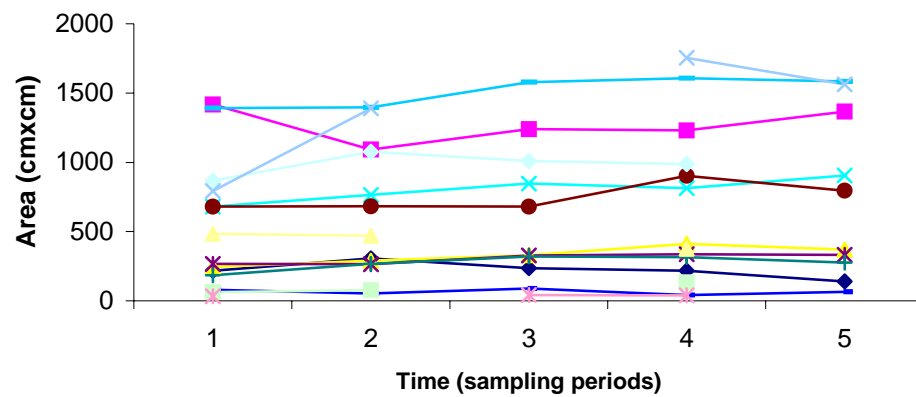
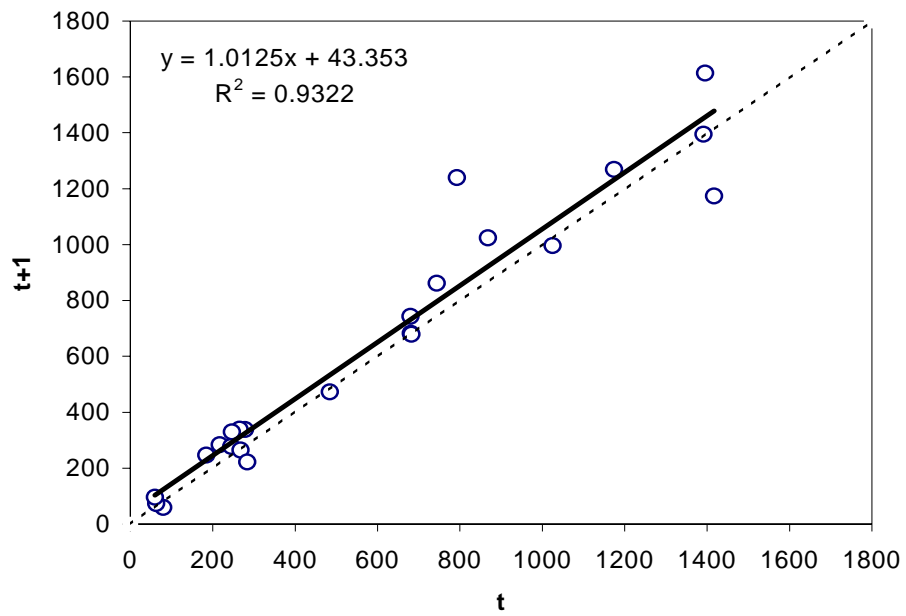


Figure 6-22. (a) Video still of *Cymbastella coralliophila* (red dots are lasers 100 mm apart). (b) The sizes of 14 individual *Cymbastella coralliophila* followed through time (32 months) from four locations around Curacao Island (1998-2000).

(a)



(b)

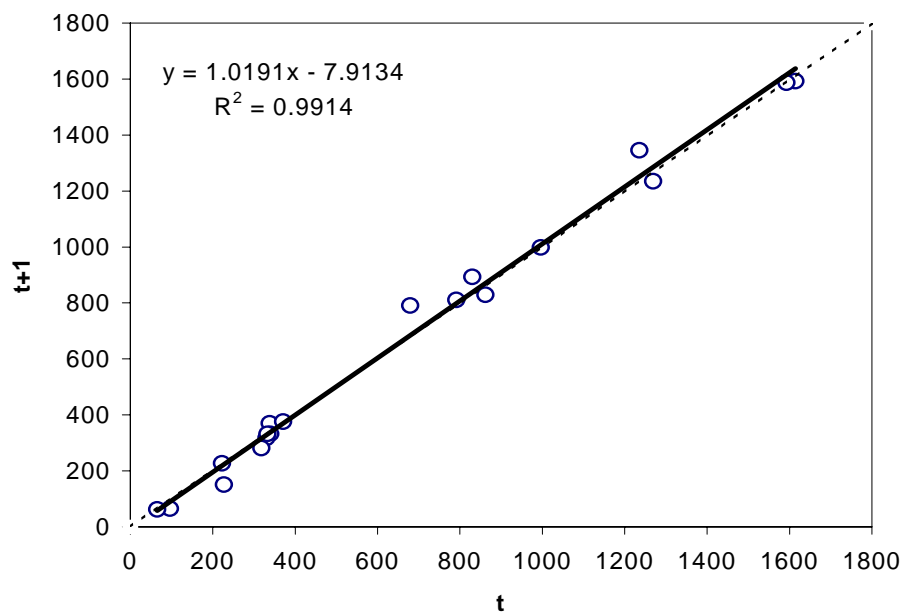


Figure 6-23. Walford-plots of *Cymbastella coralliophila* area data for pre (a) and post (b) cyclone data.

(a)



(b)

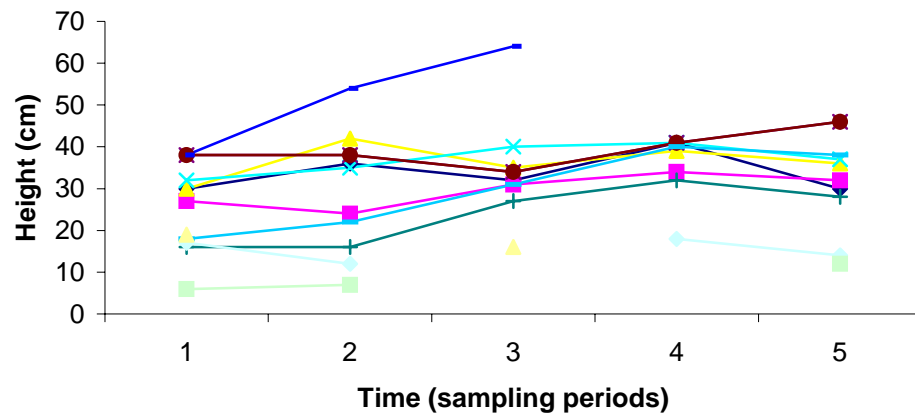


Figure 6-24. (a) Video still of *Ianthella basta* (red dots are lasers 100 mm apart). (b) The sizes of 12 individual *Ianthella basta* followed through time (32 months) from four locations around Curacao Island (1998-2000).

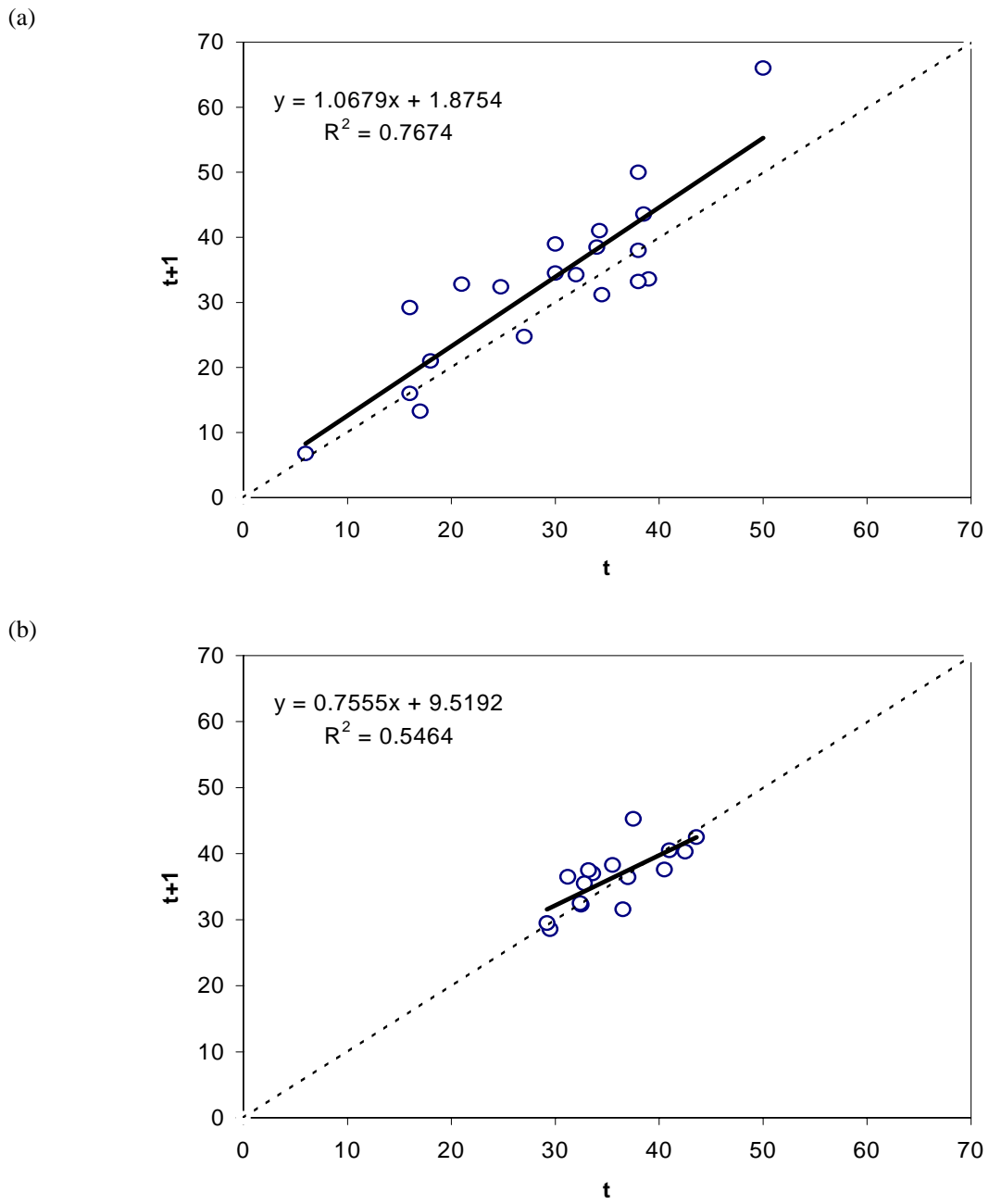
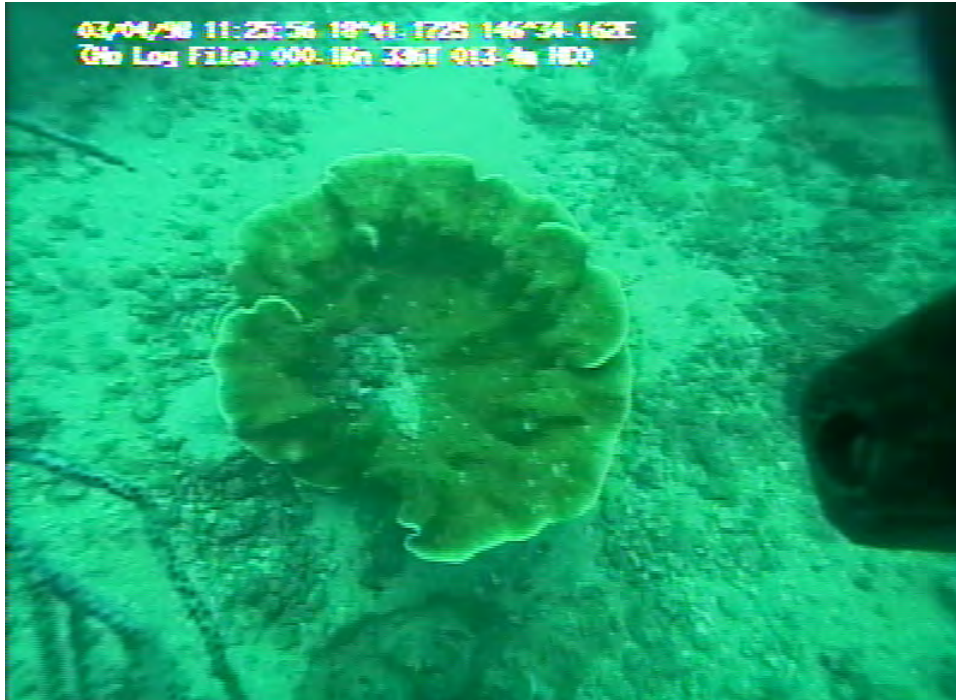


Figure 6–25. Walford-plots of *Ianthella basta* height data for pre (a) and post (b) cyclone periods.

(a)



(b)

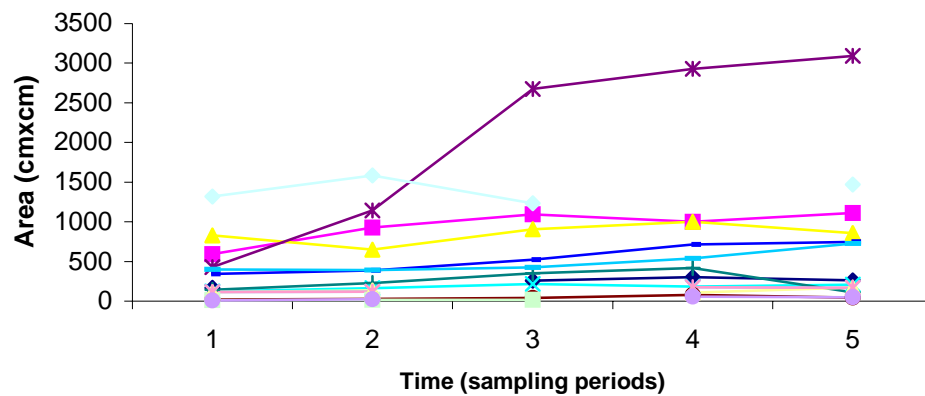


Figure 6-26. (a) Video still of *Turbinaria* sp (red dots are lasers 100 mm apart). (b) The sizes of 15 individual *Turbinaria* sp followed through time (32 months) from four locations around Curacao Island (1998-2000).

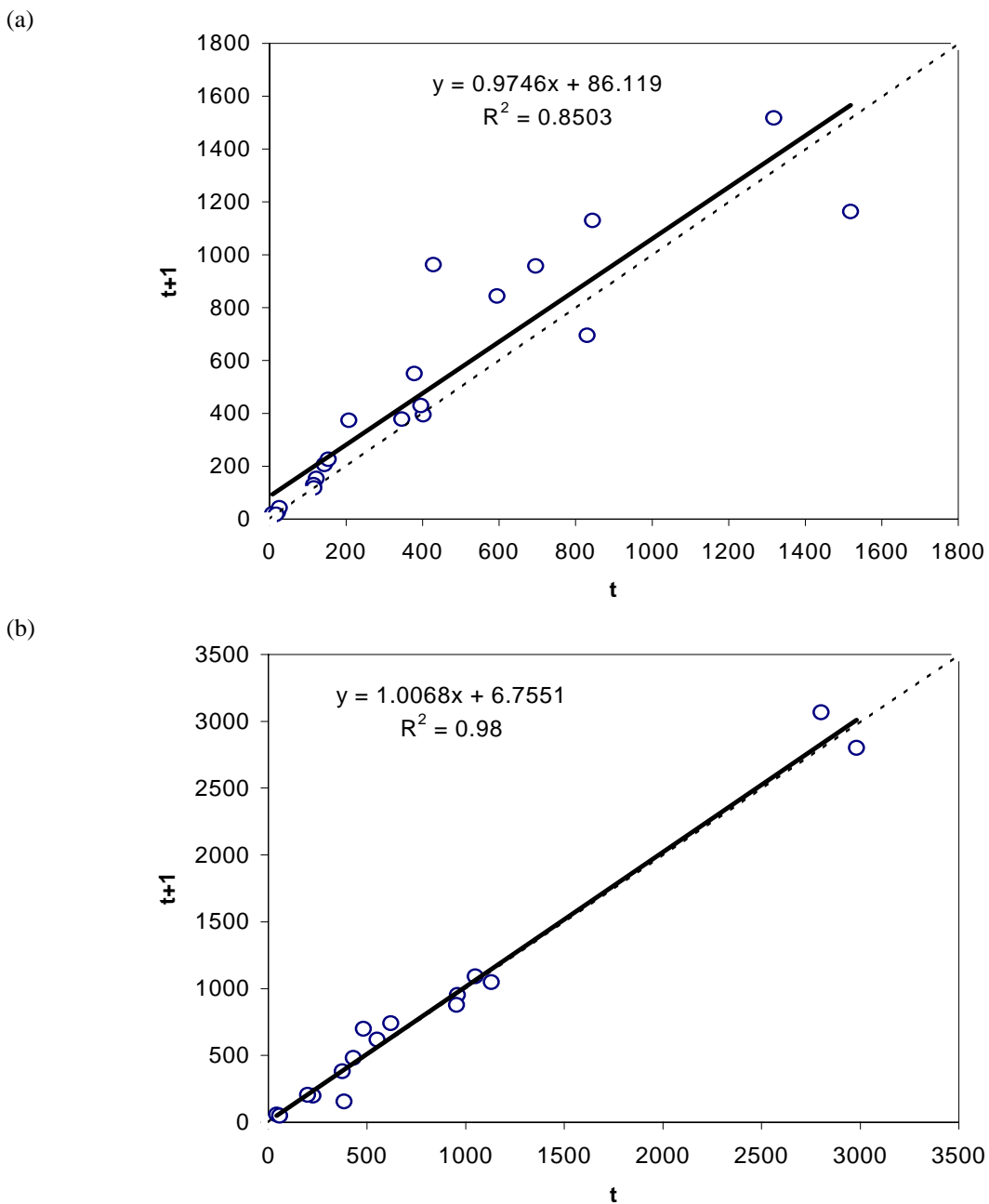


Figure 6–27. Walford-plots of *Turbinaria* sp area data for pre (a) and post (b) cyclone periods.

6.3.1.3 Mortality

There was considerable variability in mortality among species and sampling intervals (Figure 6–28). In general, highest mortalities were observed in one or other of the two cyclone affected intervals, but not necessarily both. Overall mortality across all species was about double in the cyclone affected intervals (6.5% & 9.0%, cf. 15.2% & 17.7% — $p \approx 0.004$). On a percentage basis, highest mortality occurred in the sponge (*Xestospongia testudinaria*), the gorgonian (*Semperina brunei*) and the coral (*Turbinaria* sp.) (Table 6–4), though overall

mortality among all species did not differ significantly ($p \approx 0.21$). *Ctenocella pectinata*, the most abundant gorgonian, had a mortality rate of 10%.

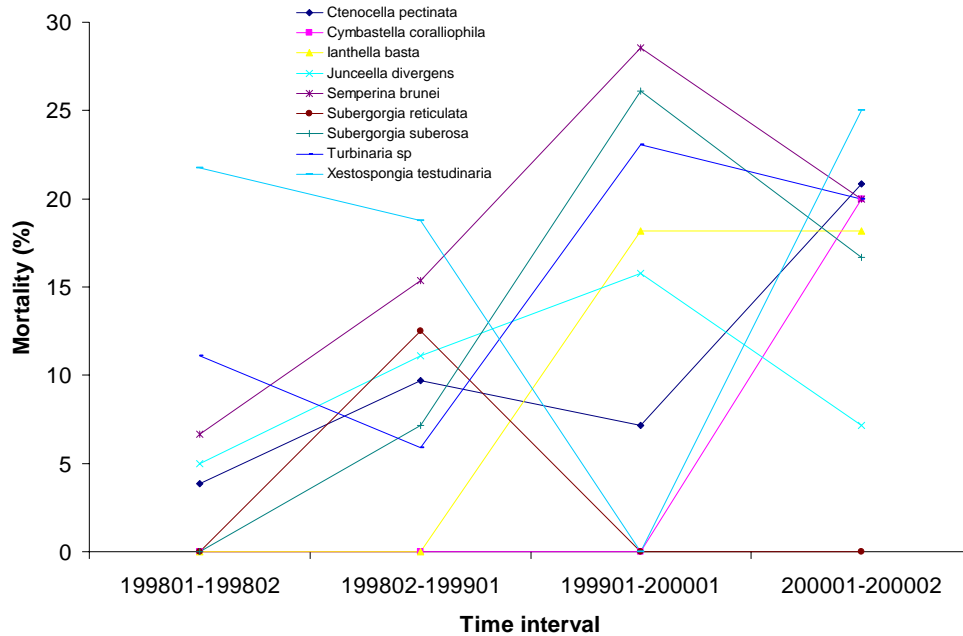


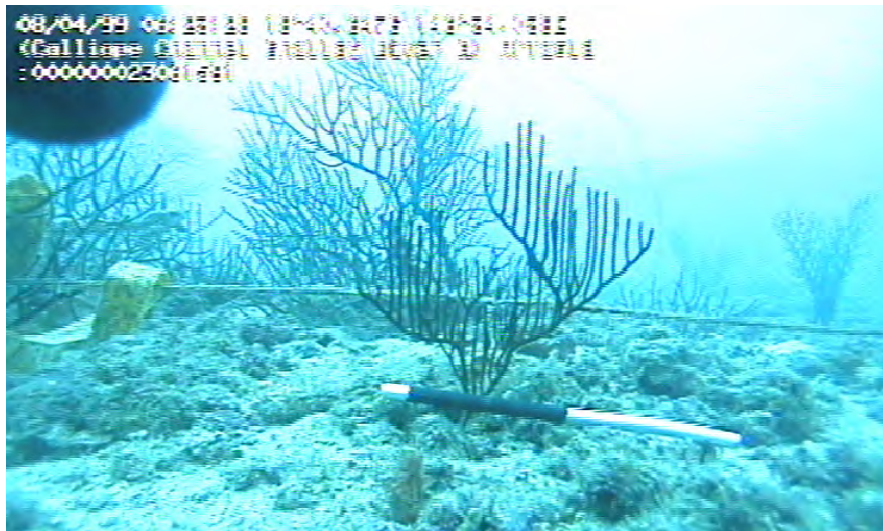
Figure 6–28. Temporal patterns of mortality of nine megabenthos species over four sampling intervals — two separate cyclones affected the third and fourth intervals.

Table 6–4. Mortality summary of tagged species in the Palm Island study sites

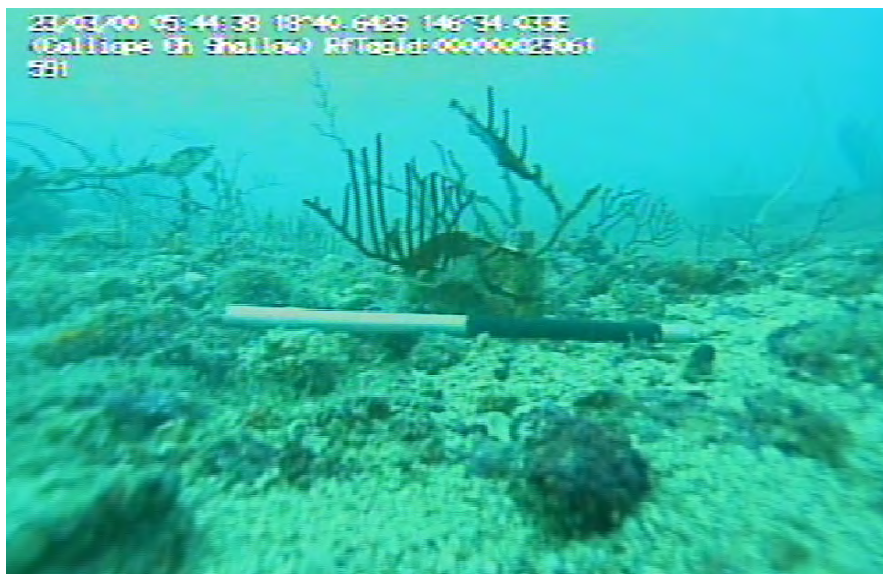
Species	Number of Deaths	Number Observations	% Mortality
<i>Xestospongia testudinaria</i>	11	59	18.6
<i>Semperina brunei</i>	9	52	17.3
<i>Turbinaria sp</i>	9	63	14.3
<i>Subergorgia suberosa</i>	11	90	12.2
<i>Ctenocella pectinata</i>	11	109	10.1
<i>Junceella divergens</i>	7	71	9.9
<i>lanthella basta</i>	4	45	8.9
<i>Cymbastella coralliophila</i>	3	52	5.8
<i>Subergorgia reticulata</i>	1	25	4.0

The death of some animals was progressive, initially involving shrinkage to a smaller size, as in the case of *Ctenocella pectinata* (Figure 6–29a,b,c). Other deaths were rapid, as in the case of the *Semperina brunei*, many of which disappeared completely between successive field-trips.

(a)



(b)



(c)



Figure 6–28. Image of *Ctenocella pectinata* (tag no. 1591) taken during (a) March 1999 (note the background - many live gorgonians); (b) March 2000 (note the changes in the background - after the first cyclone impact); (c) Oct/Nov 2000 (dead, note the algae in the background - after the second cyclone impact).

6.3.2 Reproduction

Evidence of sexual reproduction was infrequently observed. Only two specimens contained gametes or had gonads, while no larvae were found. The sponge *Axinella aruensis* (QM G313181) contained small areas of cellular material believed to be gametes, but without transmission electron microscopy it could not be determined whether they were spermatozoa or ova. The colonial ascidian *Synoicum castellatum* (QM G313186) contained zooids that had testicular follicles present in the abdomen, but no ova were found anterior to these. In general, almost no reproductive activity was detected over the 32-month experimental period.

The products of asexual reproduction were not observed in specimens. These are normally bud-like structures and/or narrowing of the skeleton and tissue, facilitating separation from the main colony.

6.4 Discussion

Sessile animals and plants are subjected to the environmental conditions in which they settled as larvae. The sponges, corals, soft corals and ascidians are no exception. The range of light, water flow, depth and sedimentation determines the success or failure of the individual species to settle, grow and survive. Many genera inhabit only narrow bands along gradients of environmental conditions (Fabricius and De'ath, 1997). Two important environmental gradients for octocorals are depth and distance from land, and gorgonians are mostly restricted to current exposed environments (Fabricius and Alderslade, 2001).

The Palm Islands study sites were all within 1 km of an island, all exposed to currents of at least 3 knots ($\sim 1.5 \text{ ms}^{-1}$) on spring tides (from nautical charts) and at two depth ranges. The study sites were dominated by gorgonians (*Ctenocella pectinata*, *Subergorgia suberosa* and *Junceella divergens*). Many of the megabenthos studied at these sites were also found in the Green Zone (GZ) of the far northern section of the Great Barrier Reef (Poiner *et al.* 1998), although densities were generally higher at the Palm Islands (Table 6–5).

Table 6–5. Density of tagged species in the Palm Islands study sites contrasted with density (estimated from inverse nearest neighbour distances NND averaged for each of 32 ROV sites) in megabenthos garden patches in the far northern section of the Great Barrier Reef (GZ). (G = gorgonian, S = sponge, C = coral)

Species	Taxon	Palm Isl density /10 m ²	Palm Isl SE mean	GZ ROV density /10 m ²	GZ ROV SE mean
<i>Ctenocella pectinata</i>	G	9.52	1.86	3.81	0.95
<i>Subergorgia suberosa</i>	G	5.71	3.95	1.29	0.82
<i>Junceella divergens</i>	G	4.76	1.29	2.07	0.45
<i>Xestospongia testudinaria</i>	S	0.95	0.27	0.21	0.07
<i>Semperina brunei</i>	G	0.95	0.55	0.03	0.06
<i>Ianthella basta</i>	S	0.95	0.39	0.13	1.20
<i>Turbinaria</i> sp	C	0.24	0.24	0.64	0.82
<i>Cymbastella coralliophila</i>	S			0.09	0.17
<i>Subergorgia reticulata</i>	G			0.14	0.32

6.4.1 Recruitment

An ROV and divers were used to monitor any recruitment of sponges, corals or gorgonians to the quadrats. There is an obvious limit to the size of recruits that would be detected (visible) by using the ROV or by divers. This limit was about 80 mm for erect animals like gorgonians and about 10 mm diameter for corals or sponges. Nevertheless, a number of recruits were detected and tagged in each quadrat. The density of recruits in our quadrats, of the species we were studying, ranged from 0.005 to 0.031 m⁻². Most studies of recruitment of corals and sponges have used tiles to get optimum rates and densities of recruitment (Gleeson, 1996; Fisk and Harriot, 1990). For corals the densities of recruits on the tiles have been as high as 3604 m⁻² (Fisk and Harriot, 1990). These high numbers of spat settling indicate that supply of coral larvae was not limited. Fisk and Harriot (1990) also found that the greatest abundance of spat occurred at the inshore fringing reefs and that there was a variation in the spat types between widely separate reefs.

Other environmental factors appear to limit the successful settlement of larvae. An obvious factor must be the availability of suitable substratum, free from sedimentation (Rogers, 1990), free from sand scour (Gotelli, 1988), free from competition by algae (Tanner, 1995; Gleeson, 1996) or grazing pressure (Fisk and Harriot, 1990). Our study sites were free neither from sedimentation nor from competition from algae, particularly after the cyclones when recruitment was lower. The presence of large boulders, extensive growth of brown algae (*Padina tenuis* and *Dictyopteris australis*) and soft corals (Nephtheidae) and notable changes in the density and condition of both tagged and untagged animals indicated that a significant

disturbance had taken place. Wulff (1995), however, found the abundance of small sponges was an order of magnitude higher after a hurricane than before.

6.4.2 Growth

The growth of individual animals within a species was highly variable; some individuals were observed to both grow and shrink in size over the study period. The decreases in width, height or area could have been due to disease, predation by fish, or breaking off during rough weather, or for reproduction (see below). Sponges are known to have negative growth rates (Leys and Lauzon, 1998) either from predation or undergoing fission by separation of parts during growth or reproduction (Meroz and Ilan, 1995). The average growth rates of the gorgonians we studied ranged from 0.8 to 3.0 cm y⁻¹. Published records of average growth rates for soft corals in the GBR are 0.5 cm y⁻¹ (Fabricius, 1995). Goh and Chou (1995) reported average growth rates for five species of gorgonians of between 2.3 cm y⁻¹ and 7.88 cm y⁻¹ (range of 0.4 to 11.5 cm y⁻¹) for gorgonians in turbid waters of Singapore. Linear growth rates for some corals (*Pocillopora damicornis*) are 0.47 to 2.46 cm y⁻¹, (*Turbinaria frondens*) 1.4 cm y⁻¹, and (faviid species) 0.26 to 0.46 cm y⁻¹ (Harriott, 1999).

There was some tendency for smaller individuals, on average, to have greater absolute growth increments (7 of 9 species; 2 significant $p < 0.05$) — probably because larger individuals more frequently regressed in size, not because potential growth increments decreased with size. The growth observed is likely to be representative of a wide range of ages, including quite young individuals, because the initial tagging deliberately covered the full range of available sizes of individuals, from small (typically <10 cm) to large (often >50 cm). Growth increments of ~5 cm between ~6 monthly surveys were not unusual, thus the smallest individuals could have been <1 to 2 years old. Thus, the size transition probabilities estimated for the modeling (Chapter 7) are likely to be representative of a realistic wide range of sizes and ages.

In this study, though the growth increments of the two post-cyclone intervals combined were not significantly different, the sizes of most individuals of several species declined after one or other of the cyclones and the cyclonic activity appeared to have had a dramatic effect on the sessile benthic assemblages in the study area. Many sessile animals were damaged or disappeared completely after the two cyclones. This was probably due to scouring by shifting sediments, as much of the seabed showed signs of heavy erosion and the deposition of large

boulders following the second cyclone. We noted large numbers of *Lemnalia* sp. (Nephtheidae; soft corals) in our study sites after the cyclones. The impacts of natural environmental disturbance such as cyclones or hurricanes have been shown to affect the natural dynamics of benthic “communities” (Rogers, 1993; Wulff, 1995). All sessile invertebrates are vulnerable to abrasion, dislodgment and fragmentation by storm surges and the associated movement of sand and rubble. Most storm damage to sessile animals occurs to those in shallow reef crests, which are dominated by hard corals. Few octocorals are found in this region and most gorgonians occur in wave protected deeper slopes with strong currents (Fabricius and Alderslade, 2001).

6.4.3 Mortality

Natural mortality occurred in a stochastic manner for number of tagged animals throughout the duration of our observations. Most notable was the loss of tagged (and untagged) gorgonians *Semperina brunei*. Several sponges (*Xestospongia testudinaria*) also disappeared within a six-month period. In the case of one small *Xestospongia testudinaria*, a large chunk was bitten out of it shortly after it was tagged; this sponge was not present on the subsequent field-trip. Tissue loss was evident in most gorgonians. Whether this was due to predation or by disease was not known. Tissue loss leading to mortality has been recorded in soft corals close to our study area following a bleaching event after high water temperatures and an influx of fresh water (Fabricius, 1999). Many of these soft coral species lost 60 to 80% of biomass two to three months after bleaching commenced, whereas the Xeniidae died and decayed within days of bleaching (Fabricius, 1999). Mass mortalities of gorgonians in the Caribbean have been attributed to infections by a terrestrial fungi (*Aspergillus*) and a secondary infection by a cyanobacterium (Smith *et al.* 1996). It was thought that the primary infection was caused by hyphea possibly associated with sediment particles flushed from land.

Mortality was generally higher under cyclonic conditions, as has been reported elsewhere. In a study of three common sponges (Wulff, 1995), nearly half the individuals and biomass were lost after the impact of a hurricane. Some of these sponges were toppled and others were fragmented. For a reef coral in Jamaica, Hughes (1984) found that a hurricane increased mortality by ~5-20% depending on the size, with larger corals being affected more severely.

6.4.4 Reproduction

In our study, we found little evidence of sexual reproduction in any of the sponge or octocoral samples collected. This may be due to the bi-annual sampling constraints on the logistics, relative to the seasonality and duration of reproductive activity. Both sexual and asexual reproduction are both dispersal or recruitment strategies used by many groups of sponges, gorgonians and corals. These groups of animals may have the male and female sexes in separate colonies or they may be hermaphroditic (Fromont and Bergquist, 1994; Fabricius and Alderslade, 2001). Several types of sexual reproduction may occur in these animals; they may broadcast their eggs and sperm or have internal brooding of larvae or eggs (Fromont and Bergquist, 1994; Benayahu, 1991). The sexual reproduction of sponges and octocorals may be seasonal in the Great Barrier Reef (GBR) (Fromont and Bergquist, 1994; Fabricius, 1997). Egg development in the sponge *Xestospongia testudinaria* in the GBR occurred over about 5 months and spawning occurred in October and November, coinciding with the lunar phase (Fromont and Bergquist, 1994). Many hard and soft corals were observed to undergo synchronous spawning in the GBR (Babcock *et al.* 1986).

We did not observe any confirmed asexual propagation of megabenthos in this study. Asexual reproduction or cloning is commonly employed as a strategy for rapid colonization by the octocorals (Walker and Bull, 1983; Dahan and Benayahu, 1997). Several mechanisms for propagation are used by these animals, including: budding, fission, fragmentation and generating new colonies from stolons. The unbranched seawhip *Junceella fragilis* pinches off the last ~10 cm of its tip which drops and attaches to the seabed to form a new individual (Walker and Bull, 1983). Using DNA studies (Coffroth *et al.* 1992), found that on one reef in Panama 59% of the colonies of *Plexaura* sp. were of one genotype. Members of two common soft coral families in the GBR, the Xeniidae and Nephtheidae, are considered 'fugitive' species, with high rates of growth and asexual reproduction (Fabricius, 1997). These traits are considered beneficial when environmental conditions change (Fabricius, 1997). About seven months after the cyclones passed over our study sites, we noted large numbers of *Lemnalia* sp. (Nephtheidae) in our study sites. Whether they had been propagated sexually or asexually was not known.

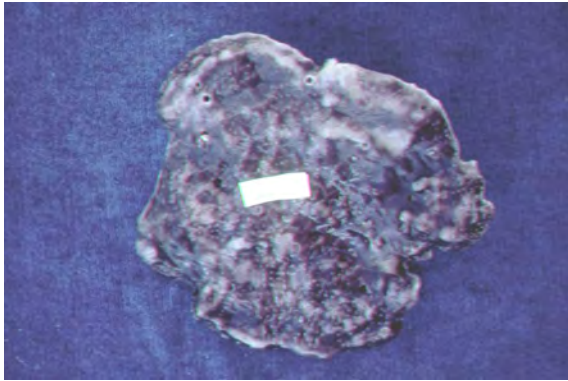
6.5 Appendices

Appendix 6.5–1. Record of the number of species collected from various locations and lodged with the Queensland Museum

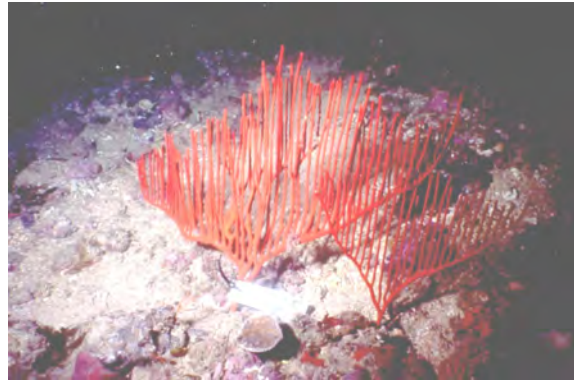
Genus	Species	Locality				Grand Total
		Calliope Deep	Calliope Shallow	Curacao Deep	Curacao Shallow	
<i>Acanthella</i>	820				1	1
<i>Aka</i>	1373					1
<i>Alertigorgia</i>	<i>orientalis</i>				1	1
<i>Amphimedon</i>	<i>terpenensis</i>					1
<i>Anthoplexaura</i>	5232			1		1
<i>Arenosclera</i>	1363					1
<i>Axinella</i>	2950				1	1
<i>Axinella</i>	<i>carteri</i>				1	1
<i>Callyspongia</i>	2022					1
<i>Callyspongia</i>	2393			1		1
<i>Callyspongia</i>	2673					1
<i>Carteriospongia</i>	<i>flabellifera</i>					1
<i>Cinachyrella</i>	1870			1		1
<i>Clathria (Clathria)</i>	<i>kylista</i>			1		1
<i>Clathria (Thalysias)</i>	<i>reinwardti</i>				1	1
<i>Clathria (Thalysias)</i>	<i>vulpina</i>				2	2
<i>Coscinoderma</i>	<i>mathewsi</i>	1	1		2	4
<i>Ctenocella</i>	<i>pectinata</i>			2	1	3
<i>Cymbastella</i>	<i>concentrica</i>			1	1	2
<i>Cymbastella</i>	<i>coralliophila</i>	1	1	1	1	5
<i>Dysidea</i>	<i>arenaria</i>	1				1
<i>Euplexaura</i>	5267			1		1
<i>Euplexaura</i>	5270				1	1
<i>Fascaplysinopsis</i>	1842				1	1
<i>Halichondria</i>	1227			1	1	2
<i>Halichondria</i>	1451		1			1
<i>Halichondria</i>	2658			1	1	2
<i>Halichondria</i>	2949				1	1
<i>Haliclona</i>	1205					1
<i>Hemiassterella</i>	2839	1				1
<i>Higginsia</i>	<i>mixta</i>					1
<i>Hyattella</i>	1366	1				1
<i>Ianthella</i>	<i>basta</i>			2	2	5
<i>Ianthella</i>	<i>cf. flabelliformis</i>			1		1
<i>Ianthella</i>	<i>cf. flabelliformis</i>					1

Genus	Species	Calliope Deep	Calliope Shallow	Curacao Deep	Curacao Shallow	Kelso Reefs	Grand Total
<i>Ianthella</i>	<i>flabelliformis</i>		1	1			2
<i>Ianthella</i>	<i>quadrangulata</i>			1			1
<i>Iotrochota</i>	377			1	1		2
<i>Iotrochota</i>	2256			1	1		2
<i>Iotrochota</i>	2682					1	1
<i>Ircinia</i>	1255					1	1
<i>Ircinia</i>	1523				1		1
<i>Ircinia</i>	2683			1		1	2
<i>Junceella (Dichotella)</i>	<i>divergens</i>			2	1		3
<i>Junceella (Junceella)</i>	<i>fragilis</i>			1			1
<i>Lendenfeldia</i>	<i>plicata</i>					1	1
<i>Lissoclinum</i>	<i>patella</i>					1	1
<i>Menella</i>	5233			1			1
<i>Mopsella</i>	5021			1			1
<i>Mopsella</i>	5268				1		1
<i>Muricella</i>	5269			1			1
<i>Myriastr</i>	<i>clavosa</i>	1		2			3
<i>Niphates</i>	1980			1			1
<i>Niphates</i>	2190			1			1
<i>Niphates</i>	2678					1	1
<i>Niphates</i>	2951			1			1
<i>Paratetilla</i>	2656				1		1
<i>Pericharax</i>	<i>heterorhaphis</i>					1	1
<i>Phakellia</i>	<i>flabellata</i>					1	1
<i>Phyllospongia</i>	<i>lamellosa</i>					1	1
<i>Phyllospongia</i>	<i>papyracea</i>					1	1
<i>Ptilocaulis</i>	<i>fusiformis</i>				1		1
<i>Raphidotethya</i>	415				1		1
<i>Raphidotethya</i>	2655				1		1
<i>Raphidotethya</i>	<i>enigmatica</i>			1	1		2
<i>Semperina</i>	<i>brunei</i>			2	1		3
<i>Siphonochalina</i>	941			1	1		2
<i>Stelletta</i>	1005			1	1		2
<i>Strepsichordaia</i>	<i>lendenfeldi</i>					1	1
<i>Subergorgia</i>	<i>reticulata</i>			3	1		4
<i>Subergorgia</i>	<i>suberosa</i>			2	1		3
<i>Xestospongia</i>	<i>pacifica</i>				1		1
<i>Xestospongia</i>	<i>testudinaria</i>	1		2	1		4
Total		7	4	42	36	22	111

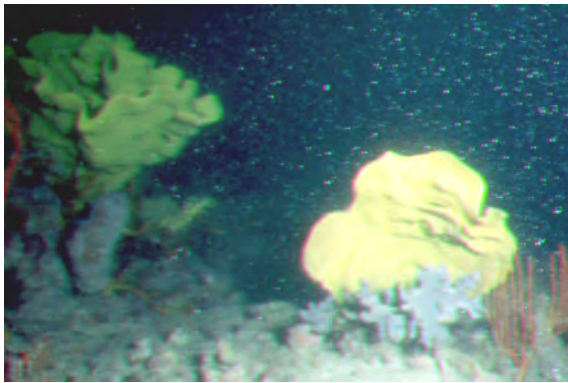
Appendix 6.5-2. Photographs of specimens of tagged species, collected and lodged with the Queensland Museum (including QM specimen reference number)



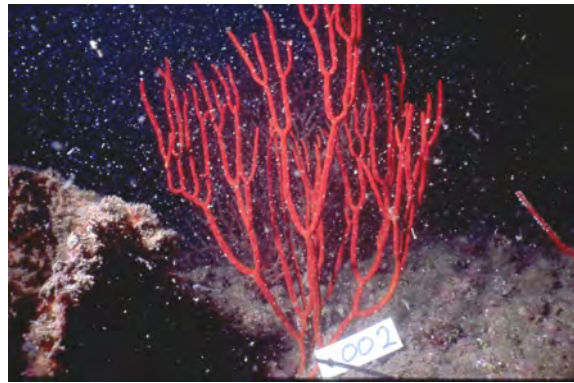
Cymbastella coralliophila G317077



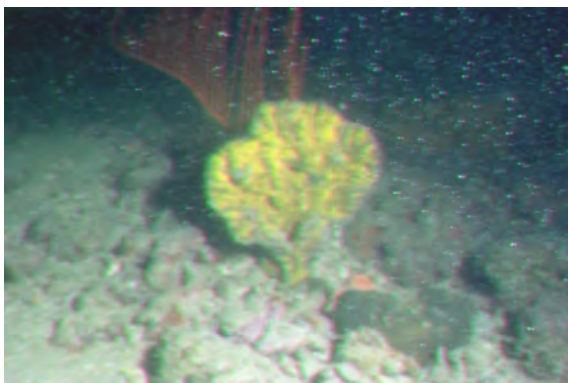
Ctenocella pectinata G314310



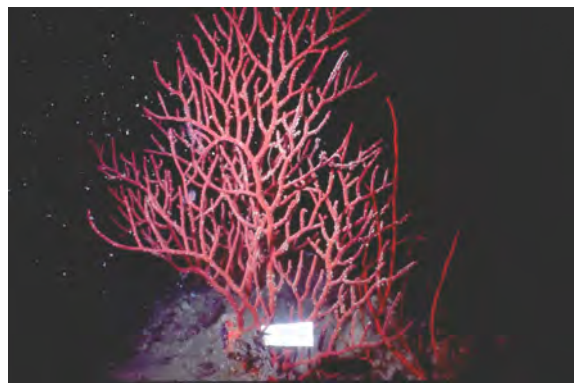
Ianthella basta G317085



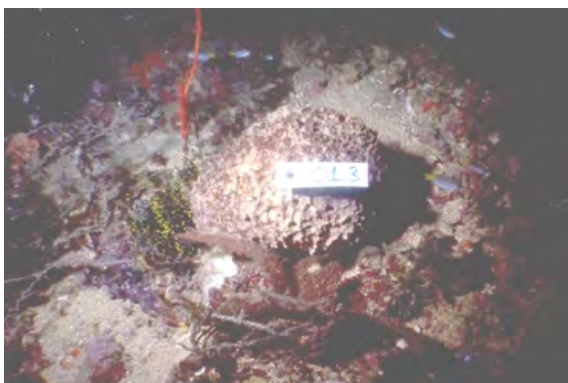
Junceella divergens G314320



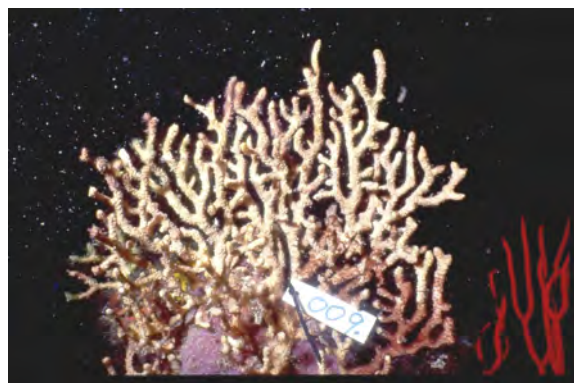
Iotrochota sp. G317102



Subergorgia suberosa G314315



Ircinia sp G314311



Semperina brunea G314325

7 Modelling the dynamics of sessile megabenthos

To model the dynamics of seabed habitat organisms and predict the potential of trawled megabenthos to recover and contribute as fisheries habitat.

Contents

7	Modeling Megabenthos Dynamics	7-105
7.1	Introduction	7-108
7.2	Methods	7-109
7.2.1	Matrix Model	7-109
7.2.2	Size Transitions	7-111
7.2.3	Mortality/Survival	7-113
7.2.4	Recruitment	7-114
7.2.5	Model Scenarios	7-116
7.3	Results	7-117
7.3.1	Recruitment Scenarios for <i>Ctenocella pectinata</i>	7-117
7.3.2	Size-Class Distributions for <i>Ctenocella pectinata</i>	7-118
7.3.3	Effect of Cyclones on <i>Ctenocella pectinata</i>	7-118
7.3.4	Effect of Trawling and Recovery of <i>Ctenocella pectinata</i>	7-122
7.3.5	Establishment Scenario for <i>Ctenocella pectinata</i>	7-122
7.3.6	Cohort Growth and Mortality of <i>Ctenocella pectinata</i>	7-123
7.3.7	Results for Other Species	7-124
7.3.7.1	Size-Class Distributions	7-124
7.3.7.2	Recruitment & Mortality Rates	7-126
7.3.7.3	Effects of Cyclones & Trawling	7-126
7.3.7.4	Recovery after Cyclones & Trawling	7-126
7.3.7.5	Establishment Scenarios	7-128
7.3.7.6	Cohort Growth and Mortality	7-128
7.4	Discussion	7-129
7.6	Appendices	7-136
7.6.1	<i>Subergorgia suberosa</i>	7-136
7.6.2	<i>Junceella divergens</i>	7-141
7.6.3	<i>Turbinaria</i> sp	7-146
7.6.4	<i>Xestospongia testudinaria</i>	7-151
7.6.5	<i>Semperina brunei</i>	7-156
7.6.6	<i>Cymbastella coralliophila</i>	7-161
7.6.7	<i>Ianthella basta</i>	7-166
7.6.8	<i>Subergorgia reticulata</i>	7-171

Tables

Table 7-1.	Width intervals for the 4 size-classes of the gorgonian <i>Ctenocella pectinata</i> , showing the upper and lower boundaries for each size-class, and the initial number of individuals in each size-class tagged during the first measurement field trip	7-111
Table 7-2.	Illustration of size-transition probabilities for the gorgonian <i>Ctenocella pectinata</i> for the 4 size-classes intervals, estimated from simulation of the regression of Size-at-t with Size-at-t+1 (Figure 7-3)	7-112
Table 7-3.	Construction of a mortality and survival vector by size-class for the pre and post cyclone periods for <i>Ctenocella pectinata</i>	7-114
Table 7-4.	Overall transition probabilities for <i>Ctenocella pectinata</i> under normal (non-cyclonic) conditions, for A: 100% external recruitment, B: 50:50 external and self-recruitment, and C: 100% self-recruitment	7-119

Table 7-5. Size-transition matrix, survival probabilities and overall transition probabilities for <i>Ctenocella pectinata</i> under cyclone affected conditions.....	7-120
Table 7-6. Size-class boundaries for size transition matrices of nine megabenthos species.....	7-125
Table 7-7. Mortality rates and required recruitment per model step (6 months) under stable normal conditions, and additional mortality due to a cyclone, a single trawl and 14 multiple trawls, for nine megabenthos species.	7-125
Table 7-8. Observed mortality rates, overall for both normal and cyclonic periods, per 6 month time-step by size-class for nine megabenthos species.	7-126
Table 7-9. Estimated half-recovery times (years) for a single cyclone and a single-trawl impacts, for three different recruitment scenarios, for nine megabenthos species.	7-127
Table 7-10. Estimated half- and full recovery times (years) for a multiple-trawl (14x) impact, for three different recruitment scenarios, for nine megabenthos species.....	7-127
Table 7-11. Estimated half- and full establishment times (years) from zero, given 50:50 external & self-recruitment, for nine megabenthos species.....	7-128
Table 7-12. Cohort annual decay mortality (after reaching a stable size-structure); years to peak Size II, III & IV numbers after recruiting to Size I; % surviving to attain Size IV; mean age & 90%-ile range of survivors attaining Size IV, for nine megabenthos species.	7-129
Table 7-13. Average residence times within each size class I to IV, without mortality, calculated directly from the size-transition matrix, for nine megabenthos species.	7-129
Table 7-14. Observed mortality, density & recruitment summary of study species, contrasted with modeled minimum recruitment to balance mortality for steady-state populations of nine megabenthos species. ..	7-133

Figures

Figure 7-1. Schematic diagram of the dynamics of a size-classified megabenthos organism. Classes I-IV represent increasing size of individuals. In each time-step, a proportion of individuals may stay in the same size-class (L), grow one two or even 3 size-classes (G), shrink one two or even 3 size-classes (S), die (M), or provide recruits to the first size class by sexual or asexual offspring (R).	7-110
Figure 7-2. Components of the matrix model for megabenthos: (a) matrix of size transitions including the proportion of surviving animals for each size class at time t that grow, shrink or remain the same from time t to $t+1$; (b) vector of the proportion animals dying for each size class and for each time-step (survival is $1-M$; note that some formulations implicitly include survival in the size transition matrix); (c) vector of [self-] recruitment for each time-step (note that either fixed external recruitment or density-dependent recruitment or a mixture were used in this report); (d) full model matrix incorporating all components.	7-110
Figure 7-3. Illustration of a “Ford-Walford” plot for <i>Ctenocella pectinata</i> whose width size-class intervals are very close to 20 cm. The continuous line shows linear regression on the paired size measurements from each field trip at time t compared with time $t+1$. The dashed line shows $Y=X$ representing no change in width. The coloured tiles represent the density of 1000 points from simulating the regression with a uniform Size-at- t distribution and normal Size-at- $t+1$ distribution with standard deviation from $s_{Y,X}$ of regression. The colours are related to the probabilities in the size-transition matrix, with dark blue indicating very small probabilities and green indicating higher probabilities.....	7-112
Figure 7-4. Illustration of the density-dependent (DD) recruitment (based on the von Bertalanffy function) for self-seeding in the megabenthos models. For example, a population that required 10 recruits every 6 months to balance mortality and maintain a population size of 100 individuals in a given area, the asymptotic maximum allowed recruitment was arbitrarily set at 1.5x this minimum requirement (ie. 15 recruits). If abundance was less than 100, recruitment exceeded mortality so that the population would grow; however, if abundance was more than 100, mortality exceeded recruitment and the population would decline. At very small population sizes, the DD & non-DD recruitment are ~same (at a rate of $R \sim 0.165$ in this example). The non-DD recruitment would lead to exponential population increase — the maximum population growth rate in this example was ~6.5% per 6 mo (or ~13.4% per year, equivalent to a logistic growth parameter $r \sim 0.126$). The replacement line indicates the level of recruitment required to balance mortality at any population level (10% in this case) — the population size would remain the same as the starting numbers or any externally induced change. Constant recruitment of 10 per time-step is also shown.....	7-115
Figure 7-5. Time trajectory of the four size-classes of <i>Ctenocella pectinata</i> in a model run with 100% external recruitment, showing the simulated impact and recovery from a cyclone, a single trawl and 14 trawls. The model takes ~8 years to half-recover from the cyclone, ~7 years to half-recover from a single trawl, ~8 years to half-recover from 14 trawls and ~38 years to fully recover.	7-120

- Figure 7-6. Time trajectory of the four size-classes of *Ctenocella pectinata* in a model run with 50:50 external & self-recruitment, showing the simulated impact and recovery from a cyclone, a single trawl and 14 trawls. The model takes ~11 years to half-recover from the cyclone, ~11 years to half-recover from a single trawl, ~14 years to half-recover from 14 trawls and ~57 years to fully recover.7-121
- Figure 7-7. Time trajectory of the four size-classes of *Ctenocella pectinata* in a model run with 100% self-recruitment, showing the simulated impact and recovery from a cyclone, a single trawl and 14 trawls. The model takes ~13 years to half-recover from the cyclone, ~15 years to half-recover from a single trawl, ~31 years to half-recover from 14 trawls and ~88 years to fully recover.7-121
- Figure 7-8. Time trajectory of the four size-classes of *Ctenocella pectinata* in a model run to establish a population from zero with 50:50 external & self-recruitment. The model takes ~17 years to half-establish, and more than 100 years to fully establish.....7-123
- Figure 7-9. Time trajectory of the four size-classes of *Ctenocella pectinata* in a model run to establish the fate of a single pulse of 100 Size I recruits (0-19 cm wide), showing survival and growth through to larger size classes. Peak Size IV (>63 cm wide) abundance of ~7% occurs ~6 years after recruitment. Approximately 24.35% of Size I recruits attain Size IV after an average of 5.9 years, with a 90-percentile range of 1.5–14 years.....7-124
- Figure 7-10. Time trajectory of four size-classes of *Agaricia agaricites* in Jamaica (Hughes 1984) in a model run with 100% external recruitment at the observed rate of approx 8.5% (1.47 times that need to sustain the observed density), showing the simulated impact and recovery from a hurricane. Total model colony numbers continued to decline for another ~10 years after the hurricane and took ~27 years to recover to the immediate post-hurricane numbers, ~37 years to half-recover from the hurricane, and ~48 years to fully recover.7-131
- Figure 7-11. (a) Indicators of vulnerability to trawling for nine megabenthos species, as a combination of resilience (complement of removal rate per trawl) and recovery rates (% of ‘carrying capacity’ recovered in first year). The scenario for 50:50 external:self-recruitment is indicated by ●, the lower interval indicates the 100% self-recruitment scenario and the upper interval indicates the 100% external-recruitment scenario. There is of course also uncertainty in the estimates of removal rates. These indicators have been positioned in the wider context of (b) estimated resilience (1-removal rate) for ~900 seabed species (from Poiner et al 1998 dataset), and (c) a hypothetical frequency distribution of species recovery rates from the knowledge that there are many more small short-lived species than large long-lived species. It is the relatively few species that do not have high resilience or fast recovery that management action needs to target in order to achieve sustainability.....7-135

7.1 Introduction

In recent years, there has been increasing community pressure and legislative requirement to ensure that fishing, and other human activities in the marine realm, are environmentally sustainable. There are now several processes that require fisheries to report with respect to environmental sustainability, including: environmental assessments under Schedule 4 of the Wildlife Protection (REI) Act and the Environmental Protection and Biodiversity Conservation Act (EPBC) and a related Ecologically Sustainable Development (ESD) reporting system being implemented by the Standing Committee on Fisheries and Aquaculture (SCFA).

To complete these assessments, indicators are required for the wider environmental risks, impacts of trawling, and preferably also for environmental status and trends. To develop these indicators, information is needed on: the spatial & temporal dynamics of the trawling process; the effects of trawling on the environment; the capacity and rate of recovery of the environment; and the distribution & abundance of ecosystems, habitats and biota that may be affected by trawling. The dynamics of the interaction between trawling and the environment also need to be placed in the context of the dynamics of the environment when no trawling is present. When such complete information is available, it is possible to achieve more than simply monitor and report environmental indicators, but to quantitatively evaluate which management strategies will best achieve environmental sustainability goals (Pitcher *et al.* 2000a) while taking into account consequences for the fishery (eg. Ellis and Pantus, 2001).

This project, and this chapter of the report specifically intends to address some of these important information needs for the interactions between trawling and sessile epifauna on tropical shelf seabeds. Specifically, by synthesizing data on the population dynamics (recruitment, growth, mortality) presented in previous chapters into relatively simple models, we intend to contribute information on the natural dynamics of dominant sessile epifauna where there is no trawling, as context for areas where there are interactions with trawling, and information on the capacity and potential rate of recovery of sessile epifauna after impacts from trawling. We also attempt to estimate the potential re-establishment times of megabenthos in areas where such fauna may have been present previously. This information can be incorporated in the Trawl Scenario Model (Ellis and Pantus, 2001) to assist development of alternative fishing strategies that have less impact on habitat.

7.2 Methods

The growth, mortality and recruitment rates measured by this study (Chapter 6) were the source of information for constructing population dynamics models of some dominant species of large sessile epibenthos. Sufficient data to attempt modeling was collected for nine species. The structure of these models was a relatively simple form, involving a matrix of transition probabilities among size categories. This type of model is based on an age-structured deterministic model (Leslie 1945), generalized to include size-structured population dynamics (reviewed in Usher 1972). Size is a more appropriate basis for describing the dynamics of colonial megabenthos such as sponges and gorgonians, not only because they are difficult to age but because they have indeterminate growth — large variability in growth rate means that individuals of the same age can be of very different sizes, whereas mortality and reproduction are more likely to be related to size (Hughes 1984). Further, the size-based matrix models can readily incorporate aspects of dynamics peculiar to colonial organisms, for example shrinkage, fragmentation, partial mortality and asexual reproduction, which also decouple the relationship between size and age (Hughes 1984). Nevertheless, age can still be important and individual history can affect future fate, though the data are difficult to obtain (Hughes & Connell 1987; Babcock 1991). Hughes (1984) provides a very readable introduction to the dynamics of colonial organisms and a generalized form of this model type (see Figure 7-1). He goes on to apply it to a Caribbean coral in a manner directly analogous to that required herein. Variations of this general form have been applied to a wide range of marine and terrestrial populations (eg. Caswell 1982ab, Hughes & Connell 1987, Crouse *et al.* 1987, Levin *et al.* 1987, Babcock 1991, Pascual & Caswel, 1991, Caswell & Brault 1992).

7.2.1 Matrix model

The empirical observations of the proportions of individuals that follow each path in Figure 7-1 per time step form the parameters of the matrix model (Figure 7-2). The size transition matrix includes the probability that individuals within each size category will grow to larger size category(s), stay in the same category, or even undergo ‘negative’ growth to smaller size category(s). The mortality vector includes the probability that individuals within each size category will die. The recruitment vector includes the probability of new individuals of observable size being added to the smallest size-category, either through asexual or sexual products. Typically all these probabilities differ among size categories.

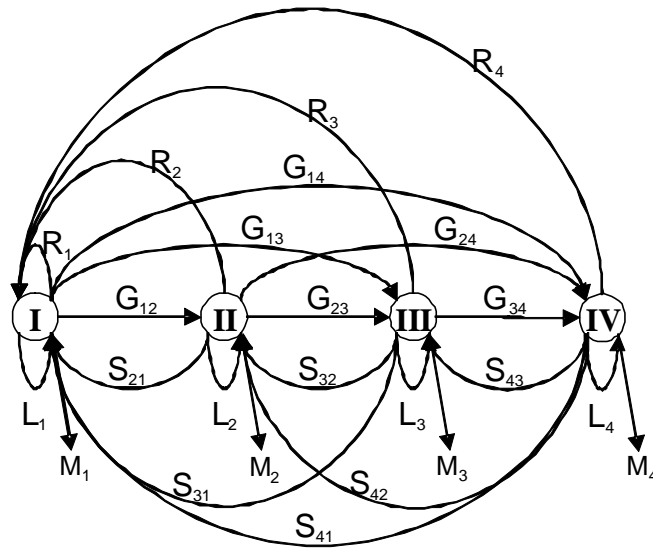


Figure 7-1. Schematic diagram of the dynamics of a size-classified megabenthos organism. Classes I-IV represent increasing size of individuals. In each time-step, a proportion of individuals may stay in the same size-class (L), grow one two or even 3 size-classes (G), shrink one two or even 3 size-classes (S), die (M), or provide recruits to the first size class by sexual or asexual offspring (R).

	Size classes at time t :	I_t II_t III_t IV_t
(a) Size transition matrix at time $t+1$:	$\begin{matrix} I_{t+1} \\ II_{t+1} \\ III_{t+1} \\ IV_{t+1} \end{matrix}$	$\begin{bmatrix} L_1 & S_{21} & S_{31} & S_{41} \\ G_{12} & L_2 & S_{32} & S_{42} \\ G_{13} & G_{23} & L_3 & S_{43} \\ G_{14} & G_{24} & G_{34} & L_4 \end{bmatrix}$
(b) Mortality vector, t to $t+1$:		$[M_1 \quad M_2 \quad M_3 \quad M_4]$
(c) Recruitment vector:		$[R_1 \quad R_2 \quad R_3 \quad R_4]$
(d) Model matrix:		$\begin{bmatrix} R_1 + L_1 \cdot (1 - M_1) & R_2 + S_{21} \cdot (1 - M_2) & R_3 + S_{31} \cdot (1 - M_3) & R_4 + S_{41} \cdot (1 - M_4) \\ G_{12} \cdot (1 - M_1) & L_2 \cdot (1 - M_2) & S_{32} \cdot (1 - M_3) & S_{42} \cdot (1 - M_4) \\ G_{13} \cdot (1 - M_1) & G_{23} \cdot (1 - M_2) & L_3 \cdot (1 - M_3) & S_{43} \cdot (1 - M_4) \\ G_{14} \cdot (1 - M_1) & G_{24} \cdot (1 - M_2) & G_{34} \cdot (1 - M_3) & L_4 \cdot (1 - M_4) \end{bmatrix}$

Figure 7-2. Components of the matrix model for megabenthos: (a) matrix of size transitions including the proportion of surviving animals for each size class at time t that grow, shrink or remain the same from time t to $t+1$; (b) vector of the proportion animals dying for each size class and for each time-step (survival is $1-M$; note that some formulations implicitly include survival in the size transition matrix); (c) vector of [self]-recruitment for each time-step (note that either fixed external recruitment or density-dependent recruitment or a mixture were used in this report); (d) full model matrix incorporating all components.

In these size-based matrix models, there is a trade-off between size-resolution and precision of the matrix parameters (Hughes 1984). For each megabenthos species modeled in this study, four size categories were used because mortality rates were low, relatively few deaths were observed (between 1-11 deaths per species) and to have attempted a greater number of size

categories would have been unwarranted. Conversely, fewer size categories would have yielded insufficient size-resolution, and where fewest deaths were observed a single overall estimate of mortality was used for each size-class. In these cases, continued observations are necessary to improve precision. For mortality, the data were divided into size-quartiles to provide a balanced number of observations for survival/mortality. For size-transitions, equal size-intervals were chosen (eg. Table 7-1), with the middle break-point between size-classes II and III related to the mean of all measurements of tagged individuals, the mean of a series of measurements of random individuals taken during the study, and the mean of individuals measured in the far northern Great Barrier Reef by another study (Pitcher *et al.* 2000b).

Table 7-1. Width intervals for the 4 size-classes of the gorgonian *Ctenocella pectinata*, showing the upper and lower boundaries for each size-class, and the initial number of individuals in each size-class tagged during the first measurement field trip.

Size class	Small	Medium Small	Medium Large	Large
Category	I	II	III	IV
Lower	0	20.48	40.97	61.46
Upper	20.48	40.97	61.46	81.95 & larger
Count	9	8	4	4

Further, during the later part of the field studies two cyclones passed through the study area. These events provided an opportunity to measure the impact of cyclones on megabenthos, though this benefit came with a drawback. The observations of size-transitions and mortality needed to be split into pre-cyclone and cyclone-affected partitions, which reduced the number of observations in each size-class within these partitions.

7.2.2 Size transitions

The measurements of size of each individual formed the basis of the size-transition matrix of each taxon. The size measurements (typically height) from each field trip (H_t) were paired with those of the same individuals from the next subsequent field trip (H_{t+1}), each typically 5-7 months apart. All size increments were standardized to 6 month intervals. These size measurement pairs were plotted in the manner of a Ford-Walford plot as applied to growth of fish populations in stock-assessment (Figure 7-3). However, the parameters of the Ford-Walford plot are inappropriate for the growth of megabenthos because megabenthos can 'shrink' substantially. For example, in the case of *Ctenocella pectinata*, the L_∞ (asymptotic size, from point where regression crosses $Y=X$, Figure 7-3) is only ~30 cm width, whereas

some of these gorgonians probably achieve this width in 3-4 years and many are much larger. An alternative approach was taken. The Ford-Walford regression was simulated to estimate transition probabilities because of the unevenness of real measurement-pairs in some size-classes for some taxa. The simulation was done by taking 1000 points from the regression with a uniform random Size-at- t distribution and normal random Size-at- $t+1$ distribution:

$$H_{t+1} = b \cdot H_t + c + N(0, s_{Y.X})$$

where b is the slope of regression, c is the intercept, and N is a normal deviate with mean 0 and standard deviation from the standard error of regression ($s_{Y.X}$). The simulated data were binned into size-classes and the probabilities in the size-transition matrix were estimated from the proportion of points in each $t+1$ size-class, relative to each t size-class (see Figure 7-3 and Table 7-2 for illustration of these methods).

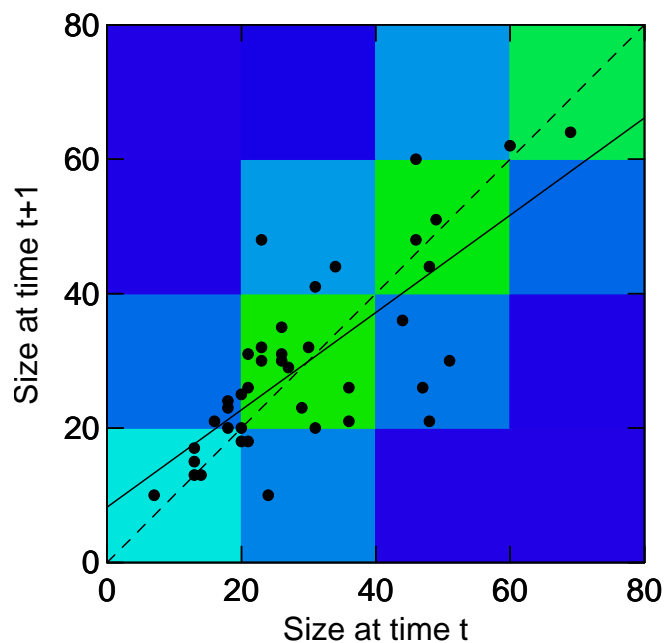


Figure 7-3. Illustration of a “Ford-Walford” plot for *Ctenocella pectinata* whose width size-class intervals are very close to 20 cm. The continuous line shows linear regression on the paired size measurements from each field trip at time t compared with time $t+1$. The dashed line shows $Y=X$ representing no change in width. The coloured tiles represent the density of 1000 points from simulating the regression with a uniform Size-at- t distribution and normal Size-at- $t+1$ distribution with standard deviation from $s_{Y.X}$ of regression. The colours are related to the probabilities in the size-transition matrix, with dark blue indicating very small probabilities and green indicating higher probabilities.

Table 7-2. Illustration of size-transition probabilities for the gorgonian *Ctenocella pectinata* for the 4 size-classes intervals, estimated from simulation of the regression of Size-at- t with Size-at- $t+1$ (Figure 7-3).

Class at t+1	Size class at t			
	I	II	III	IV
I	0.723	0.154	0.004	0.000
II	0.272	0.660	0.239	0.004
III	0.004	0.170	0.576	0.240
IV	0.000	0.015	0.182	0.756

7.2.3 Mortality/survival

The number of observations of survival & deaths of individuals during intervals between field-trips formed the basis of the mortality vector for each taxon. These observations were grouped into the size-class of the individual as measured during the field trip at the beginning of each interval, each typically 5-7 months duration.

Due to the influence of the two cyclones on the study animals and the partitioning of the data as a consequence, there were relatively few deaths observed in each combination of size-class and cyclone ‘treatment’. To avoid excessive heterogeneity due to random influences among these few fully partitioned observations, the observations were separately grouped in to size-classes for overall estimates of mortality by size-class and into cyclone ‘treatments’ for overall estimates of the influence of cyclones on mortality. This assumed that there was no difference in the pattern of mortality among size-classes in the periods before and during cyclones. This assumption was tested for those taxa with the greatest number of mortality observations (11), by chi-square test of cross-tabulated relative frequencies, and found to be non-significant (*Ctenocella pectinata*, $p=0.83$; *Subergorgia suberosa*, $p=0.36$; *Xestospongia*, $p=0.41$). In the case of *Subergorgia reticulata*, only 1 death was observed and a single overall estimate of mortality was used for each size-class and each cyclone ‘treatment’. This approach is not ideal, but additional observations are needed to improve on this situation.

The method of constructing the size-class mortality vector for each cyclone ‘treatment’ is illustrated for *Ctenocella pectinata* (Table 7-3). There were a total of 11 deaths in 109 observations for *C. pectinata* (overall $M=0.101$). For size-class I, there were 7 deaths in 32 observations ($M=0.219$); for size-class II, there was 1 death in 21 observations ($M=0.048$); for size-class III, there were 2 deaths in 30 observations ($M=0.067$); for size-class IV: there was 1 death in 26 observations ($M=0.038$). For the pre-cyclone period, there were 4 deaths in 57 observations ($M=0.071$); for the post-cyclone period, there were 7 deaths in 52 observations ($M=0.135$). The matrix model actually used survival parameters ($S=1-M$), so the mortality vector was converted to a survival vector. In the *C. pectinata* method illustration (Table 7-3), total survival was 0.899; pre-cyclone survival was 0.929; and post-cyclone survival was 0.865. The pre and post cyclone survival rates for individual size-classes were calculated from the product of the overall survival by size-class and the ratio of pre or post-cyclone survival over total survival.

Table 7-3. Construction of a mortality and survival vector by size-class for the pre and post cyclone periods for *Ctenocella pectinata*.

Vector	Size-class				Total
	I	II	III	IV	
Overall M	0.219	0.048	0.067	0.038	0.101
Overall S	0.781	0.952	0.933	0.962	0.899
Pre-Cyclone	0.808	0.985	0.965	0.994	0.929
Post-Cyclone	0.752	0.917	0.898	0.925	0.865

7.2.4 Recruitment

In the models implemented here, the numbers of recruits needed to replace animals lost due to natural mortality was estimated, and later compared with recruit densities observed in the field study sites. The source of recruitment in the field was unknown; consequently, in the models the implications of alternative hypothetical sources of recruitment was examined: either constant recruitment (ie. sourced from external sources), or from density-dependent self-recruitment, or from a 50:50 mix of both. In the case of the self-recruitment alternatives, it was necessary to implement density-dependence because a recruitment vector that was sufficient only to replace natural mortality losses would not allow the population to rebuild after any deleterious perturbation; on the other hand, a recruitment vector that provided more recruits than natural mortality losses would cause the population to grow exponentially to infinity. Any relationship for the density-dependent self-recruitment was also unknown; however, to implement this behaviour in the models, the von Bertalanffy function was used in a consistent manner for all taxa (Figure 7-4). The function for the density-dependent self-recruitment was:

$$\text{Number of recruits} = R_{\infty} \cdot \left(1 - e^{\left(\frac{-1}{R_{\infty}} \cdot \sum_{n=1}^4 (N_n \cdot R_n) \right)} \right),$$

where R_{∞} was the maximum number of recruits and was arbitrarily set at a 1.5 *multiple* of the constant number of ‘external’ recruits needed to maintain a stable meta-population size of 100 individuals in a given area and depended on the overall mortality rate of each species; N_n was the number of animals in size-class n at a given time-step; and R_n was the element from the recruitment vector. The elements of the recruitment vector were also arbitrarily set to yield sufficient recruits for replacement at a population size of 100 — in the simple case of a single size class then:

$$R = M \cdot \text{multiple} \cdot \left(-\ln \left(1 - \frac{1}{\text{multiple}} \right) \right).$$

The relativity's among the individual elements depended on the growth form of the animal: for planar growth-forms the relative contribution was related to the average area of each size-class, and for massive growth-forms the relative contribution was related to the average volume of each size-class. With the 1.5 *multiple*, this function always produced ~64% more recruits at very low abundance's than the minimum for replacement. Other multipliers >1 could have been used, eg. a 1.25 multiplier would have produced ~100% more recruits at very low abundance's than the minimum for replacement and would have lead to faster recoveries from perturbations; a multiplier of 2 would have produced ~40% more recruits at very low abundance's than the minimum for replacement and would have lead to slower recoveries from perturbations.

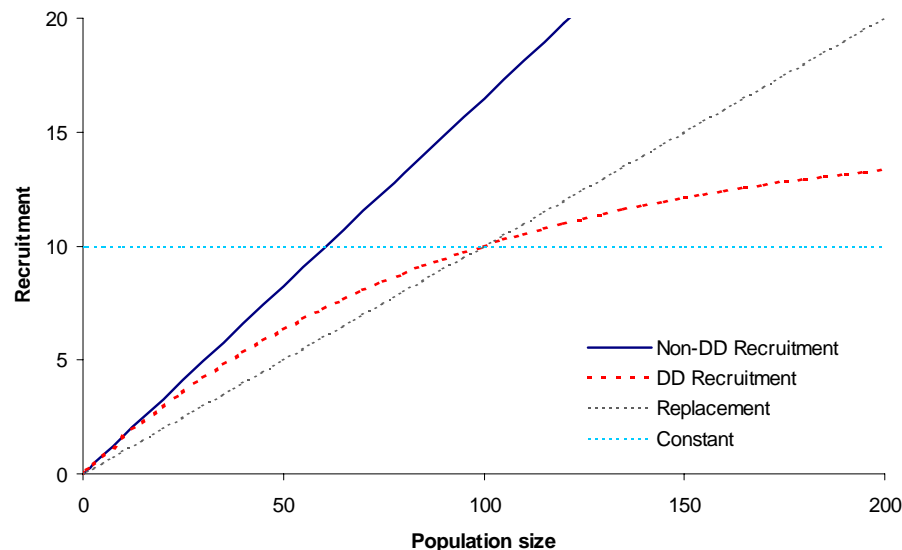


Figure 7-4. Illustration of the density-dependent (DD) recruitment (based on the von Bertalanffy function) for self-seeding in the megabenthos models. For example, a population that required 10 recruits every 6 months to balance mortality and maintain a population size of 100 individuals in a given area, the asymptotic maximum allowed recruitment was arbitrarily set at 1.5x this minimum requirement (ie. 15 recruits). If abundance was less than 100, recruitment exceeded mortality so that the population would grow; however, if abundance was more than 100, mortality exceeded recruitment and the population would decline. At very small population sizes, the DD & non-DD recruitment are ~same (at a rate of $R \sim 0.165$ in this example). The non-DD recruitment would lead to exponential population increase — the maximum population growth rate in this example was ~6.5% per 6 mo (or ~13.4% per year, equivalent to a logistic growth parameter $r \sim 0.126$). The replacement line indicates the level of recruitment required to balance mortality at any population level (10% in this case) — the population size would remain the same as the starting numbers or any externally induced change. Constant recruitment of 10 per time-step is also shown.

Although density-dependence could occur at any or all other life-stages, it was most parsimonious to include this behaviour for recruitment, given that the majority of assumptions were made for this stage, rather than complicating the observed data on growth and mortality.

The matrix models can include the possible effects of density of the same and other benthos taxa, but replicated and controlled manipulation of such factors was not possible in this project. More extensive future work may be able to identify any relationships for density-dependence in these processes. It was also not possible to obtain data on the effect of reproductive potential and proximity of larval supply sources external to the meta-populations studied, though this may be important.

7.2.5 Model scenarios

Having constructed the matrix model for each taxon, as per Figure 7-2(d), initially each model was set-up with normal (non-cyclonic) transition probabilities and starting size-class frequencies from measurements in the far northern Great Barrier Reef by another study (Pitcher *et al.* 2000b), or from measurements of random individuals taken during this study, or from measurements of tagged individuals. Then each model was run out to 100 years (200 six month time-steps) to examine the stable size-class distribution and the number of recruits required to maintain a population of 100 individuals, for the three recruitment scenarios (100% external, 100% D-D self-recruitment, 50:50 external:self-recruitment).

For each of the three hypothetical recruitment scenarios, the impact and potential recovery from a cyclone and two levels of trawling was modeled separately, after an initial period of 15 years to reach a stable size distribution. The impact of a cyclone was simulated by inserting the size-transition matrix and mortality vector from the cyclone period for a single time-step. The impact of trawling was simulated by inserting a vector incorporating trawl removal rates (from Poiner *et al.* 1998), and density and deterioration in condition of animals remaining on the seabed (from Pitcher *et al.* 2000b), between two time-steps. The two levels of trawling were a single trawl, and multiple-trawls where the trawl removal and condition deterioration rates were compounded 14-fold. To put these trawl intensities in context, about $\sim 1/2$ of recorded trawl-grounds are trawled once or more per year and about $\sim 1/200$ of recorded trawl-grounds are trawled ≥ 14 times per year (Pitcher *et al.* 2000). For the cyclone and single-trawl impact scenarios, the number of years for the population to return half-way to the pre-impact status was estimated (half-recovery time). For the multiple-trawl (14x) impact, the half-recovery times, and full recovery times (the number of years for the population to return to within 1% of the pre-impact status) were estimated.

Another model scenario was to estimate the potential establishment times of megabenthos in hypothetical areas where such fauna could grow but where they have been completely removed by some impact, which does not occur again. Half and full (99%) establishment times (years) from zero were estimated given 50:50 external & self-recruitment. This recruitment option was chosen because a fully self-recruiting population could never re-establish from a zero state and, on the other hand, a constant external recruitment is unlikely though it would lead to faster establishment times. Scenarios of this type provide an indication of how fast epibenthic habitat may recover in new refuge areas in the GBR and similar tropical seabed regions.

A final model scenario was to estimate the fate of a single cohort of 100 recruits. This helped to illustrate more clearly the time required for animals to reach larger size classes and estimate the proportion of recruits that may attain the largest size class. Average residence times in each size class were also estimated (excluding mortality) from the probabilities in the diagonal of the size-transition matrix (ie. $0.5/(1-L_n)$ years, where 0.5 represents the 6 monthly time-steps).

7.3 Results

The results are described in some detail for one species (*Ctenocella pectinata*), then summarized for the remainder, with details given in 7.5 Appendices.

7.3.1 Recruitment scenarios for *Ctenocella pectinata*

For *Ctenocella pectinata*, the normal (non-cyclonic) size-transition matrix and survival probabilities were shown in Table 7-2 and Table 7-3. The overall transition probabilities from combining the size, survival and recruitment parameters is given in Table 7-4; the result is slightly different depending on the recruitment scenario (Table 7-4 A-C). In the 100% external (constant) recruitment scenario, 6.85 recruits were required every 6 months to balance mortality and maintain a population of 100 individuals (Table 7-4 A). In the 50:50 external:self-recruitment scenario, the same total number of recruits were required every 6 months to maintain the population of 100 individuals but only 3.425 came from a constant external source and the remainder came from the population according to the self-recruitment probability vector (Table 7-4 B). In the 100% self-recruitment scenario, again the same total

number of recruits were required to maintain the population, but none came from external sources and the self-recruitment vector parameters needed to be larger (Table 7-4 C).

7.3.2 Size-class distributions for *Ctenocella pectinata*

The model rapidly departed from the initial size-class frequency, set from existing data, and settled on a somewhat different frequency distribution after about 15 years, remaining stable for the remainder of the model to 100 years (see the first 15 years of Figure 7-5, Figure 7-7, or Figure 7-6, which also show other scenarios described below). Because the model's stable size-class distribution differed from the field measured frequencies, it can be inferred that either the field frequencies were measured with error or had been perturbed from the stable state by some event(s) or that the observations leading to the model parameters were not taken from a population in a stable state. In reality it is likely that all were the case — it is highly unlikely that any of these megabenthos populations are in a stable state as any variation in recruitment, growth or survival will lead to constantly changing size-class frequencies. Nevertheless, the model size-class frequencies are not very dissimilar to field observations — the model did not diverge into highly unlikely distributions that would indicate the transition probabilities were suspect (but see below for *Turbinaria* sp., *Cymbastella coralliophila*, and *Ianthella basta*).

7.3.3 Effect of cyclones on *Ctenocella pectinata*

The cyclone affected size-transition matrix, survival probabilities and overall transition probabilities for *Ctenocella pectinata* are shown in Table 7-5. The impact and recovery from a cyclone, for each of the three recruitment scenarios is illustrated in Figure 7-5, Figure 7-7 and Figure 7-6. Overall, the cyclone appeared to cause an additional 6-7% mortality in the population (about double the normal rate) and most of the impact appeared to be on size-class II because of lower transition rates from size-classes I & III. The pattern for size-class I differs among scenarios because the model did not include self-recruitment for the immediate time-step of the cyclone. The recovery after the cyclone depended on the recruitment scenario: with 100% external recruitment, half-recovery occurred in about 8 years; with 50:50 external:self-recruitment, the half-recovery time was ~11 years; and with 100% self-recruitment scenario, half-recovery was ~13 years.

Table 7-4. Overall transition probabilities for *Ctenocella pectinata* under normal (non-cyclonic) conditions, for A: 100% external recruitment, B: 50:50 external and self-recruitment, and C: 100% self-recruitment.**A: 100% external recruitment**

Self Recruitment Probabilities

Yr+1 Class	Size class in Yr			
	I	II	III	IV
I	0.000	0.000	0.000	0.000

Overall Transition Probabilities

Yr+1 Class	Size class in Yr			
	I	II	III	IV
I	0.584	0.152	0.004	0.000
II	0.220	0.650	0.230	0.004
III	0.004	0.167	0.556	0.239
IV	0.000	0.015	0.175	0.751
TOTAL	0.808	0.985	0.965	0.994

External Recruitment Numbers

6.85

B: 50:50 external and self-recruitment

Self Recruitment Probabilities

Yr+1 Class	Size class in Yr			
	I	II	III	IV
I	0.002	0.020	0.061	0.123

Overall Transition Probabilities

Yr+1 Class	Size class in Yr			
	I	II	III	IV
I	0.586	0.173	0.065	0.123
II	0.220	0.650	0.230	0.004
III	0.004	0.167	0.556	0.239
IV	0.000	0.015	0.175	0.751
TOTAL	0.810	1.005	1.026	1.117

External Recruitment Numbers

3.425

C: 100% self-recruitment

Self Recruitment Probabilities

Yr+1 Class	Size class in Yr			
	I	II	III	IV
I	0.006	0.055	0.165	0.333

Overall Transition Probabilities

Yr+1 Class	Size class in Yr			
	I	II	III	IV
I	0.590	0.208	0.169	0.333
II	0.220	0.650	0.230	0.004
III	0.004	0.167	0.556	0.239
IV	0.000	0.015	0.175	0.751
TOTAL	0.813	1.040	1.130	1.327

External Recruitment Numbers

0

Table 7-5. Size-transition matrix, survival probabilities and overall transition probabilities for *Ctenocella pectinata* under cyclone affected conditions.

Cyclone Growth Transition Probabilities

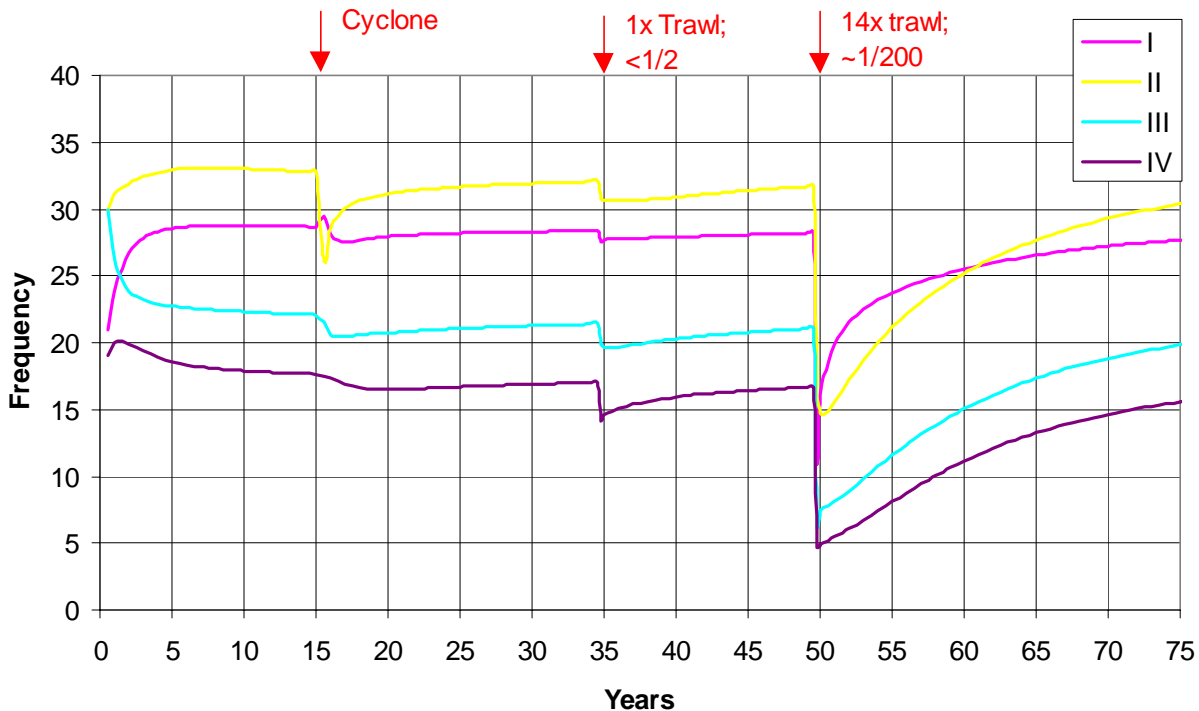
Yr+1 Class	Size class in Yr			
	I	II	III	IV
I	0.829	0.158	0.000	0.000
II	0.171	0.650	0.144	0.000
III	0.000	0.192	0.677	0.147
IV	0.000	0.000	0.179	0.853
TOTAL	1.000	1.000	1.000	1.000

Cyclone Survival Probabilities

Size class in Yr			
I	II	III	IV
0.752	0.917	0.898	0.925

Overall Cyclone Transition Probabilities

Yr+1 Class	Size class in Yr			
	I	II	III	IV
I	0.624	0.145	0.000	0.000
II	0.128	0.596	0.129	0.000
III	0.000	0.176	0.608	0.136
IV	0.000	0.000	0.161	0.790
TOTAL	0.752	0.917	0.898	0.925

**Figure 7-5.** Time trajectory of the four size-classes of *Ctenocella pectinata* in a model run with 100% external recruitment, showing the simulated impact and recovery from a cyclone, a single trawl and 14 trawls. The model takes ~8 years to half-recover from the cyclone, ~7 years to half-recover from a single trawl, ~8 years to half-recover from 14 trawls and ~38 years to fully recover.

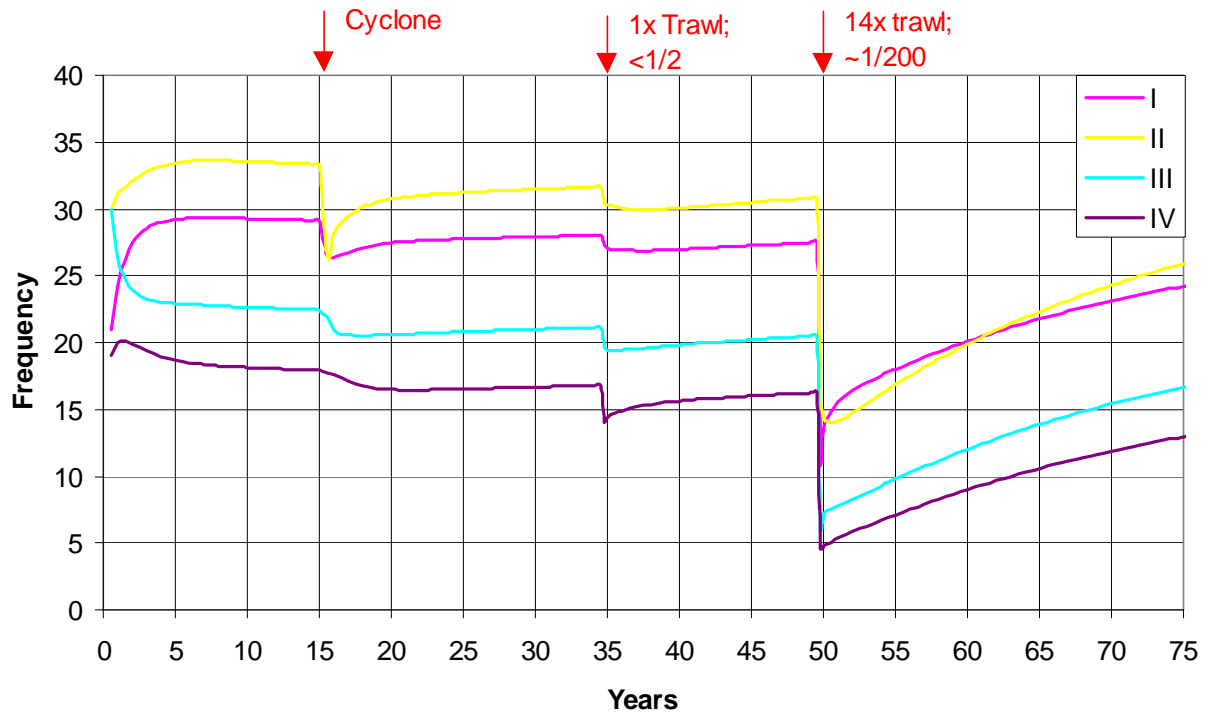


Figure 7-6. Time trajectory of the four size-classes of *Ctenocella pectinata* in a model run with 50:50 external & self-recruitment, showing the simulated impact and recovery from a cyclone, a single trawl and 14 trawls. The model takes ~11 years to half-recover from the cyclone, ~11 years to half-recover from a single trawl, ~14 years to half-recover from 14 trawls and ~57 years to fully recover.

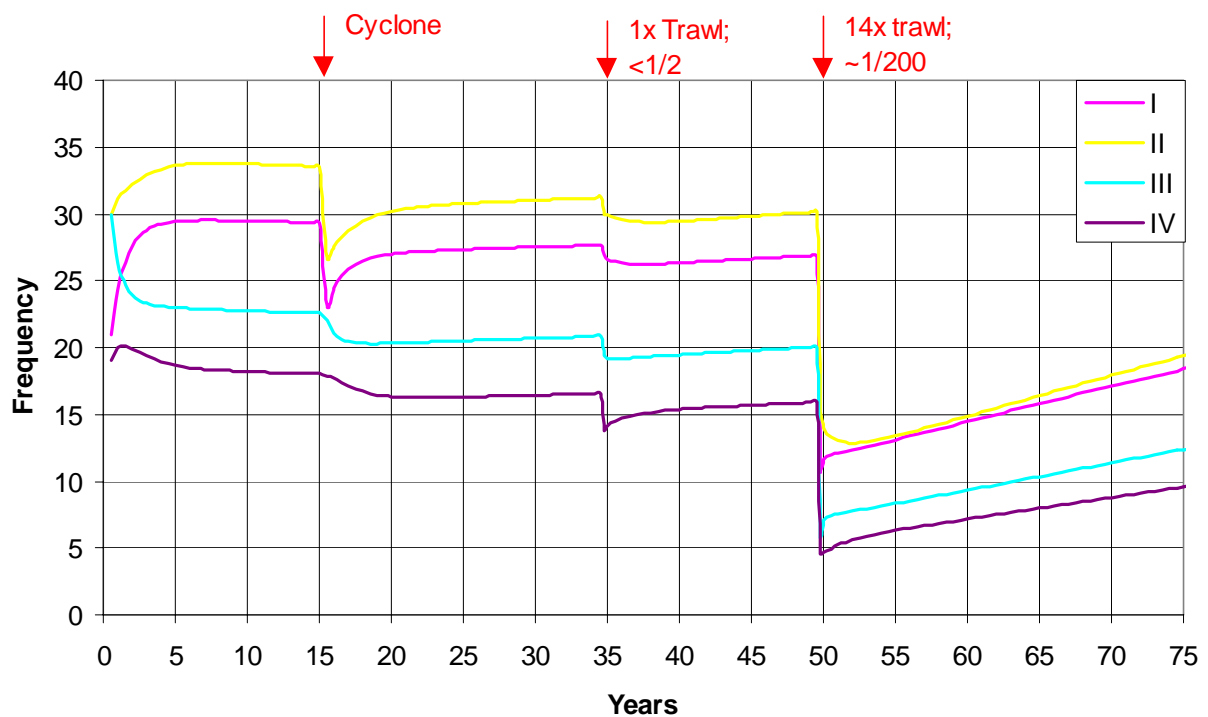


Figure 7-7. Time trajectory of the four size-classes of *Ctenocella pectinata* in a model run with 100% self-recruitment, showing the simulated impact and recovery from a cyclone, a single trawl and 14 trawls. The model takes ~13 years to half-recover from the cyclone, ~15 years to half-recover from a single trawl, ~31 years to half-recover from 14 trawls and ~88 years to fully recover.

7.3.4 Effect of trawling and recovery of *Ctenocella pectinata*

The impact and recovery of *Ctenocella pectinata* from a single trawl, for each of the three recruitment scenarios is also illustrated in Figure 7-5, Figure 7-7 and Figure 7-6. Overall, the 1x trawl appeared to cause an additional 6-7% mortality in the population (similar to a cyclone) and the impact was relatively greater on larger size-classes (Pitcher *et al.* 2000b). The recovery after the trawl was also similar to the cyclone impact and was dependent on the recruitment scenario: with 100% external recruitment, half-recovery occurred in about 7 years; with 50:50 external:self-recruitment, the half-recovery time was ~11 years; and with 100% self-recruitment scenario, half-recovery was ~13-15 years.

The impact and recovery of *Ctenocella pectinata* from the multiple-trawl (14x) impact, for each of the three recruitment scenarios is again illustrated in Figure 7-5, Figure 7-7 and Figure 7-6. Overall, the 14x trawl appeared to cause an additional ~58% mortality in the population and again the impact was relatively greater on larger size-classes. The recovery after such a large impact was lengthy and was dependent on the recruitment scenario: with 100% external recruitment, half-recovery occurred in about 7-8 years; with 50:50 external:self-recruitment, the half-recovery time was ~14-15 years; and with 100% self-recruitment, half-recovery was ~29-31 years. The time taken for “full” recovery was very imprecise because the model has asymptotic behaviour close to ‘carrying capacity’, particularly with density dependent self-recruitment. Full recovery time with 100% external recruitment was in the vicinity of 40 years; with 50:50 external:self-recruitment, the full-recovery time was ~60 years; and with 100% self-recruitment, full-recovery took ~90 years.

Clearly, recovery of *Ctenocella pectinata* from any impact will be dependent on the actual recruitment rates into affected habitats.

7.3.5 Establishment scenario for *Ctenocella pectinata*

In the hypothetical model scenario of establishment of *Ctenocella pectinata* in areas where this species could grow but where they were absent, with 50:50 external & self-recruitment, establishment times were lengthy (Figure 7-8). Half establishment times were about 17 years and full establishment may take more than 100 years. However, as above, full establishment was very imprecise because the model has asymptotic behaviour close to ‘carrying capacity’.

Further, establishment is more dependent on recruitment rates than growth rates, as the higher initial recruitment rates of the constant external scenario (6.85 recruits per time step) lead to half-establishment in 7-8 years and animals can grow to size-class IV in about 6 years (see 7.3.6 below). Nevertheless, this indicated that *Ctenocella pectinata* may take several to many decades to re-establish if they were completely removed from tropical seabed areas.

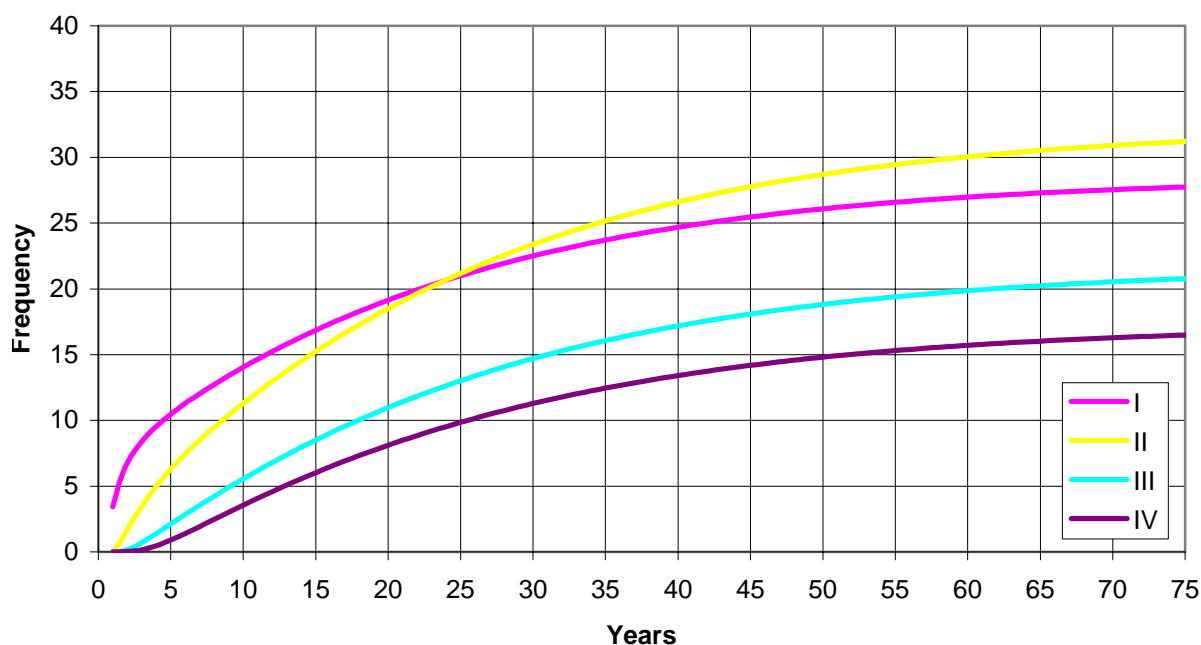


Figure 7-8. Time trajectory of the four size-classes of *Ctenocella pectinata* in a model run to establish a population from zero with 50:50 external & self-recruitment. The model takes ~17 years to half-establish, and more than 100 years to fully establish.

7.3.6 Cohort growth and mortality of *Ctenocella pectinata*

The fate of a single cohort of 100 recruits of *Ctenocella pectinata* is illustrated in Figure 7-9. The cohort decays quite rapidly due to mortality at an overall rate of ~8.1% per year, after reaching a stable size distribution. Following recruitment to Size I, some individuals grow quite rapidly and typically, Size II is attained in ~2 years and Size III in ~4 years. Size IV is attained after an average of 5.9 years (90-percentile range of 1.5–14 years) and about 24% of recruits eventually reach this size (>63 cm width). A few *Ctenocella pectinata* reach much larger sizes (up to ~1.2 m wide) and may be much older, though their ages are unknown. These growth rates coincide closely with the average residence times (excluding mortality) in each size class I to IV of 1.8, 1.5, 1.2, and 2.0 years respectively.

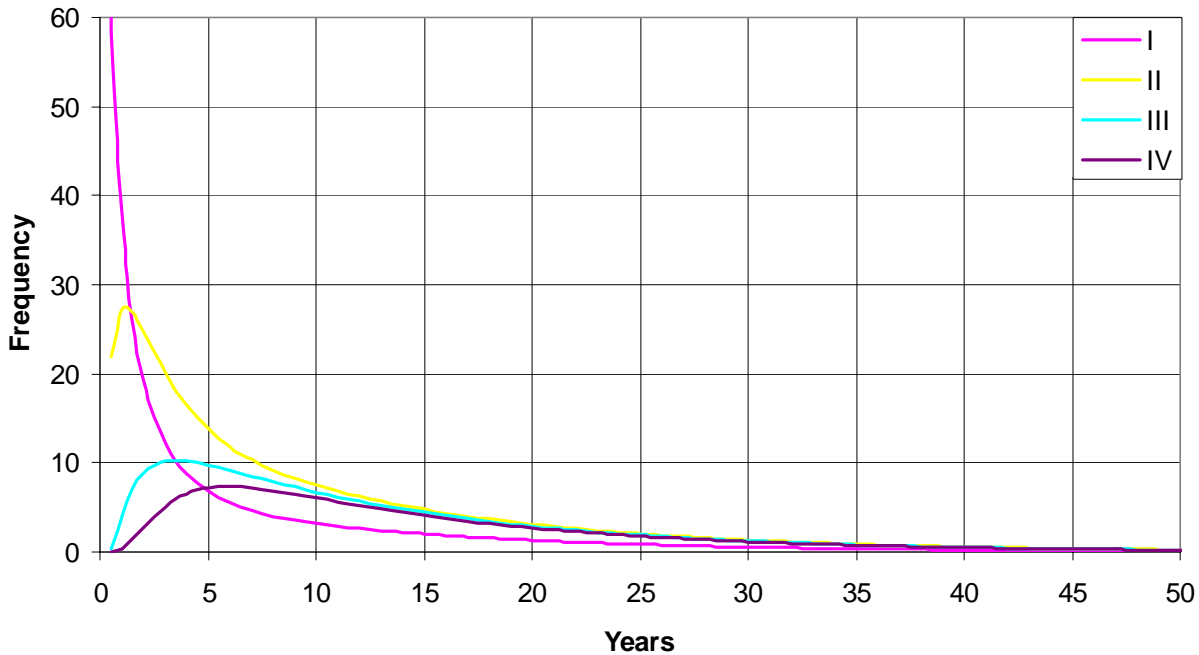


Figure 7-9. Time trajectory of the four size-classes of *Ctenocella pectinata* in a model run to establish the fate of a single pulse of 100 Size I recruits (0-19 cm wide), showing survival and growth through to larger size classes. Peak Size IV (>63 cm wide) abundance of ~7% occurs ~6 years after recruitment. Approximately 24% of Size I recruits attain Size IV after an average of 5.9 years, with a 90-percentile range of 1.5–14 years.

7.3.7 Results for other species

The results for other species are summarized here in a similar format to that just described in detail for *Ctenocella pectinata*. The detailed tables and figures for these species are provided in 7.5 Appendices.

7.3.7.1 Size-class distributions

The boundaries between the four size-classes for all nine species are shown in Table 7-6. Height was modeled for most species, but area was more appropriate for *Cymbastella* and *Turbinaria*. The approximate diameter equivalents of these area boundaries for these two species are 16.2, 27.9, 36.0 cm and 22.3, 31.7, 39.0 cm respectively.

As with *Ctenocella pectinata*, the models for other species departed from the initial size-class frequency, set from existing data, and settled on a somewhat different frequency distribution, remaining stable after about 15 years. Except for *Turbinaria* sp., *Cymbastella coralliophila*, and *Ianthella basta*, the models did not diverge into highly unlikely distributions that might indicate the transition probabilities were suspect. For these three species, under ‘normal’ (cf.

cyclonic) conditions, the size-at- t vs size-at- $t+1$ plots (eg. like Figure 7-3) remained above and ~parallel to & did not cross the $Y=X$ line, implying infinite growth. This, combined with high observed survival for all or larger size-classes, lead to an accumulation of the population into Size-Class IV, producing a size-frequency distribution that was never observed in the field, either in this study or any other. If the transitions were realistic, then some event(s) must cause disproportionately higher mortality in larger size-classes, or transitions to smaller size-classes, to lead to the observed distributions. Storms have the potential to do this. However, although the two cyclones during the study caused higher mortality in each case, these increases did not appear to be greater among larger size-classes. Notwithstanding the possibility that some non-normal conditions may control size-distributions to the observed range, for these species the mortality rate of the largest size-class was increased in the model, while keeping the total mortality constant, to bring the size-distributions within the observed ranges. More observations would be required to overcome this uncertainty.

Table 7-6. Size-class boundaries for size transition matrices of nine megabenthos species.

Species	I – II	II – III	III – IV
<i>Ctenocella pectinata</i> , width cm	20.48	40.97	61.46
<i>Cymbastella coralliophila</i> , area cm ²	206.49	612.72	1018.94
<i>Ianthella basta</i> , height cm	15.17	30.44	45.71
<i>Junceella divergens</i> , height cm	15.27	26.71	38.14
<i>Semperina brunei</i> , height cm	22.75	38.33	53.90
<i>Subergorgia reticulata</i> , height cm	25.18	50.82	76.47
<i>Subergorgia suberosa</i> , height cm	14.42	24.00	33.58
<i>Turbinaria</i> sp., area cm ²	389.90	791.71	1193.52
<i>Xestospongia testudinaria</i> , height cm	14.45	24.17	33.90

Table 7-7. Mortality rates and required recruitment per model step (6 months) under stable normal conditions, and additional mortality due to a cyclone, a single trawl and 14 multiple trawls, for nine megabenthos species.

Species	Normal mortality & recruitment	Cyclone additional mortality	1x trawl additional mortality	14x trawl additional mortality
<i>Ctenocella pectinata</i>	6.85	6.5	6.5	58.1
<i>Cymbastella coralliophila</i>	4.20	7.3	27.3	92.0
<i>Ianthella basta</i>	14.70	11.2	10.3	73.9
<i>Junceella divergens</i>	12.03	1.6	8.6	59.9
<i>Semperina brunei</i>	19.80	8.0	11.7	72.5
<i>Subergorgia reticulata</i>	4.00	0.0?	17.1	88.4
<i>Subergorgia suberosa</i>	10.75	10.9	15.8	81.9
<i>Turbinaria</i> sp.	18.10	7.5	27.2	80.4
<i>Xestospongia testudinaria</i>	20.60	0.0	5.4	57.3

7.3.7.2 Recruitment & mortality rates

Under the normal (non-cyclonic) conditions size-transition matrix and survival probabilities, the recruitment required to balance mortality ranged from 4.0 to 20.6 recruits per 100 individuals every 6 months (Table 7-7). Under stable size-distribution and constant recruitment, these required recruitment rates also reflect the overall mortality rates. Typically, smaller megabenthos individuals were observed to have a higher mortality rate than larger individuals Table 7-8.

Table 7-8. Observed mortality rates, overall for both normal and cyclonic periods, per 6 month time-step by size-class for nine megabenthos species.

Species	I	II	III	IV
<i>Ctenocella pectinata</i>	0.22	0.05	0.07	0.04
<i>Cymbastella coralliophila</i>	0.10	0.06	0.00	0.06
<i>Ianthella basta</i>	0.25	0.00	0.13	0.05
<i>Junceella divergens</i>	0.18	0.11	0.07	0.05
<i>Semperina brunei</i>	0.22	0.20	0.20	0.11
<i>Subergorgia reticulata</i>	0.00	0.00	0.09	0.00
<i>Subergorgia suberosa</i>	0.13	0.09	0.16	0.08
<i>Turbinaria</i> sp.	0.38	0.11	0.11	0.00
<i>Xestospongia testudinaria</i>	0.25	0.20	0.25	0.06

7.3.7.3 Effects of cyclones & trawling

During cyclones, mortality rates increased by an additional 0.0-11.2% over normal mortality rates (Table 7-7). In the case of *Subergorgia reticulata*, there were relatively few observations mortality and only a single was recorded. The additional mortality due to a single trawl was similar to or greater than that caused by cyclones and ranged from 5.4-27.3% (Table 7-7). The additional mortality due to a multiple-trawl (14x) impact would be substantial and ranged from 57-92%.

7.3.7.4 Recovery after cyclones & trawling

The potential recovery rates after the cyclone and trawling were very dependent on the recruitment scenario. Where all recruitment came from a constant external source, recovery was faster than with 50:50 external:self-recruitment, which in turn was faster than with 100% self-recruitment (Table 7-9). The potential recovery time after a single trawl, in most cases, was similar to recovery from a cyclone.

Table 7-9. Estimated half-recovery times (years) for a single cyclone and a single-trawl impacts, for three different recruitment scenarios, for nine megabenthos species.

Species	Cyclone			Single trawl		
	100% External Recruitment	50:50 External & self-recruitment	100% Self-recruitment	100% External Recruitment	50:50 External & self-recruitment	100% Self-recruitment
<i>Ctenocella pectinata</i>	8	11	13	7	11	15
<i>Cymbastella coralliophila</i>	7	11	17	7	10	15
<i>Ianthella basta</i>	1.5	5	6	1.5	3	4
<i>Junceella divergens</i>	2	4	6	3	5	7
<i>Semperina brunei</i>	2	5	6	2	4	6
<i>Subergorgia reticulata</i>	1	3	15	8	15	20
<i>Subergorgia suberosa</i>	4	7	10	4	6	7
<i>Turbinaria</i> sp.	3	5	7	3	5	7
<i>Xestospongia testudinaria</i>	2	5	5	2.5	7	10

The recovery after a multiple-trawl (14x) impact again was dependent on the recruitment scenario (Table 7-10). The half-recovery time with 100% external recruitment was similar to that for a single trawl or cyclone at about 2.5-8 years. With 50:50 external:self-recruitment, the half-recovery time was longer at about 4-15 years. With 100% self-recruitment, half-recovery was ~14-58 years — notably longer than for a single trawl or cyclone due to the larger impact reducing the populations to lower abundance and consequently reducing the absolute number of recruits in the self-recruiting scenario.

Table 7-10. Estimated half- and full recovery times (years) for a multiple-trawl (14x) impact, for three different recruitment scenarios, for nine megabenthos species.

Species	half recovery			full recovery		
	100% External Recruitment	50:50 External & self-recruitment	100% Self-recruitment	100% External Recruitment	50:50 External & self-recruitment	100% Self-recruitment
<i>Ctenocella pectinata</i>	8	14	31	38	57	88
<i>Cymbastella coralliophila</i>	8	11	57	25	36	150
<i>Ianthella basta</i>	2.5	5	16	11	27	43
<i>Junceella divergens</i>	4	7	16	23	36	52
<i>Semperina brunei</i>	2	4	17	11	24	50
<i>Subergorgia reticulata</i>	8	15	58	36	50	116
<i>Subergorgia suberosa</i>	4	7	28	21	29	54
<i>Turbinaria</i> sp.	3	5	35	17	23	56
<i>Xestospongia testudinaria</i>	2.5	5	14	13	28	43

The estimated time taken for “full” recovery after the multiple-trawl (14x) impact was rather imprecise, as noted above, because the model has asymptotic behaviour close to ‘carrying capacity’ — especially for the density-dependent self-recruitment scenario. Across the nine species, “full” recovery time with 100% external recruitment was in the range 11-38 years;

with 50:50 external:self-recruitment, the full-recovery time was ~23-57 years; and with 100% self-recruitment, full-recovery took ~43-150 years (Table 7-10).

7.3.7.5 *Establishment scenarios*

In the hypothetical models of establishment of other species in areas where they could grow but were absent, with 50:50 external & self-recruitment, establishment times were lengthy (Table 7-11). Half establishment times were in the range 5-18 years and full establishment in the models took about 25-150 years depending on the species. Again, however, the estimates of full establishment were imprecise because the models have asymptotic behaviour close to 'carrying capacity'. As with recovery, establishment times are more dependent on recruitment rates than growth rates, as some individuals can grow to size-class IV in about 4-9 years (see 7.3.7.6) and the higher initial recruitment rates of the constant external scenarios lead to half-establishment in ~3-9 years for overall numbers and in ~4-13 years for size-class IV. However, actual recruitment rates remain one of the most uncertain parameters, as discussed below. Nevertheless, these models do indicate that megabenthos species may take several to many decades to fully re-establish if they were completely removed from tropical continental shelf seabed habitats.

Table 7-11. Estimated half- and full establishment times (years) from zero, given 50:50 external & self-recruitment, for nine megabenthos species.

Species	half establishment	full establishment
	50:50 External & self-recruitment	50:50 External & self-recruitment
<i>Ctenocella pectinata</i>	17	106
<i>Cymbastella coralliophila</i>	14	151
<i>Ianthella basta</i>	5	30
<i>Junceella divergens</i>	8	47
<i>Semperina brunei</i>	5	26
<i>Subergorgia reticulata</i>	18	155
<i>Subergorgia suberosa</i>	7	40
<i>Turbinaria</i> sp.	6	30
<i>Xestospongia testudinaria</i>	5	33

7.3.7.6 *Cohort growth and mortality*

The model scenario of the fate of a single cohort of 100 recruits of each species showed that cohorts would decay quite rapidly due to mortality at overall rates in the range ~8-37% per year (Table 7-12). These rates differ from those presented earlier (Table 7-7) because they are annual rates and the stable size-structure for the decaying population differs from that of a population with constant recruitment and different size-classes have different mortality rates.

Table 7-12. Cohort annual decay mortality (after reaching a stable size-structure); years to peak Size II, III & IV numbers after recruiting to Size I; % surviving to attain Size IV; mean age & 90%-ile range (years) of survivors attaining Size IV, for nine megabenthos species.

Species	Decay mortality %	Peak size II	Peak size III	Peak size IV	% attain size IV	Mean size IV	90%ile range size IV
<i>Ctenocella pectinata</i>	8.1	~2	~4	~6	24%	5.9	1.5-14
<i>Cymbastella coralliophila</i>	12.4	~1.5	~4	~7	74% ?	7.7	2-18
<i>Ianthella basta</i>	36.9	~1	~2.5	~4	38% ?	4.2	1.5-8.5
<i>Junceella divergens</i>	17.5	~1	~2.5	~3.5	23%	4.0	1.5-8.5
<i>Semperina brunei</i>	32.9	~1	~1.5	~2.5	13%	3.0	1-6.5
<i>Subergorgia reticulata</i>	7.8	~1	~3.5	~5	36%	9.2	2-23
<i>Subergorgia suberosa</i>	20.2	~1	~2	~2.5	33%	3.7	1-8.5
<i>Turbinaria</i> sp.	27.3	~1	~2	~3.5	24% ?	3.9	1.5-8
<i>Xestospongia testudinaria</i>	25.8	~1	~2.5	~4	6%	3.8	1.5-7.5

Typically, the peak numbers of size-class II animals are attained in ~1-2 years after recruitment to size-class I, size-class III peaks after ~1.5-4 years and the peak size-class IV numbers occur after ~2.5-7 years (Table 7-12). Of the 13-74% of recruits that eventually reach size-class IV, the average time taken to reach this size ranges from 3.0-9.2 years with an overall 90-percentile range across all species of ~1-23 years demonstrating the plasticity of growth in these fauna. These growth rates coincide closely with the average residence times in each size class I to III, calculated directly from the transition matrix, of 1-2 years each (Table 7-13).

Table 7-13. Average residence times within each size class I to IV, without mortality, calculated directly from the size-transition matrix, for nine megabenthos species.

Species	I	II	III	IV
<i>Ctenocella pectinata</i>	1.81	1.47	1.18	2.05
<i>Cymbastella coralliophila</i>	1.27	1.96	1.91	6.14
<i>Ianthella basta</i>	2.10	1.35	1.14	7.28
<i>Junceella divergens</i>	1.24	1.11	1.21	1.39
<i>Semperina brunei</i>	1.18	1.00	0.95	1.12
<i>Subergorgia reticulata</i>	1.22	1.43	1.32	0.82
<i>Subergorgia suberosa</i>	1.07	1.05	0.91	0.94
<i>Turbinaria</i> sp.	1.52	1.16	1.30	3.32
<i>Xestospongia testudinaria</i>	1.61	1.65	1.44	2.58

7.4 Discussion

The demographic modeling results for the nine species in this study are similar to those from the few studies (Hughes 1984, Babcock 1991) that have published comparable information for the demographics of reef corals (four species). We could not find comparable studies for the

types of marine sessile megabenthos studied here, although there were a number of studies that reported one or two of the necessary demographic parameters (Chapter 6, Discussion).

In this study, the stable size-class distributions of modeled megabenthos typically diverged and differed from observed size-class frequencies. Modeling of similar information from the comparable studies showed similar patterns of divergence from frequencies observed during relatively short periods: eg. *Agaricia agaricites* in Jamaica (Hughes 1984) and *Goniastrea aspera* and *Platygyra sinensis* off Townsville (Babcock 1991). For only one of Babcock's three study species (*Goniastrea favulus*) did the modeled stable size-class frequencies remain similar to the observed frequencies. These departures between observations and models are not unexpected and indicate it is very unlikely that natural populations are in stable states (at equilibrium with respect to size-distribution or "carrying capacity"), because any variation in recruitment, growth, survival or other perturbations or impacts will lead to constantly changing size-class frequencies. The time-scale of such perturbations is likely to be shorter than the time-scale of megabenthos dynamics. Thus, current size distributions are a reflection of past dynamics, whereas measurements are made of current dynamics. Because of these random effects, more empirical studies of megabenthos demography are required to develop a more complete understanding of the typical distribution of these demographic parameters.

Mortality rates were relatively low (compared with productive fish stocks) at 5-30% per annum and typically smaller megabenthos individuals were observed to have higher mortality rates than larger individuals (~20% cf ~5% per annum, respectively). These rates were in the same range as those mortalities observed for corals (eg. Hughes 1984; Babcock 1991). These authors also observed that larger colonies, more so than small, suffered partial mortality and shrinkage — and often shrank to smaller colonies before dying, as we had observed.

Cyclones typically increased our megabenthos mortality rates by about 6% above that for normal conditions. While a number of studies have described the impact of Hurricanes on reef megabenthos, Hughes provides the only comparable information as a hurricane similarly affected his 1984 Jamaican study. In that study, the hurricane caused an additional 3% net reduction of colony numbers, as well as a substantial change to the size structure (many colonies of sizes III & IV reduced to II). After accounting for new colonies arising from fragments, the actual mortality for sizes I to IV increased by 5, 9, 15, 18% respectively (ie. substantially more so for larger colonies). Interestingly, a model of the Hughes data (Figure

7-10) indicated that the total number of colonies of his coral population would continue to decline slightly for another 10 years, despite return to the ‘calm conditions’ transition matrix immediately after the hurricane. This appeared to be because size IV colonies normally produced significant numbers of asexual offspring, but were reduced significantly.

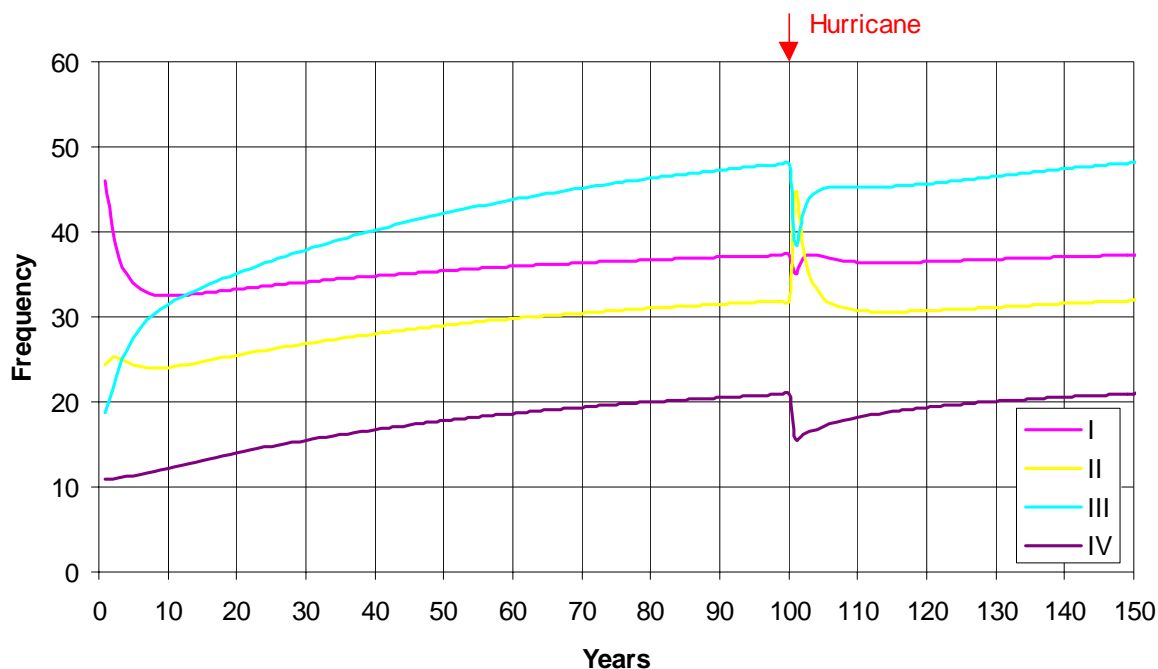


Figure 7-10. Time trajectory of four size-classes of *Agaricia agaricites* in Jamaica (Hughes 1984) in a model run with 100% external recruitment at the observed rate of approx 8.5% (1.47 times that need to sustain the observed density), showing the simulated impact and recovery from a hurricane. Total model colony numbers continued to decline slightly for another ~10 years after the hurricane and took ~27 years to recover to the immediate post-hurricane numbers, ~37 years to half-recover from the hurricane, and ~48 years to fully recover.

The trawl mortality rates applied herein were from Poiner *et al.* (1998) and Pitcher *et al.* (2000b). From this study, it can be determined that the additional mortality caused by a single trawl was of the same range as the normal undisturbed annual mortality rates. However, as Poiner *et al.* (1998) found, the additional mortality due to multiple-trawls could substantially reduce megabenthos populations if there was a coincidence of intense trawling on megabenthos habitat.

Growth rates for megabenthos could be surprisingly fast and contrasted with the lay belief in their slow growth. Typically, these fauna could achieve linear growth extensions of about 7 (2.5-14) cm per year, and attain size-class IV (lower boundary: 45-75 cm) 3-9 years post-recruitment. Nevertheless, the model estimates for the time taken for individuals to attain size-class IV ranged by more than 250%, showing that some individuals may grow very slowly

(and some more quickly) and that size is a very poor indicator of age. Many of the slow individuals may have regressed on one or more occasions. For many species, the largest (very few) individuals observed were at least twice the size of the size-class IV lower boundary. Presumably, a correspondingly longer time period is needed to attain such impressive dimensions — perhaps 20-50 years.

Recovery after cyclones or trawling could be lengthy was very dependent on the recruitment scenario, rather than growth rates. Higher recruitment, whether from a constant external source or for a species estimated to require higher recruitment, lead to faster recovery. If species are dependent on self-recruitment, recovery will be slower. Where there is significant external recruitment, the half-recovery time is similar regardless of the magnitude of impact. Of course, a population suffering a heavy impact (say down to 10%) will take absolutely longer to recover to the half-recovery point for the same population recovering from a lesser impact (say down to 90%), that is to 95%. This is not the case when there is high dependence on self-recruitment. In such cases, half-recovery times will be slower after heavy impacts, because the population has been reduced to very low abundance and, with self-recruitment, the absolute number of recruits will be lower. This result leads to a testable hypothesis for discriminating between external and self-recruiting scenarios in empirical recovery studies with contrasts in impact magnitude. In the mixed recruitment scenario, half-recovery was typically half to two decades. As a comparison, Hughes' (1984) Jamaican coral took about 37 years to half-recover from the hurricane (Figure 7-10).

Establishment scenarios were similarly more dependent on recruitment than growth rates, and half establishment times were also similar to half-recovery times. Estimates of full recovery or establishment times, however, were imprecise because the models have asymptotic behaviour as they approached 'carrying capacity'. Similarly, empirical measurements of full recovery will be imprecise because of measurement errors around population abundance such that the recovering population will become statistically indistinguishable from the before or control status before it has truly recovered. Nevertheless, the indications are that megabenthos may take several to many decades to fully recover or re-establish where they have been significantly impacted or removed. Again, as a comparison, Hughes' (1984) coral took about 48 years to fully recover from the hurricane (Figure 7-10) and would take ~27 years to half-establish and take >150 years to fully establish, given his observed recruitment rates.

This study appears to be the first to attempt to understand the demographics of off-reef tropical megabenthos and for nine species has succeeded in measuring growth-rates with adequate initial precision and description of natural variation, especially considering the mixed benefit due to the impact of the cyclones. Mortality was less precisely described, primarily because relatively few deaths occurred (Table 7-14), but again due to the cyclones. Recruitment probabilities, however, remain the most uncertain parameter — despite this study's relatively large observation plots — they have been measured only imprecisely over a 2-year period (short relative to the long time dynamics of these populations). This uncertainty is crucial given the long recovery times are critically dependent on rates of recruitment. This difficulty with recruitment is not unique, even in studies of shallow reef corals. For example, in the Hughes (1984) study, the probabilities for sexual offspring and for self-recruitment were unknown, thus Hughes had the same issue of not knowing the sources of recruitment. Nevertheless, Hughes modeled a range of (constant external sources of) recruitment scenarios, to assess their implications, and measured actual recruitment, as we did.

Table 7-14. Observed mortality, density & recruitment summary of study species, contrasted with modeled minimum recruitment to balance mortality for steady-state populations of nine megabenthos species.

Species	Number of Deaths	Number Observations	Raw % Mortality	Resident density /10 m ²	Recruit density /10 m ²	Recruit/Adult %	Model min % recruit
<i>Ctenocella pectinata</i>	11	109	10.1	9.52	0.26	2.73	6.85
<i>Cymbastella coralliophila</i>	3	52	5.8	0.00	0.00		4.20
<i>Ianthella basta</i>	4	45	8.9	0.95	0.00	0.00	14.70
<i>Junceella divergens</i>	7	71	9.9	4.76	0.10	2.19	12.03
<i>Semperina brunei</i>	9	52	17.3	0.95	0.05	5.47	19.80
<i>Subergorgia reticulata</i>	1	25	4.0	0.00	0.00		4.00
<i>Subergorgia suberosa</i>	11	90	12.2	5.71	0.31	5.47	10.75
<i>Turbinaria</i> sp.	9	63	14.3	0.24	0.10	43.75	18.10
<i>Xestospongia testudinaria</i>	11	59	18.6	0.95	0.10	10.94	20.60

Note: % mortality rates in this Table are those observed overall, whereas as those cited for the modeling results differ because the models attain stable size-distributions and have constant recruitment.

The rates of actual recruitment that we measured (Chapter 6) were typically less than that required to maintain the resident densities observed during the study. The recruit densities (per six month interval) in four plots totaling 48 m² as a ratio over resident densities in random quadrats totaling 42 m², averaged only ~8% (range 0 to ~43%) compared with the average minimum requirement of ~12% (range 0 to ~20%) (Table 7-14). Thus actual recruitment was only 20-50% (range 0-240%) of the maintenance level. It is possible that recruitment was atypically low during the period of the study, and/or the resident densities

observed reflect an earlier period of atypically high recruitment. Alternatively, mortality may have been atypically high during the period of the study and/or atypically low prior to the study. Nevertheless, this leaves open the possibility that the recovery rates discussed herein may be optimistic and, given the sensitivity of recovery rates to recruitment, emphasizes that need for additional data on rates of recruitment for these megabenthos.

This situation is not unique. Our modeling of the Babcock (1991) data (of reef top corals in the same region near Townsville) showed that observed recruitment was only 50-65% of that needed to maintain resident densities for all three species in his study and would lead to population decline. Again, perhaps recruitment may have been higher in the recent past to yield the resident densities observed. A similar result was reported for two Californian gorgonians with observed recruitment only 70-80% of that needed to maintain observed densities (Grigg, 1977). On the other hand, the recruitment observed (in 12 m²) by Hughes would have lead to population growth by 25-75% relative to resident densities in his study.

The synthesis of data on the population dynamics of sessile megabenthos that live on tropical shelf seabeds, into relatively simple models has contributed information needed for managing interactions between these types of fauna and trawling. This information can be used in the Trawl Scenario Model (Ellis and Pantus, 2001) to assist development of alternative fishing strategies that have less impact on habitat. Some of the information needed by the Trawl Scenario Model is illustrated in (Figure 7-11) and includes the per-trawl removal rates (Poiner *et al.* 1998 and Pitcher *et al.* 2000b) and the recovery rates from this Project. As a pre-cursor to the Trawl Scenario Model, Pitcher *et al.* (2000a) examined the potential large-scale implications of trawling on faunal types having high, medium and low resilience (ie. removal rates of 5%, 10% & 20% per trawl) and recovery rates ranging from slow, medium-slow, medium-fast, fast (ie. 5%, 10%, 20% & 50% of 'carrying capacity' in the first year after impact). Vulnerability to trawling is a combination of these two factors — (Figure 7-11a) illustrates these indicators for the megabenthos species studied here. Put simply, if the removal rate exceeds the recovery rate, the fauna may decline. However, the interaction is a spatially dynamic process that also requires information on the distribution and intensity of trawl effort, and the distribution & abundance of seabed biota that may be affected by trawling. With such information, quantitative environmental risk assessment is possible, and further, it would be possible to quantitatively evaluate which management strategies will best achieve environmental sustainability goals (Pitcher *et al.* 2000) while taking into account

consequences for the fishery (eg. Ellis and Pantus, 2001). Rigorous model-based assessments of this kind are needed to contribute to an objective balance between ecologically sustainable fishing and biodiversity conservation as ESD management changes are implemented in those Australian fisheries that affect seabed habitat.

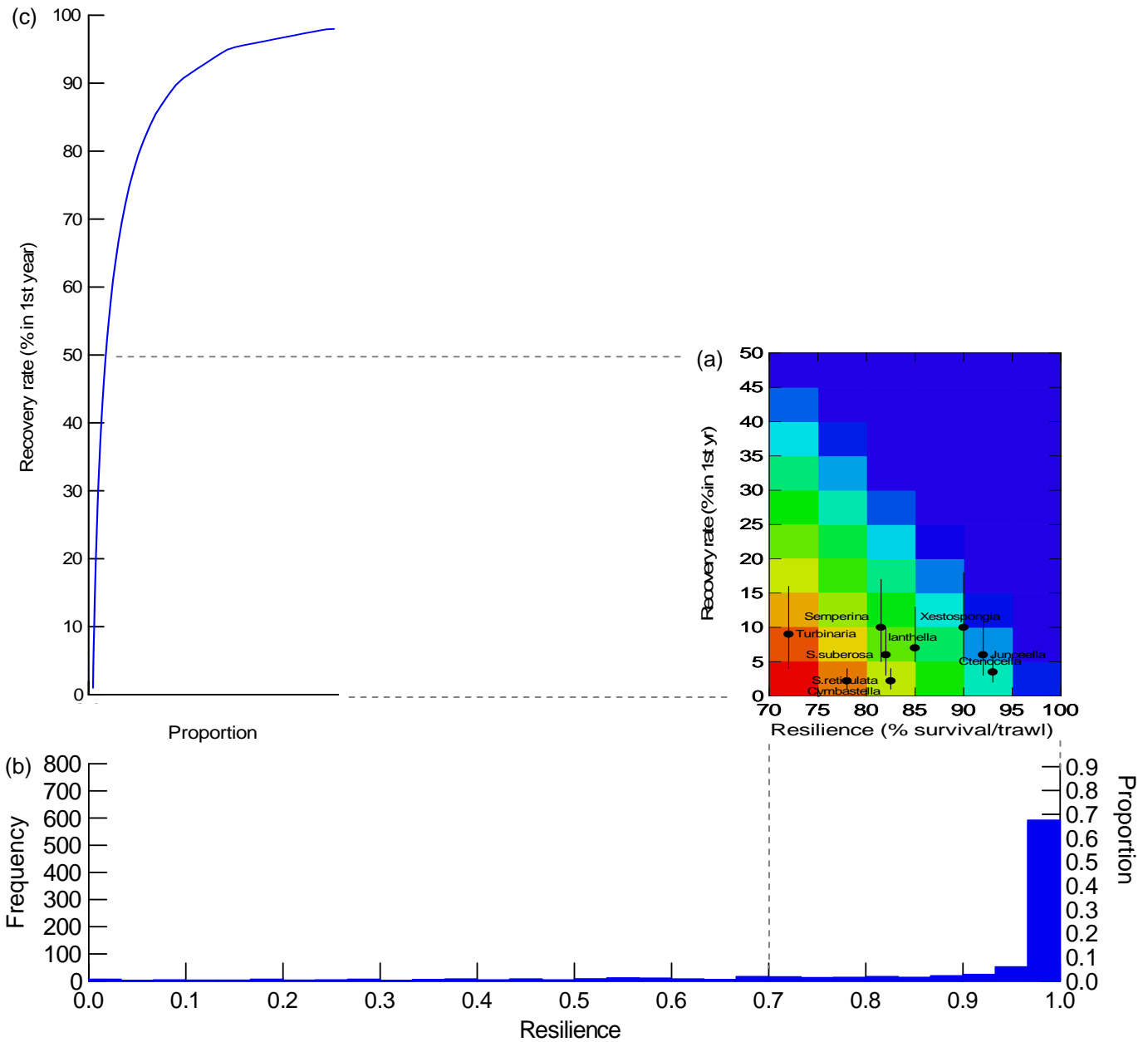


Figure 7-11. (a) Indicators of vulnerability to trawling for nine megabenthos species, as a combination of resilience (complement of removal rate per trawl) and recovery rates (% of ‘carrying capacity’ recovered in first year). The scenario for 50:50 external:self-recruitment is indicated by ●, the lower interval indicates the 100% self-recruitment scenario and the upper interval indicates the 100% external-recruitment scenario. There is of course also uncertainty in the estimates of removal rates. These indicators have been positioned in the wider context of (b) estimated resilience (1-removal rate) for ~900 seabed species (calculated from the Poiner *et al.* 1998 dataset), and (c) a hypothetical frequency distribution of species recovery rates from the knowledge that there are many more small short-lived species than large long-lived species. It is the relatively few species that do not have high resilience or fast recovery that management action needs to target in order to achieve sustainability.

7.5 Appendices

7.5.1 *Subergorgia suberosa*

Appendix 7.5–1. A: Size-transition and survival probabilities for *Subergorgia suberosa* under normal (non-cyclonic) conditions, and overall transition probabilities for B: 100% external recruitment, C: 50:50 external and self-recruitment, and D: 100% self-recruitment.

A: Normal size& survival probabilities

Normal Size Transition Probabilities

Yr+1 Class	Size class in Yr			
	I	II	III	IV
I	0.534	0.160	0.075	0.004
II	0.404	0.523	0.247	0.098
III	0.058	0.276	0.448	0.427
IV	0.005	0.041	0.230	0.470
TOTAL	1.000	1.000	1.000	1.000

Normal Survival Probabilities

Size class in Yr			
I	II	III	IV
0.882	0.921	0.851	0.928

B: 100% external recruitment

Self Recruitment Probabilities

Yr+1 Class	Size class in Yr			
	I	II	III	IV
I	0.000	0.000	0.000	0.000

Overall Transition Probabilities

Yr+1 Class	Size class in Yr			
	I	II	III	IV
I	0.471	0.148	0.064	0.004
II	0.356	0.481	0.210	0.091
III	0.051	0.254	0.381	0.397
IV	0.004	0.038	0.196	0.436
TOTAL	0.882	0.921	0.851	0.928

External Recruitment Numbers

10.750

C: 50:50 external and self-recruitment

Self Recruitment Probabilities

Yr+1 Class	Size class in Yr			
	I	II	III	IV
I	0.012	0.048	0.108	0.192

Overall Transition Probabilities

Yr+1 Class	Size class in Yr			
	I	II	III	IV
I	0.483	0.196	0.172	0.196
II	0.356	0.481	0.210	0.091
III	0.051	0.254	0.381	0.397
IV	0.004	0.038	0.196	0.436
TOTAL	0.894	0.969	0.959	1.120

External Recruitment Numbers

5.375

D: 100% self-recruitment

Self Recruitment Probabilities

Yr+1 Class	Size class in Yr			
	I	II	III	IV
I	0.033	0.130	0.293	0.520

Overall Transition Probabilities

Yr+1 Class	Size class in Yr			
	I	II	III	IV
I	0.503	0.278	0.357	0.524
II	0.356	0.481	0.210	0.091
III	0.051	0.254	0.381	0.397
IV	0.004	0.038	0.196	0.436
TOTAL	0.915	1.051	1.143	1.448

External Recruitment Numbers

0

Appendix 7.5–2. Size-transition matrix, survival probabilities and overall transition probabilities for *Subergorgia suberosa* under cyclone affected conditions.

Cyclone Size Transition Probabilities

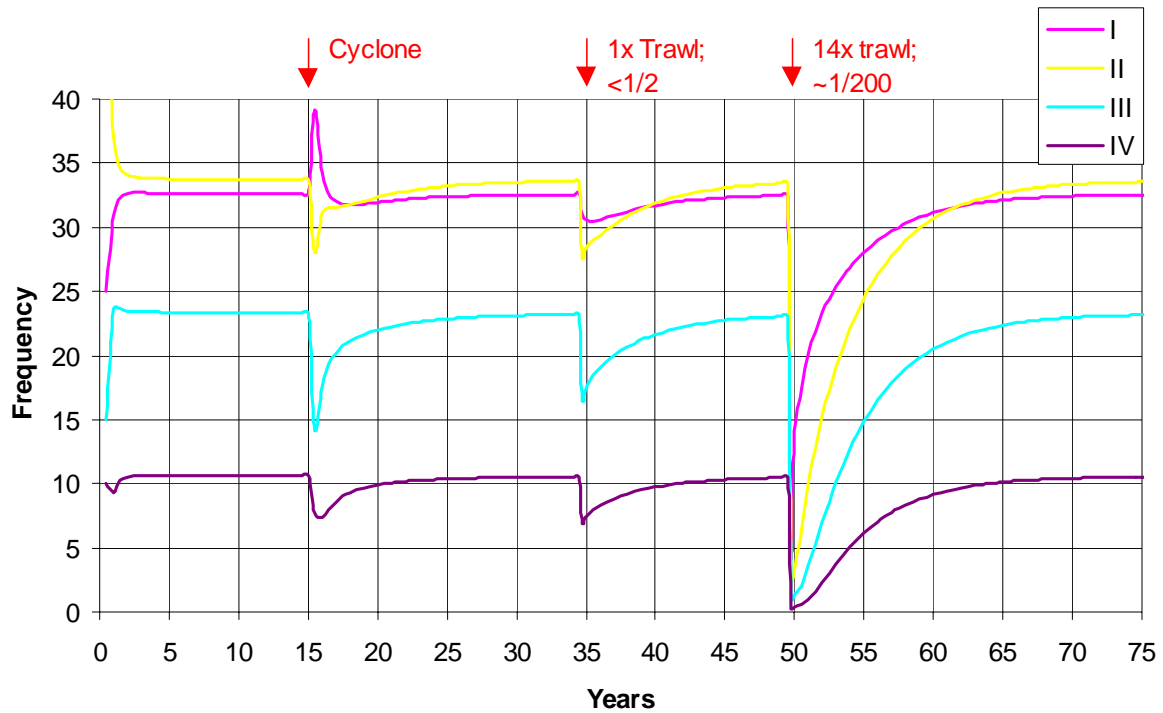
Yr+1 Class	Size class in Yr			
	I	II	III	IV
I	0.712	0.345	0.056	0.000
II	0.274	0.504	0.395	0.064
III	0.014	0.137	0.379	0.420
IV	0.000	0.013	0.169	0.516
TOTAL	1.000	1.000	1.000	1.000

Cyclone Survival Probabilities

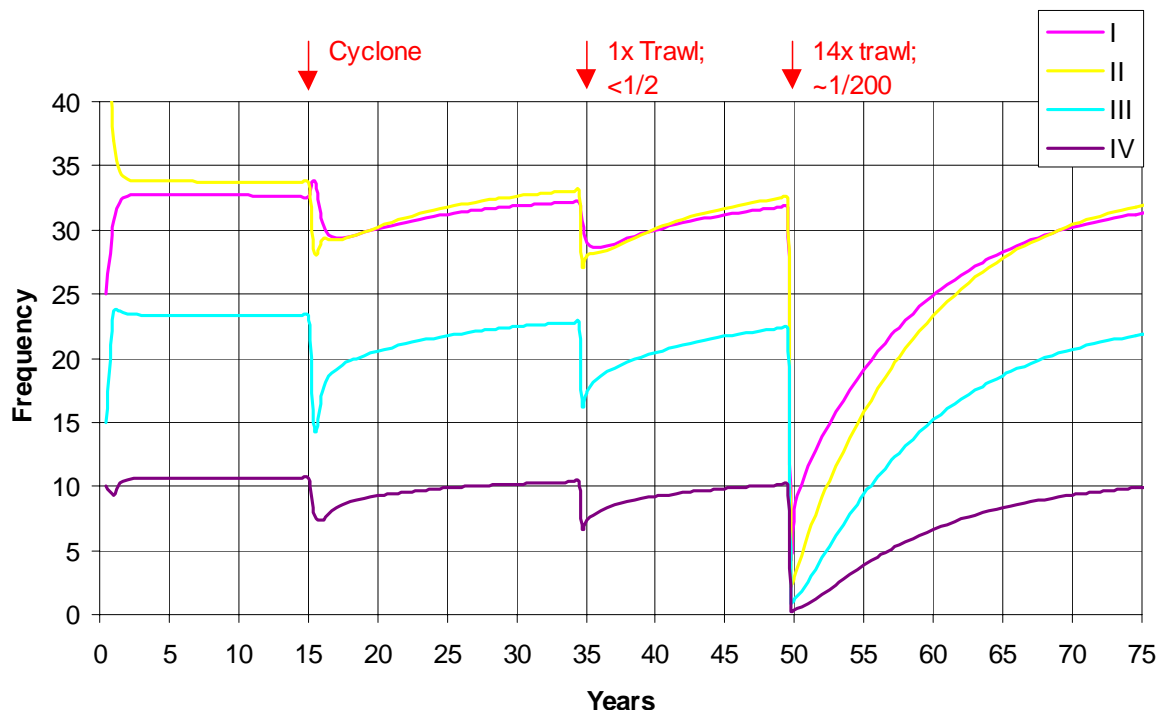
Size class in Yr			
I	II	III	IV
0.774	0.808	0.747	0.815

Overall Cyclone Transition Probabilities

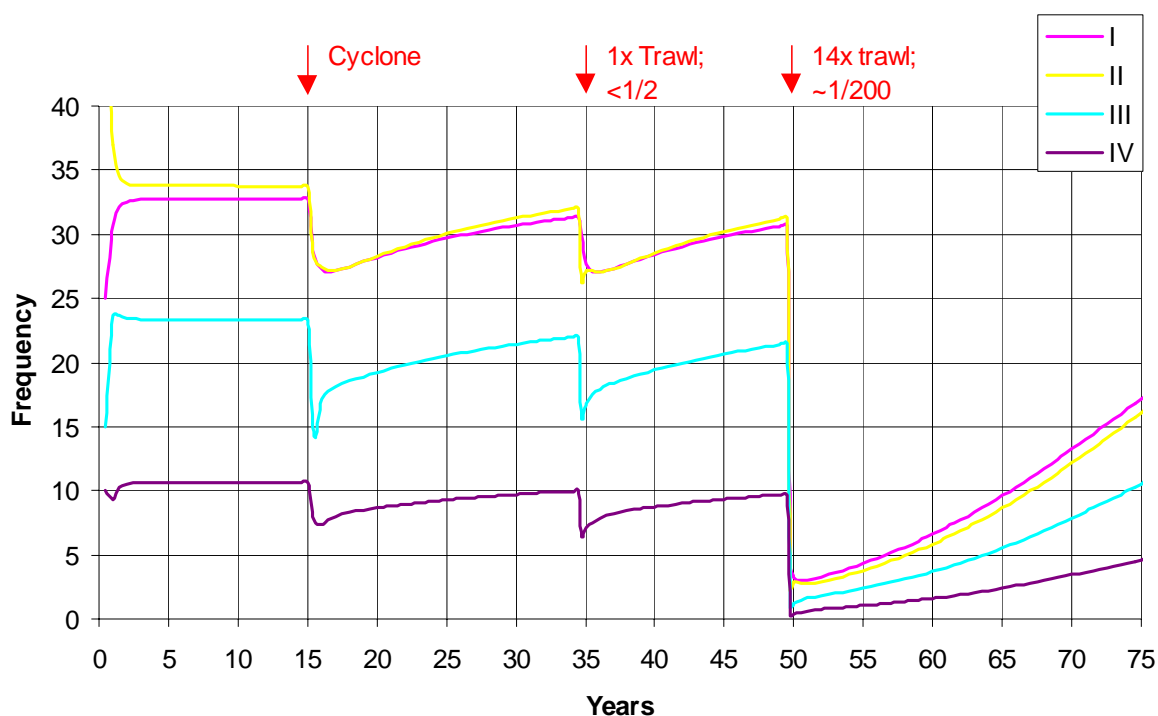
Yr+1 Class	Size class in Yr			
	I	II	III	IV
I	0.552	0.279	0.042	0.000
II	0.212	0.408	0.295	0.052
III	0.011	0.111	0.283	0.342
IV	0.000	0.011	0.126	0.421
TOTAL	0.774	0.808	0.747	0.815



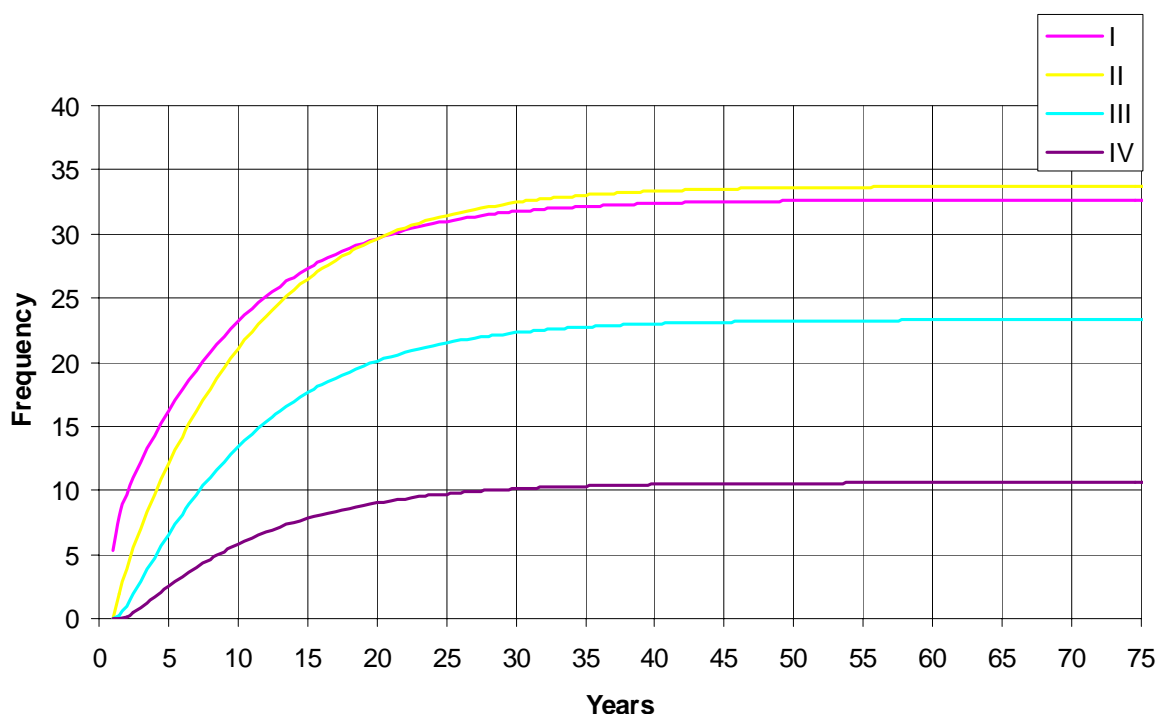
Appendix Fig. 7.5.1-1. Time trajectory of the four size-classes of *Subergorgia suberosa* in a model run with 100% external recruitment, showing the simulated impact and recovery from a cyclone, a single trawl and 14 trawls. The model takes ~4 years to half-recover from the cyclone, ~4 years to half-recover from a single trawl, ~4 years to half-recover from 14 trawls and ~21 years to fully recover.



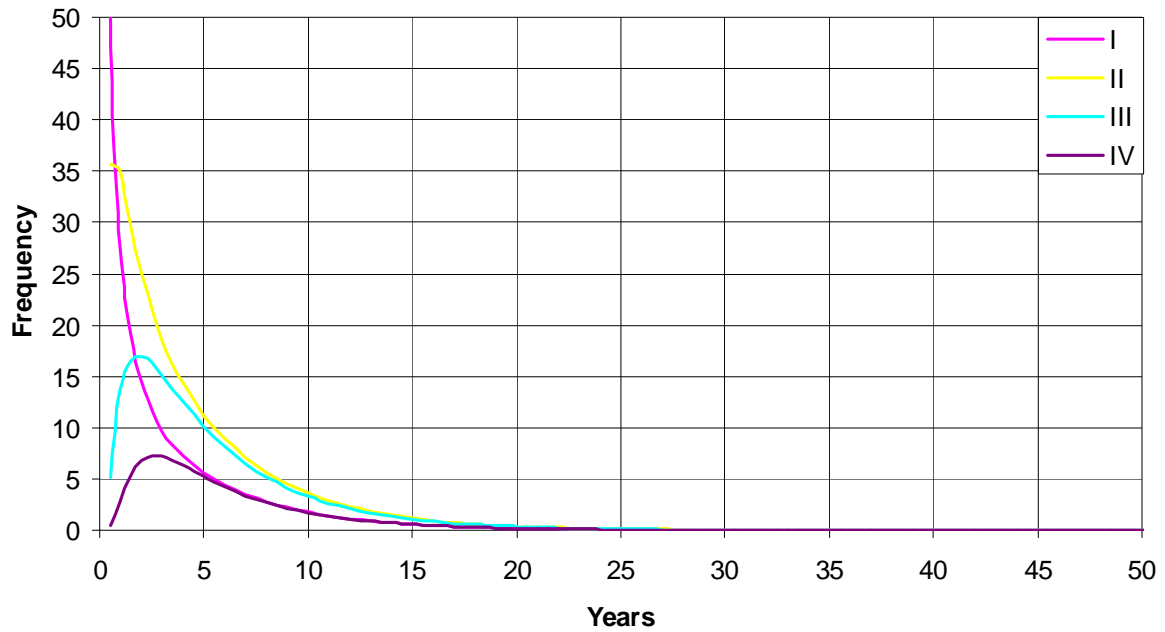
Appendix Fig. 7.5.1-2. Time trajectory of the four size-classes of *Subergorgia suberosa* in a model run with 50:50 external & self-recruitment, showing the simulated impact and recovery from a cyclone, a single trawl and 14 trawls. The model takes ~7 years to half-recover from the cyclone, ~6 years to half-recover from a single trawl, ~7 years to half-recover from 14 trawls and ~29 years to fully recover.



Appendix Fig. 7.5.1-3. Time trajectory of the four size-classes of *Subergorgia suberosa* in a model run with 100% self-recruitment, showing the simulated impact and recovery from a cyclone, a single trawl and 14 trawls. The model takes ~10 years to half-recover from the cyclone, ~7 years to half-recover from a single trawl, ~28 years to half-recover from 14 trawls and ~54 years to fully recover.



Appendix Fig. 7.5.1-4. Time trajectory of the four size-classes of *Subergorgia suberosa* in a model run to establish a population from zero with 50:50 external & self-recruitment. The model takes ~7 years to half-establish, and ~40 years to fully establish.



Appendix Fig. 7.5.1-5. Time trajectory of the four size-classes of *Subergorgia suberosa* in a model run to establish the fate of a single pulse of 100 Size I recruits (0-14 cm high), showing survival and growth through to larger size classes. Peak Size IV (>34 cm wide) abundance of ~7% occurs ~3 years after recruitment. Approximately 33% of Size I recruits attain Size IV after an average of 3.7 years, with a 90-percentile range of 1–8.5 years.

7.5.2 *Junceella divergens*

Appendix 7.5–3. A: Size-transition and survival probabilities for *Junceella divergens* under normal (non-cyclonic) conditions, and overall transition probabilities for B: 100% external recruitment, C: 50:50 external and self-recruitment, and D: 100% self-recruitment.

A: Normal size & survival probabilities

Normal Size Transition Probabilities

Yr+1 Class	Size class in Yr			
	I	II	III	IV
I	0.595	0.172	0.004	0.000
II	0.391	0.548	0.198	0.033
III	0.014	0.264	0.588	0.325
IV	0.000	0.017	0.210	0.642
TOTAL	1.000	1.000	1.000	1.000

Normal Survival Probabilities

	Size class in Yr			
	I	II	III	IV
	0.817	0.882	0.922	0.947

B: 100% external recruitment

Self Recruitment Probabilities

Yr+1 Class	Size class in Yr			
	I	II	III	IV
I	0.000	0.000	0.000	0.000

Overall Transition Probabilities

Yr+1 Class	Size class in Yr			
	I	II	III	IV
I	0.487	0.151	0.004	0.000
II	0.320	0.484	0.183	0.031
III	0.011	0.233	0.542	0.308
IV	0.000	0.015	0.194	0.608
TOTAL	0.817	0.882	0.922	0.947

External Recruitment Numbers

12.030

C: 50:50 external and self-recruitment

Self Recruitment Probabilities

Yr+1 Class	Size class in Yr			
	I	II	III	IV
I	0.010	0.048	0.114	0.208

Overall Transition Probabilities

Yr+1 Class	Size class in Yr			
	I	II	III	IV
I	0.497	0.199	0.117	0.208
II	0.320	0.484	0.183	0.031
III	0.011	0.233	0.542	0.308
IV	0.000	0.015	0.194	0.608
TOTAL	0.827	0.930	1.035	1.155

External Recruitment Numbers

6.015

D: 100% self-recruitment

Self Recruitment Probabilities

Yr+1 Class	Size class in Yr			
	I	II	III	IV
I	0.027	0.129	0.308	0.563

Overall Transition Probabilities

Yr+1 Class	Size class in Yr			
	I	II	III	IV
I	0.513	0.280	0.311	0.563
II	0.320	0.484	0.183	0.031
III	0.011	0.233	0.542	0.308
IV	0.000	0.015	0.194	0.608
TOTAL	0.844	1.011	1.229	1.510

External Recruitment Numbers

0

Appendix 7.5-4. Size-transition matrix, survival probabilities and overall transition probabilities for *Junceella divergens* under cyclone affected conditions.

Cyclone Size Transition Probabilities

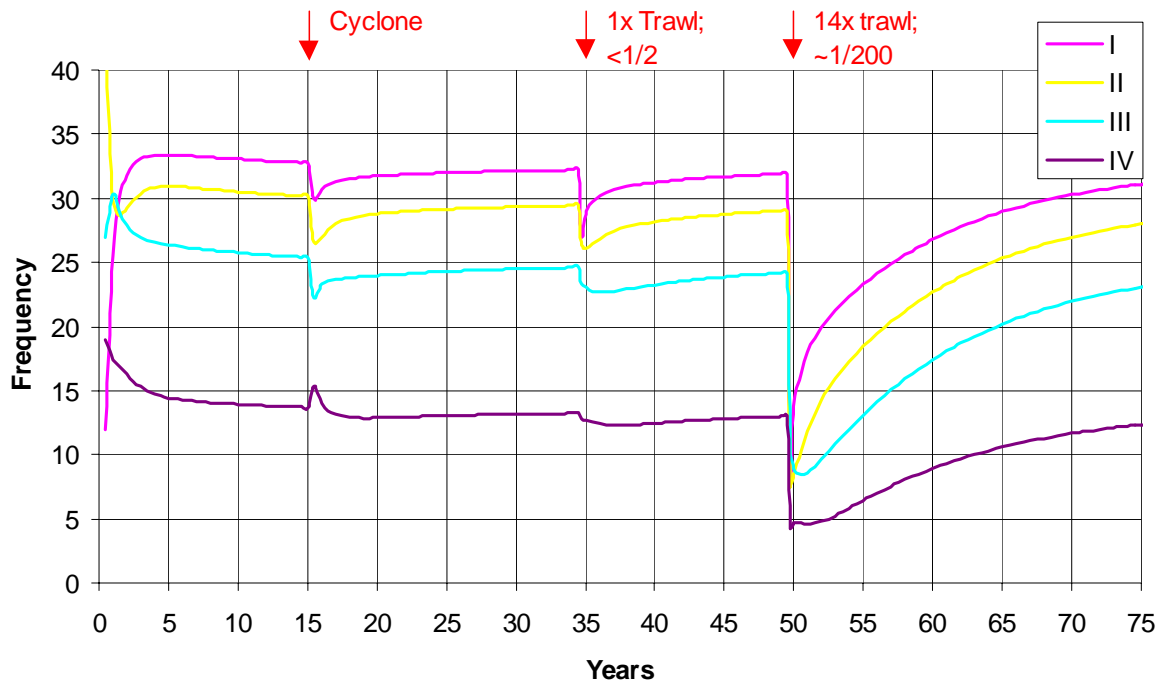
Yr+1 Class	Size class in Yr			
	I	II	III	IV
I	0.633	0.251	0.031	0.000
II	0.328	0.455	0.236	0.056
III	0.040	0.226	0.471	0.350
IV	0.000	0.068	0.262	0.594
TOTAL	1.000	1.000	1.000	1.000

Cyclone Survival Probabilities

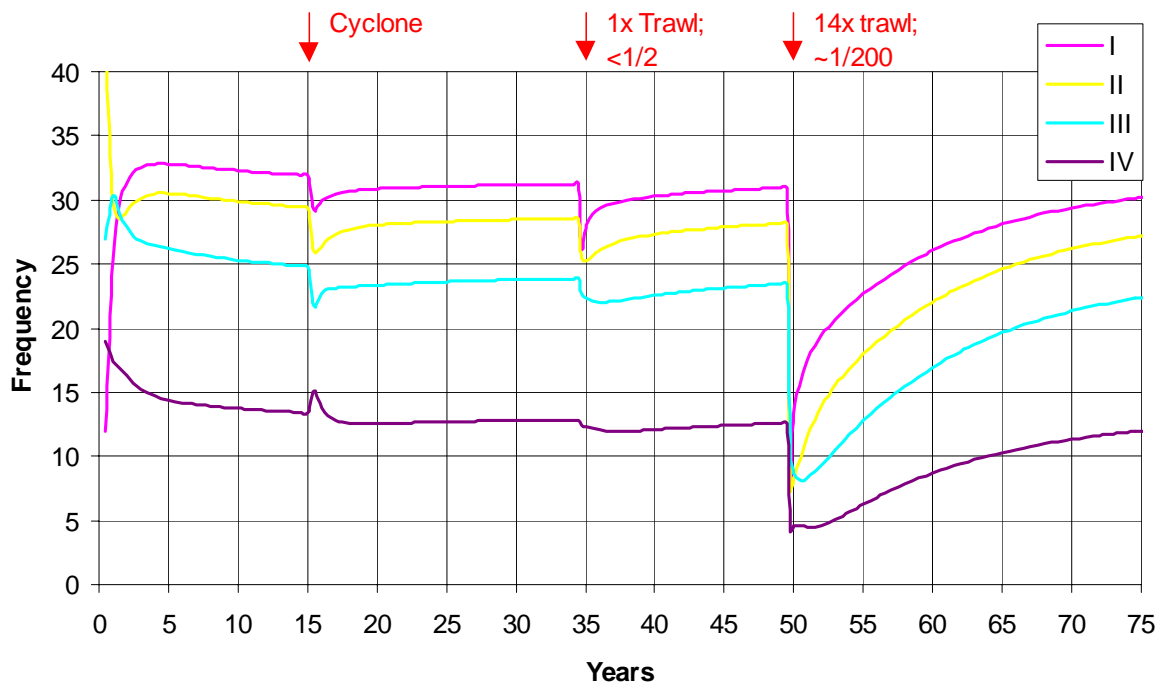
		Size class in Yr			
		I	II	III	IV
		0.803	0.867	0.905	0.931

Overall Cyclone Transition Probabilities

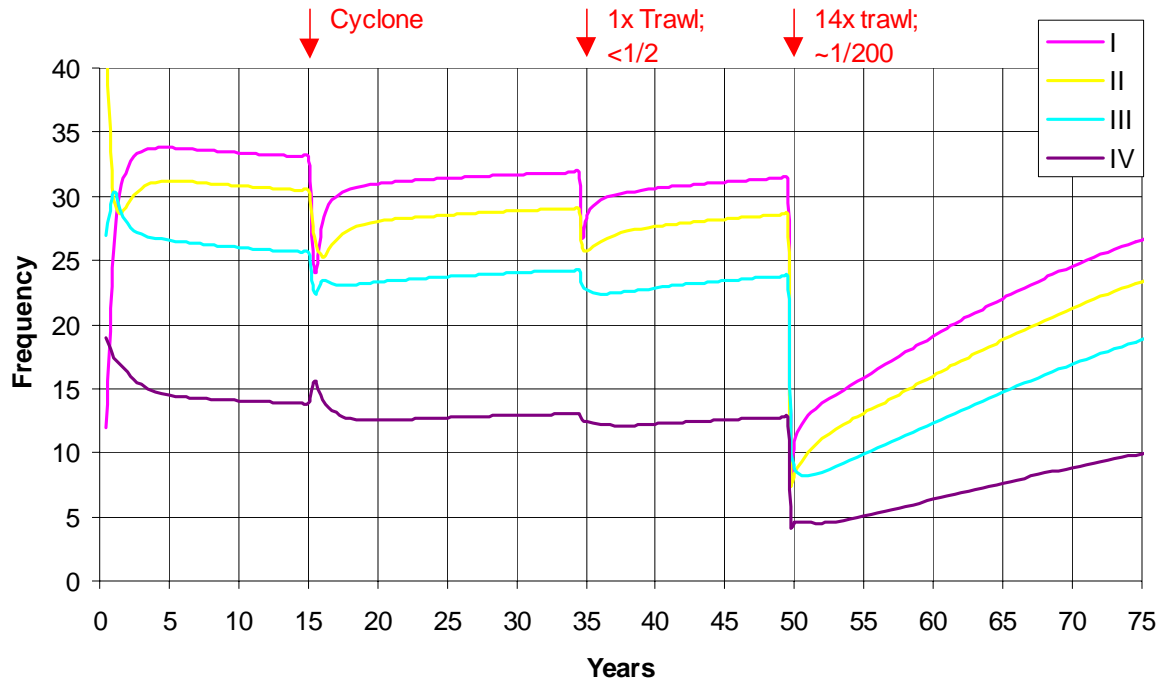
Yr+1 Class	Size class in Yr			
	I	II	III	IV
I	0.508	0.218	0.028	0.000
II	0.263	0.395	0.213	0.052
III	0.032	0.195	0.426	0.326
IV	0.000	0.059	0.237	0.553
TOTAL	0.803	0.867	0.905	0.931



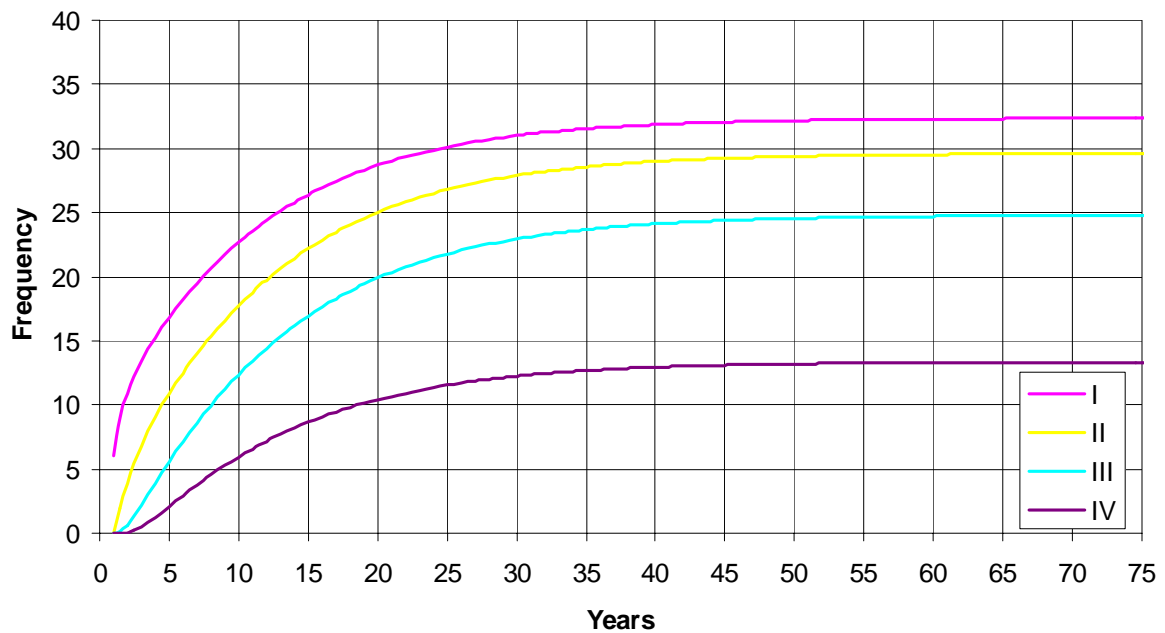
Appendix Fig. 7.5.2-1. Time trajectory of the four size-classes of *Junceella divergens* in a model run with 100% external recruitment, showing the simulated impact and recovery from a cyclone, a single trawl and 14 trawls. The model takes ~2 years to half-recover from the cyclone, ~3 years to half-recover from a single trawl, ~4 years to half-recover from 14 trawls and ~23 years to fully recover.



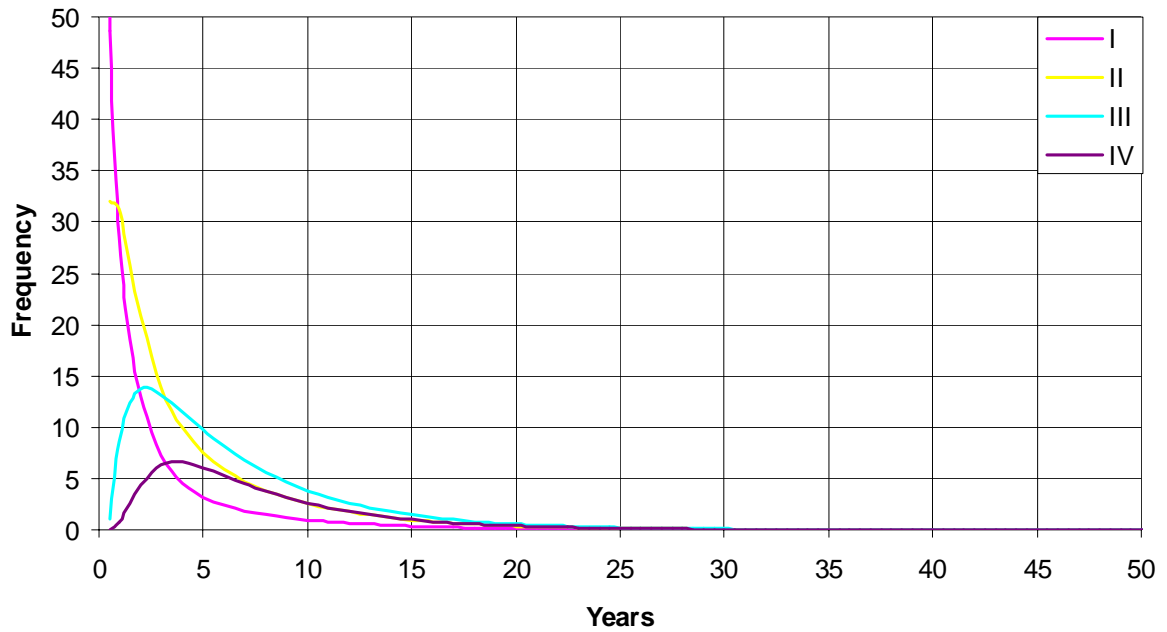
Appendix Fig. 7.5.2-2. Time trajectory of the four size-classes of *Junceella divergens* in a model run with 50:50 external & self-recruitment, showing the simulated impact and recovery from a cyclone, a single trawl and 14 trawls. The model takes ~4 years to half-recover from the cyclone, ~5 years to half-recover from a single trawl, ~7 years to half-recover from 14 trawls and ~36 years to fully recover.



Appendix Fig. 7.5.2-3. Time trajectory of the four size-classes of *Junceella divergens* in a model run with 100% self-recruitment, showing the simulated impact and recovery from a cyclone, a single trawl and 14 trawls. The model takes ~6 years to half-recover from the cyclone, ~7 years to half-recover from a single trawl, ~16 years to half-recover from 14 trawls and ~52 years to fully recover.



Appendix Fig. 7.5.2-4. Time trajectory of the four size-classes of *Junceella divergens* in a model run to establish a population from zero with 50:50 external & self-recruitment. The model takes ~8 years to half-establish, and ~47 years to fully establish.



Appendix Fig. 7.5.2-5. Time trajectory of the four size-classes of *Junceella divergens* in a model run to establish the fate of a single pulse of 100 Size I recruits (0-15 cm height), showing survival and growth through to larger size classes. Peak Size IV (>38 cm wide) abundance of ~7% occurs ~4 years after recruitment. Approximately 23% of Size I recruits attain Size IV after an average of 4.0 years, with a 90-percentile range of 1.5–8.5 years.

7.5.3 *Turbinaria* sp.

Appendix 7.5-5. A: Size-transition and survival probabilities for *Turbinaria* sp. under normal (non-cyclonic) conditions, and overall transition probabilities for B: 100% external recruitment, C: 50:50 external and self-recruitment, and D: 100% self-recruitment.

A: Normal size & survival probabilities

Normal Size Transition Probabilities

Yr+1 Class	Size class in Yr			
	I	II	III	IV
I	0.671	0.123	0.000	0.000
II	0.325	0.570	0.102	0.000
III	0.004	0.298	0.614	0.151
IV	0.000	0.009	0.283	0.849
TOTAL	1.000	1.000	1.000	1.000

Normal Survival Probabilities

Size class in Yr			
I	II	III	IV
0.673	0.957	0.964	0.750*

B: 100% external recruitment

Self Recruitment Probabilities

Yr+1 Class	Size class in Yr			
	I	II	III	IV
I	0.000	0.000	0.000	0.000

Overall Transition Probabilities

Yr+1 Class	Size class in Yr			
	I	II	III	IV
I	0.452	0.118	0.000	0.000
II	0.218	0.546	0.099	0.000
III	0.003	0.285	0.592	0.113
IV	0.000	0.008	0.273	0.637
TOTAL	0.673	0.957	0.964	0.750

External Recruitment Numbers

18.7

C: 50:50 external and self-recruitment

Self Recruitment Probabilities

Yr+1 Class	Size class in Yr			
	I	II	III	IV
I	0.034	0.102	0.172	0.241

Overall Transition Probabilities

Yr+1 Class	Size class in Yr			
	I	II	III	IV
I	0.485	0.220	0.172	0.241
II	0.218	0.546	0.099	0.000
III	0.003	0.285	0.592	0.113
IV	0.000	0.008	0.273	0.637
TOTAL	0.707	1.059	1.135	0.991

External Recruitment Numbers

9.35

D: 100% self-recruitment

Self Recruitment Probabilities

Yr+1 Class	Size class in Yr			
	I	II	III	IV
I	0.091	0.277	0.466	0.654

Overall Transition Probabilities

Yr+1 Class	Size class in Yr			
	I	II	III	IV
I	0.543	0.395	0.466	0.654
II	0.218	0.546	0.099	0.000
III	0.003	0.285	0.592	0.113
IV	0.000	0.008	0.273	0.637
TOTAL	0.764	1.234	1.429	1.404

External Recruitment Numbers

0

Appendix 7.5–6. Size-transition matrix, survival probabilities and overall transition probabilities for *Turbinaria sp.* under cyclone affected conditions.

Cyclone Size Transition Probabilities

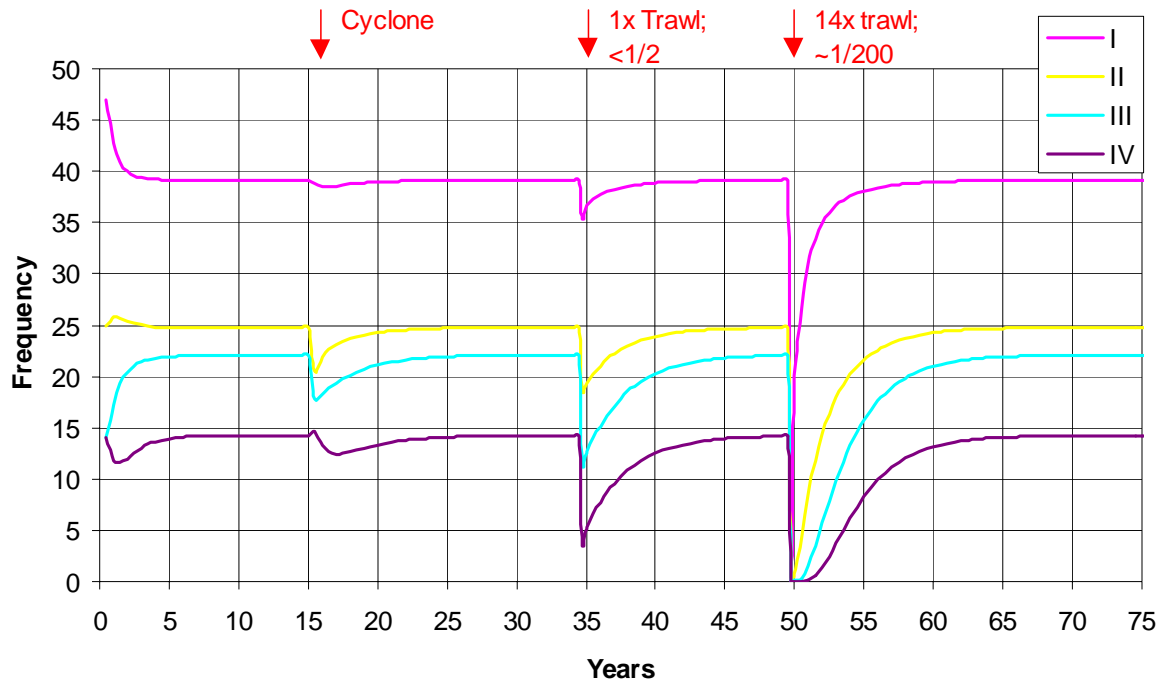
Yr+1 Class	Size class in Yr			
	I	II	III	IV
I	0.817	0.120	0.000	0.000
II	0.183	0.701	0.126	0.000
III	0.000	0.178	0.723	0.087
IV	0.000	0.000	0.150	0.913
TOTAL	1.000	1.000	1.000	1.000

Cyclone Survival Probabilities

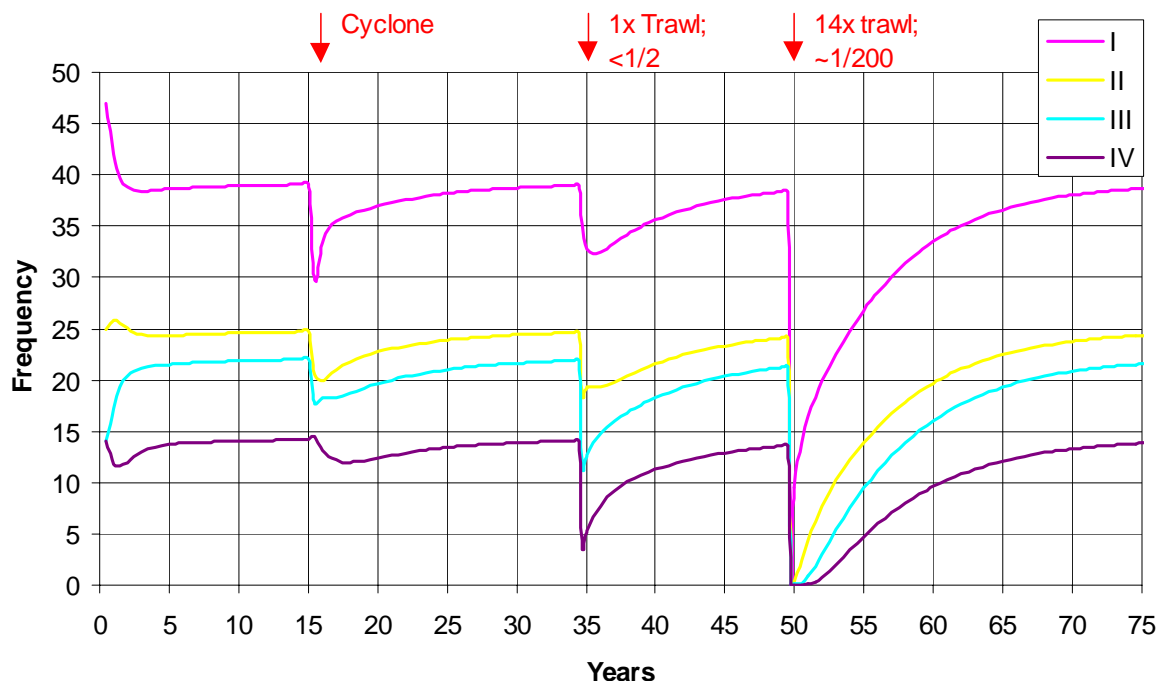
	Size class in Yr			
	I	II	III	IV
	0.573	0.815	0.820	0.917

Overall Cyclone Transition Probabilities

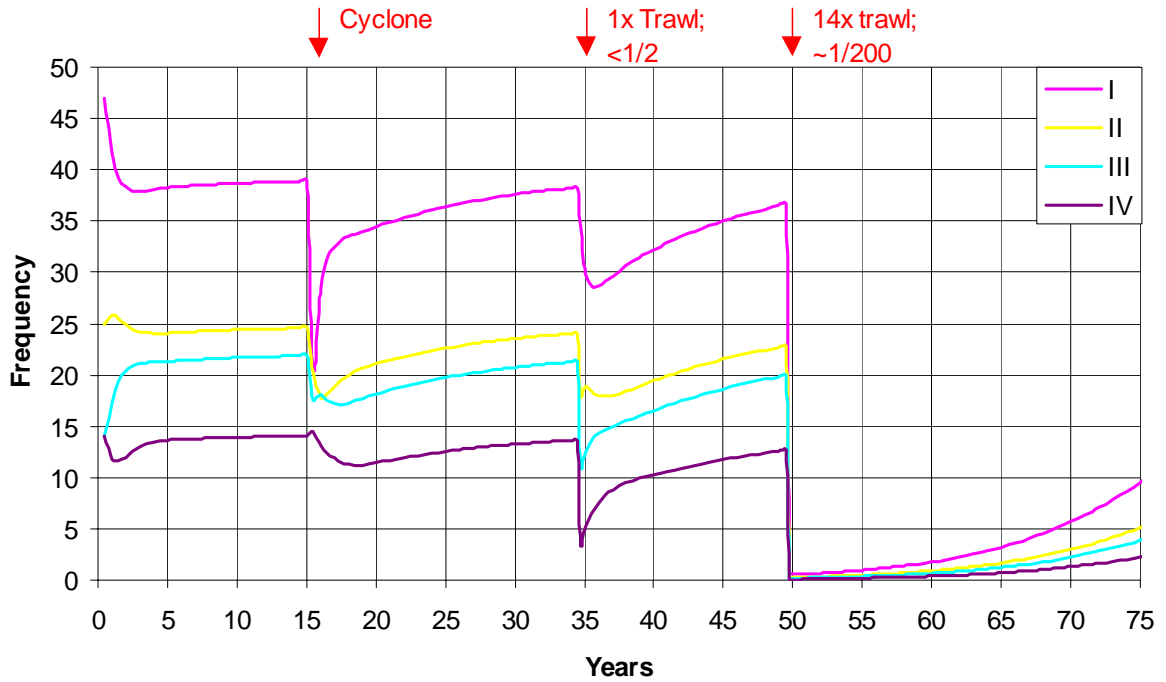
Yr+1 Class	Size class in Yr			
	I	II	III	IV
I	0.468	0.098	0.000	0.000
II	0.105	0.571	0.104	0.000
III	0.000	0.145	0.593	0.080
IV	0.000	0.000	0.123	0.837
TOTAL	0.573	0.815	0.820	0.917



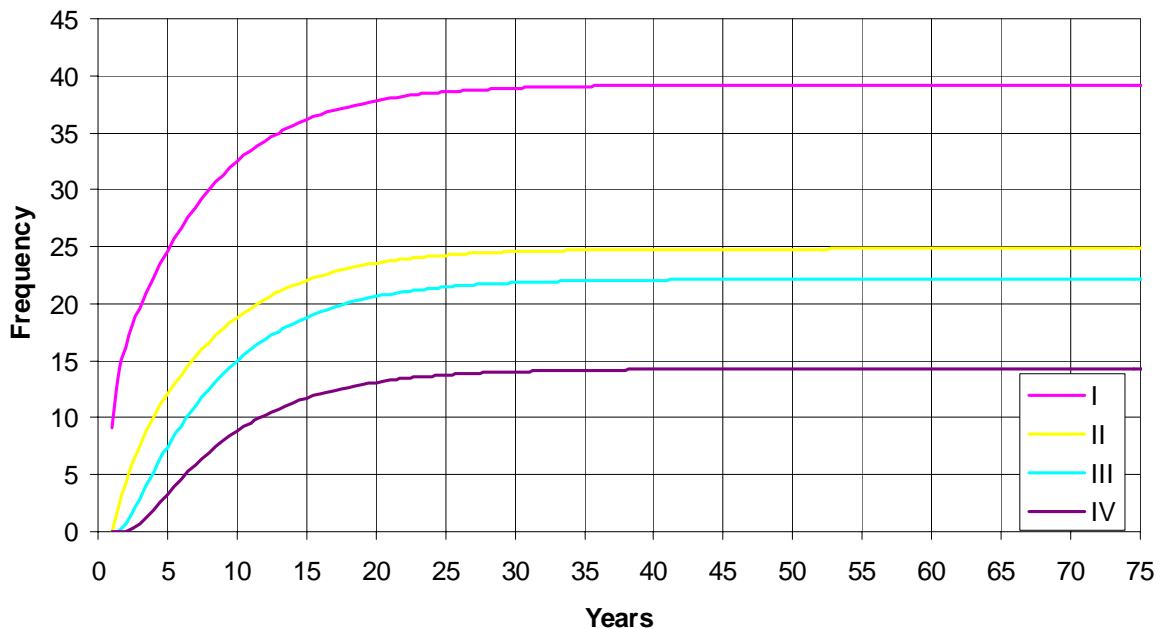
Appendix Fig. 7.5.3-1. Time trajectory of the four size-classes of *Turbinaria* sp. in a model run with 100% external recruitment, showing the simulated impact and recovery from a cyclone, a single trawl and 14 trawls. The model takes ~ 3 years to half-recover from the cyclone, ~ 3 years to half-recover from a single trawl, ~ 3 years to half-recover from 14 trawls and ~ 17 years to fully recover.



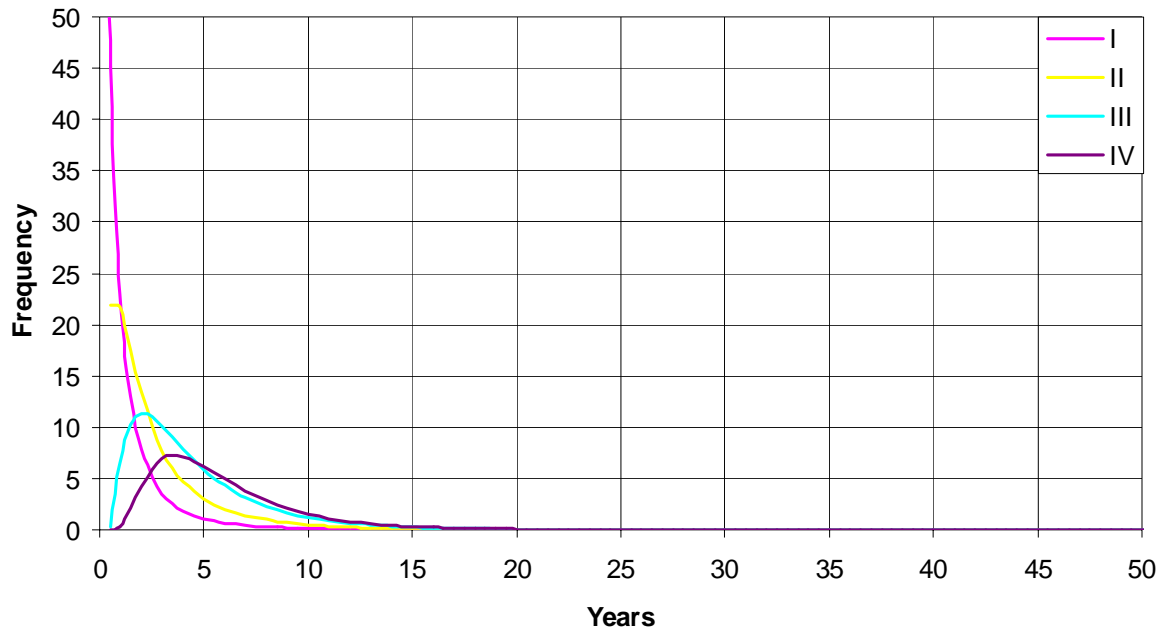
Appendix Fig. 7.5.3-2. Time trajectory of the four size-classes of *Turbinaria* sp. in a model run with 50:50 external & self-recruitment, showing the simulated impact and recovery from a cyclone, a single trawl and 14 trawls. The model takes ~ 5 years to half-recover from the cyclone, ~ 5 years to half-recover from a single trawl, ~ 5 years to half-recover from 14 trawls and ~ 23 years to fully recover.



Appendix Fig. 7.5.3-3. Time trajectory of the four size-classes of *Turbinaria sp.* in a model run with 100% self-recruitment, showing the simulated impact and recovery from a cyclone, a single trawl and 14 trawls. The model takes ~7 years to half-recover from the cyclone, ~7 years to half-recover from a single trawl, ~35 years to half-recover from 14 trawls and ~56 years to fully recover.



Appendix Fig. 7.5.3-4. Time trajectory of the four size-classes of *Turbinaria sp.* in a model run to establish a population from zero with 50:50 external & self-recruitment. The model takes ~6 years to half-establish, and ~30 years to fully establish.



Appendix Fig. 7.5.3-5. Time trajectory of the four size-classes of *Turbinaria sp.* in a model run to establish the fate of a single pulse of 100 Size I recruits (0-22 cm across), showing survival and growth through to larger size classes. Peak Size IV (>40 cm across) abundance of ~7% occurs ~4 years after recruitment. Approximately 24% of Size I recruits attain Size IV after an average of 3.9 years, with a 90-percentile range of 1.5–8 years.

7.5.4 *Xestospongia testudinaria*

Appendix 7.5–7. A: Size-transition and survival probabilities for *Xestospongia testudinaria* under normal (non-cyclonic) conditions, and overall transition probabilities for B: 100% external recruitment, C: 50:50 external and self-recruitment, and D: 100% self-recruitment.

A: Normal size & survival probabilities

Normal Size Transition Probabilities

Yr+1 Class	Size class in Yr			
	I	II	III	IV
I	0.689	0.104	0.008	0.000
II	0.311	0.697	0.177	0.000
III	0.000	0.199	0.654	0.194
IV	0.000	0.000	0.161	0.806
TOTAL	1.000	1.000	1.000	1.000

Normal Survival Probabilities

Size class in Yr			
I	II	III	IV
0.765	0.816	0.765	0.960

B: 100% external recruitment

Self Recruitment Probabilities

Yr+1 Class	Size class in Yr			
	I	II	III	IV
I	0.000	0.000	0.000	0.000

Overall Transition Probabilities

Yr+1 Class	Size class in Yr			
	I	II	III	IV
I	0.527	0.085	0.006	0.000
II	0.238	0.569	0.136	0.000
III	0.000	0.163	0.500	0.186
IV	0.000	0.000	0.123	0.774
TOTAL	0.765	0.816	0.765	0.960

External Recruitment Numbers

20.6

C: 50:50 external and self-recruitment

Self Recruitment Probabilities

Yr+1 Class	Size class in Yr			
	I	II	III	IV
I	0.011	0.091	0.311	0.740

Overall Transition Probabilities

Yr+1 Class	Size class in Yr			
	I	II	III	IV
I	0.538	0.176	0.317	0.740
II	0.238	0.569	0.136	0.000
III	0.000	0.163	0.500	0.186
IV	0.000	0.000	0.123	0.774
TOTAL	0.776	0.907	1.076	1.700

External Recruitment Numbers

10.3

D: 100% self-recruitment

Self Recruitment Probabilities

Yr+1 Class	Size class in Yr			
	I	II	III	IV
I	0.030	0.248	0.845	2.010

Overall Transition Probabilities

Yr+1 Class	Size class in Yr			
	I	II	III	IV
I	0.557	0.333	0.851	2.010
II	0.238	0.569	0.136	0.000
III	0.000	0.163	0.500	0.186
IV	0.000	0.000	0.123	0.774
TOTAL	0.795	1.064	1.610	2.970

External Recruitment Numbers

0

Appendix 7.5-8. Size-transition matrix, survival probabilities and overall transition probabilities for *Xestospongia testudinaria* under cyclone affected conditions.

Cyclone Size Transition Probabilities

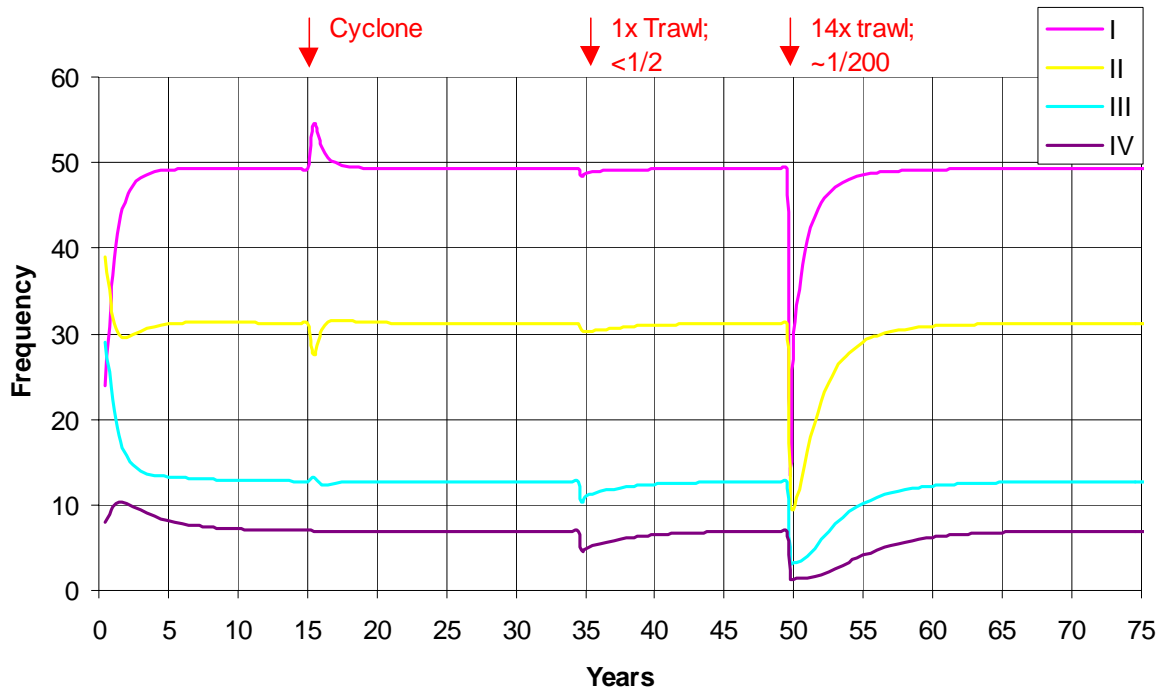
Yr+1 Class	Size class in Yr			
	I	II	III	IV
I	0.760	0.178	0.000	0.000
II	0.235	0.632	0.195	0.005
III	0.005	0.186	0.655	0.232
IV	0.000	0.004	0.150	0.763
TOTAL	1.000	1.000	1.000	1.000

Cyclone Survival Probabilities

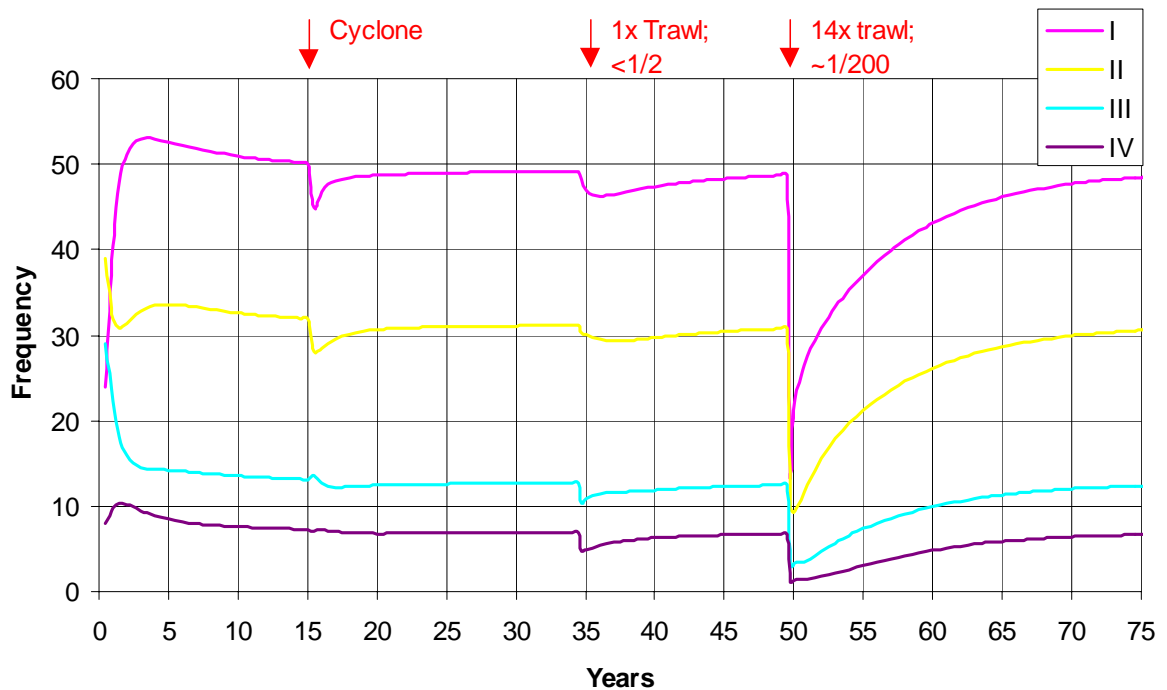
Size class in Yr			
I	II	III	IV
0.784	0.836	0.784	0.983

Overall Cyclone Transition Probabilities

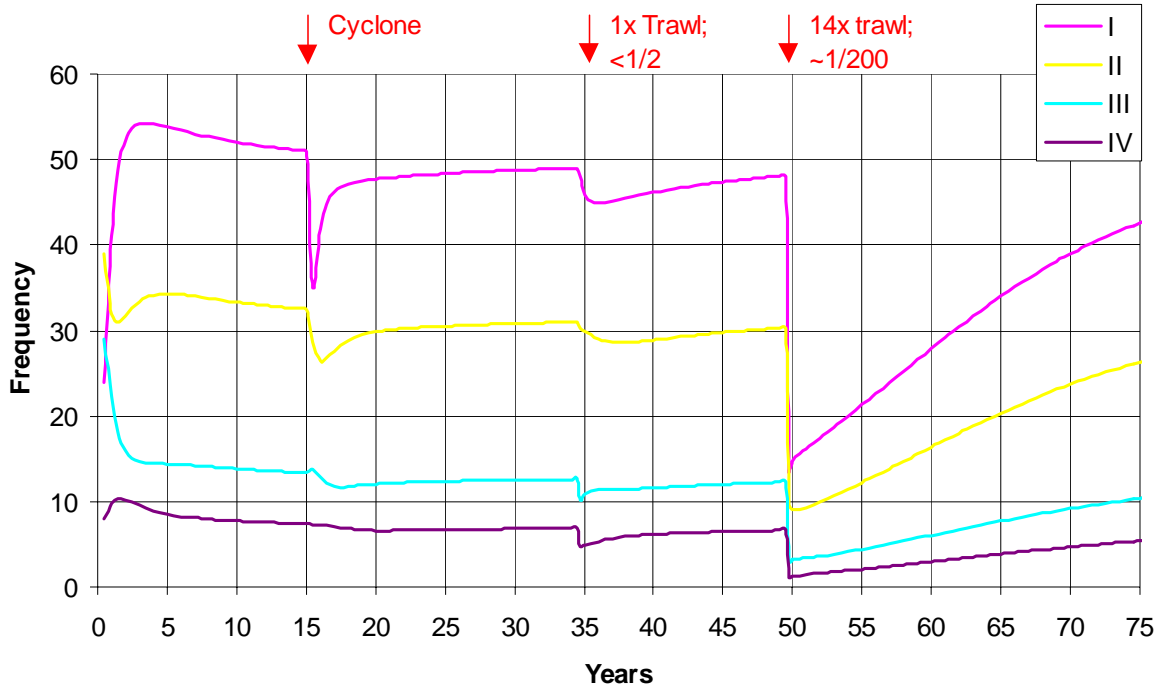
Yr+1 Class	Size class in Yr			
	I	II	III	IV
I	0.596	0.149	0.000	0.000
II	0.184	0.528	0.153	0.005
III	0.004	0.155	0.514	0.228
IV	0.000	0.003	0.117	0.750
TOTAL	0.784	0.836	0.784	0.983



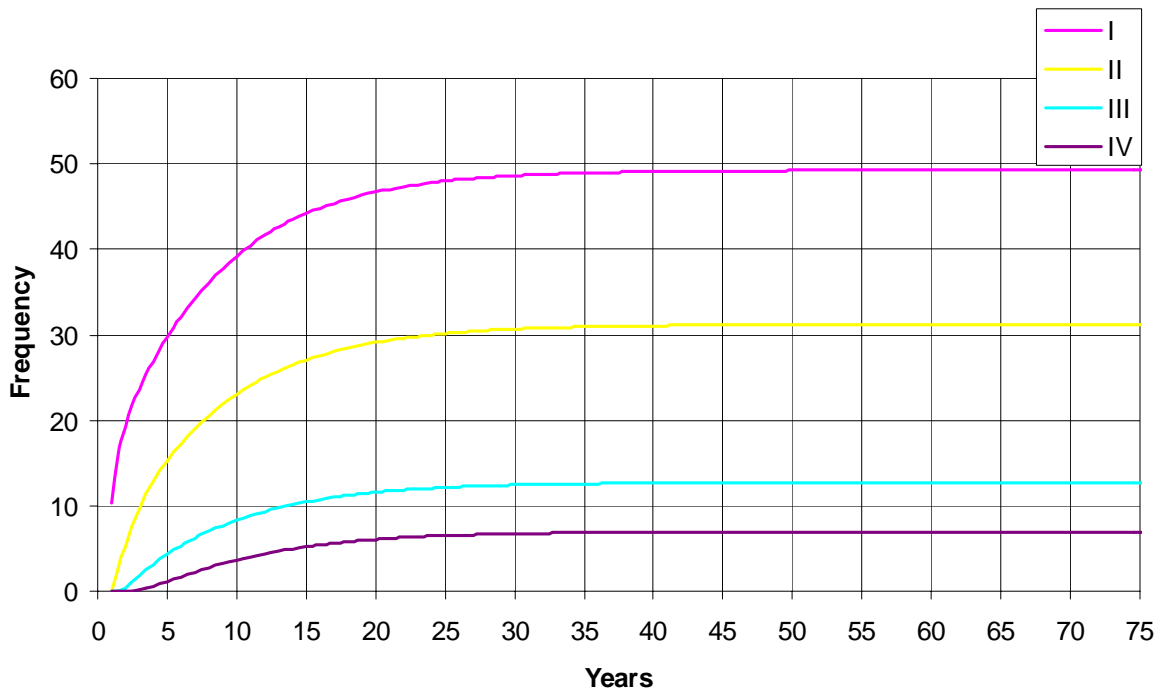
Appendix Fig. 7.5.4-1. Time trajectory of the four size-classes of *Xestospongia testudinaria* in a model run with 100% external recruitment, showing the simulated impact and recovery from a cyclone, a single trawl and 14 trawls. The model takes ~ 2 years to half-recover from the cyclone, ~ 2.5 years to half-recover from a single trawl, ~ 2.5 years to half-recover from 14 trawls and ~ 13 years to fully recover.



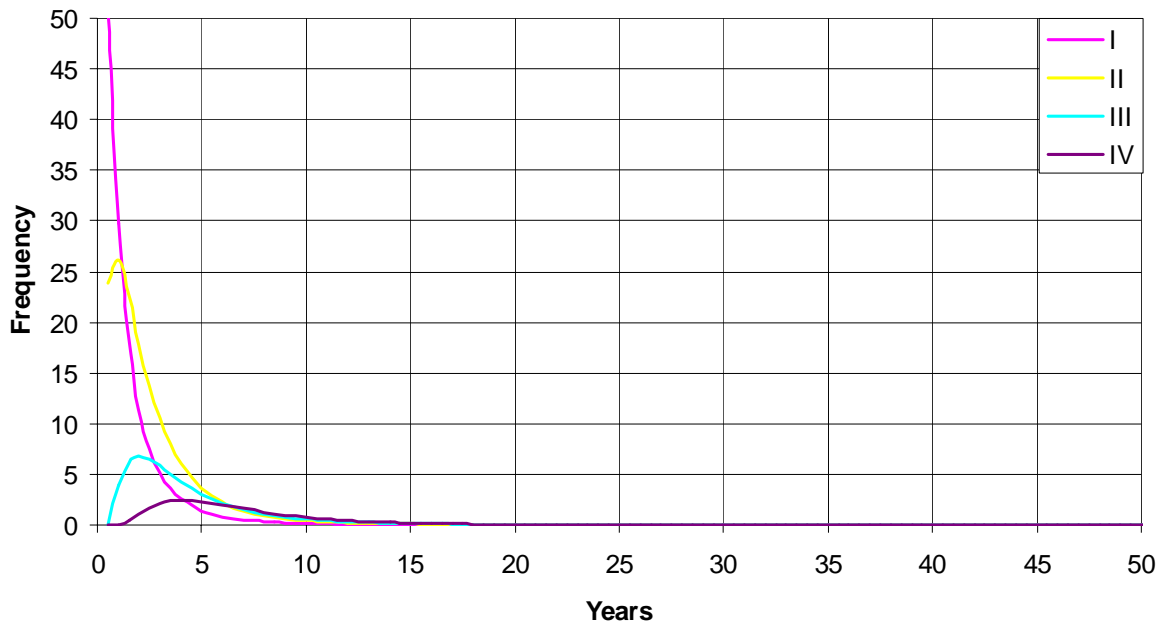
Appendix Fig. 7.5.4-2. Time trajectory of the four size-classes of *Xestospongia testudinaria* in a model run with 50:50 external & self-recruitment, showing the simulated impact and recovery from a cyclone, a single trawl and 14 trawls. The model takes ~ 5 years to half-recover from the cyclone, ~ 7 years to half-recover from a single trawl, ~ 5 years to half-recover from 14 trawls and ~ 28 years to fully recover.



Appendix Fig. 7.5.4-3. Time trajectory of the four size-classes of *Xestospongia testudinaria* in a model run with 100% self-recruitment, showing the simulated impact and recovery from a cyclone, a single trawl and 14 trawls. The model takes ~5 years to half-recover from the cyclone, ~10 years to half-recover from a single trawl, ~14 years to half-recover from 14 trawls and ~43 years to fully recover.



Appendix Fig. 7.5.4-4. Time trajectory of the four size-classes of *Xestospongia testudinaria* in a model run to establish a population from zero with 50:50 external & self-recruitment. The model takes ~5 years to half-establish, and ~33 years to fully establish.



Appendix Fig. 7.5.4-5. Time trajectory of the four size-classes of *Xestospongia testudinaria* in a model run to establish the fate of a single pulse of 100 Size I recruits (0-14 cm height), showing survival and growth through to larger size classes. Peak Size IV (>34 cm height) abundance of ~2.5% occurs ~4 years after recruitment. Approximately 6% of Size I recruits attain Size IV after an average of 3.8 years, with a 90-percentile range of 1.5–7.5 years.

7.5.5 *Semperina brunei*

Appendix 7.5–9. A: Size-transition and survival probabilities for *Semperina brunei* under normal (non-cyclonic) conditions, and overall transition probabilities for B: 100% external recruitment, C: 50:50 external and self-recruitment, and D: 100% self-recruitment.

A: Normal size & survival probabilities

Normal Size Transition Probabilities

Yr+1 Class	Size class in Yr			
	I	II	III	IV
I	0.576	0.227	0.065	0.004
II	0.384	0.500	0.247	0.071
III	0.040	0.240	0.476	0.370
IV	0.000	0.033	0.212	0.555
TOTAL	1.000	1.000	1.000	1.000

Normal Survival Probabilities

Size class in Yr			
I	II	III	IV
0.784	0.806	0.806	0.902

B: 100% external recruitment

Self Recruitment Probabilities

Yr+1 Class	Size class in Yr			
	I	II	III	IV
I	0.000	0.000	0.000	0.000

Overall Transition Probabilities

Yr+1 Class	Size class in Yr			
	I	II	III	IV
I	0.451	0.183	0.052	0.004
II	0.301	0.403	0.199	0.064
III	0.032	0.193	0.384	0.333
IV	0.000	0.027	0.171	0.500
TOTAL	0.784	0.806	0.806	0.902

External Recruitment Numbers

19.8

C: 50:50 external and self-recruitment

Self Recruitment Probabilities

Yr+1 Class	Size class in Yr			
	I	II	III	IV
I	0.027	0.114	0.261	0.467

Overall Transition Probabilities

Yr+1 Class	Size class in Yr			
	I	II	III	IV
I	0.479	0.298	0.313	0.471
II	0.301	0.403	0.199	0.064
III	0.032	0.193	0.384	0.333
IV	0.000	0.027	0.171	0.500
TOTAL	0.811	0.921	1.067	1.369

External Recruitment Numbers

9.9

D: 100% self-recruitment

Self Recruitment Probabilities

Yr+1 Class	Size class in Yr			
	I	II	III	IV
I	0.074	0.310	0.707	1.265

Overall Transition Probabilities

Yr+1 Class	Size class in Yr			
	I	II	III	IV
I	0.526	0.493	0.759	1.269
II	0.301	0.403	0.199	0.064
III	0.032	0.193	0.384	0.333
IV	0.000	0.027	0.171	0.500
TOTAL	0.858	1.116	1.513	2.167

External Recruitment Numbers

0

Appendix 7.5–10. Size-transition matrix, survival probabilities and overall transition probabilities for *Semperina brunei* under cyclone affected conditions.

Cyclone Size Transition Probabilities

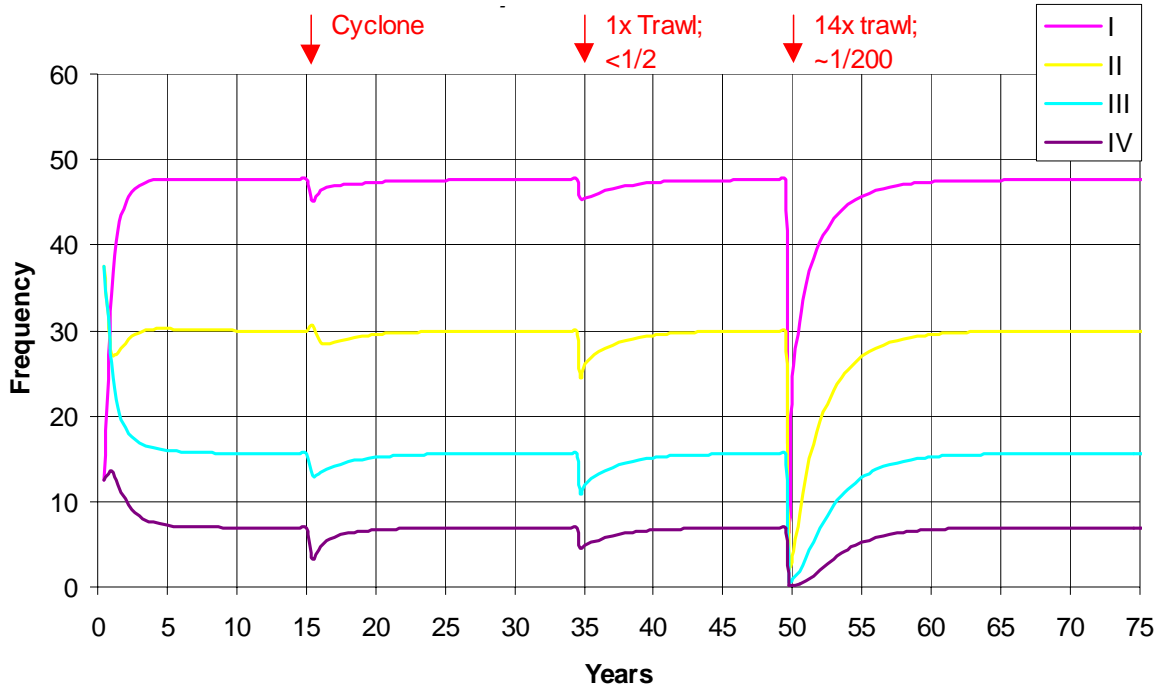
Yr+1 Class	Size class in Yr			
	I	II	III	IV
I	0.645	0.167	0.004	0.000
II	0.350	0.693	0.318	0.025
III	0.004	0.133	0.619	0.550
IV	0.000	0.007	0.059	0.424
TOTAL	1.000	1.000	1.000	1.000

Cyclone Survival Probabilities

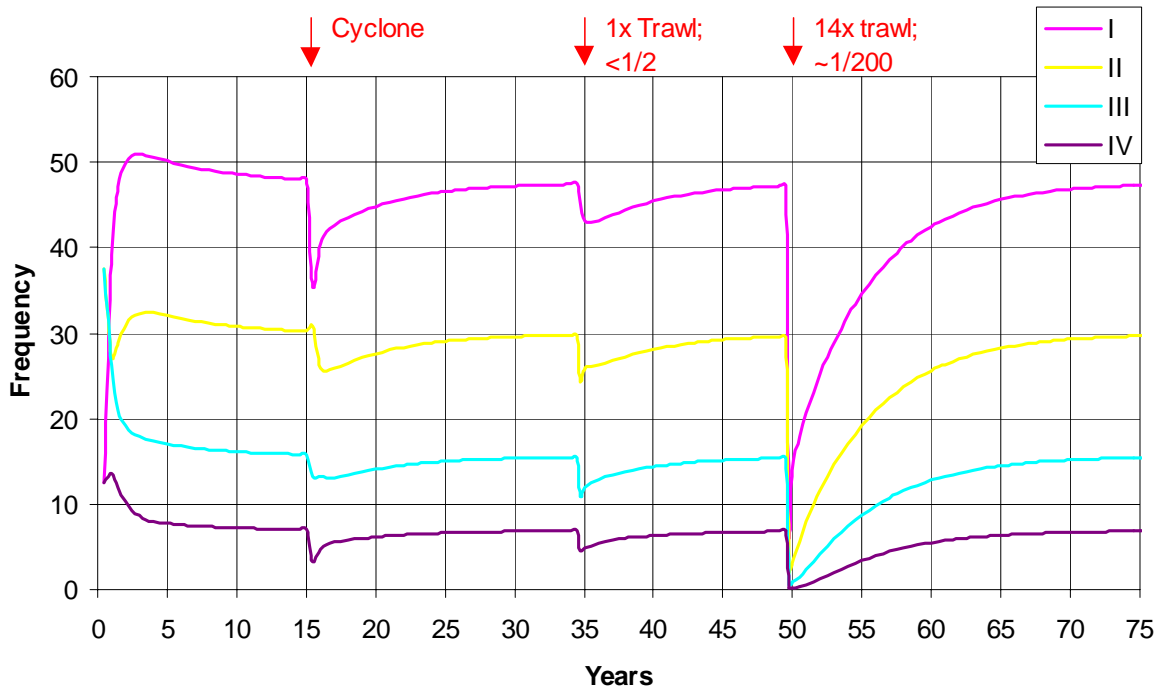
Size class in Yr			
I	II	III	IV
0.705	0.726	0.726	0.812

Overall Cyclone Transition Probabilities

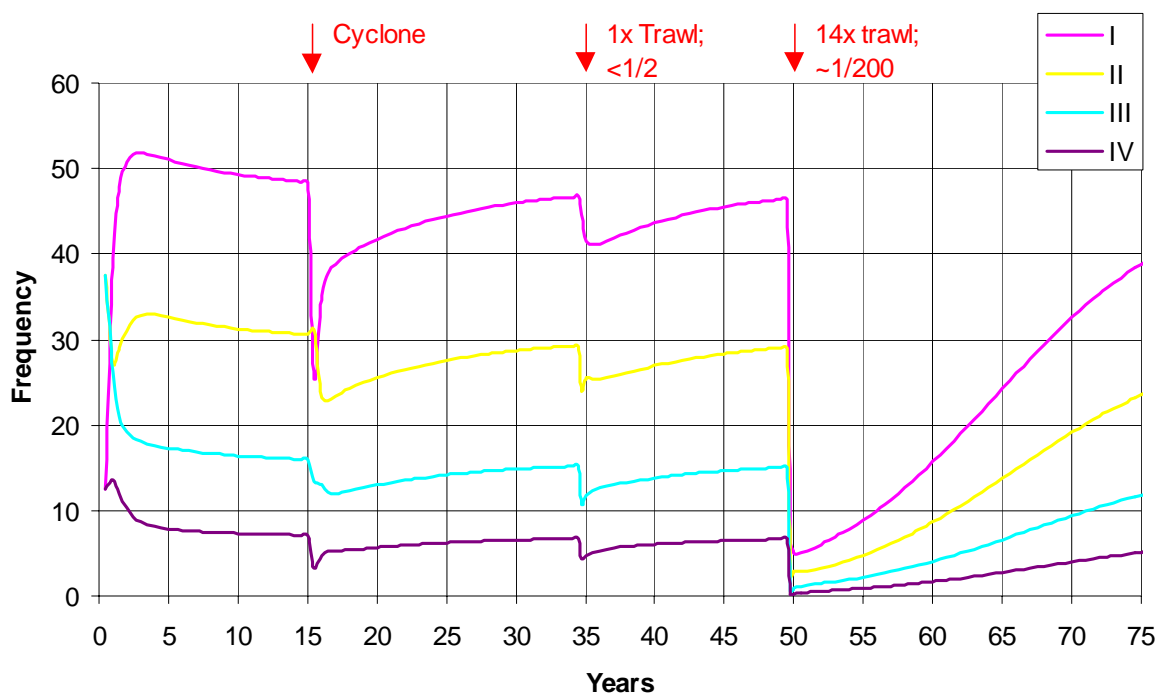
Yr+1 Class	Size class in Yr			
	I	II	III	IV
I	0.455	0.121	0.003	0.000
II	0.247	0.503	0.231	0.020
III	0.003	0.097	0.449	0.447
IV	0.000	0.005	0.043	0.344
TOTAL	0.705	0.726	0.726	0.812



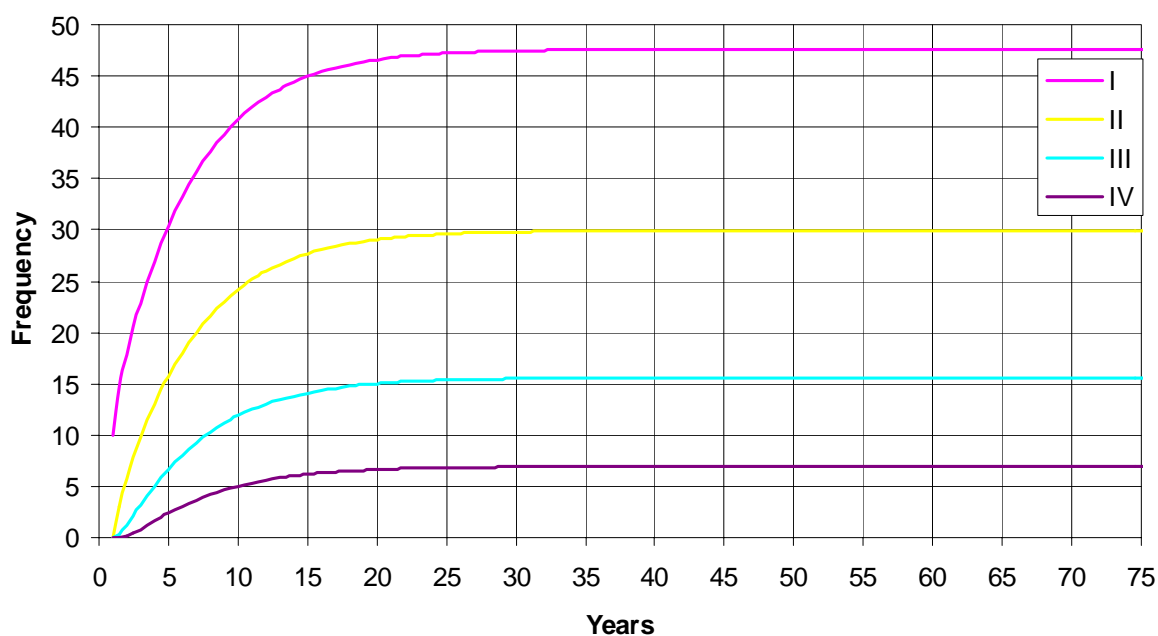
Appendix Fig. 7.5.5-1. Time trajectory of the four size-classes of *Semperina brunei* in a model run with 100% external recruitment, showing the simulated impact and recovery from a cyclone, a single trawl and 14 trawls. The model takes ~2 years to half-recover from the cyclone, ~2 years to half-recover from a single trawl, ~2 years to half-recover from 14 trawls and ~11 years to fully recover.



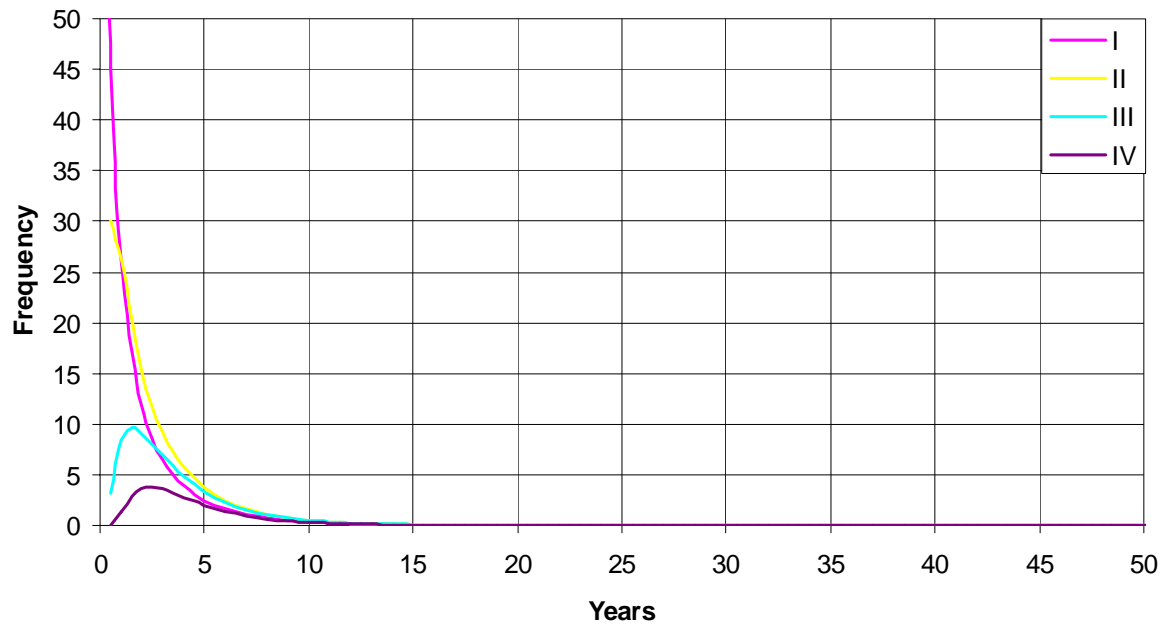
Appendix Fig. 7.5.5-2. Time trajectory of the four size-classes of *Semperina brunei* in a model run with 50:50 external & self-recruitment, showing the simulated impact and recovery from a cyclone, a single trawl and 14 trawls. The model takes ~5 years to half-recover from the cyclone, ~4 years to half-recover from a single trawl, ~4 years to half-recover from 14 trawls and ~24 years to fully recover.



Appendix Fig. 7.5.5-3. Time trajectory of the four size-classes of *Semperina brunei* in a model run with 100% self-recruitment, showing the simulated impact and recovery from a cyclone, a single trawl and 14 trawls. The model takes ~6 years to half-recover from the cyclone, ~6 years to half-recover from a single trawl, ~17 years to half-recover from 14 trawls and ~50 years to fully recover.



Appendix Fig. 7.5.5-4. Time trajectory of the four size-classes of *Semperina brunei* in a model run to establish a population from zero with 50:50 external & self-recruitment. The model takes ~5 years to half-establish, and ~26 years to fully establish.



Appendix Fig. 7.5.5-5. Time trajectory of the four size-classes of *Semperina brunei* in a model run to establish the fate of a single pulse of 100 Size I recruits (0–23 cm wide), showing survival and growth through to larger size classes. Peak Size IV (>54 cm wide) abundance of ~4% occurs ~2.5 years after recruitment. Approximately 13% of Size I recruits attain Size IV after an average of 3 years, with a 90-percentile range of 1–6.5 years.

7.5.6 *Cymbastella coralliophila*

Appendix 7.5–11. A: Size-transition and survival probabilities for *Cymbastella coralliophila* under normal (non-cyclonic) conditions, and overall transition probabilities for B: 100% external recruitment, C: 50:50 external and self-recruitment, and D: 100% self-recruitment.

A: Normal size & survival probabilities

Normal Size Transition Probabilities

Yr+1 Class	Size class in Yr			
	I	II	III	IV
I	0.607	0.072	0.000	0.000
II	0.393	0.746	0.081	0.000
III	0.000	0.183	0.739	0.081
IV	0.000	0.000	0.181	0.919
TOTAL	1.000	1.000	1.000	1.000

Normal Survival Probabilities

Size class in Yr			
I	II	III	IV
0.990	0.990	0.990	0.850*

B: 100% external recruitment

Self Recruitment Probabilities

Yr+1 Class	Size class in Yr			
	I	II	III	IV
I	0.000	0.000	0.000	0.000

Overall Transition Probabilities

Yr+1 Class	Size class in Yr			
	I	II	III	IV
I	0.601	0.071	0.000	0.000
II	0.389	0.738	0.080	0.000
III	0.000	0.181	0.731	0.069
IV	0.000	0.000	0.179	0.781
TOTAL	0.990	0.990	0.990	0.850

External Recruitment Numbers

4.2

C: 50:50 external and self-recruitment

Self Recruitment Probabilities

Yr+1 Class	Size class in Yr			
	I	II	III	IV
I	0.004	0.016	0.031	0.047

Overall Transition Probabilities

Yr+1 Class	Size class in Yr			
	I	II	III	IV
I	0.605	0.087	0.031	0.047
II	0.389	0.738	0.080	0.000
III	0.000	0.181	0.731	0.069
IV	0.000	0.000	0.179	0.781
TOTAL	0.994	1.006	1.021	0.897

External Recruitment Numbers

2.1

D: 100% self-recruitment

Self Recruitment Probabilities

Yr+1 Class	Size class in Yr			
	I	II	III	IV
I	0.011	0.043	0.086	0.129

Overall Transition Probabilities

Yr+1 Class	Size class in Yr			
	I	II	III	IV
I	0.612	0.114	0.086	0.129
II	0.389	0.738	0.080	0.000
III	0.000	0.181	0.731	0.069
IV	0.000	0.000	0.179	0.781
TOTAL	1.001	1.033	1.076	0.979

External Recruitment Numbers

0

Appendix 7.5–12. Size-transition matrix, survival probabilities and overall transition probabilities for *Cymbastella coralliophila* under cyclone affected conditions.

Cyclone Size Transition Probabilities

Yr+1 Class	Size class in Yr			
	I	II	III	IV
I	0.892	0.057	0.000	0.000
II	0.108	0.869	0.029	0.000
III	0.000	0.074	0.917	0.044
IV	0.000	0.000	0.054	0.956
TOTAL	1.000	1.000	1.000	1.000

Cyclone Survival Probabilities

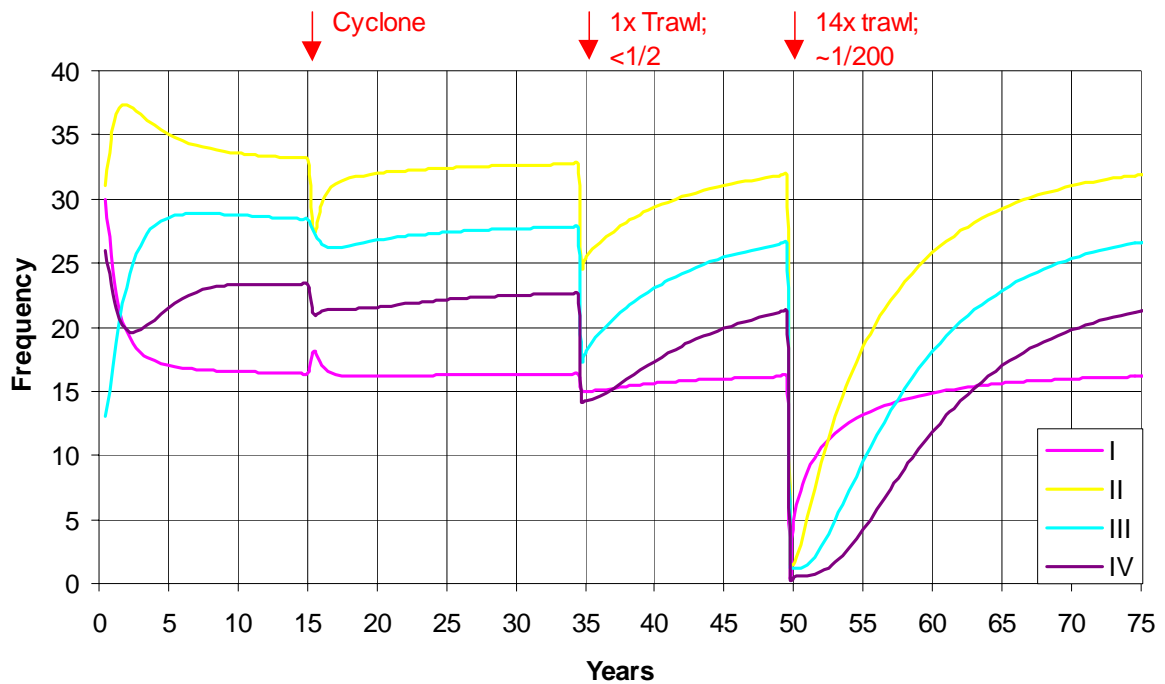
Size class in Yr				
	I	II	III	IV
	0.840	0.879	0.934	0.879

Cyclone Self Recruitment Probabilities

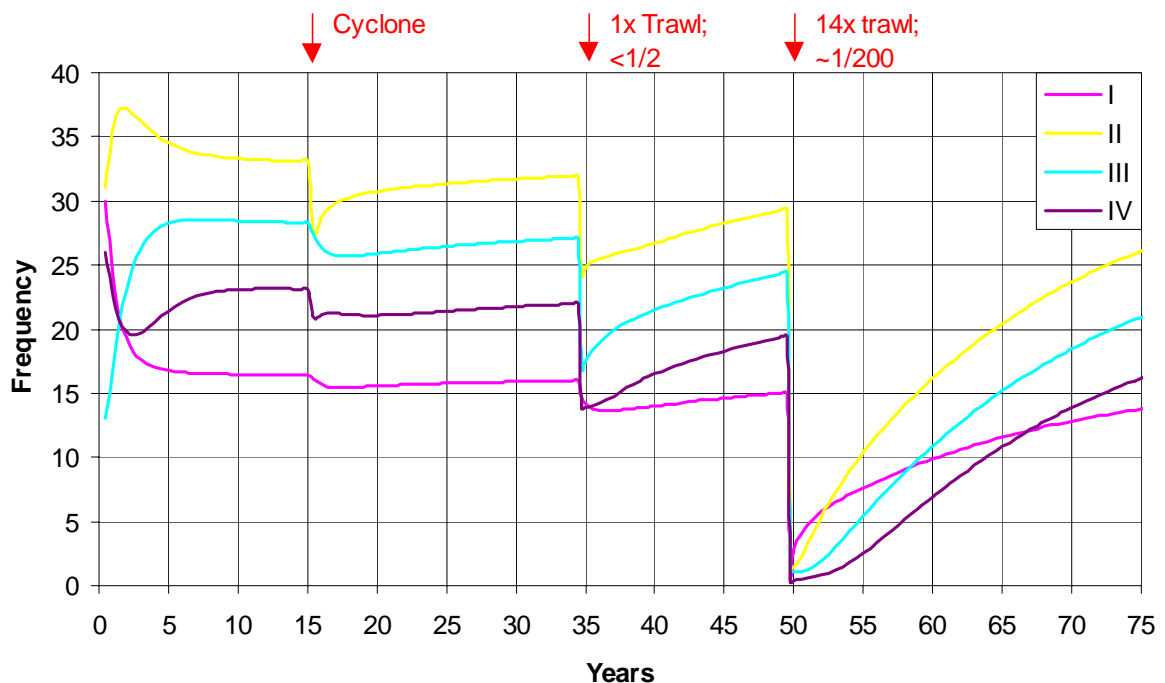
Yr+1 Class	Size class in Yr			
	I	II	III	IV
I	0.000	0.000	0.000	0.000

Overall Cyclone Transition Probabilities

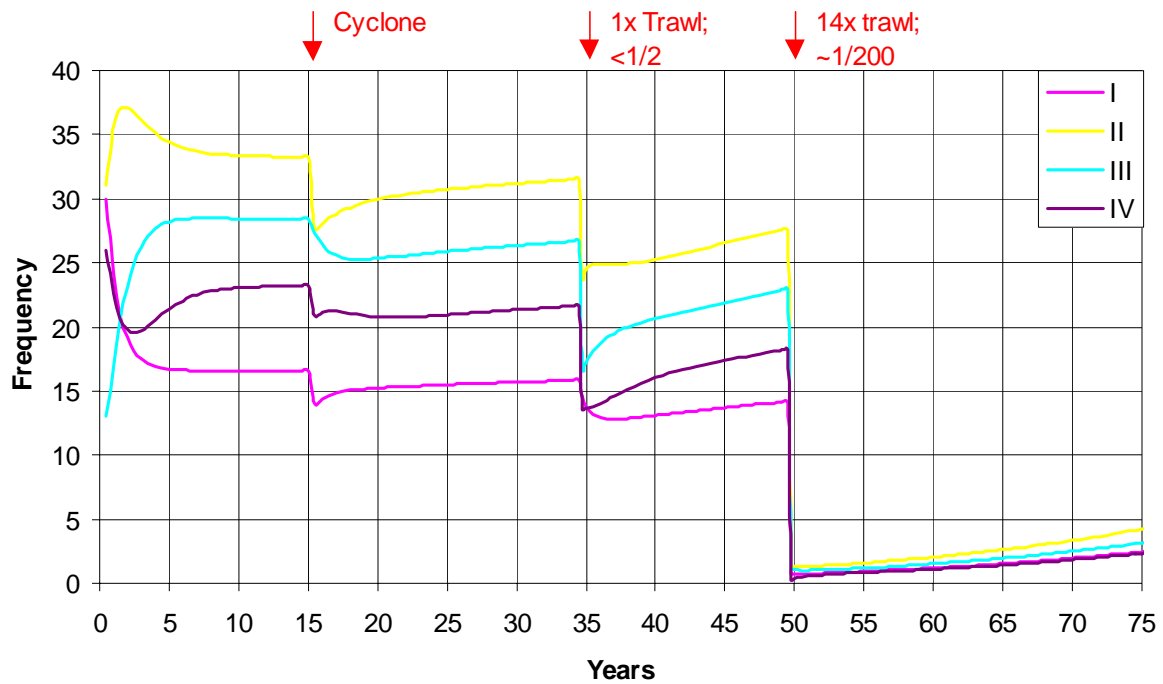
Yr+1 Class	Size class in Yr			
	I	II	III	IV
I	0.749	0.050	0.000	0.000
II	0.091	0.764	0.027	0.000
III	0.000	0.065	0.856	0.039
IV	0.000	0.000	0.051	0.840
TOTAL	0.840	0.879	0.934	0.879



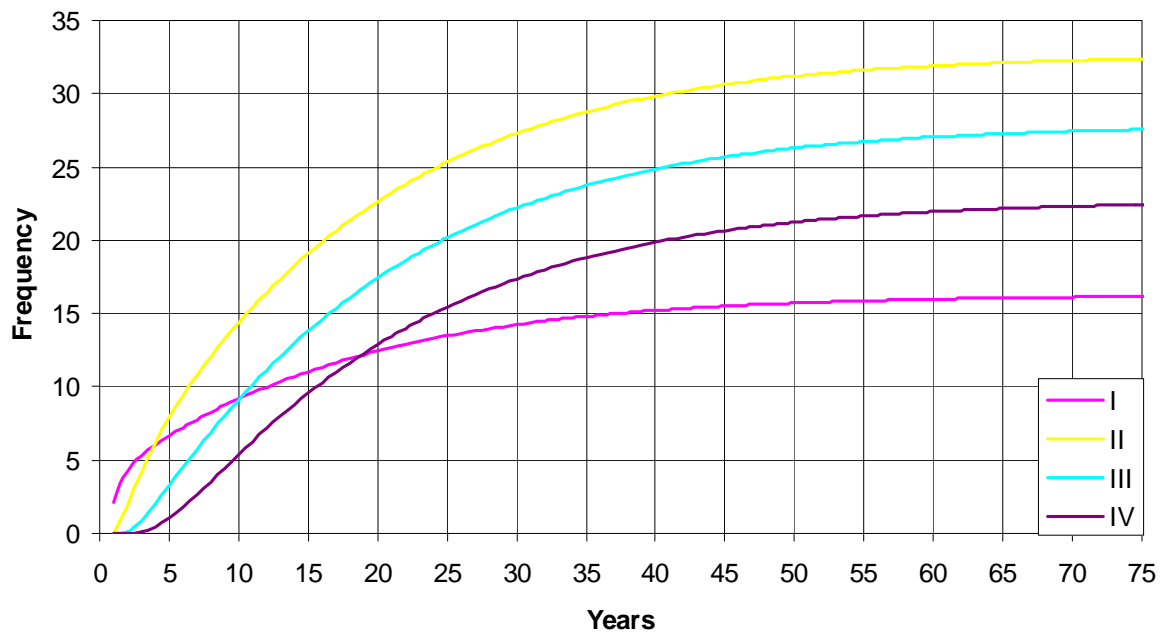
Appendix Fig. 7.5.6-1. Time trajectory of the four size-classes of *Cymbastella coralliophila* in a model run with 100% external recruitment, showing the simulated impact and recovery from a cyclone, a single trawl and 14 trawls. The model takes ~ 7 years to half-recover from the cyclone, ~ 7 years to half-recover from a single trawl, ~ 8 years to half-recover from 14 trawls and ~ 25 years to fully recover.



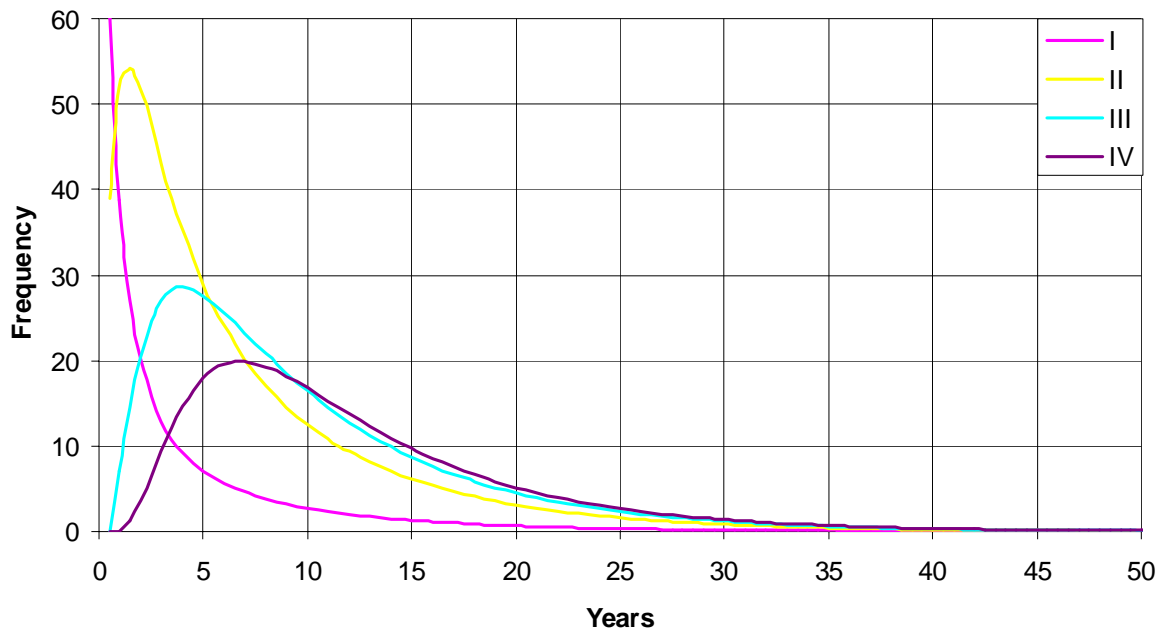
Appendix Fig. 7.5.6-2. Time trajectory of the four size-classes of *Cymbastella coralliophila* in a model run with 50:50 external & self-recruitment, showing the simulated impact and recovery from a cyclone, a single trawl and 14 trawls. The model takes ~ 11 years to half-recover from the cyclone, ~ 10 years to half-recover from a single trawl, ~ 11 years to half-recover from 14 trawls and ~ 36 years to fully recover.



Appendix Fig. 7.5.6-3. Time trajectory of the four size-classes of *Cymbastella coralliophila* in a model run with 100% self-recruitment, showing the simulated impact and recovery from a cyclone, a single trawl and 14 trawls. The model takes ~17 years to half-recover from the cyclone, ~15 years to half-recover from a single trawl, ~57 years to half-recover from 14 trawls and ~150 years to fully recover.



Appendix Fig. 7.5.6-4. Time trajectory of the four size-classes of *Cymbastella coralliophila* in a model run to establish a population from zero with 50:50 external & self-recruitment. The model takes ~14 years to half-establish, and more than 100 years to fully establish.



Appendix Fig. 7.5.6-5. Time trajectory of the four size-classes of *Cymbastella coralliophila* in a model run to establish the fate of a single pulse of 100 Size I recruits (0-16 cm across), showing survival and growth through to larger size classes. Peak Size IV (>36 cm across) abundance of ~20% occurs ~7 years after recruitment. Approximately 74% of Size I recruits attain Size IV after an average of 7.7 years, with a 90-percentile range of 2–18 years.

7.5.7 *Ianthella basta*

Appendix 7.5–13. A: Size-transition and survival probabilities for *Ianthella basta* under normal (non-cyclonic) conditions, and overall transition probabilities for B: 100% external recruitment, C: 50:50 external and self-recruitment, and D: 100% self-recruitment.

A: Normal size & survival probabilities

Normal Size Transition Probabilities

Yr+1 Class	Size class in Yr			
	I	II	III	IV
I	0.762	0.065	0.000	0.000
II	0.238	0.629	0.053	0.000
III	0.000	0.302	0.561	0.069
IV	0.000	0.004	0.386	0.931
TOTAL	1.000	1.000	1.000	1.000

Normal Survival Probabilities

Size class in Yr			
I	II	III	IV
0.812	0.990	0.947	0.650*

B: 100% external recruitment

Self Recruitment Probabilities

Yr+1 Class	Size class in Yr			
	I	II	III	IV
I	0.000	0.000	0.000	0.000

Overall Transition Probabilities

Yr+1 Class	Size class in Yr			
	I	II	III	IV
I	0.619	0.065	0.000	0.000
II	0.193	0.622	0.050	0.000
III	0.000	0.299	0.531	0.045
IV	0.000	0.004	0.366	0.605
TOTAL	0.812	0.990	0.947	0.650

External Recruitment Numbers

14.8

C: 50:50 external and self-recruitment

Self Recruitment Probabilities

Yr+1 Class	Size class in Yr			
	I	II	III	IV
I	0.006	0.055	0.153	0.300

Overall Transition Probabilities

Yr+1 Class	Size class in Yr			
	I	II	III	IV
I	0.625	0.119	0.153	0.300
II	0.193	0.622	0.050	0.000
III	0.000	0.299	0.531	0.045
IV	0.000	0.004	0.366	0.605
TOTAL	0.818	1.045	1.100	0.950

External Recruitment Numbers

7.4

D: 100% self-recruitment

Self Recruitment Probabilities

Yr+1 Class	Size class in Yr			
	I	II	III	IV
I	0.016	0.149	0.415	0.815

Overall Transition Probabilities

Yr+1 Class	Size class in Yr			
	I	II	III	IV
I	0.635	0.214	0.415	0.815
II	0.193	0.622	0.050	0.000
III	0.000	0.299	0.531	0.045
IV	0.000	0.004	0.366	0.605
TOTAL	0.829	1.139	1.363	1.465

External Recruitment Numbers

0

Appendix 7.5–14. Size-transition matrix, survival probabilities and overall transition probabilities for *Ianthella basta* under cyclone affected conditions.

Cyclone Size Transition Probabilities

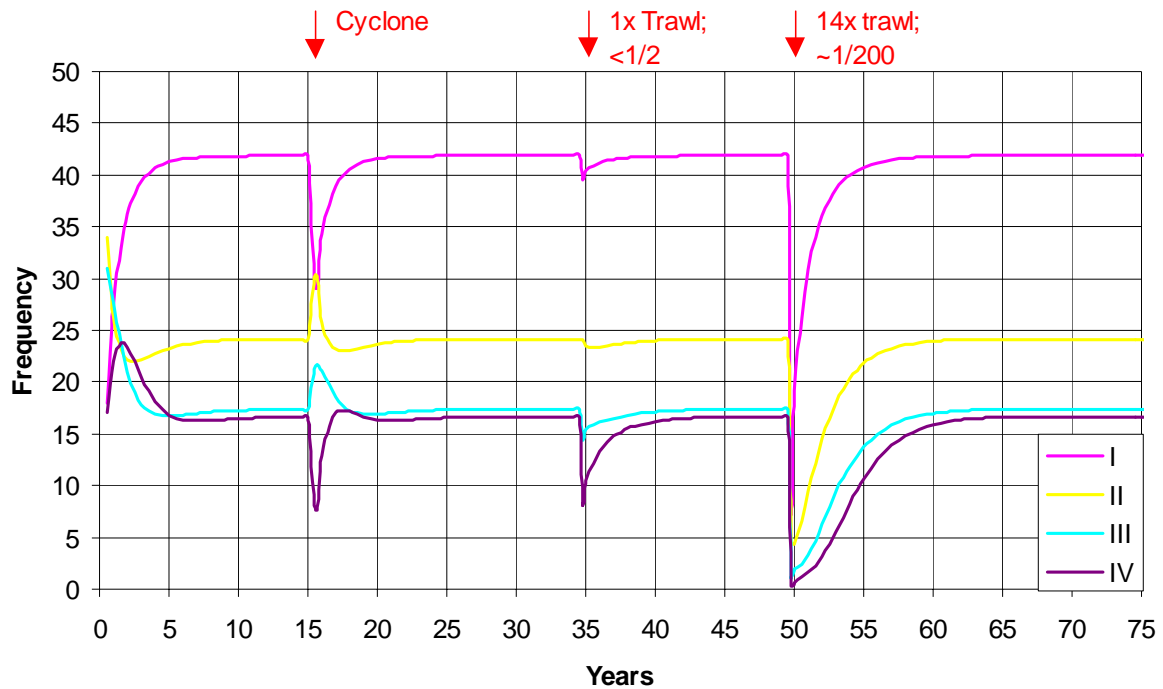
Yr+1 Class	Size class in Yr			
	I	II	III	IV
I	0.498	0.010	0.000	0.000
II	0.502	0.710	0.037	0.000
III	0.000	0.280	0.934	0.227
IV	0.000	0.000	0.029	0.773
TOTAL	1.000	1.000	1.000	1.000

Cyclone Survival Probabilities

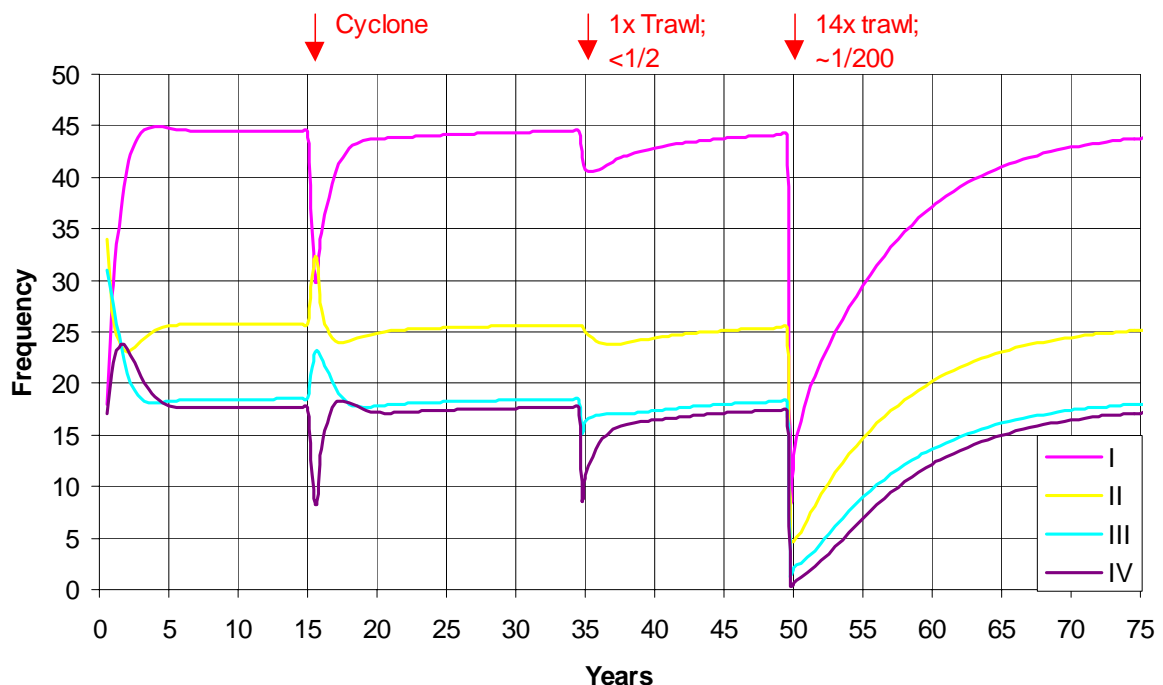
Size class in Yr				
	I	II	III	IV
	0.706	0.861	0.824	0.566

Overall Cyclone Transition Probabilities

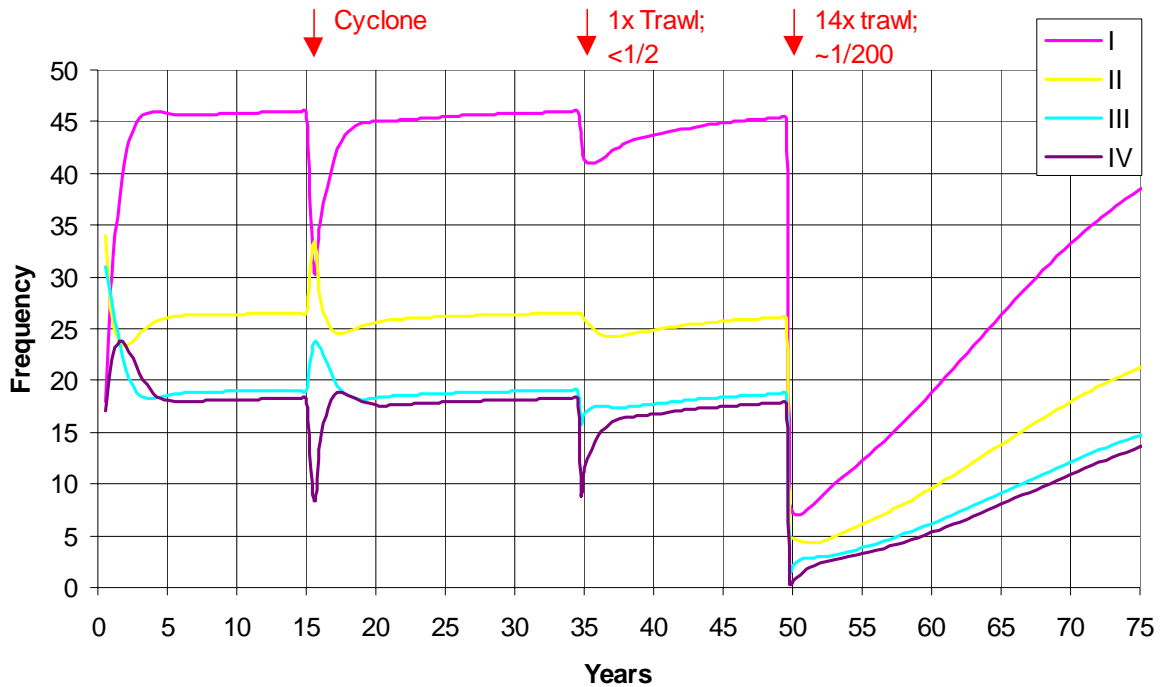
Yr+1 Class	Size class in Yr			
	I	II	III	IV
I	0.352	0.009	0.000	0.000
II	0.355	0.611	0.030	0.000
III	0.000	0.241	0.770	0.128
IV	0.000	0.000	0.024	0.437
TOTAL	0.706	0.861	0.824	0.566



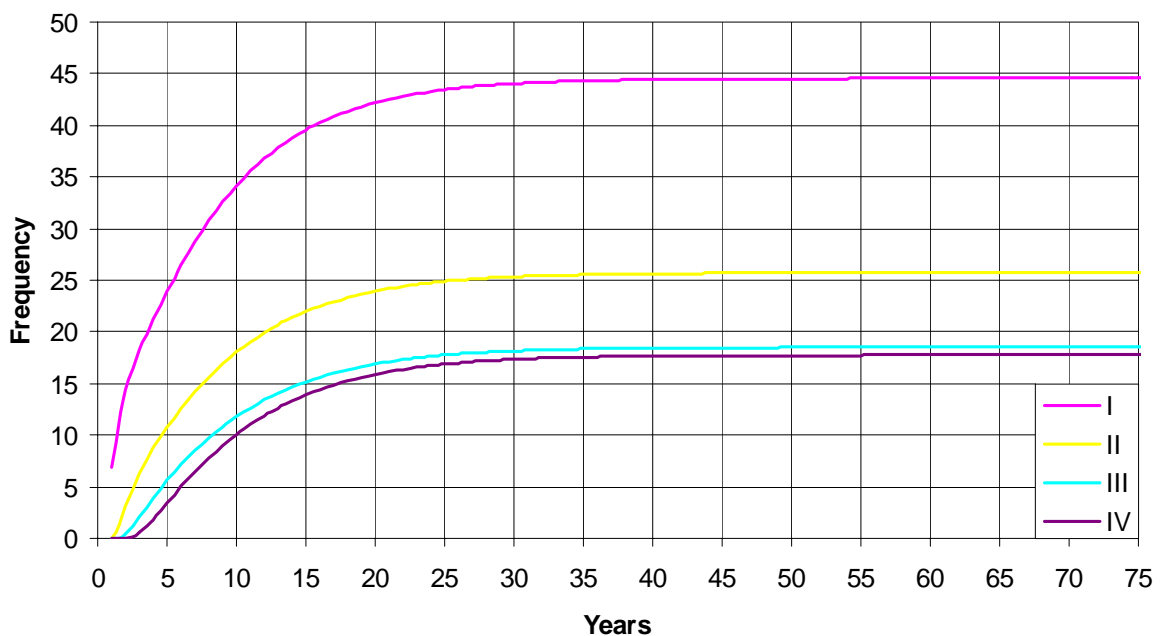
Appendix Fig. 7.5.7-1. Time trajectory of the four size-classes of *Ianthella basta* in a model run with 100% external recruitment, showing the simulated impact and recovery from a cyclone, a single trawl and 14 trawls. The model takes ~1.5 years to half-recover from the cyclone, ~1.5 years to half-recover from a single trawl, ~2.5 years to half-recover from 14 trawls and ~11 years to fully recover.



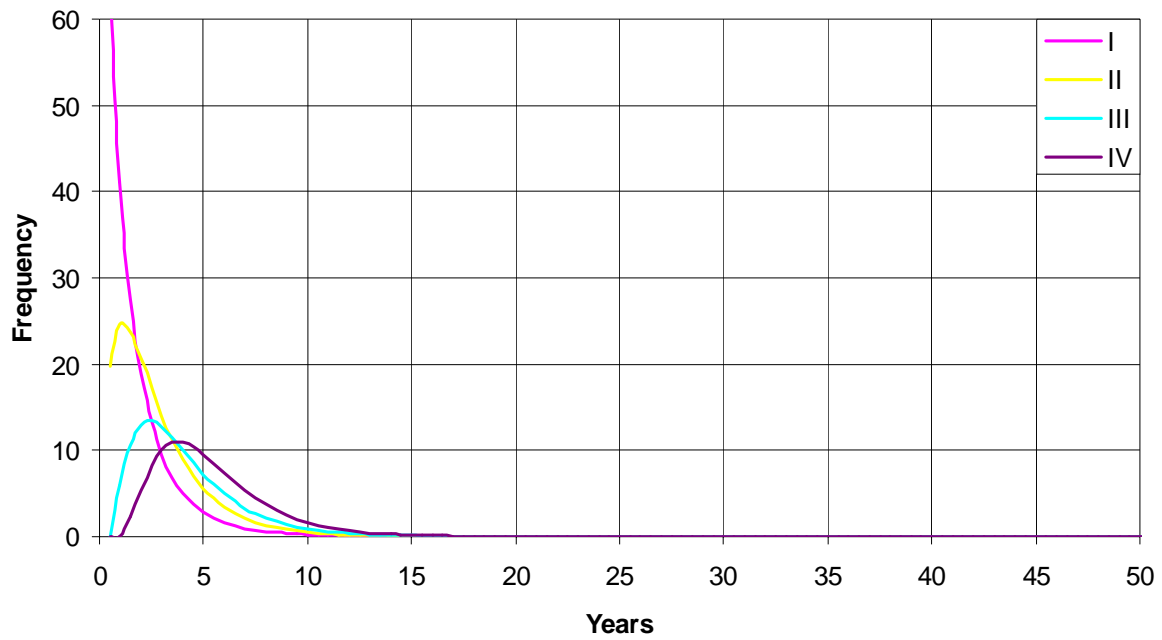
Appendix Fig. 7.5.7-2. Time trajectory of the four size-classes of *Ianthella basta* in a model run with 50:50 external & self-recruitment, showing the simulated impact and recovery from a cyclone, a single trawl and 14 trawls. The model takes ~5 years to half-recover from the cyclone, ~3 years to half-recover from a single trawl, ~5 years to half-recover from 14 trawls and ~27 years to fully recover.



Appendix Fig. 7.5.7-3. Time trajectory of the four size-classes of *Ianthella basta* in a model run with 100% self-recruitment, showing the simulated impact and recovery from a cyclone, a single trawl and 14 trawls. The model takes ~6 years to half-recover from the cyclone, ~4 years to half-recover from a single trawl, ~16 years to half-recover from 14 trawls and ~43 years to fully recover.



Appendix Fig. 7.5.7-4. Time trajectory of the four size-classes of *Ianthella basta* in a model run to establish a population from zero with 50:50 external & self-recruitment. The model takes ~5 years to half-establish, and ~30 years to fully establish.



Appendix Fig. 7.5.7-5. Time trajectory of the four size-classes of *Ianthella basta* in a model run to establish the fate of a single pulse of 100 Size I recruits (0-15 cm height), showing survival and growth through to larger size classes. Peak Size IV (>38 cm height) abundance of ~11% occurs ~4 years after recruitment. Approximately 38% of Size I recruits attain Size IV after an average of 4.2 years, with a 90-percentile range of 1.5–8.5 years.

7.5.8 *Subergorgia reticulata*

Appendix 7.5–15. A: Size-transition and survival probabilities for *Subergorgia reticulata* under normal (non-cyclonic) conditions, and overall transition probabilities for B: 100% external recruitment, C: 50:50 external and self-recruitment, and D: 100% self-recruitment.

A: Normal size & survival probabilities

Normal Size Transition Probabilities

Yr+1 Class	Size class in Yr			
	I	II	III	IV
I	0.555	0.112	0.000	0.000
II	0.432	0.677	0.284	0.020
III	0.014	0.207	0.640	0.571
IV	0.000	0.004	0.077	0.409
TOTAL	1.000	1.000	1.000	1.000

Normal Survival Probabilities

Size class in Yr			
I	II	III	IV
0.960	0.960	0.960	0.960

B: 100% external recruitment

Self Recruitment Probabilities

Yr+1 Class	Size class in Yr			
	I	II	III	IV
I	0.000	0.000	0.000	0.000

Overall Transition Probabilities

Yr+1 Class	Size class in Yr			
	I	II	III	IV
I	0.532	0.107	0.000	0.000
II	0.415	0.650	0.272	0.019
III	0.013	0.199	0.614	0.548
IV	0.000	0.004	0.074	0.393
TOTAL	0.960	0.960	0.960	0.960

External Recruitment Numbers

4

C: 50:50 external and self-recruitment

Self Recruitment Probabilities

Yr+1 Class	Size class in Yr			
	I	II	III	IV
I	0.002	0.016	0.044	0.087

Overall Transition Probabilities

Yr+1 Class	Size class in Yr			
	I	II	III	IV
I	0.534	0.123	0.044	0.087
II	0.415	0.650	0.272	0.019
III	0.013	0.199	0.614	0.548
IV	0.000	0.004	0.074	0.393
TOTAL	0.962	0.976	1.004	1.047

External Recruitment Numbers

2

D: 100% self-recruitment

Self Recruitment Probabilities

Yr+1 Class	Size class in Yr			
	I	II	III	IV
I	0.005	0.043	0.119	0.235

Overall Transition Probabilities

Yr+1 Class	Size class in Yr			
	I	II	III	IV
I	0.537	0.150	0.119	0.235
II	0.415	0.650	0.272	0.019
III	0.013	0.199	0.614	0.548
IV	0.000	0.004	0.074	0.393
TOTAL	0.965	1.003	1.079	1.195

External Recruitment Numbers

0

Appendix 7.5–16. Size-transition matrix, survival probabilities and overall transition probabilities for *Subergorgia reticulata* under cyclone affected conditions.

Cyclone Size Transition Probabilities

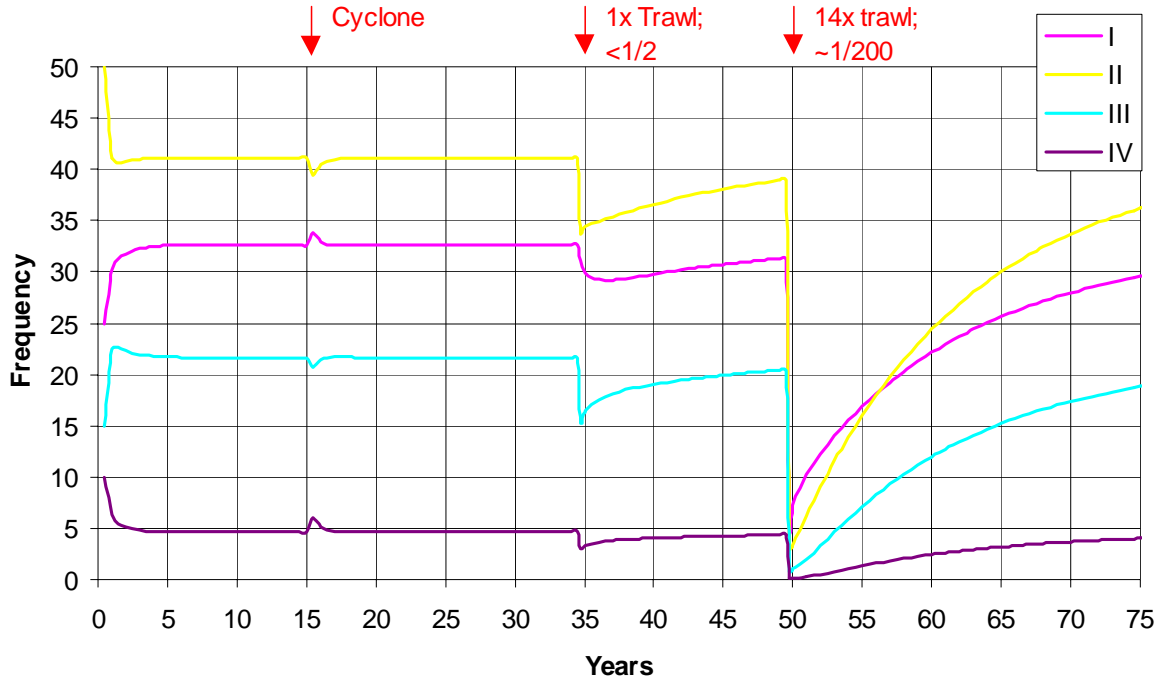
Yr+1 Class	Size class in Yr			
	I	II	III	IV
I	0.647	0.208	0.032	0.000
II	0.332	0.581	0.289	0.049
III	0.021	0.208	0.494	0.440
IV	0.000	0.004	0.186	0.510
TOTAL	1.000	1.000	1.000	1.000

Cyclone Survival Probabilities

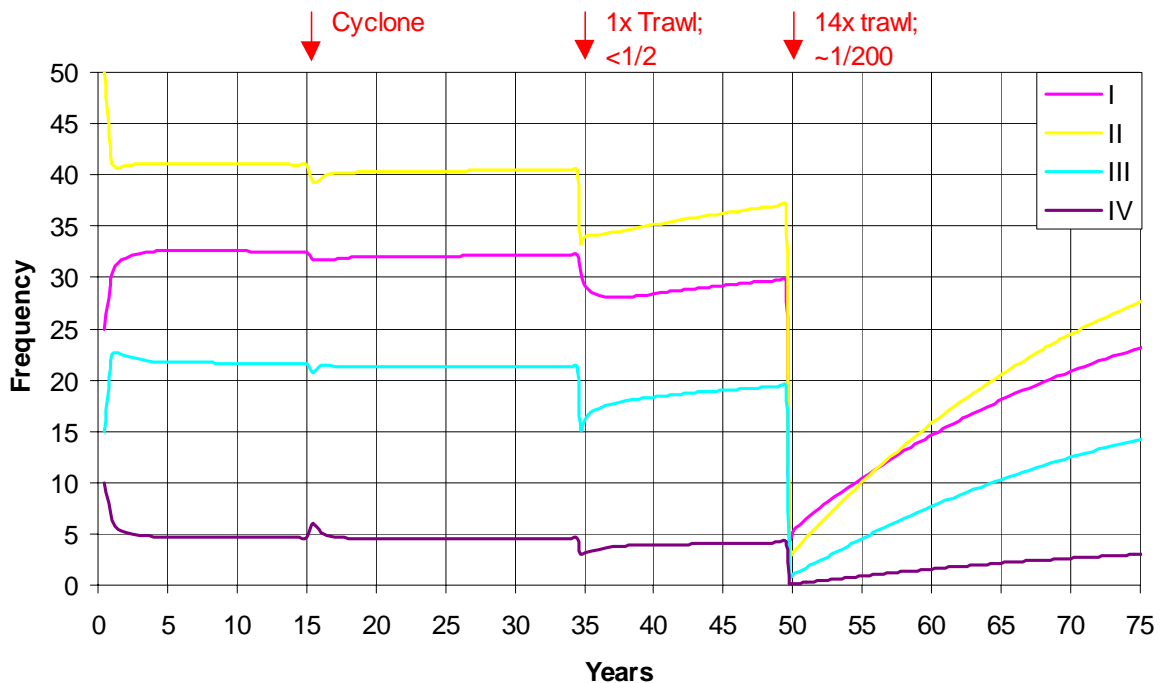
		Size class in Yr			
		I	II	III	IV
		0.960	0.960	0.960	0.960

Overall Cyclone Transition Probabilities

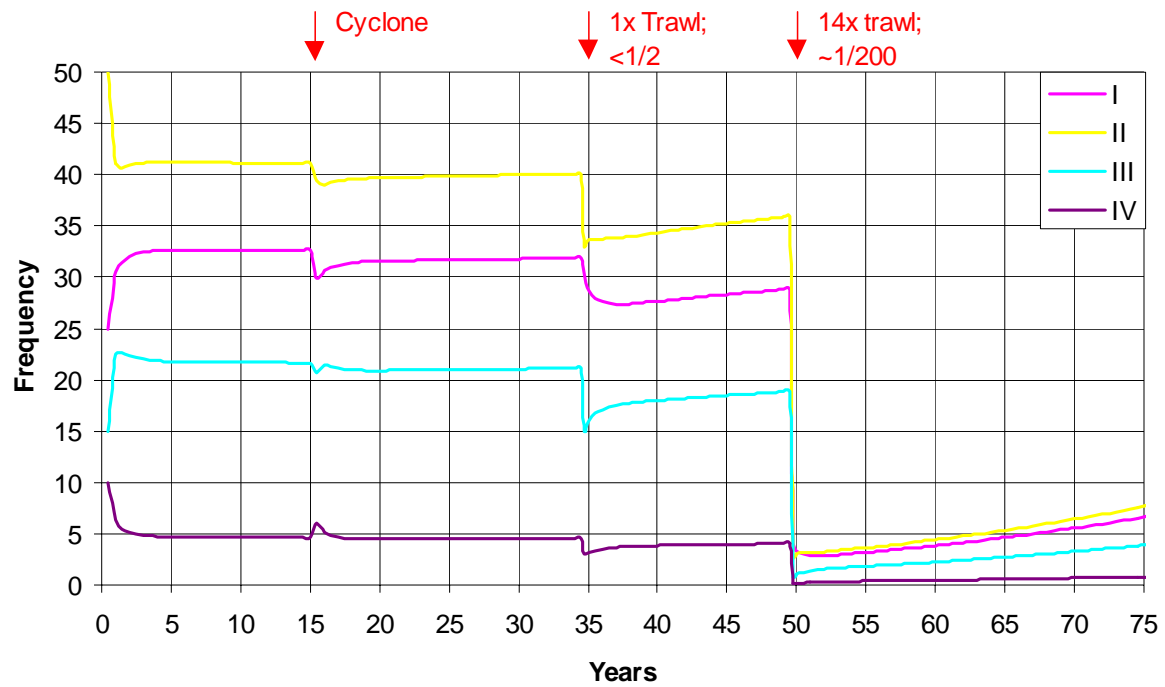
Yr+1 Class	Size class in Yr			
	I	II	III	IV
I	0.621	0.199	0.030	0.000
II	0.318	0.557	0.277	0.047
III	0.020	0.199	0.474	0.423
IV	0.000	0.004	0.178	0.490
TOTAL	0.960	0.960	0.960	0.960



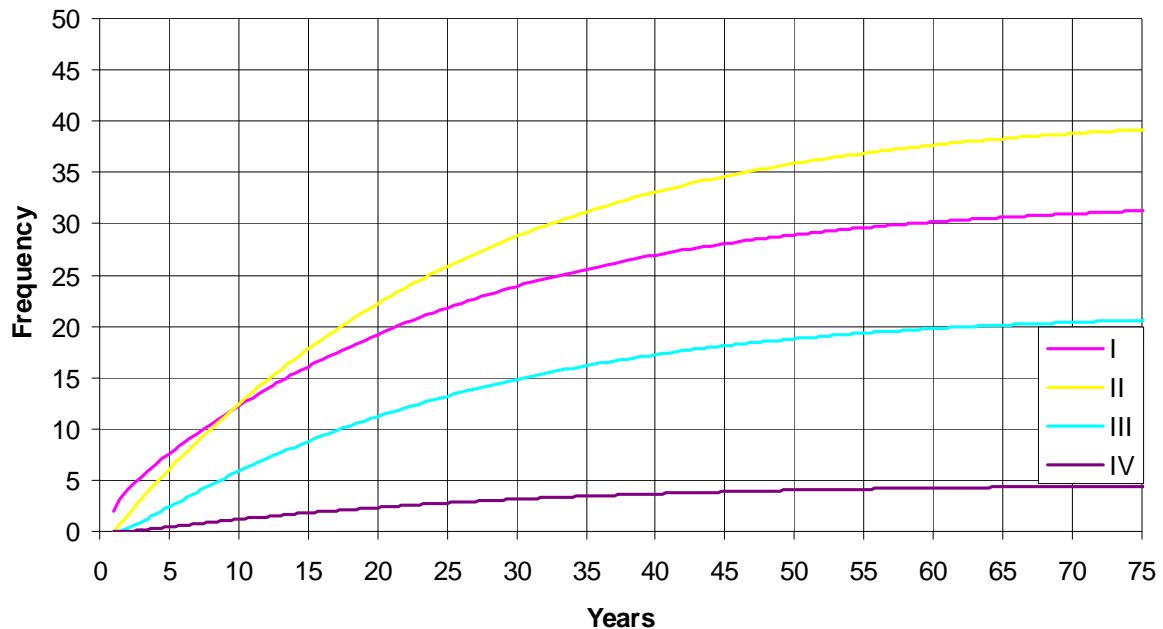
Appendix Fig. 7.5.8-1. Time trajectory of the four size-classes of *Subergorgia reticulata* in a model run with 100% external recruitment, showing the simulated impact and recovery from a cyclone, a single trawl and 14 trawls. The model takes ~1 year to half-recover from the cyclone, ~8 years to half-recover from a single trawl, ~8 years to half-recover from 14 trawls and ~36 years to fully recover.



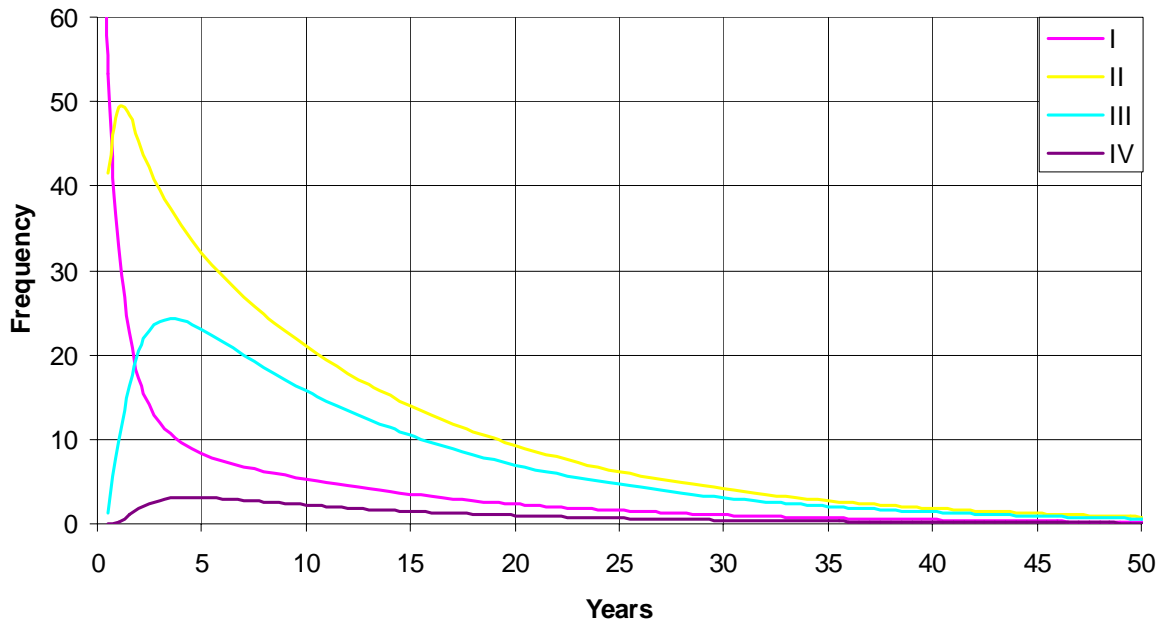
Appendix Fig. 7.5.8-2. Time trajectory of the four size-classes of *Subergorgia reticulata* in a model run with 50:50 external & self-recruitment, showing the simulated impact and recovery from a cyclone, a single trawl and 14 trawls. The model takes ~3 years to half-recover from the cyclone, ~15 years to half-recover from a single trawl, ~15 years to half-recover from 14 trawls and ~50 years to fully recover.



Appendix Fig. 7.5.8-3. Time trajectory of the four size-classes of *Subergorgia reticulata* in a model run with 100% self-recruitment, showing the simulated impact and recovery from a cyclone, a single trawl and 14 trawls. The model takes ~15 years to half-recover from the cyclone, ~20 years to half-recover from a single trawl, ~58 years to half-recover from 14 trawls and ~116 years to fully recover.



Appendix Fig. 7.5.8-4. Time trajectory of the four size-classes of *Subergorgia reticulata* in a model run to establish a population from zero with 50:50 external & self-recruitment. The model takes ~18 years to half-establish, and more than 100 years to fully establish.



Appendix Fig. 7.5.8-5. Time trajectory of the four size-classes of *Subergorgia reticulata* in a model run to establish the fate of a single pulse of 100 Size I recruits (0-25 cm height), showing survival and growth through to larger size classes. Peak Size IV (>76 cm height) abundance of ~4% occurs ~5 years after recruitment. Approximately 36% of Size I recruits attain Size IV after an average of 9.2 years, with a 90-percentile range of 2–23 years.

8 The ecological usage of epibenthic habitat by key commercial finfish species

To document the ecological usage of living epibenthic habitat by key commercial finfish species, in terms of species micro-distribution, shelter requirements, and food chain links.

To assess fishery-independent and “environmentally-friendly” techniques for surveying tropical finfish resource abundance in inter-reefal areas, including fish-traps, remote (baited) video stations.

Contents

8	The ecological usage of epibenthic habitat by key commercial finfish species	8-176
8.1	Introduction	8-179
8.2	Methods	8-181
8.2.1	Fish Traps	8-182
8.2.2	Fish Dissections	8-186
8.2.3	Remote Underwater Video Stations.....	8-187
8.2.3.1	“TrapCam”.....	8-189
8.3	Results	8-190
8.3.1	Trap catches.....	8-190
8.3.2	Remote Underwater Video Stations.....	8-194
8.3.2.1	TrapCAM results	8-194
8.3.2.2	RUVS – baited and unbaited comparisons	8-197
8.3.2.3	RUVS – fish community associations with habitat type.....	8-200
8.3.3	The location and habitat of “reds” grounds	8-208
8.3.3.1	Feeding habits of major species	8-211
8.3.4	Stereo-BRUVS development.....	8-212
8.4	Discussion.....	8-212
8.5	Appendices	8-219

Tables

Table 8–1.	Operations carried out during 3 phases of the study using 44 days at sea	8-181
Table 8–2.	The total number of operations with each sampling method carried out at the sampling locations in 44 sea days. Method codes are unbaited video (RUVS), baited video (BRUVS), baited video in stereo combination (SBRUV), video in baited traps (TRAPCAM), video during counts by diver (UVC), baited traps (TRAP) and handlines (HOOK).	8-181
Table 8–3.	Summary of effort and catch, and mean, standard deviation and coefficient of variation in catch rate (fish trapped per hour fishing time), in trapping operations by site.....	8-191
Table 8–4.	Summary of effort and catch, and mean, standard deviation and coefficient of variation in catch rate (fish trapped per hour fishing time), in trapping operations by trap design.....	8-191
Table 8–5.	Summary of effort and catch, and mean, standard deviation and coefficient of variation in catch rate (CPUE – fish per hour fishing time), in trapping operations over different parts of the day, with different trap types and galvanic-timed-releases (GTRs) governing fishing times.	8-191
Table 8–6.	Trap catch by location.	8-192

Table 8–7. Numbers in 27 families (in descending order of diversity) recorded by video outside (<i>Species out</i>), and inside (<i>Species in</i>), and in the final catches of fish traps (<i>Species caught</i>) in 36 sets at Rib and Davies Reefs. Inside the brackets are numbers of individual fish in those species seen outside (<i>Nout</i>), seen entering (<i>Nenter</i>), seen inside the traps (<i>Nin</i>) and finally caught (<i>Ncaught</i>).	8-196
Table 8–8. Number of fish of 30 species (in descending order of abundance in final catches) filmed inside 36 trap sets at Rib & Davies Reefs. Fish numbers outside (<i>Nout</i>), seen entering (<i>Nenter</i>), seen inside the traps (<i>Nin</i>) and finally caught (<i>Ncaught</i>) are shown. Values in brackets are the proportions of fish seen entering, seen inside and finally caught, expressed as percentages (rounded to the nearest whole number) of <i>Nout</i> , <i>Nenter</i> and <i>Nin</i>	8-197
Table 8–9. The Kruskal-Wallis (KW) values of the top 10 species influencing the classification by sites/habitat types, with average abundance ($avgMaxN \pm$ std dev) in each group in brackets. Species are shown in descending order of KW in each group.	8-207
Table 8–10. The number of stomachs examined <i>N</i> , with the number <i>n food</i> containing items other than pilchard bait, and the prey taxa in descending order of prevalence.	8-211
Table 8–11. Frequency of observation of various fish genera in different demersal habitats, based on analysis of 2,720 frames of a photographic survey on the North-West Shelf. Habitats were defined by cluster analysis, and the benthos consisted mostly of sponges, gorgonians and alcyonarians. Table adapted from Sainsbury (1987).	8-217
Table 8–12. Frequency of observation of various fish genera in different demersal habitats, based on analysis of 130 baited and unbaited video sets in the current study. Habitats were defined by cluster analysis, and the benthos consisted mostly of gorgonians and sponges growing on Pleistocene reef remnants on the mid-shelf, and gorgonians, sponges and alcyonarians growing on various substrata in the Palm Islands.	8-217

Figures

Figure 8–1. “Z” Trap on RV James Kirby with largest catch of “redfish” <i>Lutjanus erythropterus</i> and <i>L. malabaricus</i> from Robbery Shoals.	8-183
Figure 8–2. (a) Collapsed trap, and (b) with side panels open to start assembly.	8-184
Figure 8–3. Trap assembly pulling top panel along its long axis, and sides fall downward.	8-184
Figure 8–4. Insertion of trap funnel for assembly, bait replacement and catch removal.	8-185
Figure 8–5. Assembled trap.	8-185
Figure 8–6. Fleet of 10 collapsed traps stacked on shipping pallet.	8-185
Figure 8–7. Baited Remote Underwater Video Station (BRUVS) with prototype bait arm without measuring grids.	8-188
Figure 8–8. BRUVS bait arm with “gunsight” grids for measurement of fish feeding on the bait canister.	8-188
Figure 8–9. Relationships between depth and size of exploited “reds” in the central GBR region between latitudes –18.560 and –19.147 . Data from our trapping study are supplemented with those from trawl, trap and handline surveys in Newman <i>et al.</i> (2000) and Cappo <i>et al.</i> (2000). Regression lines forced through the origin are shown with sample sizes.	8-193
Figure 8–10. Entry of a juvenile red emperor <i>Lutjanus sebae</i> filmed with “TrapCam”. A sweetlip <i>Lethrinus semisinctus</i> is feeding on the bait canister.	8-194
Figure 8–11. Escape of <i>Lethrinus sp2</i> through the trap entrance.	8-195
Figure 8–12. Plot of average number of species sighted, \pm standard deviation, from 50 random selections of tape interrogations for baited (BRUVS – upper curve) and unbaited (RUVS – lower curve) video sets at Davies Reef.	8-199
Figure 8–13. Plots of simulated species-accumulation curves for baited (BRUVS – upper curve; $Y = 27.5 \ln(X) + 20.393$) and unbaited (RUVS – lower curve; $Y = 6.5945 \ln(X) + 1.2634$) video sets at Davies Rf. ...	8-199
Figure 8–14. Classification of sites based on the abundance of 147 species recorded on at least 2 sets of baited and unbaited video, using the classification methods described in the text.	8-201
Figure 8–15. Tabulation of top 10 species influencing the classification shown in Figure 8–14, in descending order of Kruskal-Wallis values, and plots of the untransformed, average abundance ($Av (MaxN) + 1$ stdev) of 9 of these species in Groups 1 (Robbery Shoals), 2 (Palm Islands) and 3 (Mid-Shelf Reefs).....	8-202
Figure 8–16. Classification of sites based on the abundance of 123 species recorded on at least 2 sets of the baited (BRUVS) video, using the classification methods described in the text. The 3 primary groups are Inshore (Deep), Inshore (Shallow) and Mid-Shelf Reefs.	8-203
Figure 8–17. Tabulation of top 10 species influencing the classification of only BRUVS data shown in Figure 8–16, in descending order of Kruskal-Wallis values, and plots of the untransformed, average abundance ($Av (MaxN) + 1$ stdev) of the top 3 of these species in each of Groups 1 (Inshore - Deep), 2 (Inshore - Shallow) and 3 (Mid-Shelf Reefs).	8-204

- Figure 8–18. Classification of habitat types based on the abundance of 194 species recorded on at least one set of the baited (BRUVS) and unbaited (RUVS) video, using the classification methods described in the text. There are two levels of primary grouping – “Mid-Shelf Reefs” and “Inshore” groups, followed by 5 secondary groups based on the “benthic habitat categories” derived from video footage.....8-205
- Figure 8–19. Tabulation of the top 10 species influencing the classification of BRUVS and RUVS data shown in Figure 8–18, in descending order of Kruskal-Wallis values, with bold-face type* for species common to both patterns. Plots of $Av (MaxN) + 1$ stdev of the top 9 species in classification of 5 groups of habitat types are shown. Note that Group 1 is “inshore megabenthos and *Sargassum*”, group 3 is “mid-shelf megabenthos” and groups 4 and 5 are “mid-shelf sand and *Halimeda*” at 2 different reefs.....8-206
- Figure 8–20. The location of BRUVS/RUVS and trap sets (small flags) around the 4 Kelso Reefs and Shoals in relation to “benthos” (brown shading) and “no benthos” (blue shading) categories derived from towed video transects. The locations of capture or sighting of “redfish” (*Lutjanus sebae* and *L.malabaricus*) are shown with the depth in metres.....8-209
- Figure 8–21. The location of BRUVS/RUVS and trap sets (small flags) around the Palms Islands in relation to “benthos” (red or light shading) and “no benthos” (blue or dark shading) categories derived from towed video transects. The locations of capture or sighting of “redfish” (SEBA *Lutjanus sebae* and MALA *L.malabaricus*) are shown by fish symbols with the species and depth in metres for the major concentrations.....8-210
- Figure 8–22. A large Queensland groper (~158 cm Total Length) measured with a baited stereo-video prototype.8-212

8.1 Introduction

The major demersal fish of commercial and recreational importance in the “inter-reef” areas, that may be exposed to fishing by prawn trawlers, are in the families lutjanidae (sea perches), lethrinidae (sweetlip emperors) and serranidae (coral trout and cod), including the red emperor (*Lutjanus sebae*), red-throat sweetlip (*Lethrinus miniatus*) and common coral trout (*Plectropomus leopardus*).

These three families of fish are diverse, often have low densities and/or have highly clumped distributions, inhabit rugose topography and are known or suspected to closely associate with specific sediment types or "megabenthos" patches (eg Sainsbury, 1987). Much, if not most, of the fishery for the lutjanids and lethrinids occurs below the 20 metre depth contour, below the range to which scientific SCUBA diving is generally restricted (Williams and Russ, 1994).

Recent reviews have shown that these distributions and associations can make stock assessment very difficult when using common sampling techniques. This is caused not only by selectivity of the techniques, but moreso by the nature of the variance in the data (see Cappo and Brown, 1996). Trapping and Underwater Visual Census (UVC) have been widely used to survey lutjanids, lethrinids and serranids. In the best case, fishery-independent UVC surveys of the common coral trout populations in the GBR have been refined, tested and proven powerful in detecting changes in density – but these surveys are entirely restricted to depths ≤ 30 metres.

For other species, both techniques can be characterised as producing a few samples with high catches (traps) or sightings (UVC) but the most common samples have zero catches/sightings. To further complicate statistical analysis of abundance, trapping surveys produce a significant linear correlation between the mean of a sample and its standard deviation, and in UVC there is a similar relationship between the mean and its variance (Williams *et al.* 1997).

For both techniques, relatively high levels of variance can occur at all densities of fish and increasing the levels of replication can do little to reduce the variance after a certain point. In the case of fish trapping, it can be argued that the trapping effort needed to overcome the poor power of statistical tests (see simulations in Williams *et al.* 1997) may prove either

logistically or socially unacceptable, or both, when employing catch-and-release — even to detect major changes such as halving of the population size. Logistically, this is because traps are large and consume deck-space, and ethically because the survival of trapped fish after the trauma of capture and swimbladder deflation is jeopardised. Put simply, a very large proportion of the population must be trapped to overcome the sampling variance in traditional stock assessments, which may cause higher levels of mortality than the original effect size to be measured.

Clearly, alternative sampling techniques must be developed to describe the distributions and abundance of inter-reef fishes below the limits of SCUBA. Following the leads of Whitelaw *et al.* (1991) and Ellis and DeMartini (1995) in using underwater video we sought to develop a hybrid survey technique using low-cost, Remote Underwater Video Systems (RUVS) to enhance the advantages, but overcome the biases, of both trapping and UVC to census demersal fish. Here we report on results of the comparative advantages, sampling power and limitations of data obtained from these video techniques applied to answer questions about the associations of fish assemblages with “megabenthos” patches.

Our approach to develop and demonstrate this “environmentally-friendly” technique was to:

- place RUVS inside “industry-standard” fish traps to assess comparative sampling power
- deploy baited and un-baited RUVS at spatial coordinates known to be “hot-spots” from previous major studies using fish traps.

The major, primary aim of these developments was to apply them to key questions concerning the relationship between fish requirements for food and shelter and the distribution of sponge, gorgonian and algal “megabenthos”. We therefore deployed RUVS and traps to address the following questions;

- what is the nature of fish assemblages inside and outside megabenthos patches?
- what benthos and sediments characterise some known “hotspots” for inter-reef lutjanids?
- what food items are found in stomachs from fish caught in “megabenthos” patches?

After initial surveys to find suitable sampling sites (MBD Trip 1, Chapter 5), we divided the study into three phases, to fulfill our objectives (see Table 8–1).

8.2 Methods

The details of deployment of devices and sampling techniques in the 3 fieldwork phases are shown in Tables 8–1 and 8–2. Here we describe the different components.

Table 8–1. Operations carried out during 3 phases of the study, during 44 days at sea.

Phase	Operations	Location	Trip number, vessel and dates
1	Set baited fish traps on known or suspected “redfish hotspots”, and megabenthos patches.	Kelso, Curacao, Calliope, Robbery Shoals	MBD Trip 2 - RV James Kirby ; 26 March - 7 April, 1998
2	Deploy collapsible fish traps with Galvanic-Timed-Release closing devices and other modifications to reduce escapement	Kelso, Curacao, Calliope	MBD Trip 3 - RV James Kirby; 26 – 29 October, 1998 MBD Trip 4 – RV James Kirby; 11 – 19 April, 1999.
2	Conduct pilot studies to develop video hardware and deployment approaches for use inside traps and in megabenthos patches	Kelso, Curacao, Calliope	MBD Trip 4 – RV James Kirby; 11 – 19 April, 1999.
3	Set baited and unbaited RUVS inside and outside of megabenthos patches, and on “marks” known to produce catches of key “redfish” species.	Curacao, Calliope, Robbery Shoals, Kelso	MBD Trip 6 – RV James Kirby; 24 March – 10 April, 2000. (broken for 7 days by cyclone)
3	Set baited and unbaited RUVS, and RUVS inside baited fish traps, on “marks” known to produce outstanding catches in 1992 trap surveys	Rib Reef, Davies Reef	AIMS Trip – RV Lady Basten; 30 September – 5 October, 2000.

Table 8–2. The total number of operations with each sampling method carried out at the sampling locations in 44 sea days. Method codes are unbaited video (RUVS), baited video (BRUVS), baited video in stereo combination (SBRUV), video in baited traps (TRAPCAM), video during counts by diver (UVC), baited traps (TRAP) and handlines (HOOK).

Location	RUVS	BRUVS	SBRUV	TRAPCAM	UVC	TRAP	HOOK	Total
Calliope Channel	6	14				9		29
Curacao Channel	21	27		12		40		100
Davies Reef	9	9	1	18	8			45
Kelso Shoals	18	18		16		99	5	156
Rib Reef	9	9	1	18	16		1	54
Robbery Shoals	3	3				4		10
Total	66	80	2	64	24	152	6	394

8.2.1 Fish traps

The gear selectivity of fish traps has been well-documented and includes such factors as bait type, mesh size, trap volume and shape, and entrance size, shape and position (see Cappo and Brown, 1996 for review). In our sampling region, intensive trapping by Newman and Williams (1995) and Williams *et al.* (1997) was done with an “O” trap design having 2 entrances of 250 mm × 100 mm. Those studies focussed on smaller lutjanids, lethrinids and serranids -- such as hussars (*Lutjanus adetii* and *L. vitta*), “grassy” sweetlips (*Lethrinus semisinctus* and *L. sp2*) and common coral trout (*Plectropomus leopardus*).

We wished to sample the greatest possible diversity of sizes and species of fishes in megabenthos patches and were concerned that such small entrances would prevent the entry of larger, deep-bodied, fish of commercial and recreational importance – such as red emperor (*L. sebae*), scarlet sea-perches (*L. malabaricus* and *L. erythropterus*), spangled emperors (*L. nebulosus*) and larger serranids such as black-spot cod (*Epinephelus malabaricus*) and flowery cod (*E. fuscoguttatus*).

We therefore used a fleet of 2 large Antillean “Z” traps and 2 “Arrowhead” or Chevron traps (both designs 1800 mm long × 1200mm wide × 560 mm high). One replicate of each design had hexagonal wire mesh sizes of 40 mm and the other had rectangular weld-mesh of 50 mm (Figure 8–1). These traps were baited with 2 perforated canisters of the Newman and Williams (1995) design each containing 1.5 kg of crushed pilchards. Entrance funnel dimensions were 560 mm × 80 mm. Soft-plastic mesh liners were attached to the trap floors to aid in release of healthy fish after capture. Sacrificial wire panels were used to prevent “ghost fishing” in case of irretrievable snagging and loss.

These traps proved too large and bulky to store and handle safely from the RV James Kirby and a better, collapsible design was sought, so that the number of replicates could be increased. A rectangular (1500 mm long × 1200 mm wide × 600 mm high), collapsible model developed and applied by Richard Mounsey and “Mac” MaCartie of the Northern Territory Department of Primary Industries and Fisheries (NTDPIF) was copied to produce a fleet of 10 “industry standard” traps suitable for redfish.



Figure 8-1. “Z” Trap on RV James Kirby with largest catch of “redfish” *Lutjanus erythropterus* and *L. malabaricus* from Robbery Shoals.

The collapsible traps consisted of 3 separate pieces – 2 entrance funnels and one articulated assembly of 6 rectangular panels of 10 mm “reo-rod” to which 50 mm weld-mesh was butt-welded. The 2 end panels were fixed to the adjacent top and bottom panel by loose clasp rings (Figure 8-2a). The 2 long sides had square openings for entrance funnels at opposite ends (Figure 8-2b). These sides were fixed one to the bottom panel and one to the top panel by these clasps. This allowed the trap to be collapsed along its long axis, by rotation within the clasp rings, with the side panels then folded back over the top panel and under the bottom panel. During assembly the sides were folded down or up into position and the trap was pulled back off the deck along the long axis to expand into the final box-shape (Figure 8-3). To remove catch and insert bait canisters a single entrance funnel was removed (Figure 8-4). The long sides were then wired to the adjacent panels, and the entrance funnels were inserted and wired into place (Figure 8-5). This allowed a neat stack of 10 traps to be transported on a standard pallet (Figure 8-6). The funnel entrances were 380 mm × 160 mm. The traps were deployed and retrieved over the rear port gunwhale of the RV James Kirby using a pot-tipper.

(a)



(b)



Figure 8–2. (a) Collapsed trap, and (b) with side panels open to start assembly.



Figure 8–3. Trap assembly pulling top panel along its long axis, and sides fall downward.



Figure 8-4. Insertion of trap funnel for assembly, bait replacement and catch removal.



Figure 8-5. Assembled trap.



Figure 8-6. Fleet of 10 collapsed traps stacked on shipping pallet.

Soak times were determined by our need to share RV James Kirby amongst four main functions on the field trips 2 and 3 -- trapping, SCUBA diving, video-tows and ROV deployments. The restriction of trap deployment and retrieval to long (>3 hour) soaks in daylight hours therefore made it necessary to develop techniques that reliably governed the time that the collapsible traps were actually fishing, as opposed to the entire soak time.

We used sets of Galvanic Timed Releases (GTRs) to govern precisely:

- the time at which traps ceased fishing, by using spring-loaded doors in the funnels
- the time at which bait and bait plumes were released after the trap was set, by using hinged and sealed containers around the bait canisters.

The process of calibrated, timed erosion in seawater of known temperature before use allowed us to fix fishing times at 2.5 and 5.5 hours. For example, the GTRs manufactured to give a 6 hour bond at 22°C were soaked in seawater for 2.5 hours at this temperature to produce links with a 3.5 hour bond life. The 6 hour GTR was attached to hold the 2 spring-loaded doors open, and the 3.5 hour GTR was attached to hold shut the sealed bait dispenser. This meant that a trap set with doors open at 1700 hrs released the bait to begin fishing at 2030 hrs, and the doors closed at 2300 hrs. This shortening of fishing time was essential to guarantee true nocturnal fishing from dusk-dawn sets and was desirable to reduce egress of fish after feeding in the trap. It freed the vessel to carry out other functions.

The trap entrance funnels were also modified and filmed in some tests by inserting a mesh sleeve to produce a side-ways bend in the entry route and by attaching inward-pointing, overlapping “fingers” of flexible plastic (cable ties). These modifications were intended to make it more difficult for fish to leave the collapsible traps, and all entrances in “TrapCam” deployments were reduced to 350 mm × 70 mm.

8.2.2 Fish dissections

The following parameters were measured for all fish caught in traps:

- Size: total length TL, fork length FL, standard length SL, girth GIRTH, body depth BD
- Weight (total weight TWT, filleted weight (no skin) CLNWT)
- Sex and reproductive state ; on a scale of 1 (immature) to 5 (running ripe)

- Feeding morphometry (head length HL, snout length SNL, upper jaw length UJL, eye diameter ED, inter-orbital IO).

The stomach contents were noted, then removed and frozen for further analysis.

8.2.3 Remote Underwater Video Stations

Following pilot studies with the single video station used by Hill and Wassenberg (2000), we developed a fleet of 6 Remotely Operated Underwater Video Stations (RUVS) for daylight use with bait (BRUVS) or without bait (RUVS). Our approach differed from Hill and Wassenberg (2000), Willis *et al.* (2000) and Yau *et al.* (2001) in the sampling power afforded by replication, in the much greater amount of bait we used, and in the fact that RUVS were not attached to the vessel but were set apart with buoy ropes and floats like fish traps.

The RUVS had clear, acrylic dome ports housing Sony Hi-8 Handycams (model TR516E) with wide-angle lenses (Hama 0.5). The Hama wide-angle lens had a factor of 0.5, reducing the set focal length by 50%. Each housing (made from 12mm UPVC “blue brute” sewer pipe) was clamped into a galvanised “roll-bar” frame with lugs for ballasting and lifting, and a pipe mount for pinning bait arms (Figure 8–7). Bait arms were 1500 mm long electrical conduit of 20 mm diameter. The flexible conduit sustained vigorous attacks by predators on the bait bag and broke away at the pin-holes when snagging occurred during retrieval or when sharks attacked. A 300 mm × 200 mm plastic mesh bait bag was sewn along the arm immediately between 2 “scale grids” of 50 mm × 52 mm. This alignment was intended to allow measurement of fish feeding on the bait bag between the scale grids (Figure 8–8). The bait was finely-crushed pilchards that produced a visible oily plume around the station.

The housings and frames were designed and fabricated by the AIMS mechanical workshops and were pressure tested to the equivalent of 80 m depth (the maximum available at the AIMS testing facility).

Exposure was set to “Auto”, focus was set to infinity/manual, short-play (90 minutes) or long-play mode (180 minutes) was selected, and date/time codes were overlaid on footage. The bait consisted of 750 grams of crushed pilchard set in the middle field of view (see Figure 8–8). The RUVS were deployed in 30-70 m depth and retrieved in the same manner as fish traps,

with polypropylene rope and marker buoys attached, and the time, depth, latitude and longitude was recorded for each set.



Figure 8–7. Baited Remote Underwater Video Station (BRUVS) with prototype bait arm without measuring grids.



Figure 8–8. BRUVS bait arm with “gunsight” grids for measurement of fish feeding on the bait canister.

Interrogation of each tape provided:

- a classification of the habitat at each set, based on estimated sediment composition and/or the nature of epibenthos
- the time the RUVS settle on the seabed (*TOB*)
- the time of first sighting of a taxa (*TFS*)
- a coarse classification of “Adult” or “Juvenile” for these taxa based on size and shape
- the time of first feeding of taxa (*TFF*) in the field of view,
- the maximum number of each taxa seen together, or readily identifiable, in any one time on the whole tape (*MaxN*),
- the time at which this maxima occurred (*TMaxN*)
- the behaviour of each taxa toward the bait (*passing, scavenging, or feeding*), and
- the time at which all bait was exhausted if such an event occurred.

The habitat categories recognised were: megabenthos, *Sargassum*, *Halimeda*, low algae, mud, fine sand, coarse sand, rubble, and “near benthos”. The “near benthos” category covered sets where the video units landed on sand, but in the far field of view, or during the deployment or retrieval, significant patches of rock or megabenthos were seen.

Image grabs also allowed size estimates of fish directly above the scale grid on the bait canister, but there was insufficient time to gather these data for the current report. We also developed and tested a prototype stereo-video system (SBRUV) with collaboration of Dr Euan Harvey (University of Western Australia) at Rib and Davies Reefs.

8.2.3.1 “TrapCam”

We placed RUVS inside baited, collapsible traps to directly compare the sampling efficiency of the traps with the observed number and species composition of fish recorded outside the trap by the RUVS. The RUVS were wired into one end of the trap, so that the bait canister and one entrance were in the field of view (Figure 8–9). During tape interrogation for each taxa the following parameters were recorded:

- time the trap settled on the seabed (*TOB*)
- time of first sighting of a taxa outside the trap (*TFSO*)
- a coarse classification of “Adult” or “Juvenile” for these taxa based on size and shape

- time the taxa first seen entering the trap (*TFET*)
- time the taxa first seen feeding in the trap (*TFFT*)
- time the taxa first seen escaping from the trap (*TFXT*)
- maximum number of the taxa seen together, or readily identifiable, in any one time outside the trap and inside the trap (*MaxNout* and *MaxNin*),
- time at which these maxima occurred (*TmaxNout* and *TmaxNin*)
- behaviour of each taxa toward the trap and bait (*passing, trying to enter, scavenging, feeding, trying to escape, escaping*, or combinations of these 6 categories),
- last time at which the taxa was seen inside (*Tlastin*) and/or outside the trap (*Tlastout*), and
- time at which all bait was exhausted if such an event occurred.

These deployments were made in the same locations at Rib and Davies Reefs (often at the same GPS coordinates) as those trapped previously by Newman and Williams (1996), Newman *et al.* (1997) and Williams *et al.* (1997), and identified by them as “hotspots” of unusually high catch.

8.3 Results

8.3.1 Trap catches

In the first phase, traps were set without any means of directly sensing the seabed habitat on which the trap settled, and the catches were generally poor, in comparison to previous studies by Whitelaw *et al.* (1991) and Williams *et al.* (1997). Only 20 species were caught -- mainly carnivores from the families lutjanidae and lethrinidae (Table 8–6). Catch rates were generally low, only reaching more than one fish trapped per hour fishing at Davies Reefs sets (Table 8–3). There was little evidence of difference in overall catch rate with trap design (Table 8–4). Data were few and the coefficients of variation were high, so there was little basis for comparisons of catch rate by different trap designs in day and night sets and with addition of galvanic timed releases to govern fishing time (Table 8–5). At best, there was a suggestion that the use of the GTRs to open bait canisters after dusk and shut doors before midnight caused a doubling in catch rate of collapsible traps in overnight sets.

Table 8–3. Summary of effort and catch, and mean, standard deviation and coefficient of variation in catch rate (fish trapped per hour fishing time), in trapping operations by site.

Location	Trap Sets	Trap Effort (Hours)	Fish Catch (Numbers)	Mean Cpue \pm Stdev	Cv Cpue (%)
Calliope Channel	9	91.5	9	0.08 \pm 0.17	212
Curacoa Channel	48	490.7	87	0.16 \pm 0.24	146
Robbery Shoals	4	50.5	30	0.58 \pm 1.06	183
Kelso Shoals	107	832.6	62	0.11 \pm 0.32	289
Rib Reef	18	38.4	15	0.41 \pm 0.69	167
Davies Reef	18	37.9	39	1.09 \pm 1.62	148
Totals	204	1541.6	242		

Table 8–4. Summary of effort and catch, and mean, standard deviation and coefficient of variation in catch rate (fish trapped per hour fishing time), in trapping operations by trap design.

Trap_Type	Trap Sets	Trap Effort (Hours)	Fish Catch (Numbers)	Mean Cpue \pm Stdev	Cv Cpue (%)
Ztrap	49	642.8	141	.26 \pm .51	197
Collapsible	155	898.8	101	.24 \pm .69	289

Table 8–5. Summary of effort and catch, and mean, standard deviation and coefficient of variation in catch rate (CPUE – fish per hour fishing time), in trapping operations over different parts of the day, with different trap types and galvanic-timed-releases (GTRs) governing fishing times.

Trap Type	Fishing Period	GTR	N Trap Sets	Trap Effort (hours)	Fish Catch (numbers)	Mean CPUE \pm StDev	CV CPUE (%)
Z trap	day	no	19	124.1	26	0.31 \pm 0.64	208
Z trap	overnight	no	30	518.7	115	0.23 \pm 0.41	182
Collapsible	day	no	64	246.6	60	0.45 \pm 1.02	228
Collapsible	day	yes	32	102.3	10	0.09 \pm 0.19	211
Collapsible	overnight	no	27	469.9	21	0.05 \pm 0.15	280
Collapsible	overnight	yes	32	80	10	0.12 \pm 0.24	190

The length range in trap catches showed a trend for increase in length of *L. sebae* and *L. malabaricus* with increasing distance offshore (Table 8–7). When supplemented by measurements from previous surveys in the same region the trend is clearer (Figure 8–9), with an increase in the length of the 3 “redfish” species increasing by roughly 100 millimetres for every 10 metre increase in depth.

Table 8–6. Trap catch by location.

Species	Family	Curacoa Channel	Calliope Channel	Robbery Shoals	Kelso Shoals	Rib Reef	Davies Reef
<i>Abalistes stellaris</i>	Balistidae	4					
<i>Sufflamen frenatus</i>	Balistidae					1	1
<i>Caesio cuning</i>	Caesionidae						15
<i>Chaetodontoplus meredithi</i>	Pomacanthidae						1
<i>Cheilinus fasciatus</i>	Labridae						1
<i>Choerodon venustus</i>	Labridae	3				1	
<i>Diagramma pictum</i>	Haemulidae	8			1	3	
<i>Lethrinus laticaudis</i>	Lethrinidae	5					
<i>Lethrinus miniatus</i>	Lethrinidae				15		2
<i>Lethrinus semisinctus</i>	Lethrinidae				8		10
<i>Lethrinus spB</i>	Lethrinidae				12	10	1
<i>Lutjanus adetii</i>	Lutjanidae				5		
<i>Lutjanus carponotatus</i>	Lutjanidae	14					
<i>Lutjanus erythropterus</i>	Lutjanidae			23			
<i>Lutjanus malabaricus</i>	Lutjanidae	22		7	15		
<i>Lutjanus russelli</i>	Lutjanidae	11	7		1		3
<i>Lutjanus sebae</i>	Lutjanidae	13			6		
<i>Lutjanus vitta</i>	Lutjanidae	7	2				1
<i>Plectropomus leopardus</i>	Serranidae				6		4
<i>Rhizoprionodon taylori</i>	Carcharhinidae				1		

Table 8–7. Length range (FL mm) of fish trapped at different locations.

Species	Curacoa Channel	Calliope Channel	Robbery Shoals	Kelso Shoals	Rib Reef	Davies Reef
<i>Abalistes stellaris</i>	293 - 356					
<i>Sufflamen frenatus</i>					305	275
<i>Caesio cuning</i>						221 - 272
<i>Ch. meredithi</i>						175
<i>Cheilinus fasciatus</i>						274
<i>Choerodon venustus</i>	255 - 331				355	
<i>Diagramma pictum</i>	277 - 535			640	517 - 541	
<i>Lethrinus laticaudis</i>	269 - 370					
<i>Lethrinus miniatus</i>				371 - 490		465 - 515
<i>Lethrinus semisinctus</i>				217 - 256		228 - 255
<i>Lethrinus spB</i>				222 - 274	232 - 272	247
<i>Lutjanus adetii</i>				223 - 278		
<i>Lutjanus carponotatus</i>	235 - 341					
<i>Lut. erythropterus</i>			309 - 448			
<i>Lutjanus malabaricus</i>	170 - 368		440 - 532	455 - 797		
<i>Lutjanus russelli</i>	210 - 315	185 - 218		254		292 - 354
<i>Lutjanus sebae</i>	196 - 325			495 - 735		
<i>Lutjanus vitta</i>	198 - 265	200 - 220				277
<i>Plec. leopardus</i>				390 - 571		325 - 426
<i>Rhizop. taylori</i>				755		

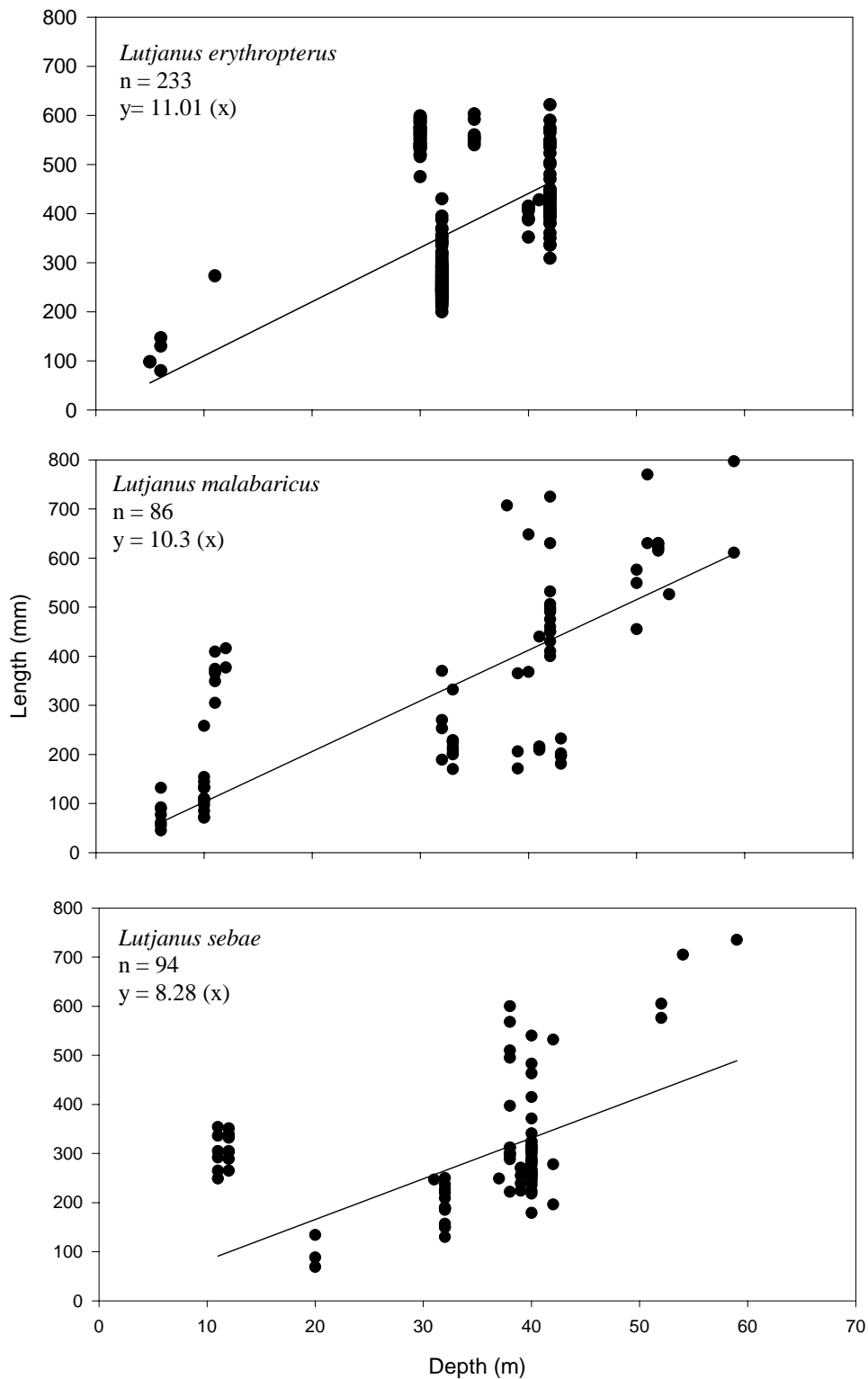


Figure 8-9. Relationships between depth and size of exploited “reds” in the central GBR region between latitudes -18.560 and -19.147 . Data from our trapping study are supplemented with those from trawl, trap and handline surveys in Newman *et al.* (2000) and Cappo *et al.* (2000). Regression lines forced through the origin are shown with sample sizes.

8.3.2 Remote Underwater Video Stations

8.3.2.1 TrapCAM results

A total of 1623 fish of 97 species (the sum of *MaxNout*) were recorded in the video camera field-of-view (FOV) around 36 trap sets (Table 8–8). Of this “pool” of available fish we filmed only 180 incursions through the FOV entrance by separate, or the same, individuals of 28 species (Figure 8–10). A further 2 species were seen inside the traps, but entered through the entrance outside the FOV. The sum of the greatest number of species *i* seen in any given FOV inside the traps (*MaxNin i*) for these 30 species was 230 fish, but only 54 individuals of 12 species were eventually caught when the traps were retrieved. Numerous fish were filmed leaving the trap through the entrance during the trap “soak” on the seabed (Figure 8–11).

It must be borne in mind that we could only see one of the two trap entrances in the FOV and could not discern individuals entering, leaving and entering traps again, nor could we account for fish outside the FOV in and around the trap, so our sampling statistics of the number of fish entering, and *MaxNin* inside, are underestimates of the true “traffic” of fish in and out of the traps.

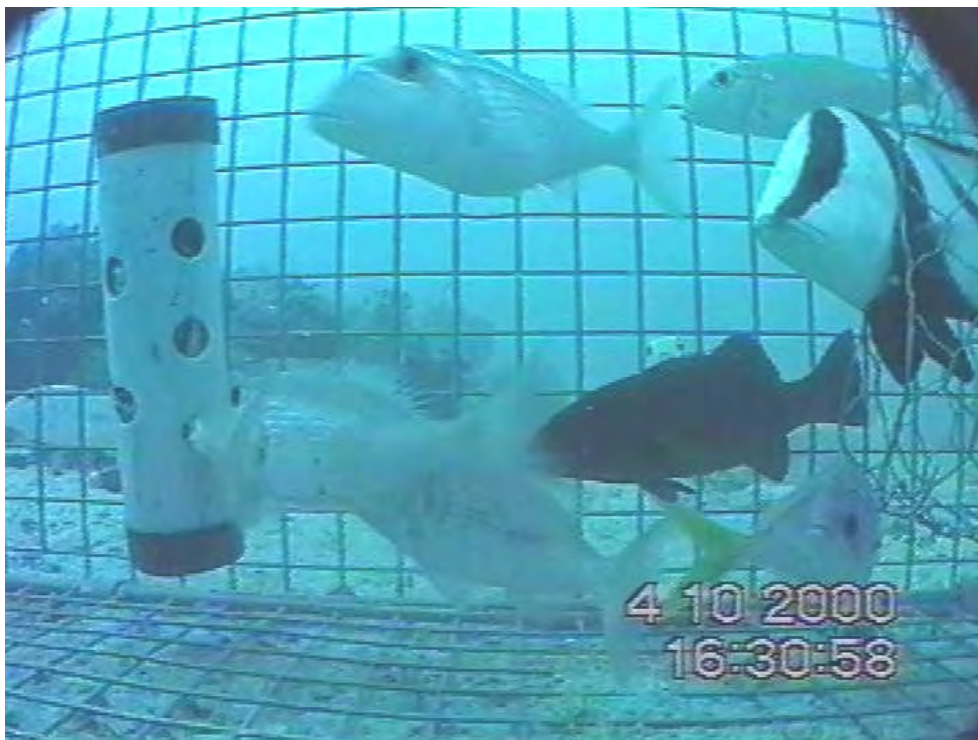


Figure 8–10. Entry of a juvenile red emperor *Lutjanus sebae* filmed with “TrapCam”. A sweetlip *Lethrinus semisinctus* is feeding on the bait canister.

The species composition of sightings outside and inside the trap (Tables 8–8 and 8–9) show that there were marked differences between fish families, and between species within fish families, in the inclination to enter traps and in their ability to escape. In terms of fish diversity, the top 5 families seen on video around the traps were labrids, serranids, lutjanids, carangids and lethrinids, yet the diversity in trap catches was dominated by caesionids, lethrinids, serranids, haemulids and lutjanids. In terms of fish numbers, the top two families in trap catches matched the top two families seen on the video (651 caesionids and 213 lethrinids), but traps did not sample at all the families ranked third (169 siganids) and fifth (106 mullids) on video. The labrids were ranked fourth in abundance on video (116 fish), and first in diversity (17 species), yet were ranked last in trap catches of only two individuals of two species.



Figure 8–11. Escape of *Lethrinus sp2* through the trap entrance.

The relationships between video sightings and trap catches are shown in Tables 8–8 and 8–9. The “probability of entry” might be gauged from the ratio of fish seen inside and outside traps, while the “probability of retention” might be gauged by the ratio of the number fish caught to the number seen inside the trap. For example, the data in Table 8–9 for *Lethrinus semisinctus* show that 73 fish were seen outside the traps, and of these 79% were seen to enter, 104% were seen inside the traps, and 14% were finally caught. Of the 58 fish seen to enter 131% were seen inside the traps and 17% were finally caught. Of the 76 *L. semisinctus*

seen inside the traps 13% were finally caught. The percentages greater than 100% implies that some individual fish made multiple ingress/egress from traps, and that they entered outside the FOV. This species could be considered to have a high probability of entry and a low probability of retention in the trap design we used.

Table 8–8. Numbers in 27 families (in descending order of diversity) recorded by video outside (*Species out*), and inside (*Species in*), and in the final catches of fish traps (*Species caught*) in 36 sets at Rib and Davies Reefs. Inside the brackets are numbers of individual fish in those species seen outside (*Nout*), seen entering (*Nenter*), seen inside the traps (*Nin*) and finally caught (*Ncaught*).

Family	Species out (Nout)	Species in (Nin)	Species caught (Ncaught)
Labridae	17(116)	6(14)	2(2)
Serranidae	10(56)	4(17)	1(4)
Lutjanidae	9(25)	5(12)	2(4)
Carangidae	7(84)	0(0)	0(0)
Lethrinidae	7(213)	4(121)	3(23)
Chaetodontidae	6(37)	0(0)	0(0)
Mullidae	4(106)	1(1)	0(0)
Nemipteridae	4(18)	2(6)	0(0)
Pomacanthidae	4(27)	1(3)	1(1)
Siganidae	4(169)	0(0)	0(0)
Acanthuridae	3(6)	0(0)	0(0)
Balistidae	3(31)	2(4)	1(2)
Pomacentridae	3(26)	1(1)	0(0)
Caesionidae	2(651)	2(47)	1(15)
Scaridae	2(35)	0(0)	0(0)
Echeneidae	1(4)	0(0)	0(0)
Ginglymostomatidae	1(1)	0(0)	0(0)
Grammistidae	1(5)	0(0)	0(0)
Haemulidae	1(6)	1(3)	1(3)
Loliginidae	1(1)	0(0)	0(0)
Malacanthidae	1(1)	0(0)	0(0)
Muraenidae	1(1)	0(0)	0(0)
Pinguipedidae	1(0)	1(1)	0(0)
Rhynchobatidae	1(1)	0(0)	0(0)
Sphyrnidae	1(1)	0(0)	0(0)
Stegastomatidae	1(1)	0(0)	0(0)
Tetraodontidae	1(1)	0(0)	0(0)
TOTALS	97(1623)	30(230)	12(54)

The overall results show that only 14% of all fish seen as “available” around the traps were actually filmed inside the traps and only 3% of the available fish were actually caught by the traps. Most importantly, the percentages in Table 8–9 show that some visibly abundant families of fish never entered traps (most notably the carangidae, scaridae, chaetodontidae) or very seldom entered (mullidae). Some species were very likely to enter, and re-enter, the traps (*Lethrinus spB*, *L.semisinctus*) and escape, with overall retention factors of 13%-29%. Others had high probability of both entry and retention (50% and 100% for *Diagramma pictum*), or low probability of entry and moderate probability of retention (11% and 40% for *Plectropomus leopardus*, and 6% and 42% for *Caesio cuning*). The data show poor

performance of the traps to survey both biodiversity and abundance of fish inside and outside the megabenthos habitats of interest in the current study.

Table 8–9. Number of fish of 30 species (in descending order of abundance in final catches) filmed inside 36 trap sets at Rib & Davies Reefs. Fish numbers outside (*Nout*), seen entering (*Nenter*), seen inside the traps (*Nin*) and finally caught (*Ncaught*) are shown. Values in brackets are the proportions of fish seen entering, seen inside and finally caught, expressed as percentages (rounded to the nearest whole number) of *Nout*, *Nenter* and *Nin*.

Species	Nout (%enter, %in, %caught)	Nenter (%in,%caught)	Nin (%caught)	Ncaught
<i>Caesio cuning</i>	251 (10,14,6)	26 (138,58)	36 (42)	15
<i>Lethrinus spB</i>	59 (41,64,19)	24 (158,46)	38 (29)	11
<i>Lethrinus semisinctus</i>	73 (79,104,14)	58 (131,17)	76 (13)	10
<i>Plectropomus leopardus</i>	37 (27,27,11)	10 (100,40)	10 (40)	4
<i>Diagramma pictum</i>	6 (50,50,50)	3 (100,100)	3 (100)	3
<i>Lutjanus russelli</i>	3 (33,33,100)	1 (100,300)	1 (300)	3
<i>Lethrinus miniatus</i>	11 (27,27,18)	3 (100,67)	3 (67)	2
<i>Sufflamen frenatus</i>	23 (13,9,9)	3 (67,67)	2 (100)	2
<i>Chaetodontoplus meredithi</i>	19 (11,16,5)	2 (150,50)	3 (33)	1
<i>Cheilinus fasciatus</i>	25 (8,8,4)	2 (100,50)	2 (50)	1
<i>Choerodon venustus</i>	13 (31,23,8)	4 (75,25)	3 (33)	1
<i>Lutjanus vitta</i>	3 (67,100,33)	2 (150,50)	3 (33)	1
<i>Abalistes stellaris</i>	7 (29,29,0)	2 (100,0)	2 (0)	
<i>Cephalopholis boenak</i>	5 (20,60,0)	1 (300,0)	3 (0)	
<i>Cheilinus diagramma</i>	12 (17,17,0)	2 (100,0)	2 (0)	
<i>Choerodon fasciatus</i>	20 (25,25,0)	5 (100,0)	5 (0)	
<i>Choerodon vitta</i>	12 (8,8,0)	1 (100,0)	1 (0)	
<i>Epinephelus areolatus</i>	2 (150,150,0)	3 (100,0)	3 (0)	
<i>Epinephelus rivulatus</i>	1 (100,100,0)	1 (100,0)	1 (0)	
<i>Gymnocranius audleyi</i>	64 (13,6,0)	8 (50,0)	4 (0)	
<i>Lutjanus adetii</i>	6 (33,83,0)	2 (250,0)	5 (0)	
<i>Lutjanus quinquelineatus</i>	4 (50,25,0)	2 (50,0)	1 (0)	
<i>Lutjanus sebae</i>	3 (67,67,0)	2 (100,0)	2 (0)	
<i>Parapercis hexophtalma</i>	0 (0,0,0)	1 (100,0)	1 (0)	
<i>Parupeneus multifasciatus</i>	12 (8,8,0)	1 (100,0)	1 (0)	
<i>Pentapodus sp2 (Randall)</i>	3 (167,133,0)	5 (80,0)	4 (0)	
<i>Pomacentrus nagasakiensis</i>	19 (5,5,0)	1 (100,0)	1 (0)	
<i>Pterocaesio marri</i>	400 (1,3,0)	3 (367,0)	11 (0)	
<i>Scolopsis bilineatus</i>	2 (50,100,0)	1 (200,0)	2 (0)	
<i>Thalassoma lunare</i>	(0,0,0)	1 (100,0)	1 (0)	
TOTALS	1623 (11,14,3)	180 (128,30)	230 (23)	54

8.3.2.2 RUVS – baited and unbaited comparisons

We developed these video stations to detect associations between fish assemblages and seabed habitats in the belief that baited stations might better “accumulate” information about fish biodiversity in a given habitat because of attraction up a spreading bait plume. It is well known that baited traps catch mainly carnivores and omnivores, and unbaited traps catch herbivores (see Cappo and Brown , 1996), so it could immediately be argued that such an attractant biases the video technique to sample only (or mainly) carnivores and scavengers and would not adequately represent the fish assemblage.

To account for this bias we set baited and unbaited RUVS in alternating sequence in the habitats of interest and found the major differences lie only in the vastly superior performance of baited stations in accumulating information on fish biodiversity. The baited stations recorded fish from all trophic groups.

The most diverse fish fauna was recorded at Davies Reef, where 9 sets of BRUVS and RUVS were made, although one RUVS set could not be interrogated after it settled on its back end, pointing upward to the sea surface. To demonstrate species accumulation rates with increasing levels of replication we chose this diverse Davies Reef fauna to make the following simulation.

If we wish to hindcast the optimum number of tapes to interrogate to accumulate a species list for each location, the order in which the tapes are analysed becomes very important. This is because benthic assemblages are patchy, and the strings of 3 baited BRUVS and 3 unbaited RUVS may have been set within patches. If, for example, the first string of RUVS sampled sandy areas with lower diversity within a region, and the last string sampled rugose habitat with high diversity within a region, then sequential interrogation of the tapes from first to last would indicate that a species list is accumulated slowly – and that many RUVS sets are needed. To exclude this bias we ran 50 random sequences of tape selection from the 17 sets at Davies Reef and we took an average of the 50 species accumulation curves for the baited and unbaited RUVS.

These plots in Figures 8–12 and 8–13 show the best approximation to the accumulation of species by baited RUVS was an exponential decline in the number of newly recorded species with each additional deployment. The 9 sets made with baited stations at Davies Reef had accumulated diversity of over 80 species, close to an asymptote. The curve formulae were used in simulations in Figure 8–13 to predict fewer than 2 additional species per set would be expected by a 14th set. In contrast, the unbaited RUVS reached his low level of accumulation by only the 4th set. The RUVS could account for only 20% of the species recorded by the BRUVS at Davies Reef. The curves in Figure 8–13 are converging, implying the different shapes at the beginning of the curves represent the action of bait attraction and fish behaviour. Our observations show fish were not independent in their response to either the bait or the activity of other fish (see “following behaviour” below).

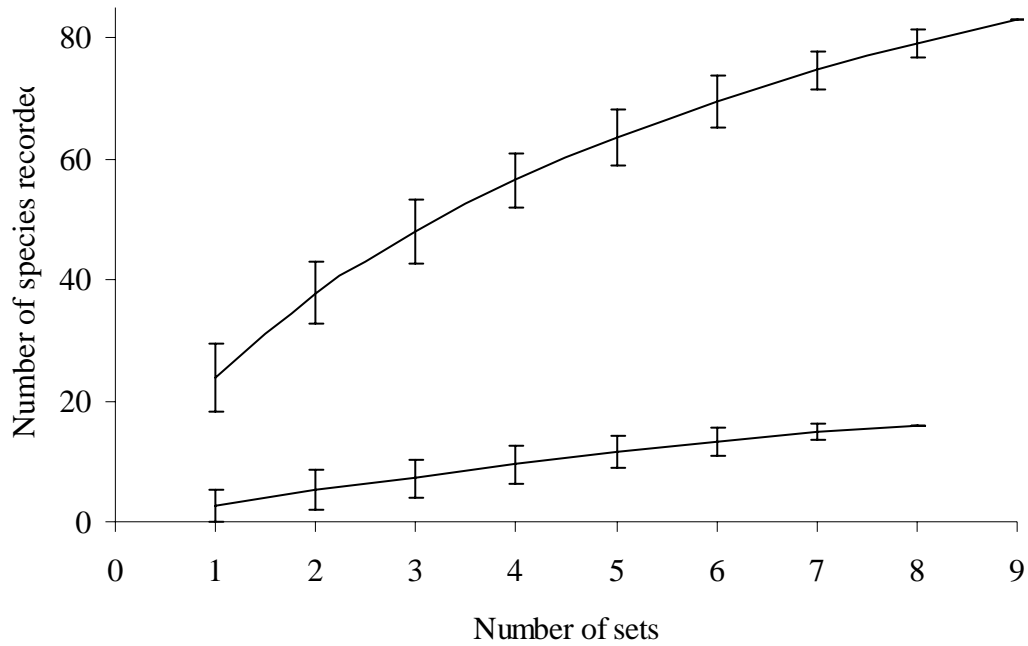


Figure 8-12. Plot of average number of species sighted, \pm standard deviation, from 50 random selections of tape interrogations for baited (BRUVS – upper curve) and unbaited (RUVS – lower curve) video sets at Davies Reef.

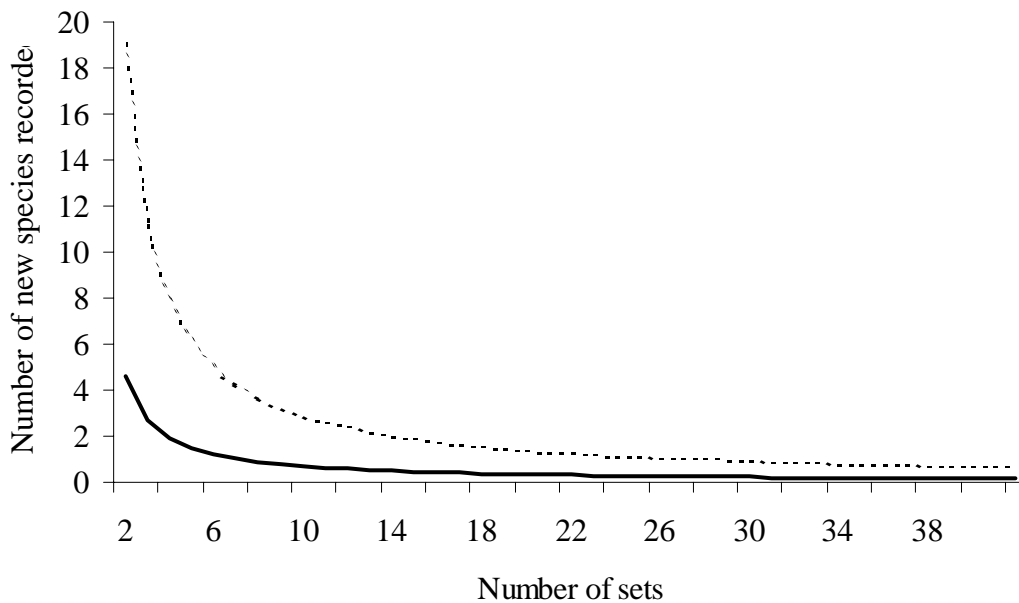


Figure 8-13. Plots of simulated species-accumulation curves for baited (BRUVS – upper curve; $Y = 27.5 \ln(X) + 20.393$) and unbaited (RUVS – lower curve; $Y = 6.5945 \ln(X) + 1.2634$) video sets at Davies Reef.

In Phase 3 of the study we made 132 deployments of RUVS and BRUVS, but failures due mostly to unfavorable landings on the seabed with inversion of the camera to point skywards, and occasionally due to camera malfunction, reduced the useful number of sets to 122 — 58 for RUVS and 64 for BRUVS. The number of sets on which a species was sighted

(prevalence), average number sighted (mean of *MaxN*) and its standard deviation are shown in descending order of prevalence for BRUVS in Appendix 8.1 and for RUVS in Appendix 8.2. There were 224 taxa recognised on the videos (including sea snakes, squid and different life-stages of the same fish species). There were 185 species sighted in 64 BRUVS sets, and 128 species sighted in 58 RUVS sets. There were 87 species sighted only on the BRUVS (of which 21 species had a prevalence of 3 to 6 tapes), and 30 species sighted only on the RUVS (of which only 3 species had a prevalence = 3 tapes).

It is important to note that the top 5 of the species prevalent only on baited video were scavenger/omnivores (silver toadfish *Lagocephalus sceleratus*), mobile piscivores (milk sharks *Loxodon macrorhinos*, and Queensland school mackerel *Scomberomorus queenslandicus*), ambush predators (coral cod *Cephalopholis miniata*), and very large benthic carnivores (white-spot shovelnose ray *Rhynchobatus djiddensis*). Some of these species had considerable influence in the clustering of sites by fish assemblages.

8.3.2.3 RUVS – fish community associations with habitat type

Multivariate analyses of the RUVS and BRUVS data were carried out to assess the importance of:

- cross-shelf location of habitat
- depth of habitat
- habitat type (categories such as “megabenthos”, “coarse sand”, “fine sand” etc)
- effect of bait

in classifying the fish assemblages.

Multivariate analyses of fish abundance on videos were based on the untransformed statistic *MaxN*. PATN software (Belbin, 1987) was employed for classification and ordination analyses. Bray-Curtis dissimilarity measures (Bray and Curtis, 1957) and “flexible, group average sorting” with a beta value of -0.1 were used to produce groupings of sites and habitats based on their fish assemblages (Clifford and Stephenson, 1975). The relative contributions of each fish species in distinguishing the groupings were investigated using Kruskal-Wallis values.

The number of taxa recognised on the videos (including sea snakes, squid and different life-stages of the same fish species) was 224 (see Appendices 7.1 and 7.2). The “non-fish” taxa were excluded from analyses, leaving 194 taxa of fish, sharks and rays in the classification of benthic habitats. The datasets were reduced further by selecting only those species sighted on at least 2 sets, leaving 123 species in the classification of sites using only the BRUVS data, and 147 species in the classification of sites using both the BRUVS and RUVS data.

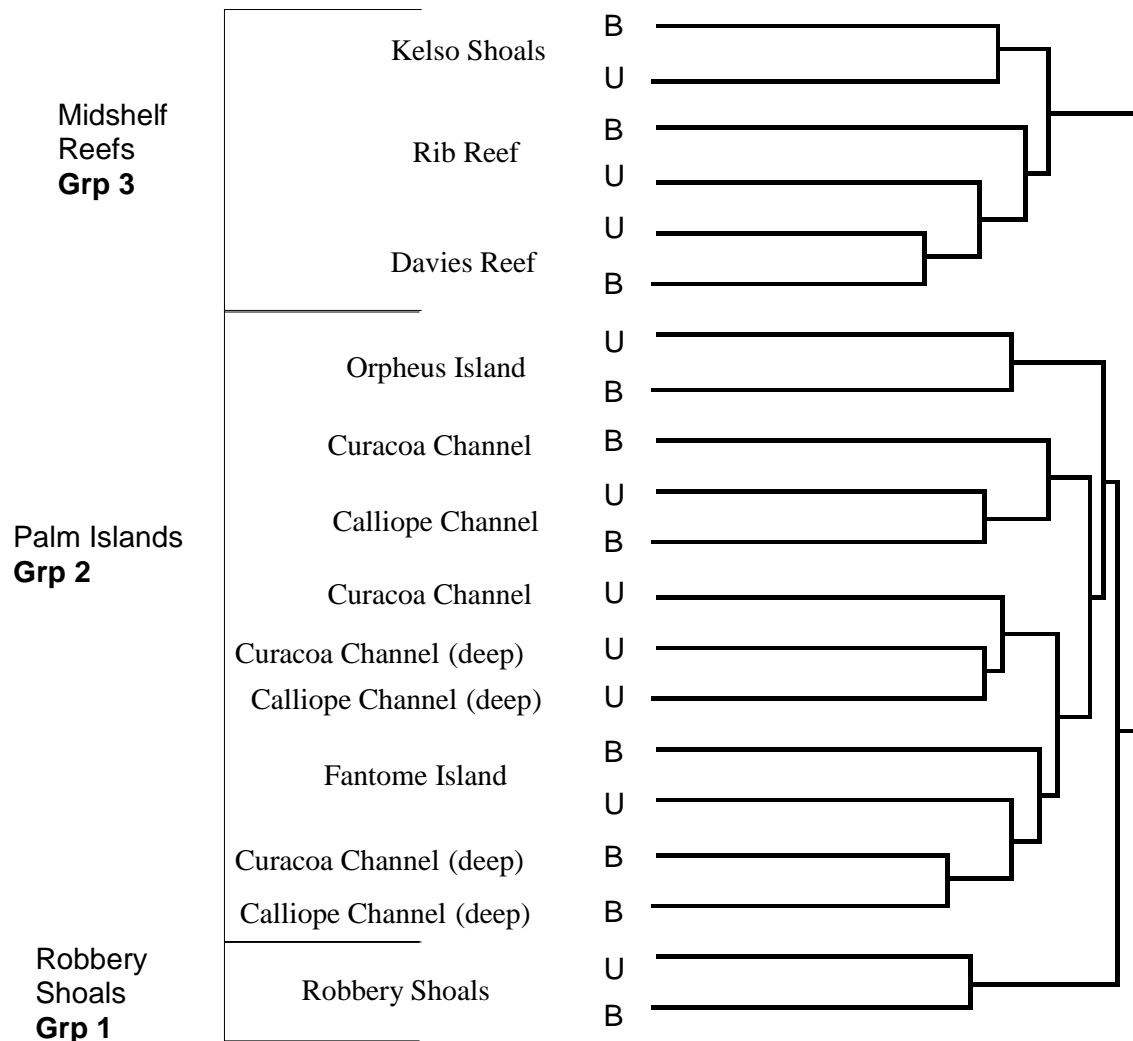


Figure 8–14. Classification of sites based on the abundance of 147 species recorded on at least 2 sets of baited (B: BRUVS) and unbaited (U: RUVS) video, using the classification methods described in the text.

The classification in Figure 8–14 shows that the primary split by sites occurs between the mid-shelf reef sites, the Palm Island sites and Robbery Shoals. Within the Palm Islands sites there are further clustering of sites of different depth. The difference between baited and unbaited sets is of far less significance in classifying the sites by their fish assemblage

structure. The species influencing the classification into 3 groups are shown in Figure 8–15. The black-banded kingfish (*Seriolina nigrofasciata*) was seen only at Robbery Shoals, but most of the other top 10 species of influence were found only on the mid-shelf reefs. They included planktivorous caesionids, piscivorous coral trout, and benthic carnivores (mullids and labrids).

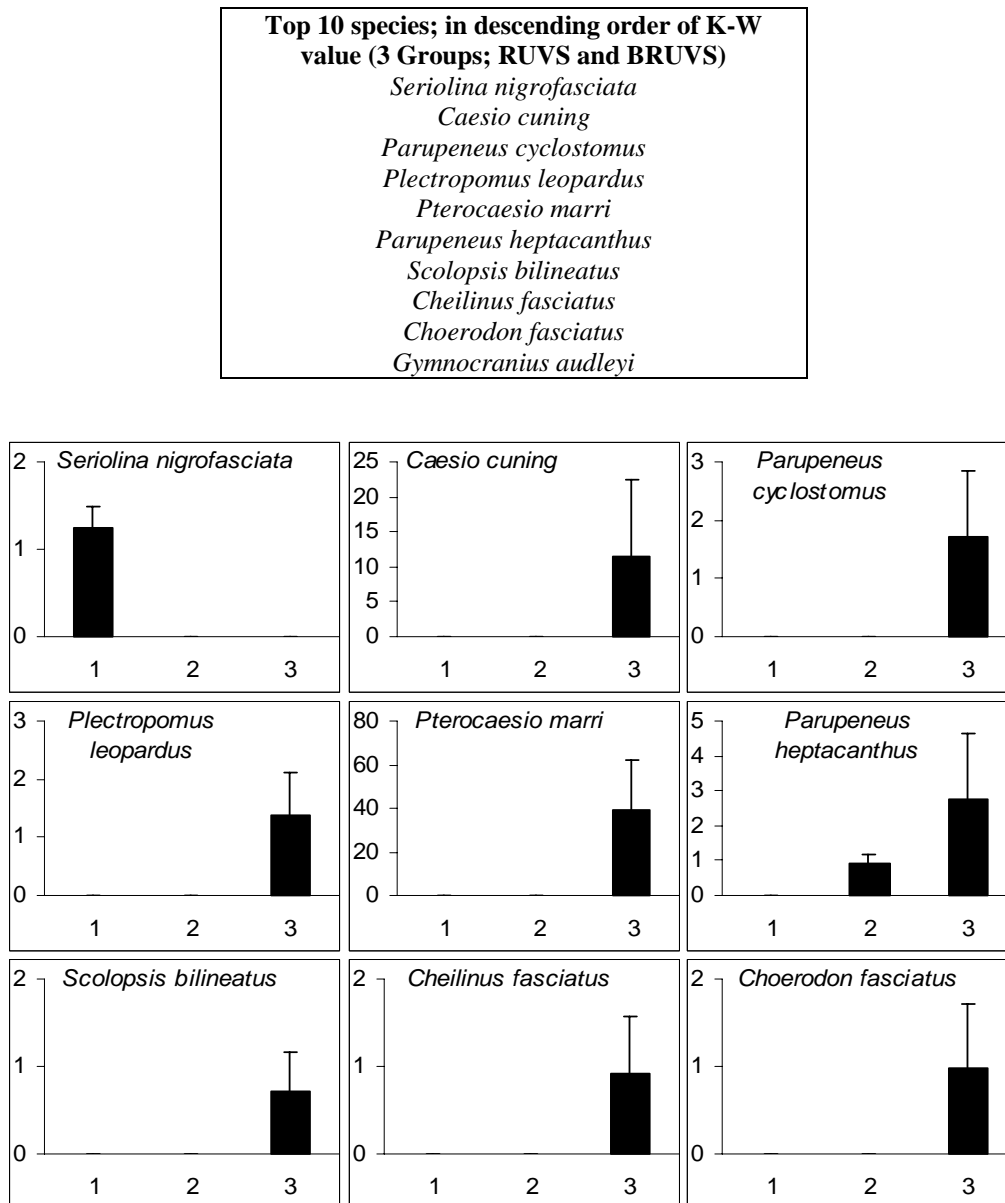


Figure 8–15. Tabulation of top 10 species influencing the classification shown in Figure 8–14, in descending order of Kruskal-Wallis values, and plots of the untransformed, average abundance ($Av(MaxN) + 1$ stdev) of 9 of these species in Groups 1 (Robbery Shoals), 2 (Palm Islands) and 3 (Mid-Shelf Reefs).

The integrity of the inshore-offshore split is demonstrated further in Figure 8–16 where only the data from baited (BRUVS) sets were used. The primary groups classified together the

mid-shelf reef sites, the shallow inshore Palm Islands sites, and the deep inshore Palm Islands and Robbery Shoals sites. Again, the mid-shelf reef species had the highest influence in the classification.

In Figure 8–17 the top 10 species of influence within each group are shown in decreasing order of Kruskal-Wallis values. The large black-spot cod (*Epinephelus malabaricus*) and red throat emperor (*Lethrinus miniatus*) were important in mid-shelf reef sites, the small, schooling carangid *Alepes spp* was notable in classifying the shallow inshore sites, and the black-spot tuskfish (*Choerodon schoenleinii*) and whiptail (*Pentapodus paradiseus*) had major influence in the deep inshore sites.

A number of species helped discriminate more than one group, with different levels of abundance. For example, the cinnabar goatfish *Parupeneus heptacanthus* occurred rarely inshore in shallow sites and most commonly offshore in the mid-shelf reef sites, and the black-spot tuskfish was most abundant in the mid-shelf reef sites.

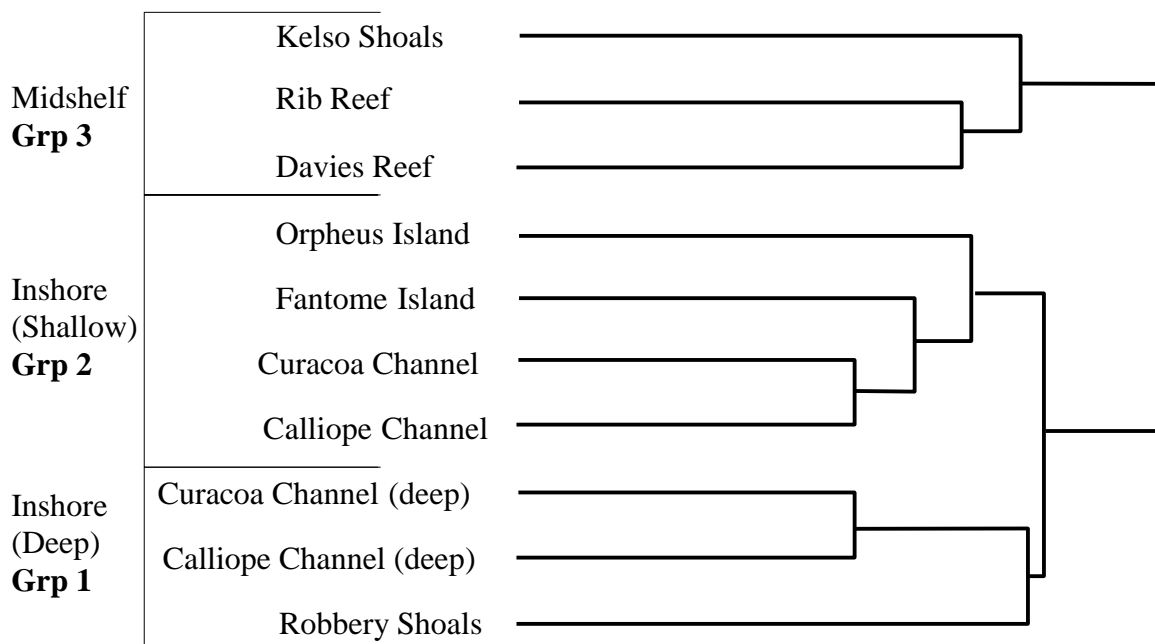


Figure 8–16. Classification of sites based on the abundance of 123 species recorded on at least 2 sets of the baited (BRUVS) video, using the classification methods described in the text. The 3 primary groups are Inshore (Deep), Inshore (Shallow) and Mid-Shelf Reefs.

Grp 3 (Mid-Shelf Reefs)	Grp 2 (Inshore - Shallow)	Grp 1 (Inshore - Deep)
<i>Epinephelus malabaricus</i>	<i>Alepes spp</i>	<i>Choerodon schoenleinii</i>
<i>Lethrinus miniatus</i>	<i>Parupeneus heptacanthus</i>	<i>Pentapodus paradiseus</i>
<i>Pomacanthus semicirculatus</i>	<i>Scolopsis margaritifer</i>	<i>Lutjanus vitta</i>
<i>Lethrinus lentjan</i>	<i>Pentapodus paradiseus</i>	<i>Symphorus nematophorus</i>
<i>Pterocaesio marri</i>	<i>Symphorus nematophorus</i>	<i>Lutjanus sebae</i>
<i>Caesio cuning</i>	<i>Nemipterus furcosus</i>	<i>Carangoides chrysophrys</i>
<i>Dascyllus trimaculatus</i>	<i>Upeneus tragula</i>	<i>Cantherines valentini</i>
<i>Gymnocranius audleyi</i>	<i>Carangoides gymnostethus</i>	<i>Echeneis naucrates</i>
<i>Plectropomus leopardus</i>	<i>Pomacanthus sexstriatus</i>	<i>Heniochus acuminatus</i>
<i>Parupeneus cyclostomus</i>	<i>Echeneis naucrates</i>	<i>Parupeneus barberinus</i>

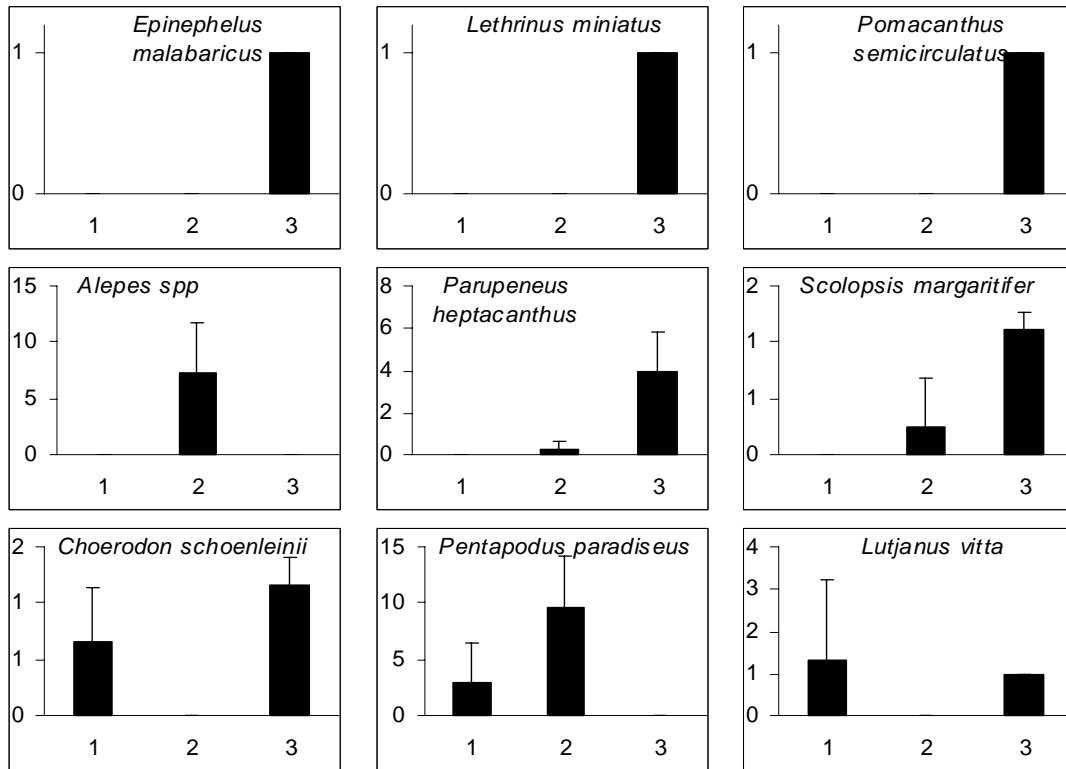


Figure 8–17. Tabulation of top 10 species influencing the classification of only BRUVS data shown in Figure 8–16, in descending order of Kruskal-Wallis values, and plots of the untransformed, average abundance (A_v ($MaxN$) + 1 stdev) of the top 3 of these species in each of Groups 1 (Inshore - Deep), 2 (Inshore - Shallow) and 3 (Mid-Shelf Reefs).

The classification was applied to the habitat categories recognized on the baited and unbaited video sets in Figure 8–18. Again, the primary split occurred between mid-shelf reefs and inshore locations, but there were also significant differences between “megabenthos” and “off-benthos” habitats in terms of fish assemblages. These differences classified 5 secondary groups – “megabenthos and *Sargassum*, inshore” (Grp 1), “mud, sand, rubble and *Sargassum*, Palm Islands” (Grp 2), “megabenthos, Rib and Davies Reefs” (Grp 3), “sand and *Halimeda*, Kelso Shoals” (Grp 4), and “sand and *Halimeda*, north-eastern side of Rib Reef” (Grp 5).

Notable species separating primary “inshore” and “offshore” groups were red-throat emperor, grey reef sharks *Carcharhinus amblyrhynchos* and goldsaddle goatfish *Parupeneus cyclostomus*. A number of species had high influence in separating both the primary and secondary splits into 5 habitat groups. These included the common coral trout, collared sea bream *Gymnocranius audleyi*, whiptails *Pentapodus paradiseus* and yellowfin parrotfish *Scarus flavipectoralis* (Figure 8–19).

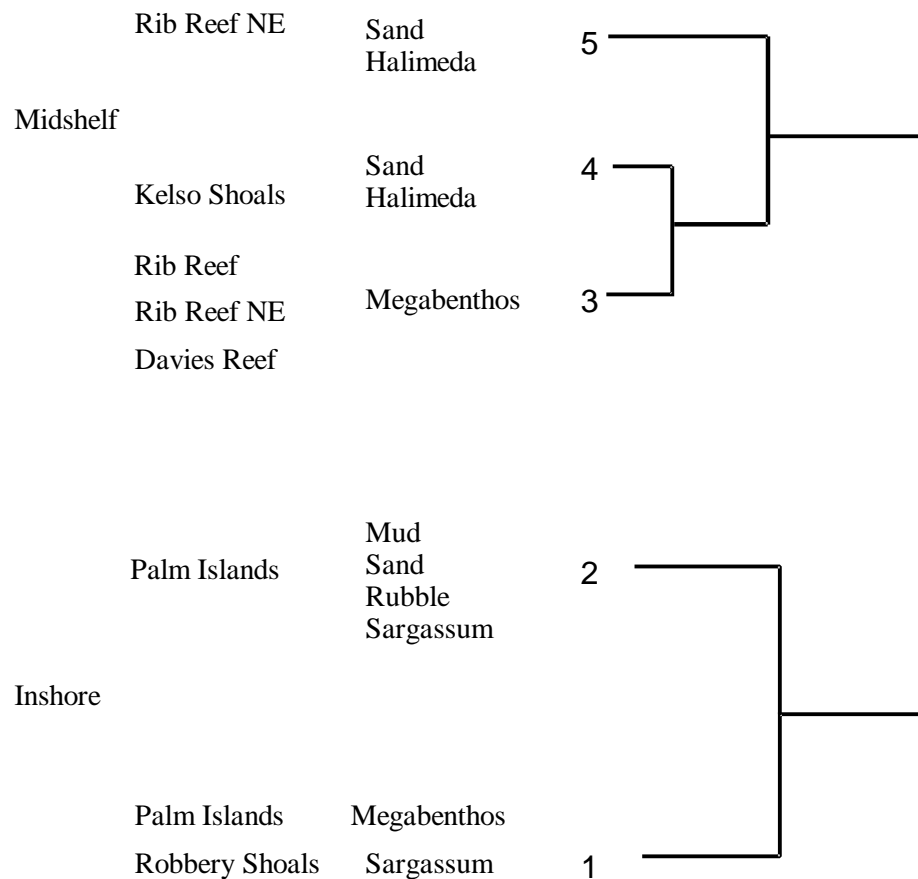


Figure 8–18. Classification of benthic habitat types based on the abundance of 194 species recorded on at least one set of the baited (BRUVS) and unbaited (RUVS) video, using the classification methods described in the text. There are two levels of primary grouping – “Mid-Shelf Reefs” and “Inshore” groups, followed by 5 secondary groups based on the “benthic habitat categories” derived from video footage.

In terms of highest influence, the species associated with offshore megabenthos were fusiliers (*Caesio cuning*), red-breasted maori wrasse (*Cheilinus fasciatus*), common coral trout, collared sea bream and harlequin tusk fish (*Choerodon fasciatus*). Whiptails were absent from the mid-shelf reef sites, and their high abundance strongly influenced the inshore megabenthos group, even though they were more abundant in the mud/sand/rubble/*Sargassum* habitat types. The dash-dot goatfish (*Parupeneus barberinus*) was found in sites with megabenthos, both inshore and offshore, but with greatest abundance on mid-shelf megabenthos.

A species of strong influence in both the inshore and offshore “off benthos” groups was the rosy threadfin bream (*Nemipterus furcosus*), sighted in large numbers on sandy habitats – but absent from sites with megabenthos. A variety of carangids were seen in the sandy habitats, but only the thicklip trevally (*Carangoides orthogrammus*) had high influence in discriminating sand/*Halimeda* habitats at Kelso Shoals.

Benthic habitat (2 primary groups)	Benthic habitat (5 secondary groups)
<i>Gymnocranius audleyi</i> *	<i>Cheilinus fasciatus</i> *
<i>Pentapodus paradiseus</i> *	<i>Caesio cuning</i> *
<i>Parupeneus eptacanthus</i>	<i>Plectropomus leopardus</i> *
<i>Plectropomus leopardus</i> *	<i>Gymnocranius audleyi</i> *
<i>Lethrinus miniatus</i>	<i>Pentapodus paradiseus</i> *
<i>Caesio cuning</i> *	<i>Choerodon fasciatus</i>
<i>Carcharhinus amblyrhynchos</i>	<i>Carangoides orthogrammus</i>
<i>Cheilinus fasciatus</i> *	<i>Parupeneus barberinus</i>
<i>Scarus flavipectoralis</i> *	<i>Nemipterus furcosus</i>
<i>Parupeneus cyclostomus</i>	<i>Scarus flavipectoralis</i> *

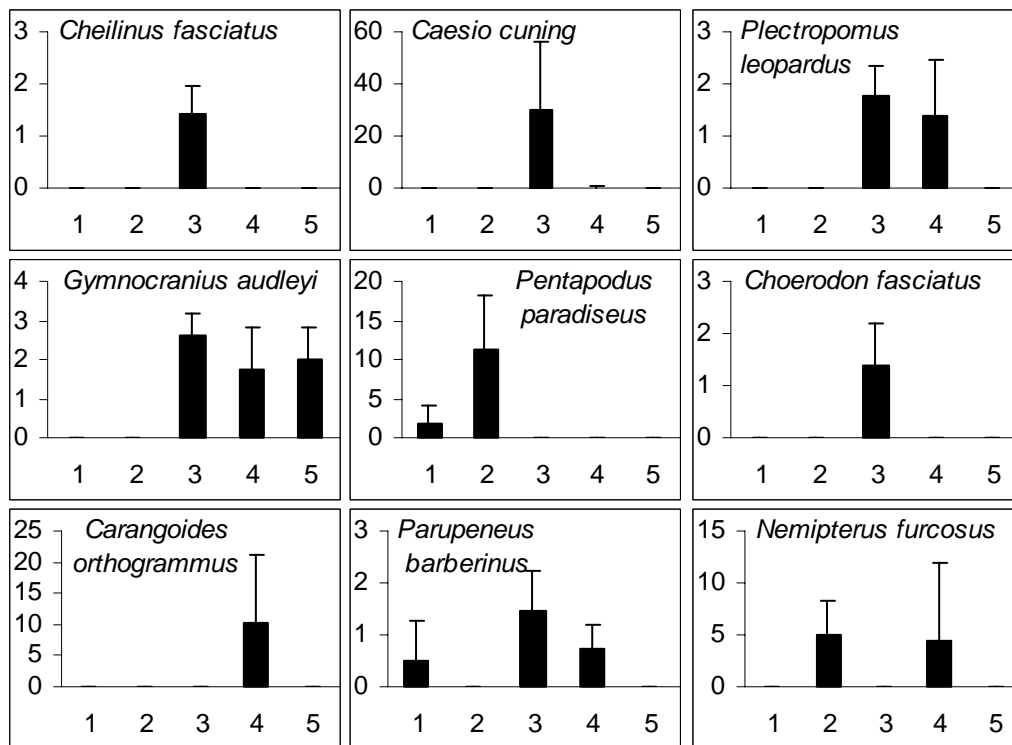


Figure 8–19. Tabulation of the top 10 species influencing the classification of BRUVS and RUVS data shown in Figure 8–18, in descending order of Kruskal-Wallis values, with * indicating species common to both patterns. Plots of $A_v (MaxN) + 1$ stdev of the top 9 species in classification of 5 groups of habitat types are shown. Note that Group 1 is “inshore megabenthos and *Sargassum*”, group 3 is “mid-shelf megabenthos” and groups 4 and 5 are “mid-shelf sand and *Halimeda*” at 2 different reefs.

Table 8–10. The Kruskal-Wallis (KW) values of the top 10 species influencing the classification by sites/habitat types, with average abundance (avgMaxN ± std dev) in each group in brackets. Species are shown in descending order of KW in each group.

Grp 1 – megabenthos and Sargassum, inshore	Grp 2 – mud,sand,rubble and Sargassum, inshore	Grp 3 – megabenthos, mid-shelf reefs	Grp 4 – sand and Halimeda, Kelso Shoals	Grp 5 – sand and Halimeda, Rib Reef NE
<i>Pentapodus paradiseus</i> 20.69 (1.9 ± 2.2)	<i>Pentapodus paradiseus</i> 20.69 (11.2 ± 7.0)	<i>Cheilinus fasciatus</i> 25.72 (1.4 ± 0.5)	<i>Caesio cuning</i> 22.98 (0.3 ± 0.4)	<i>Gymnocranius audleyi</i> 21.6 (2.0 ± 0.8)
<i>Parupeneus barberinus</i> 16.63 (0.5 ± 0.8)	<i>Nemipterus furcosus</i> 16.49 (5.0 ± 3.3)	<i>Caesio cuning</i> 22.98 (29.7 ± 26.1)	<i>Plectropomus leopardus</i> 21.67 (1.4 ± 1.1)	<i>Parupeneus heptacanthus</i> 15.75 (6.7 ± 4.1)
<i>Parupeneus heptacanthus</i> 15.75 (0.2 ± 0.4)	<i>Carangoides fulvoguttatus</i> 12.65 (3.9 ± 4.7)	<i>Plectropomus leopardus</i> 21.67 (1.8 ± 0.6)	<i>Gymnocranius audleyi</i> 21.6 (1.8 ± 1.1)	<i>Leptojulius sp</i> 8 (0.7 ± 0.9)
<i>Chaetodontoplus meredithi</i> 14.27 (0.3 ± 0.7)	<i>Alepes spp</i> 9.46 (4.5 ± 5.8)	<i>Gymnocranius audleyi</i> 21.6 (2.6 ± 0.5)	<i>Carangoides orthogrammus</i> 18.61 (10.4 ± 10.8)	<i>Carangoides ferdau</i> 6.11 (0.3 ± 0.5)
<i>Coradion chrysozonus</i> 13.89 (0.5 ± 0.8)	<i>Scomberomorus queenslandicus</i> 8.97 (0.6 ± 0.7)	<i>Choerodon fasciatus</i> 19.73 (1.4 ± 0.8)	<i>Parupeneus barberinus</i> 16.63 (0.8 ± 0.4)	<i>Lethrinus rubrioperculatus</i> 6.11 (0.3 ± 0.5)
<i>Scolopsis monogramma</i> 12.97 (1.2 ± 0.9)	<i>Lagocephalus scleratus</i> 8.13 (0.1 ± 0.3)	<i>Parupeneus barberinus</i> 16.63 (1.5 ± 0.8)	<i>Nemipterus furcosus</i> 16.49 (4.4 ± 7.6)	<i>Epinephelus malabaricus</i> 6.03 (0.3 ± 0.5)
<i>Choerodon vitta</i> 12.92 (1.4 ± 1.2)	<i>Nemipterus nematopus</i> 8.13 (0.2 ± 0.6)	<i>Scarus flavipectoralis</i> 16.46 (1.1 ± 0.7)	<i>Scarus flavipectoralis</i> 16.46 (0.3 ± 0.4)	<i>Carangoides gymnostethus</i> 5.74 (1.0 ± 0.8)
<i>Carangoides fulvoguttatus</i> 12.65 (4.3 ± 2.0)	<i>Scomberomorus commersonianus</i> 7.58 (0.1 ± 0.3)	<i>Lethrinus miniatus</i> 15.97 (0.8 ± 0.4)	<i>Lethrinus miniatus</i> 15.97 (0.5 ± 0.5)	<i>Lethrinus lentjan</i> 4.52 (0.7 ± 0.9)
<i>Diagramma pictum</i> 12.08 (0.2 ± 0.4)	<i>Nemipterus sp1</i> 7.55 (1.2 ± 3.5)	<i>Parupeneus heptacanthus</i> 15.75 (1.6 ± 1.4)	<i>Parupeneus heptacanthus</i> 15.75 (4.2 ± 4.9)	<i>Choerodon venustus</i> 3.7 (0.7 ± 0.9)
<i>Lethrinus nebulosus</i> 11.94 (0.2 ± 0.4)	<i>Sepioteuthis lessoniana</i> 6.48 (0.4 ± 0.7)	<i>Loxodon macrorrhinos</i> 14.41 (0.2 ± 0.4)	<i>Loxodon macrorrhinos</i> 14.41 (1.0 ± 0.7)	<i>Gnathanodon speciosus</i> 2.48 (11.3 +- 16.0)

A number of highly ranked species in Appendices 8.1 and 8.2 are notable by their absence from the “species of high influence” listed in the classifications presented here. To aid in interpreting the patterns for such species we have selected the top 10 species (in terms of Kruskal-Wallis values) influencing each of the 5 habitat groups, and given their abundance, in Table 8–10. Some of these species were sighted in most or all habitat types at most or all locations – and hence had little influence and low Kruskal-Wallis values in discriminating groups. The most notable of these were the ubiquitous starry triggerfish (*Abalistes stellaris*) and venus tusk fish (*Choerodon venustus*) seen in all habitat groups, and the common schools of goldspot trevally (*Carangoides fulvoguttatus*).

The abundance of common coral trout in both megabenthos and sand/*Halimeda* habitats at Kelso Shoals is somewhat surprising. It may be that the individuals seen over the sand were attracted by bait far from shelter elsewhere to venture out over the open, flat sediments. It is also possible that the video sets landed nearby, but did not record, bommies or other structure. Alternatively, there may be significant use of “off reef” habitats by coral trout and other species normally closely associated with topographically complex, hard substrata.

8.3.3 The location and habitat of “reds” grounds

We obtained the GPS coordinates (“marks”) of known “redfish” grounds from Captains Jim Dalling and Joe Linton, in the vicinity of Robbery Shoals, Davies Reef and Old Reef. Towed video was deployed though and around these marks, but the seabed was remarkably free of “structure” or megabenthos at all sites, with the exception of a wrecked plane at Robbery Shoals, some scattered very sparse epibenthos near Davies Reef, and some Pleistocene reef pinnacles near Old Reef. The ROV was deployed around the wrecked plane and large numbers of sub-adult *Lutjanus erythropterus* and *L. malabaricus* were filmed and later trapped around it. At the Robbery Shoals and Davies Reef grounds the seabed did have large, steep-sided holes where dead shell, rubble and clay was visible. Echosounder traces of these holes had an appearance of “rough ground”. Fine sediment was piled up into mounds around these holes, and they bore striking resemblance to video footage of “wonky holes” where freshwater seeps up into the GBR lagoon through extinct, gravel-filled river beds of the Herbert and Burdekin Rivers (pers. comm. T. Stieglitz, James Cook University).

The trapping in Phase 1 at Kelso Shoals was guided by the experience of Don Battersby (skipper of RV James Kirby), and immediately located a very small patch (50 m²) of seabed that produced consistent catches of large *L. malabaricus* and *L. sebae*. This “mark” was in the deepest water (52 metres) in a channel between Slashers #2 (Reef 18-043) and the un-named Reef 18-042. Other reds were trapped within 300 metres away from this mark, in 52 metres, and 800 metres away at the bottom of a very steep dropoff from 32 metres to 59 metres (see Figure 8–20). Deployment of pilot “Trapcam” in Phase 2 confirmed the presence of *L. sebae* and *L. malabaricus* at the mark, and entry and escape of several specimens was filmed (none were caught). The seabed on the trapcam video at the mark appeared to be very flat “coarse sediments with some *Halimeda*” with abundant hermit crabs. The towed video was deployed through and around the mark and no benthos or other structure was found in the vicinity.

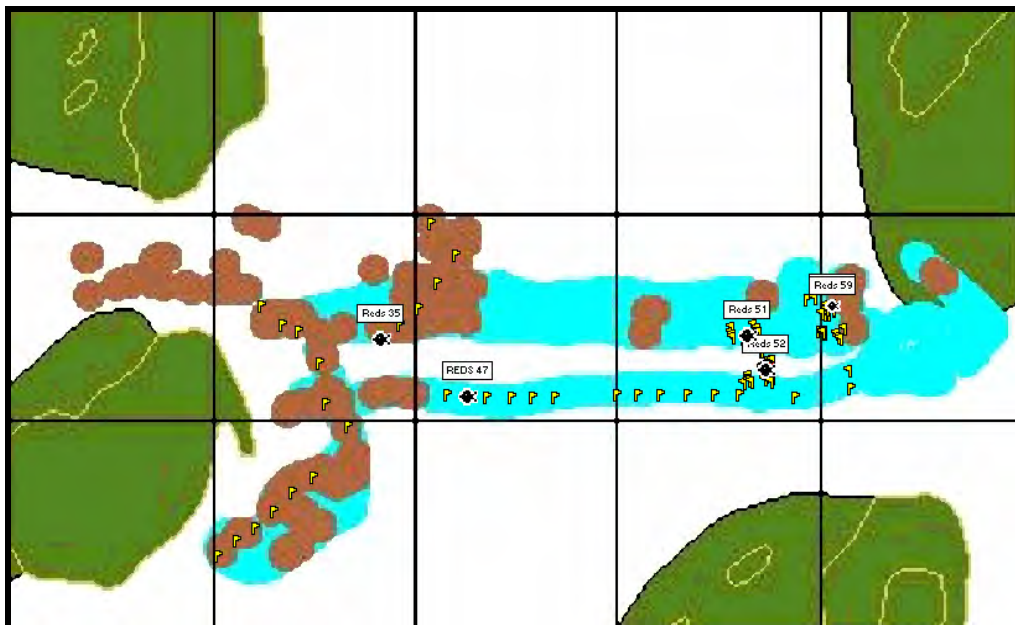


Figure 8–20. The location of BRUVS/RUVS and trap sets (small flags) around the 4 Kelso Reefs and Shoals in relation to “benthos” (brown shading) and “no benthos” (blue shading) categories derived from towed video transects. The locations of capture or sighting of “redfish” (*Lutjanus sebae* and *L. malabaricus*) are shown with the depth in metres.

In Phase 3 at Kelso, the BRUVS and RUVS were deployed “on” and “off” benthos found by the towed video transects, and at the “redfish” marks (see Figures 8–20 and 8–21). A small number of large *Lutjanus sebae* (1) and *L. malabaricus* (4) were sighted on 3 of the video sets near the same marks, and further west toward Little Kelso Reef. The sightings were confined to sites classified from the towed video as “off” benthos, with the exception of some fish seen in deep water at dropoffs from shallows bearing coral or other megabenthos (see Figure 8–20). The seabed and benthos on the BRUVS/RUVS in which redfish were sighted was

described as “heavily bioturbated soft sediment with *Halimeda*/seagrass in very sparse, low pieces”, and “flat plain of very coarse sediments, some algal blades and odd pieces of rubble, on the edge of a gutter”, and “coarse bioturbated sediments, moderate density of *Halimeda* and sparse, low (2-5 cm) unidentified benthos”.

All these lines of evidence indicate that adult redfish are not restricted to megabenthos gardens or rugose topography in the study area, but probably prefer to forage (at least in daylight hours) over coarse flat sediments in deep gutters.

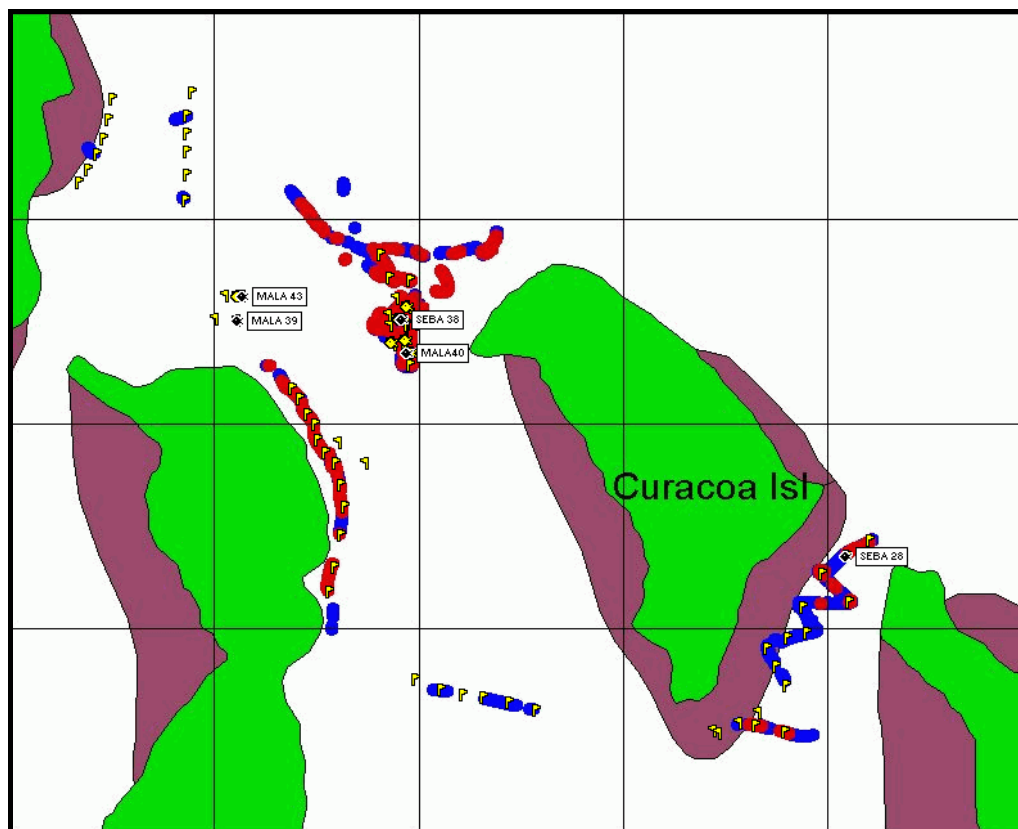


Figure 8–21. The location of BRUVS/RUVS and trap sets (small flags) around the Palms Islands in relation to “benthos” (red or light shading) and “no benthos” (blue or dark shading) categories derived from towed video transects. The locations of capture or sighting of “redfish” (SEBA *Lutjanus sebae* and MALA *L. malabaricus*) are shown by fish symbols with the species and depth in metres for the major concentrations.

The juvenile *L. sebae* were trapped and filmed in the habitats dominated by megabenthos, but in such moderate numbers that they had no major influence in the classifications presented here. We conclude that they are an important component of the fish assemblage associated with megabenthos, but we cannot predict if they are restricted to such habitats. Sub-adult *Lutjanus malabaricus* were also occasionally trapped in habitats thought to be dominated by

megabenthos in Curacoa Channel, but the greatest concentration occurred (with catches of juvenile *L. erythropterus*) in several trap sets at the base of a steep sandy drop-off in 25 metres depth at the western side of Curacoa Channel near Fantome Island (Figure 8–21). Neither *L. erythropterus* or *L. malabaricus* juveniles were sighted on BRUVS or RUVS in the Palms during this study.

8.3.4 Feeding habits of major species

Analyses of stomach contents were dominated by: empty stomachs, stomachs packed with pilchard bait from the traps, and everted stomachs (caused by embolism of the swimbladder during trap retrieval). Some of the items in Table 8–11 may also be artifacts of the trapping procedure. For example, the isopods found in the stomachs were also found in the bait canisters, so they may have been consumed incidentally when fish fed on the pilchard bait. Secondly, the whole fish found in the coral trout might have been eaten inside the trap. In the TrapCam footage we filmed a coral trout approximately 500 mm long capture and eat a large fusilier about 280 mm long. None of the prey items found could confidently be related to megabenthos habitats. The most prevalent items in *Lutjanus malabaricus* were small “coral prawns” *Metapenaeopsis* spp, but juvenile and adult *L. malabaricus* also consumed some very large squid and cuttlefish relative to their own body size. Members of the *Metapenaeopsis* genus lives in a wide variety of sediment types, from mud and sand to “hard ground”.

Table 8–11. The number of stomachs examined *N*, with the number *n food* containing items other than pilchard bait, and the prey taxa in descending order of prevalence.

Species	<i>N</i> (<i>n food</i>)	Prey taxa
<i>Abalistes stellaris</i>	4 (0)	
<i>Choerodon venustus</i>	2 (0)	
<i>Diagramma pictum</i>	5 (0)	
<i>Lethrinus laticaudis</i>	2 (0)	
<i>Lethrinus miniatus</i>	15 (1)	<i>Octopus</i> sp.
<i>Lethrinus semicinctus</i>	8 (0)	
<i>Lethrinus</i> sp.2	8 (1)	Fish remains
<i>Lutjanus adetii</i>	1 (0)	
<i>Lutjanus carponotatus</i>	1 (0)	
<i>Lutjanus malabaricus</i>	32 (10)	Decapods (prawns <i>Metapenaeopsis</i> spp and <i>Squilla</i> sp.), crabs (Portunidae <i>Thalamita</i> sp. and Grapsidae), cephalopods (<i>Photololigo</i> sp., <i>Sepia</i> sp.), Isopoda sp., fish remains
<i>Lutjanus russelli</i>	9 (0)	
<i>Lutjanus sebae</i>	11 (2)	Isopoda sp.
<i>Lutjanus vitta</i>	6 (0)	
<i>Plectropomus leopardus</i>	4 (1)	<i>Lutjanus kasmira</i>

8.3.5 Stereo-BRUVS development

Measurements of fish from single-camera video systems with “gunsight” measuring grids were prone to large errors, whereas stereo systems allow precise and accurate measurements. For this reason, a stereo-camera system was developed in collaboration with Dr Euan Harvey of the University of Western Australia by mounting the BRUVS housings on a frame with an angle of convergence of 12° in the focal plane. The unit was calibrated and tested in 2 deployments at Rib and Davies Reef, with a large Queensland groper *Epinephelus lanceolatus* the subject of measurement (Figure 8–22).



Figure 8–22. A large Queensland groper (~158 cm Total Length) measured with a baited stereo-video prototype.

8.4 Discussion

In this study we have focused on developing and applying appropriate techniques to determine the associations between fish assemblages and benthic substrata and encrusting assemblages. The use of baited and unbaited video cameras, set in strings of replicates in habitat types known or unknown from complementary surveys, was demonstrated to offer a powerful tool for daytime collection of information on biodiversity and relative abundance of

fishes. The action of the bait plume made a great difference in the rate of accumulation of fish biodiversity data in the sites and habitats, and there was no evidence it deterred species from attending the video stations. The presence of the video system, the bait plume, and the behaviour and abundance of conspecifics and other species were all evidently involved in the attraction of the fish to the units.

In contrast, fish traps were very poor sampling tools, though improvement was evident when galvanic timed releases were used to govern fishing time and increase probability of retention. This was because probability of capture was shown to depend not just on the probability of retention but also on the probability of entry — and the majority of species seen around the traps showed no interest in entering the traps in daytime sets. Species with a high probability of one or other, or both, of these species-specific factors were caught in traps, giving a very limited picture of biodiversity in different habitat types. Only 14% of all fish seen as “available” around the traps were actually filmed inside the traps and only 3% of the available fish were actually caught by the traps, with some notably important families of fish never entering. Video sets are non-extractive and can provide opportunity for extremely accurate and precise measurements of fish length *in situ* (Harvey *et al.* 2001a, 2001b), whereas the advantage of traps lies in the research opportunities for ageing and dietary studies provided by the sampled specimens. In the north-west of Australia “industry standard” traps have been considered effective tools for providing information for fishery-independent stock assessment for a limited suite of commercially important species (pers. comm. S. Newman). Traps can also be used overnight, as can video techniques when low-power, cost-effective lighting systems are applied.

Our primary objective was to determine the roles of megabenthos in providing food and shelter and thus structuring fish assemblages. At the coarsest spatial scales, a number of studies have documented bioregional (Ramm *et al.* 1990), latitudinal (long-shelf) and longitudinal (cross-shelf) patterns in distribution and abundance of both demersal fishes (eg Williams, 1982, Williams and Hatcher, 1983; Newman and Williams, 1996) and megabenthos (eg Long *et al.* 1995; Fabricius, 2001). At the next scale downward, there has also been strong pattern detected amongst different zones (eg windward slope versus back-reef) of reefs (eg Fabricius and D’earth, 1997; Newman *et al.* 1997) and different habitats within zones (eg Sluka *et al.* 2001) for economically important emperors, snappers and groupers. Studies at even smaller scales are, however, needed to determine the shelter and food requirements of

fish associated with megabenthos. The importance and function of such microhabitats is reviewed in Sale (1991) for numerous small-scale studies of fishes on coral reefs. Given that a strictly “coral reef” fish fauna does not exist (see Bellwood, 1998), it is likely that the same approaches are needed for lethrinids, lutjanids and serranids in other demersal shelf habitats where benthic structure and topographic complexity exist. The major problem in emulating such autecological approaches is the depth of water in the inter-reef, beyond the limits of safe SCUBA diving.

The scale of study we attempted was (by logistical necessity) at the level of habitat type (“off” and “on” benthos) amongst inshore and mid-shelf locations. The classification of sites by the abundance of fish assemblage components was dominated by a very strong cross-shelf difference, followed by secondary groupings according to depth of the inshore sites, and significant discrimination of inshore megabenthos/*Sargassum* and mid-shelf megabenthos from other sites having “bare substrata/algae” habitats. In view of recent analysis of lethrinid, lutjanid and serranid distributions in the same region we could expect even greater differences had we included habitats at outer-shelf locations (see Newman and Williams, 1996).

Patterns were clear in the video data presented here, but the task of interpreting them in terms of associations between fish and their benthic habitat has been confounded by four major features in the scale of sampling in this study.

First, on the basis of previous experience in the far northern GBR, the presence of large “megabenthos gardens” patches was expected to form the basis of our planned “inside” versus “outside” megabenthos comparisons, to be done with analysis of variance in regions representative of mid-shelf (red-spot king and tiger prawn) trawling grounds. Our first exploratory seabed surveys on RV Lady Basten at 105 stations spanning several degrees of latitude failed to discover significant large patches or “gardens” of megabenthos in the mid-shelf areas, despite concentrating on areas of higher seabed current shear stress known to encourage growth of such sessile filter-feeders elsewhere. Instead, we found the megabenthos to be scant in the mid-shelf, and so, much of our study was restricted to the channels between the Palm Islands — where the fish assemblages were demonstrably different to those around the mid-shelf reefs.

Secondly, the mid-shelf megabenthos patches that we did find were small, sparse and associated with Pleistocene reef edges and other eroded reef remnants. Multivariate analyses clustering sites and seabed habitat types by fish assemblages were then chosen as the most plausible approach to elucidate associations. It was not strictly possible, however, to determine if the patterns we described were related to the influence of the encrusting megabenthos, or to the shelter offered by the Pleistocene structures, or to both. We cannot tell from the scale of our study. The topographic complexity of the extinct reef skeleton alone might provide shelter, and incoming detritus or food chains based on encrusting algae might support invertebrates living in the interstices, which might support foraging fish. Alternatively, the branching and thallose megabenthos might offer the primary shelter for these prey and their fish predators (see Cappo and Kelley, 2001). It is unlikely that sponges, gorgonians and alcyonarians provide major detrital subsidies or other basis for food chains (pers. comm. K. Fabricius, AIMS), but studies are lacking.

Thirdly, both the megabenthos patches we found, and the “footprints” of the BRUVS/RUVS and the towed video used in classifying seabed habitats, were so small that “misclassification” of habitat types was likely. In the first instance, the video tows, with a swathe no more than 2 metres wide were used to pick “on” and “off” benthos sites for later sets of BRUVS and RUVS, yet the accuracy of GPS and deployment was such that the video sets sometimes landed off the intended habitat type, or the video footage itself showed a different habitat type than expected from the video tow. In the second instance, BRUVS dropped on bare substrata were sometimes known or suspected to be close to megabenthos patches – perhaps enough to influence the fish assemblage recorded on the video. For example, we sometimes recorded coral trout over bare sediments on BRUVS sets, but these fish may have been attracted by the bait plume from nearby Pleistocene reef remnants with or without encrusting megabenthos. Matching the “footprints” of complementary sensors, from the wide swath of side-scan sonar to the narrow track of video to the smaller quadrant of digital “frame grabs” was identified as a bottleneck in R&D at the recent national workshop on the use of video in Australian fisheries and mariculture habitats (see Harvey and Cappo, 2001).

Effects of the sampling technique in modifying the distribution of the target fish are difficult to measure, and often encountered in studying distributions of fish in “habitat mosaics” (see Harvey *et al.* 2001a,b). In the case of underwater visual census of serranids, Sluka *et al.* (2001) concluded that these fish were most abundant on the most topographically complex

hard substrata, yet it could be argued that the presence of the SCUBA diver scared fish into the “core area” containing their shelter holes. Our video sets on specific habitat types were not accompanied by sufficient intelligence on the proximity of other habitat types to enable us to assess the degree of “smearing” of fish-habitat associations by the attraction afforded by the bait. It is conceivable that fish moved between habitat types toward the baited video, but we cannot account for this. An obvious test would be to set the baited videos at different, known distances from specific habitat types, but high resolution habitat maps giving complete coverage of the seabed would be necessary to establish such tests.

Finally, our video footage was made with a focal plane along the seabed, rather than perpendicular to it (eg. Willis *et al.* 2000; Yau *et al.* 2001). This was ideal to identify fish, but could not provide data on the seabed “coverage” of different types of epibenthos – other than to note its presence. This prevented us from following the approach of Sainsbury *et al.* (1997) who used camera frame “stills” to conclude that there was a significantly higher probability of occurrence of *Lethrinus* and *Lutjanus* in areas of the North West Shelf where large (>25 cm) benthic organisms were present than in areas with no large epibenthos. Conversely *Nemipterus* and *Saurida* showed a significantly higher probability of occurrence in areas without large epibenthos. Those surveys have not been published in detail, but a comparison of the summaries for the North-West Shelf in Table 8–12 with the same families in our study (Table 8–13) shows three major differences.

Firstly, we did not sight the lizardfish genus *Saurida* on video sets. Secondly, while *Nemipterus* were absent from megabenthos habitats at all locations there were major differences in the sand/*Halimeda* habitat type between Kelso Shoals and Rib Reef, where *Nemipterus* was not recorded. Cross-shelf differences were also marked, with more *Lethrinus* and *Lutjanus* in the megabenthos on the mid-shelf than inshore, and with both these genera commonly sighted in sand/*Halimeda* habitats.

The implications of these differences are twofold. First, the results show that the cross-shelf location in studies of fish-habitat associations is a prime determinant in the results. Second, we cannot presume to transfer results from this study to all situations involving disturbance of megabenthos. Separate, location-specific studies are needed to address sustainability of inshore banana-prawn trawling, lagoon trawling for tiger prawns, and inter-reef trawling for

red-spot king prawns. Furthermore, it is likely there are long-shore, latitudinal differences in fish-habitat associations that could not be covered by the current study.

Table 8–12. Frequency of observation of various fish genera in different demersal habitats, based on analysis of 2,720 frames of a photographic survey on the North-West Shelf. Habitats were defined by cluster analysis, and the benthos consisted mostly of sponges, gorgonians and alcyonarians. Table adapted from Sainsbury (1987).

Genus	N Frames containing Genus	“Open Sand”	“Patchy Benthos and Open Sand”	“Dense Benthos”
<i>Saurida</i> (Lizardfish)	454 (17%)	232 (65%)	108 (30%)	14 (3%)
<i>Nemipterus</i> (Threadfin bream)	232 (8%)	124 (53%)	78 (33%)	30 (13%)
<i>Lethrinus</i> (Emperors)	40 (1.5%)	12 (30%)	7 (17%)	21 (52%)
<i>Lutjanus</i> (Snappers)	40 (1.5%)	12 (30%)	6 (15%)	22 (55%)
		1752	764	204

Table 8–13. Frequency of observation of various fish genera in different demersal habitats, based on analysis of 130 baited and unbaited video sets in the current study. Habitats were defined by cluster analysis, and the benthos consisted mostly of gorgonians and sponges growing on Pleistocene reef remnants on the mid-shelf, and gorgonians, sponges and alcyonarians growing on various substrata in the Palm Islands.

Genus	N sets containing Genus	“Inshore megabenthos and <i>Sargassum</i> ” Grp 1	“Inshore Mud, sand, rubble, <i>Sargassum</i> ” Grp 2	“Mid-shelf megabenthos” Grp 3	“mid-shelf sand, <i>Halimeda</i> Kelso Shoals” Grp 4	“mid-shelf sand, <i>Halimeda</i> Rib Reef” Grp 5
<i>Saurida</i> (Lizardfish)	-	-	-	-	-	-
<i>Nemipterus</i> (Threadfin bream)	28 (21%)	-	17 (59%)		11 (32%)	
<i>Lethrinus</i> (Emperors)	35 (27%)	3 (14%)	1 (3%)	16 (89%)	9 (26%)	6 (35%)
<i>Lutjanus</i> (Snappers)	21 (16%)	3 (14%)	1 (3%)	6 (33%)	5 (14%)	6 (35%)
	130	22	29	18	34	17

In terms of our focus on economically important species, we found no indication of a dependency of adult “redfish” (*Lutjanus sebae*, *L. malabaricus*, *L. erythropterus*) on megabenthos. Trap catches and video sightings of the adults were restricted to coarse carbonate sediments and sand/*Halimeda* habitats in deep gutters. The few charter boat “hotspots” we surveyed for these species were found to have rugose sandy seabeds, without significant megabenthos (only 0 to ~2% very sparse), with the exception of a wrecked plane at Robbery Shoals. Juvenile *L. sebae*, with their striking vertical bands, were most commonly caught and sighted in megabenthos habitats. Our data also showed ontogenetic changes in

habitat of “redfish” from juveniles in shallow inshore waters to adults in deep, offshore waters (see McPherson and Squire, 1992; Cappo and Kelley, 2001). Data on feeding were few, but the *Lutjanus malabaricus* stomach contents were dominated by small *Metapenaeopsis* spp “coral prawns” and cephalopods. Members of the *Metapenaeopsis* genus lives in a wide variety of sediment types, from mud and sand to “hard ground”.

We recommend that baited and unbaited video sets are a useful, non-extractive tool in studying the fish-habitat associations below the limits of SCUBA, if used in conjunction with underwater television and side-scan sonar to produce detailed maps of the study area. These maps of habitat are necessary to interpret the patterns of fish abundance on the videos in terms of the true mosaic of available habitat and the density and coverage of specific types of benthos. We used the video techniques only in daylight hours, but we know from the overnight trapping that a variety of important fish families are active by night, so lighting systems will need to be developed. The techniques and opportunities are reviewed in Harvey and Cappo (2001).

8.5 Appendices

Appendix 8.1. Prevalence (P number of tapes on which species sighted), sum of $MaxN$, average of $MaxN \pm$ standard deviation of 185 species sighted in 64 baited (BRUVS) video sets in the Palm Islands, Robbery and Kelso Shoals, Rib and Davies Reefs. Asterisks * highlight the 87 species seen only on BRUVS.

Species	Family	P	$\Sigma(MaxN)$	Avg($MaxN$)
<i>Carangoides fulvoguttatus</i>	Carangidae	29	131	4.5 ± 5.4
<i>Abalistes stellaris</i>	Balistidae	27	39	1.4 ± .8
<i>Choerodon venustus</i>	Labridae	22	29	1.3 ± .5
<i>Pentapodus paradiseus</i>	Nemipteridae	21	181	8.6 ± 6.4
<i>Gymnocranius audleyi</i>	Lethrinidae	20	54	2.7 ± 1.4
<i>Lethrinus spB</i>	Lethrinidae	20	100	5.0 ± 3.7
<i>Plectropomus leopardus</i>	Serranidae	19	37	1.9 ± .8
<i>Parupeneus heptacanthus</i>	Mullidae	18	79	4.4 ± 4.0
<i>Parupeneus barberinus</i>	Mullidae	17	22	1.3 ± .7
<i>Caesio cuning</i>	Caesionidae	14	307	21.9 ± 31.9
<i>Echeneis naucrates</i>	Echeneidae	13	17	1.3 ± .6
<i>Cheilinus fasciatus</i>	Labridae	12	21	1.8 ± .9
<i>Choerodon vitta</i>	Labridae	12	26	2.2 ± 1.6
<i>Scarus flavipectoralis</i>	Scaridae	12	17	1.4 ± .9
<i>Lethrinus miniatus</i>	Lethrinidae	11	11	1.0 ± .0
<i>Pterocaesio marri</i>	Caesionidae	11	388	35.3 ± 29.8
<i>Scolopsis monogramma</i>	Nemipteridae	11	19	1.7 ± .6
<i>Nemipterus furcosus</i>	Nemipteridae	11	88	8.0 ± 6.6
<i>Symphorus nematophorus</i>	Lutjanidae	10	12	1.2 ± .6
<i>Alepes spp</i>	Carangidae	9	73	8.1 ± 7.1
<i>Sufflamen frenatus</i>	Balistidae	9	11	1.2 ± .4
<i>Lethrinus semisinctus</i>	Lethrinidae	9	65	7.2 ± 2.9
<i>Choerodon fasciatus</i>	Labridae	9	19	2.1 ± .8
<i>Coradion chrysozonus</i>	Chaetodontidae	8	10	1.3 ± .5
<i>Lethrinus nebulosus</i>	Lethrinidae	8	8	1.0 ± .0
<i>Chaetodontoplus meredithi</i>	Pomacanthidae	7	9	1.3 ± .5
<i>Diagramma pictum</i>	Haemulidae	7	17	2.4 ± 2.2
<i>Chelmon rostratus</i>	Chaetodontidae	7	13	1.9 ± .4
<i>Parupeneus multifasciatus</i>	Mullidae	7	8	1.1 ± .4
<i>Cheilinus diagramma</i>	Labridae	7	11	1.6 ± .8
<i>Carangoides gymnostethus</i>	Carangidae	6	25	4.2 ± 5.4
<i>Upeneus tragula</i>	Mullidae	6	14	2.3 ± 1.4
<i>Scomberomorus queenslandicus*</i>	Scombridae	6	8	1.3 ± .5
<i>Scolopsis margaritifera</i>	Nemipteridae	6	7	1.2 ± .4
<i>Pomacanthus sexstriatus</i>	Pomacanthidae	6	11	1.8 ± 1.2
<i>Plectropomus maculatus</i>	Serranidae	6	13	2.2 ± 1.6
<i>Parupeneus cyclostomus</i>	Mullidae	6	10	1.7 ± .8
<i>Loxodon macrorhinos*</i>	Carcharhinidae	6	7	1.2 ± .4
<i>Lagocephalus scleratus*</i>	Tetraodontidae	6	31	5.2 ± 4.8
<i>Choerodon schoenleinii</i>	Labridae	6	7	1.2 ± .4
<i>Carangoides uii</i>	Carangidae	6	16	2.7 ± 1.9
<i>Carangoides orthogrammus</i>	Carangidae	6	52	8.7 ± 10.4
<i>Aprion virescens</i>	Lutjanidae	5	6	1.2 ± .4
<i>Lutjanus vitta</i>	Lutjanidae	5	9	1.8 ± 1.3
<i>Siganus doliatus</i>	Siganidae	5	9	1.8 ± .4
<i>Scarus ghobban</i>	Scaridae	5	12	2.4 ± 1.7
<i>Rhynchobatus djiddensis*</i>	Rhynchobatidae	5	5	1.0 ± .0
<i>Parupeneus indicus</i>	Mullidae	5	5	1.0 ± .0
<i>Nemipterus sp1</i>	Nemipteridae	5	59	11.8 ± 7.6
<i>Gnathanodon speciosus</i>	Carangidae	5	81	16.2 ± 12.0
<i>Heniochus acuminatus</i>	Chaetodontidae	5	12	2.4 ± 3.1
<i>Cephalopholis boenak</i>	Serranidae	5	8	1.6 ± .5
<i>Chaetodon auriga*</i>	Chaetodontidae	5	8	1.6 ± .5
<i>Cephalopholis miniata*</i>	Serranidae	5	6	1.2 ± .4
<i>Carangoides chrysophrys</i>	Carangidae	5	7	1.4 ± .9
<i>Canthigaster valentini</i>	Tetraodontidae	4	6	1.5 ± .6
<i>Siganus argenteus*</i>	Siganidae	4	10	2.5 ± 1.7
<i>Scomberomorus commersonianus</i>	Scombridae	4	4	1.0 ± .0
<i>Pomacentrus nagasakiensis</i>	Pomacentridae	4	8	2.0 ± 1.4

Species	Family	P	$\Sigma(MaxN)$	Avg(MaxN)
<i>Paramonacanthus oblongus (japonicus)</i>	Monacanthidae	4	5	1.3 ± .5
<i>Lutjanus sebae*</i>	Lutjanidae	4	4	1.0 ± .0
<i>Gymnothorax flavimarginatus*</i>	Muraenidae	4	4	1.0 ± .0
<i>Gymnocranius grandoculis</i>	Lethrinidae	4	7	1.8 ± 1.5
<i>Dascyllus trimaculatus*</i>	Pomacentridae	4	12	3.0 ± 1.6
<i>Coradion altivelis</i>	Chaetodontidae	4	5	1.3 ± .5
<i>Cheilinus undulatus</i>	Labridae	4	5	1.3 ± .5
<i>Chaetodon rainfordi</i>	Chaetodontidae	4	6	1.5 ± .6
<i>Carcharhinus amblyrhynchos</i>	Carcharhinidae	4	4	1.0 ± .0
<i>Aetobatus narinari*</i>	Myliobatididae	3	3	1.0 ± .0
<i>Chaetodontoplus duboulayi*</i>	Pomacanthidae	3	4	1.3 ± .6
<i>Carangoides ferdau</i>	Carangidae	3	3	1.0 ± .0
<i>Argyrops spinifer*</i>	Sparidae	3	7	2.3 ± 1.5
<i>Carcharhinus dussumieri*</i>	Carcharhinidae	3	3	1.0 ± .0
<i>Sufflamen chrysopterus</i>	Balistidae	3	3	1.0 ± .0
<i>Sepioteuthis lessoniana</i>	Loliginidae	3	4	1.3 ± .6
<i>Scarus microrhinos</i>	Scaridae	3	4	1.3 ± .6
<i>Nemipterus nematopus*</i>	Nemipteridae	3	40	13.3 ± 10.6
<i>Nebrius ferrugineus*</i>	Ginglymostomatidae	3	3	1.0 ± .0
<i>Lutjanus quinquelineatus</i>	Lutjanidae	3	4	1.3 ± .6
<i>Lutjanus adetii*</i>	Lutjanidae	3	31	10.3 ± 12.9
<i>Lethrinus olivaceus</i>	Lethrinidae	3	3	1.0 ± .0
<i>Lethrinus lentjan*</i>	Lethrinidae	3	5	1.7 ± .6
<i>Lethrinus laticaudis*</i>	Lethrinidae	3	3	1.0 ± .0
<i>Gymnothorax undulatus*</i>	Muraenidae	3	4	1.3 ± .6
<i>Pomacanthus semicirculatus</i>	Pomacanthidae	3	3	1.0 ± .0
<i>Nemipterus sp (thin)</i>	Nemipteridae	3	9	3.0 ± 2.6
<i>Galeocerdo cuvieri</i>	Carcharhinidae	3	3	1.0 ± .0
<i>Epinephelus malabaricus*</i>	Serranidae	3	3	1.0 ± .0
<i>Diploprion bifasciatum</i>	Grammistidae	3	3	1.0 ± .0
<i>Coris sp</i>	Labridae	3	8	2.7 ± 1.2
<i>Chrysiptera rollandi</i>	Pomacentridae	3	4	1.3 ± .6
<i>Amblyglyphidodon aureus*</i>	Pomacentridae	2	3	1.5 ± .7
<i>Chaetodon lineolatus</i>	Chaetodontidae	2	3	1.5 ± .7
<i>Epibulus insidiator</i>	Labridae	2	2	1.0 ± .0
<i>sea snake*</i>	sea snake	2	2	1.0 ± .0
<i>Sphyraena jello*</i>	Sphyraenidae	2	2	1.0 ± .0
<i>Scolopsis bilineatus</i>	Nemipteridae	2	2	1.0 ± .0
<i>Pentapodus sp2 (Randall)</i>	Nemipteridae	2	4	2.0 ± 1.4
<i>Pentapodus nagasakiensis</i>	Nemipteridae	2	3	1.5 ± .7
<i>Parupeneus pleurostigma*</i>	Mullidae	2	3	1.5 ± .7
<i>Parapercis nebulosa</i>	Pinguipedidae	2	4	2.0 ± .0
<i>Naso brevirostris*</i>	Acanthuridae	2	26	13.0 ± 17.0
<i>Meiacanthus luteus</i>	Blenniidae	2	2	1.0 ± .0
<i>Lutjanus russelli*</i>	Lutjanidae	2	2	1.0 ± .0
<i>Lutjanus malabaricus</i>	Lutjanidae	2	4	2.0 ± .0
<i>Lethrinus rubrioperculatus*</i>	Lethrinidae	2	2	1.0 ± .0
<i>Hemigymnus melapterus</i>	Labridae	2	2	1.0 ± .0
<i>Pseudochromis paccagnellae</i>	Pseudochromidae	2	2	1.0 ± .0
<i>Pomacentrus brachialis</i>	Pomacentridae	2	3	1.5 ± .7
<i>Plectropomus laevis*</i>	Serranidae	2	2	1.0 ± .0
<i>Epinephelus quoyanus*</i>	Serranidae	2	2	1.0 ± .0
<i>Epinephelus areolatus*</i>	Serranidae	2	3	1.5 ± .7
<i>Arothron stellatus*</i>	Tetraodontidae	2	2	1.0 ± .0
<i>Cephalopholis sp*</i>	Serranidae	2	2	1.0 ± .0
<i>Chaetodon aureofasciatus*</i>	Chaetodontidae	2	4	2.0 ± 1.4
<i>Acanthurus dussumieri*</i>	Acanthuridae	1	4	4.0 ± .0
<i>Balistoides viridescens*</i>	Balistidae	1	1	1.0 ± .0
<i>Balistoides conspicillum*</i>	Balistidae	1	1	1.0 ± .0
<i>Negaprion acutidens*</i>	Carcharhinidae	1	1	1.0 ± .0
<i>Naso vlamingii*</i>	Acanthuridae	1	1	1.0 ± .0
<i>Cheilinus unifasciatus*</i>	Labridae	1	1	1.0 ± .0
<i>Cheilinus trilobatus*</i>	Labridae	1	1	1.0 ± .0
<i>Cheilinus oxycephalus*</i>	Labridae	1	1	1.0 ± .0
<i>Chaetodontoplus conspicillatum*</i>	Pomacanthidae	1	1	1.0 ± .0

Species	Family	P	$\Sigma(MaxN)$	Avg(MaxN)
<i>Chaetodon kleinii</i> *	Chaetodontidae	1	2	2.0 ± .0
<i>Cetoscarus bicolor</i> *	Scaridae	1	1	1.0 ± .0
<i>Centropyge tibicen</i> *	Pomacanthidae	1	1	1.0 ± .0
<i>Carcharhinus melanopterus</i> *	Carcharhinidae	1	1	1.0 ± .0
<i>Carangoides sp</i> *	Carangidae	1	1	1.0 ± .0
<i>Carangoides plagiotaenia</i> *	Carangidae	1	6	6.0 ± .0
<i>Lutjanus argentimaculatus</i> *	Lutjanidae	1	3	3.0 ± .0
<i>Lethrinus sp</i> *	Lethrinidae	1	5	5.0 ± .0
<i>Lethrinus ornatus</i> *	Lethrinidae	1	1	1.0 ± .0
<i>Leptojulius sp</i>	Labridae	1	2	2.0 ± .0
<i>Hologymnosus doliatus</i> *	Labridae	1	1	1.0 ± .0
<i>Halichoeres prosopoeion</i>	Labridae	1	1	1.0 ± .0
<i>Gymnothorax favagineus</i> *	Muraenidae	1	1	1.0 ± .0
<i>Gymnothorax chilospilus</i> *	Muraenidae	1	1	1.0 ± .0
<i>Sphyrna mokarran</i> *	Sphyrnidae	1	1	1.0 ± .0
<i>Siganus puellus</i> *	Siganidae	1	1	1.0 ± .0
<i>Siganus javus</i> *	Siganidae	1	8	8.0 ± .0
<i>Seriolina nigrofasciata</i>	Carangidae	1	1	1.0 ± .0
<i>Scarus niger</i> *	Scaridae	1	1	1.0 ± .0
<i>Rhizoprionodon taylori</i> *	Carcharhinidae	1	1	1.0 ± .0
<i>Rachycentron canadus</i> *	Rachycentridae	1	2	2.0 ± .0
<i>Pygoplites diacanthus</i>	Pomacanthidae	1	1	1.0 ± .0
unknown	unknown	1	4	4.0 ± .0
<i>Thamnaconus modestoides</i>	Monacanthidae	1	1	1.0 ± .0
<i>Thalassoma lunare</i>	Labridae	1	1	1.0 ± .0
<i>Symphoricichthys spilurus</i>	Lutjanidae	1	1	1.0 ± .0
<i>Sufflamen bursa</i> *	Balistidae	1	1	1.0 ± .0
<i>Stegastes apicalis</i> *	Pomacentridae	1	2	2.0 ± .0
<i>Platax batavianus</i> *	Ephippidae	1	1	1.0 ± .0
<i>Pastinachus sephen</i>	Dasyatidae	1	1	1.0 ± .0
<i>Parupeneus barberinoides</i> *	Mullidae	1	1	1.0 ± .0
<i>Paramonacanthus otisensis</i> *	Monacanthidae	1	2	2.0 ± .0
<i>Paramonacanthus lowei</i>	Monacanthidae	1	1	1.0 ± .0
<i>Panulirus versicolor</i> *	Palinuridae	1	1	1.0 ± .0
<i>Nemipterus sp2 (stripe) *</i>	Nemipteridae	1	1	1.0 ± .0
<i>Nemipterus peronii</i> *	Nemipteridae	1	1	1.0 ± .0
<i>Pristipomoides sp</i> *	Lutjanidae	1	1	1.0 ± .0
<i>Pomacentrus wardi</i> *	Pomacentridae	1	1	1.0 ± .0
<i>Meiacanthus lineatus</i>	Blenniidae	1	1	1.0 ± .0
<i>Malacanthus latovittatus</i>	Malacanthidae	1	1	1.0 ± .0
<i>Lutjanus monostigma</i>	Lutjanidae	1	1	1.0 ± .0
<i>Lutjanus lemniscatus</i> *	Lutjanidae	1	1	1.0 ± .0
<i>Lutjanus fulviflamma</i> *	Lutjanidae	1	1	1.0 ± .0
<i>Lutjanus erythropterus</i> *	Lutjanidae	1	2	2.0 ± .0
<i>Lutjanus carponotatus</i>	Lutjanidae	1	2	2.0 ± .0
<i>Lutjanus bohar</i> *	Lutjanidae	1	1	1.0 ± .0
<i>Gymnocranius sp</i> *	Lethrinidae	1	1	1.0 ± .0
<i>Grammatorcynus bicarinatus</i>	Scombridae	1	1	1.0 ± .0
<i>Fistularia commersonianus</i> *	Fistulariidae	1	1	1.0 ± .0
<i>Euthynnus affinis</i> *	Scombridae	1	1	1.0 ± .0
<i>Epinephelus rivulatus</i> *	Serranidae	1	1	1.0 ± .0
<i>Elegatis bipinnulatus</i> *	Carangidae	1	1	1.0 ± .0
<i>Dascyllus reticulatus</i> *	Pomacentridae	1	4	4.0 ± .0
<i>Ctenochaetus striatus</i>	Acanthuridae	1	3	3.0 ± .0
<i>Bodianus mesothorax</i> *	Labridae	1	1	1.0 ± .0
<i>Anchisomus multistriatus</i> *	Tetraodontidae	1	1	1.0 ± .0
<i>Acanthurus nigroris</i> *	Acanthuridae	1	1	1.0 ± .0
<i>Arothron nigropunctatus</i> *	Tetraodontidae	1	1	1.0 ± .0
<i>Balistapus undulatus</i> *	Balistidae	1	1	1.0 ± .0
<i>Amblyglyphidodon curacao</i> *	Pomacentridae	1	2	2.0 ± .0
<i>Aethaloperca rogaea</i>	Serranidae	1	1	1.0 ± .0

Appendix 8.2. Prevalence (P number of tapes on which species sighted), sum of $MaxN$, average of $MaxN$ \pm standard deviation of 128 species sighted in 58 unbaited (RUVS) video sets in the Palm Islands, Robbery and Kelso Shoals, Rib and Davies Reefs. Asterisks * highlight the 30 species seen only on RUVS.

Species	Family	P	$\Sigma(MaxN)$	Avg($MaxN$)
<i>Pentapodus paradiseus</i>	Nemipteridae	16	52	3.3 \pm 3.5
<i>Carangoides fulvoguttatus</i>	Carangidae	15	37	2.5 \pm 2.3
<i>Parupeneus heptacanthus</i>	Mullidae	11	30	2.7 \pm 2.0
<i>Chaetodontoplus meredithi</i>	Pomacanthidae	10	11	1.1 \pm .3
<i>Scarus flavipectoralis</i>	Scaridae	9	19	2.1 \pm 2.3
<i>Caesio cuning</i>	Caesionidae	8	85	10.6 \pm 20.3
<i>Cheilinus fasciatus</i>	Labridae	7	7	1.0 \pm .0
<i>Gymnocranius audleyi</i>	Lethrinidae	7	10	1.4 \pm .8
<i>Scolopsis monogramma</i>	Nemipteridae	7	7	1.0 \pm .0
<i>Abalistes stellaris</i>	Balistidae	6	6	1.0 \pm .0
<i>Choerodon fasciatus</i>	Labridae	6	7	1.2 \pm .4
<i>Paramonacanthus oblongus (japonicus)</i>	Monacanthidae	6	7	1.2 \pm .4
<i>Upeneus tragula</i>	Mullidae	6	9	1.5 \pm .8
<i>Scolopsis margaritifera</i>	Nemipteridae	6	6	1.0 \pm .0
<i>Plectropomus leopardus</i>	Serranidae	6	8	1.3 \pm .8
<i>Chaetodon rainfordi</i>	Chaetodontidae	5	5	1.0 \pm .0
<i>Choerodon schoenleinii</i>	Labridae	5	5	1.0 \pm .0
<i>Lethrinus spB</i>	Lethrinidae	5	10	2.0 \pm 2.2
<i>Pomacanthus sexstriatus</i>	Pomacanthidae	5	6	1.2 \pm .4
<i>Nemipterus furcosus</i>	Nemipteridae	5	20	4.0 \pm 5.7
<i>Parupeneus barberinus</i>	Mullidae	5	9	1.8 \pm 1.3
<i>Lethrinus semisinctus</i>	Lethrinidae	5	8	1.6 \pm .9
<i>Cheilinus diagramma</i>	Labridae	5	5	1.0 \pm .0
<i>Cheilinus undulatus</i>	Labridae	4	4	1.0 \pm .0
<i>Symphorus nematophorus</i>	Lutjanidae	4	5	1.3 \pm .5
<i>Scarus microrhinos</i>	Scaridae	4	4	1.0 \pm .0
<i>Pterocaesio marri</i>	Caesionidae	4	218	54.5 \pm 34.8
<i>Pomacentrus nagasakiensis</i>	Pomacentridae	4	12	3.0 \pm 2.4
<i>Plectropomus maculatus</i>	Serranidae	4	6	1.5 \pm 1.0
<i>Parupeneus cyclostomus</i>	Mullidae	4	9	2.3 \pm 1.3
<i>Nemipterus sp1</i>	Nemipteridae	4	7	1.8 \pm 1.0
<i>Hemigymnus melapterus</i>	Labridae	4	4	1.0 \pm .0
<i>Coradion chrysozonus</i>	Chaetodontidae	4	5	1.3 \pm .5
<i>Choerodon venustus</i>	Labridae	4	4	1.0 \pm .0
<i>Carangoides uii</i>	Carangidae	3	7	2.3 \pm 1.5
<i>Choerodon vitta</i>	Labridae	3	7	2.3 \pm 2.3
<i>Symphoricichthys spilurus</i>	Lutjanidae	3	3	1.0 \pm .0
<i>Scolopsis bilineatus</i>	Nemipteridae	3	3	1.0 \pm .0
<i>Pygoplites diacanthus</i>	Pomacanthidae	3	3	1.0 \pm .0
<i>Pseudochromis paccagnellae</i>	Pseudochromidae	3	3	1.0 \pm .0
<i>Pomacanthus semicirculatus</i>	Pomacanthidae	3	3	1.0 \pm .0
<i>Diploprion bifasciatum</i>	Grammistidae	3	3	1.0 \pm .0
<i>Meiacanthus luteus</i>	Blenniidae	3	3	1.0 \pm .0
<i>Hemigymnus fasciatus*</i>	Labridae	3	3	1.0 \pm .0
<i>Diagramma pictum</i>	Haemulidae	3	6	2.0 \pm 1.0
<i>Cirrhilabrus sp*</i>	Labridae	3	11	3.7 \pm 4.6
<i>Carcharhinus amblyrhynchos</i>	Carcharhinidae	3	3	1.0 \pm .0
<i>Choerodon jordani*</i>	Labridae	3	4	1.3 \pm .6
<i>Alepes spp</i>	Carangidae	2	9	4.5 \pm 2.1
<i>Pentapodus nagasakiensis</i>	Nemipteridae	2	2	1.0 \pm .0
<i>Parupeneus multifasciatus</i>	Mullidae	2	2	1.0 \pm .0
<i>Lutjanus quinquelineatus</i>	Lutjanidae	2	4	2.0 \pm .0
<i>Lethrinus nebulosus</i>	Lethrinidae	2	2	1.0 \pm .0
<i>Lactoria sp*</i>	Ostraciidae	2	2	1.0 \pm .0
<i>Halichoeres prosopeion</i>	Labridae	2	2	1.0 \pm .0
<i>Epibulus insidiator</i>	Labridae	2	2	1.0 \pm .0
<i>Dasyatis kuhlii*</i>	Dasyatidae	2	2	1.0 \pm .0
<i>unknown</i>	unknown	2	2	1.0 \pm .0
<i>Siganus doliatus</i>	Siganidae	2	3	1.5 \pm .7
<i>Seriolina nigrofasciata</i>	Carangidae	2	3	1.5 \pm .7
<i>Pomacentrus nigromarginatus*</i>	Pomacentridae	2	3	1.5 \pm .7
<i>Pomacentrus brachialis</i>	Pomacentridae	2	7	3.5 \pm 2.1
<i>Carangoides orthogrammus</i>	Carangidae	2	12	6.0 \pm 7.1

Species	Family	P	$\Sigma(MaxN)$	Avg(MaxN)
<i>Carangoides ferdau</i>	Carangidae	2	25	12.5 ± 16.3
<i>Chrysiptera rollandi</i>	Pomacentridae	2	5	2.5 ± .7
<i>Ctenochaetus striatus</i>	Acanthuridae	2	2	1.0 ± .0
<i>Coris sp</i>	Labridae	2	9	4.5 ± 4.9
<i>Cephalopholis boenak</i>	Serranidae	2	3	1.5 ± .7
<i>Aprion virescens</i>	Lutjanidae	2	2	1.0 ± .0
<i>Aethaloperca rogaa</i>	Serranidae	1	1	1.0 ± .0
<i>Triaenodon obesus</i> *	Hemigaleidae	1	1	1.0 ± .0
<i>Thamnaconus modestoides</i>	Monacanthidae	1	2	2.0 ± .0
<i>Thalassoma lunare</i>	Labridae	1	1	1.0 ± .0
<i>Sufflamen frenatus</i>	Balistidae	1	1	1.0 ± .0
<i>Sufflamen chrysopterus</i>	Balistidae	1	1	1.0 ± .0
<i>Sphyaena obtusata</i> *	Sphyaenidae	1	4	4.0 ± .0
<i>Sepioteuthis lessoniana</i>	Loliginidae	1	2	2.0 ± .0
<i>Scomberomorus commersonianus</i>	Scombridae	1	1	1.0 ± .0
<i>Scarus ghobban</i>	Scaridae	1	1	1.0 ± .0
<i>Pseudobalistes flavimarginatus</i> *	Balistidae	1	1	1.0 ± .0
<i>Pomacanthus imperator</i> *	Pomacanthidae	1	1	1.0 ± .0
<i>Platax teira</i> *	Ephippidae	1	1	1.0 ± .0
<i>Pervagor janthinosoma</i> *	Monacanthidae	1	1	1.0 ± .0
<i>Pentapodus sp2 (Randall)</i>	Nemipteridae	1	1	1.0 ± .0
<i>Lutjanus malabaricus</i>	Lutjanidae	1	1	1.0 ± .0
<i>Lutjanus carponotatus</i>	Lutjanidae	1	1	1.0 ± .0
<i>Lethrinus olivaceus</i>	Lethrinidae	1	1	1.0 ± .0
<i>Lethrinus miniatus</i>	Lethrinidae	1	1	1.0 ± .0
<i>Lethrinus genivittatus</i> *	Lethrinidae	1	1	1.0 ± .0
<i>Lethrinus erythracanthus</i> *	Lethrinidae	1	1	1.0 ± .0
<i>Leptojulius sp</i>	Labridae	1	4	4.0 ± .0
<i>Lepidozygus tapeinosoma</i> *	Pomacentridae	1	3	3.0 ± .0
<i>Pastinachus sephen</i>	Dasyatidae	1	1	1.0 ± .0
<i>Parupeneus indicus</i>	Mullidae	1	1	1.0 ± .0
<i>Parapercis nebulosa</i>	Pinguipedidae	1	1	1.0 ± .0
<i>Paramonacanthus lowei</i>	Monacanthidae	1	1	1.0 ± .0
<i>Parachaetodon ocellatus</i> *	Chaetodontidae	1	1	1.0 ± .0
<i>Nemipterus sp (thin)</i>	Nemipteridae	1	2	2.0 ± .0
<i>Naso unicornis</i> *	Acanthuridae	1	1	1.0 ± .0
<i>Naso lituratus</i> *	Acanthuridae	1	1	1.0 ± .0
<i>Monotaxis grandoculis</i> *	Lethrinidae	1	1	1.0 ± .0
<i>Meiacanthus lineatus</i>	Blenniidae	1	1	1.0 ± .0
<i>Malacanthus latovittatus</i>	Malacanthidae	1	2	2.0 ± .0
<i>Lutjanus vitta</i>	Lutjanidae	1	2	2.0 ± .0
<i>Lutjanus monostigma</i>	Lutjanidae	1	1	1.0 ± .0
<i>Heniochus acuminatus</i>	Chaetodontidae	1	2	2.0 ± .0
<i>Gymnocranius grandoculis</i>	Lethrinidae	1	1	1.0 ± .0
<i>Grammatorcynus bicarinatus</i>	Scombridae	1	1	1.0 ± .0
<i>Gnathanodon speciosus</i>	Carangidae	1	4	4.0 ± .0
<i>Galeocerdo cuvieri</i>	Carcharhinidae	1	1	1.0 ± .0
<i>Epinephelus fasciatus</i> *	Serranidae	1	1	1.0 ± .0
<i>Echeneis naucrates</i>	Echeneidae	1	1	1.0 ± .0
<i>Coradion altivelis</i>	Chaetodontidae	1	1	1.0 ± .0
<i>Chrysiptera talboti</i> *	Pomacentridae	1	1	1.0 ± .0
<i>Chromis xanthochira</i> *	Pomacentridae	1	6	6.0 ± .0
<i>Chromis nitida</i> *	Pomacentridae	1	32	32.0 ± .0
<i>Chromis margaritifer</i> *	Pomacentridae	1	1	1.0 ± .0
<i>Chelmon rostratus</i>	Chaetodontidae	1	2	2.0 ± .0
<i>Chaetodon lineolatus</i>	Chaetodontidae	1	2	2.0 ± .0
<i>Cephalopholis argus</i> *	Serranidae	1	1	1.0 ± .0
<i>Centropyge bicolor</i> *	Pomacanthidae	1	1	1.0 ± .0
<i>Carangoides gymnostethus</i>	Carangidae	1	3	3.0 ± .0
<i>Canthigaster valentini</i>	Tetraodontidae	1	2	2.0 ± .0
<i>Carangoides chrysophrys</i>	Carangidae	1	1	1.0 ± .0
<i>Cantherhines dumerilii</i> *	Monacanthidae	1	1	1.0 ± .0
<i>Bodianus loxozonus</i> *	Labridae	1	1	1.0 ± .0
<i>Aluterus scriptus</i> *	Monacanthidae	1	1	1.0 ± .0
<i>Anthias sp*</i>	Serranidae	1	1	1.0 ± .0

9 Acoustic techniques for surveying tropical demersal finfish resources in inter-reefal areas.

To assess fishery-independent and “environmentally-friendly” techniques for surveying tropical finfish resource abundance in inter-reefal areas, including, remote video and quantitative acoustics.

Contents

9	Acoustic techniques for surveying tropical demersal finfish resources in inter-reefal areas.	9-224
9.1	Introduction	9-226
9.2	Desktop Approach	9-227
9.2.1	Characteristics of Tropical Demersal Fish Assemblages.....	9-227
9.2.2	Acoustic Techniques for Fish Stock Surveys	9-228
9.2.3	Issues in Acoustic Stock Surveys for Tropical Demersal Fish	9-230
9.3	Field Survey Approach.....	9-231
9.3.1	Methods	9-232
9.3.1.1	Video Ground Truth Data Analysis and Finfish Identification.....	9-233
9.3.1.2	Acoustic Data Analysis.....	9-235
9.3.1.3	Correlation Analysis - Acoustic and Finfish/Video	9-242
9.3.2	Results	9-244
9.3.2.1	Video Ground Truth Data Analysis and Finfish Identification.....	9-245
9.3.2.2	Acoustic Data Analysis.....	9-250
9.3.2.3	Correlation Analysis - Acoustic and Finfish/Video	9-255
9.4	Discussion.....	9-265
9.5	Appendices	9-226

Tables

Table 9-1:	List of the commercially important species of fish found in northern Australia, including the Great Barrier Reef. These fish were observed at sites across the shelf off Townsville in approximately decreasing order of importance (value). Shaded species are present in video ground truth observations for this project (dark shading to species, lighter shading to family level only).....	9-246
Table 9-2:	Finfish sighting events and summary statistics (number of sighting events, number of sites with event, total number of finfish, mean and standard deviation of fish per event, percentage of event class, and percentage of total) by class of fish (commercial and non commercial), fish identification (family and species) if known, recorded from video transects.....	9-247
Table 9-3:	SA (mean area backscatter coefficient) index summary statistics (number of acoustic integration cells per site, total SA (acoustic backscatter) over site, mean and standard deviation SA), for each video and acoustic transect site.	9-254
Table 9-4:	Table of Correlation Coefficient (Regression R^2 and Statistical Significance p) between Total SA (mean area backscatter coefficient) and Fish Observed, for various analysis and filtering schema.	9-257
Table 9-5:	Stratified video fish count analysis results – total video fish count (all fish – commercial and non-commercial) and 90% confidence interval	9-262
Table 9-6:	Stratified acoustic analysis results using mean area backscatter coefficient (SA - m^2/nm^2) for each of the ground-truth 500m transect sample. Table shows total SA and 90% confidence interval	9-262
Table 9-7:	Stratified acoustic analysis results using mean area backscatter coefficient (SA - m^2/nm^2) for acoustic data collected over the entire sample area from equivalent 500m segments. Table shows total SA and 90% confidence interval	9-262
Appendix 9.5-1:	Number of finfish sighting events, type of fish, fish identification (family and species) and total number of fish, from video transects, by site.....	9-269

Figures

- Figure 9–1: Echogram showing the complexity of tropical inter-reefal finfish assemblage structure, including mixtures of both commercial (or target) species as well as non-commercial species. The assemblage ranges from solitary fish to aggregations. The habitat range is from benthic, benthopelagic to pelagic.9-231
- Figure 9–2: Screen Capture of ECHO acoustics analysis software showing Simrad EY500 echogram data with fish marks (Site L115: Trout, Snapper and Non-commercial species). The screen capture also shows other significant components of the acoustic echogram signal including seabed signal, background and other noise and plankton signals, as well as cross-reference navigation data.9-236
- Figure 9–3: Poor Simrad EY500 bottom detection, results in erroneous echogram data. This data was edited out of the echogram worksheet, where possible.9-236
- Figure 9–4: Hi-res bottom locked echogram showing good benthic fish marks close to the seabed (red line shows the beginning of the integration layer).9-237
- Figure 9–5: School of benthic non-commercial fish, Note the close association with the seabed – it is difficult to distinguish where the school finishes and where the bottom starts. Also; note where the acoustic dead zone has an effect on ability to distinguish fish from seabed, especially on slopes.9-238
- Figure 9–6: Bottom locked echogram shows the effect of poor bottom picks in defining the benthic echo integration layer.9-239
- Figure 9–7: ECHO acoustics analysis software showing echogram data. This figure highlights the analysis layer used to calculate the acoustic estimate of tropical finfish. This benthic integration analysis layer (outlined in red) extends from 0.5m above the detected seabed (light blue) to 10m into water column. The along track analysis sections are also shown as the grid.9-240
- Figure 9–8: Effect of integrating plankton signals in the echogram, where resulting backscatter coefficients are skewed by this planktonic noise signal. This signal may be significant across the entire transect.9-241
- Figure 9–9: Pelagic marks while not included in the integration layer for analysis, never the less affect the acoustic signal which is analysed.9-241
- Figure 9–10: Scott Reef South sample area showing sample sites and habitat strata.9-243
- Figure 9–11: Estimated Total Number and Class of Fish Observed during Video Transects.9-246
- Figure 9–12: Relationship between the total number of fish (commercial and non-commercial) and the total number of commercial fish sighted on a video transect.9-248
- Figure 9–13: Occurrences of Fish Count ‘Levels’ Estimated from Video.9-249
- Figure 9–14: Clear fish events in the echogram data, however, no finfish were tagged in the video database.9-250
- Figure 9–15: Site M113 showing two significant schools of non-commercial fish.9-251
- Figure 9–16: Good fish marks close to bottom (bottom locked). Individual fish marks are circled.9-252
- Figure 9–17: Whole transect of hi-res bottom referenced echograms, show the errors introduced by poor bottom picks at the start of the transect. Values are as large as (or in some cases larger) those produced by valid fish marks later in the transect.9-252
- Figure 9–18: Boxplot of Mean Area Acoustic Backscattering Coefficients (SA) showing range, mean, one standard deviation and outliers for each Acoustic and Video Ground-truth transect site.9-253
- Figure 9–19: Mean area backscattering coefficient histogram for echo integration cells over the whole study area.9-255
- Figure 9–20: Echogram of entire transect for site F114, shows the two significant schools of non-commercial fish (a school of unidentified fish estimated to be ~100, a school of approximately 50 *Caesio*) and a solitary Coral Trout (*Serranidae plectropomus* sp.) identified from the video.9-256
- Figure 9–21: Backscatter coefficient vs fish abundance for both commercial fish and non-commercial fish.9-258
- Figure 9–22: Filtered backscatter coefficient vs fish abundance estimate for both commercial fish non-commercial fish.9-258
- Figure 9–23: Backscatter Coefficient vs Fish Abundance Estimate for Commercial Fish only and for Non-Commercial Fish only.9-259
- Figure 9–24: Scott Reef South sample area showing acoustic sampling results overlaying the habitat strata (refer to Figure 9–10) used in the analysis. The mean area backscatter coefficient (SA - m^2/nm^2) is shown for each of the ground-truth 500m transect sample sites (large square symbols). SA values are shown for acoustic data collected over the entire sample area (small round symbols) from equivalent 500m segments. The SA (m^2/nm^2) scale ranges from low (yellow) to medium (green) to high (blue).9-261
- Figure 9–25: Stratified acoustic and video fish count estimates by habitat strata.9-264
- Figure 9–26: Stratified acoustic estimates by habitat strata. Compares acoustic estimates from ground-truth sample sites with data collected over the entire area.9-264
- Figure 9–27: Total area SA estimates (including 90% confidence interval) for each sampling technique; video fish counts, acoustic estimates derived from 500m transects at sample sites and acoustic estimates derived from 500m segments over entire survey area (converted to fish counts using regression relationship)...9-265

9.1 Introduction

Through this project we have attempted to assess three fishery-independent and "environmentally-friendly" techniques for surveying tropical finfish resource abundance in inter-reefal areas. The techniques we have assessed included fish-traps, remote (baited) video stations (Chapter 8). In this chapter we outline our assessment of the quantitative acoustic technique.

The principle of quantitative acoustic techniques for fisheries resource abundance is relatively simple. The acoustic technique uses an echosounder as a means of sampling fish resources. The echosounder transmits a pulse of sound, which is reflected by water column targets such as fish. The amount of acoustic signal reflected by each fish depends on the species of fish and the size of fish. The reflected acoustic signal is received by the echosounder and allows the user to detect, locate and count fish.

In practice, there are a number of factors that may affect the results of acoustic sampling of fish resources. For example fish may be hard to detect when they occur close to the seabed or in areas of high relief such as reefs. The problem we address in this chapter is whether acoustic sampling of tropical demersal fish resources is feasible and practical.

There are two complementary approaches to addressing the objective of assessing quantitative acoustics as a fishery-independent and "environmentally-friendly" technique for surveying tropical finfish resource abundance in inter-reefal areas.

1. Combine the understanding of the physics of quantitative underwater acoustics with the understanding of the characteristics of tropical demersal fish assemblages. This "desktop" approach was carried out through a survey of literature relating to the subject.
2. Examine the first approach by comparing observations by two technologies (acoustics and another ground-truth sampling device e.g. video) deployed simultaneously over the same seabed under conditions like that which actual acoustic surveys may be carried out. This "field survey" approach was carried out through direct observation of the technique and through analysis of the results.

Conclusions made from the “desktop” approach were then used to inform the interpretation of the subsequent “field survey” approach. An assessment of quantitative acoustics was then made integrating the information gained from both approaches.

9.2 Desktop approach

We surveyed literature relating to the habitats of tropical demersal fish of importance to reef-line, charter and recreational fishers in northern Australia, including the Great Barrier Reef. The goal was to gain an understanding of general characteristics of these fish and fish assemblages that would be relevant to the application of acoustic approaches in assessing their abundance.

We also surveyed literature relating to general underwater acoustic techniques for assessing fish stocks. The goal was to gain an understanding of what aspects of the physics of this sampling technique would be relevant to its application to those tropical demersal fish species.

9.2.1 Characteristics of tropical demersal fish assemblages

Tropical demersal fish of relevance to this study are in the families *Lutjanidae* (sea perches / snappers), *Lethrinidae* (sweetlip / emperors) and *Serranidae* (coral trout, *Plectropomus* sp. and cod, *Epinephelus* sp.).

These families of fish generally are known to be closely associated with coral reef seabed habitats or are often found in their vicinity. Kailola *et al.* (1993, pp 256) states that “*coral trout (Plectropomus sp.) generally inhabit shallow water to 100m, often in association with coral reefs*”. Randall *et al.* (1990, pp 176) found “*most snappers (Lutjanidae sp.) dwell in shallow to intermediate depths (to 100m) in the vicinity of reefs*”. Randall *et al.* (1990, pp 196) also found for emperors (*Lethrinidae* sp.) that “*most species occur on the sandy fringe of reefs where they actively forage on sand dwelling invertebrates*”. Kailola *et al.* (1993, pp 307) states “*emperors (Lethrinidae sp.) inhabit continental shelf waters including coral reef and lagoon areas over substrates of hard coral, gravel, sand or rubble*”, or as Sainsbury (1987) found, are associated with sponge and gorgonian-dominated megabenthos habitats,

which are the particular subject of this project. These findings are also confirmed in recent work by Kulbicki *et al.* (2000) “*Many species in particular Lethrinidae, Lutjanidae and [Carangidae] are found both on reefs and in adjacent biotopes*”.

These families of fish occur in sparse or patchy abundance (Connell *et al.* 1998). Particularly the *Serranidae* family, which includes the coral trout (*Plectropomus* sp.) which may be considered a solitary fish (Kulbicki *et al.* 2000) unless forming spawning aggregations. The association of these fish to reef or megabenthos habitat structures may be attributed to shelter and feeding requirements. These habitat associations are not limited to these species of interest alone. Other fishes also share the same habitat. As such, when found these fish often may be seen in diverse multi-species assemblages.

Thus we may conclude that tropical demersal fish such as snappers (*Lutjanidae* sp.), emperors (*Lethrinidae* sp.) and coral trout (*Plectropomus* sp.) inhabit areas near the seabed, of complex, high relief or rugged topography; particularly habitats such as coral reefs or megabenthos patches. These fish most often occur in sparse abundance, (particularly coral trout) or form patchy aggregations or assemblages that often consist of multiple species.

9.2.2 Acoustic techniques for fish stock surveys

Over the last thirty years acoustic techniques for assessing the distribution and abundance of fish have become a useful adjunct to conventional fisheries sampling using trawls (MacLennan and Holliday, 1996; Misund, 1997; Thomas and Kirsch, 2000). Quantitative acoustic techniques began with the advent of echo integration. Echo integration sums the reflected echo signals (in this case, from fish) over intervals of depth and distance travelled. The technique of echo integration depends on the fundamental assumption (based on a random phase approximation) that acoustic scattering by fish is a linear process (MacLennan and Holliday, 1996). The assumption of linearity has been shown experimentally (Foote, 1983). The principle is that the total scattering strength of a fish school equals the summation of the scattering from each individual fish as though no other fish are present (Alvarez and Ye, 1999). The echosounder may also be calibrated using targets (usually metal spheres) of known acoustic backscattering strength. The principle of acoustic stock surveying is then,

that if the backscattering strength of a particular fish is known, the calibrated and integrated echos may be converted to units of density for that fish (Misund, 1997).

While the principle of acoustic measurement of fish abundances may be simple; there are a number of influences which may affect the interpretation of results when the technique is applied in practice. For example, the target strength of a fish depends on a number of factors including the species of fish, the size of the fish (especially the swim-bladder, which may account for up to 90% of the reflecting strength), the orientation of the fish and the distribution through the water column (Misund, 1997, Alvarez and Ye, 1999). The acoustic reflecting properties of fish are also influenced by the frequency of sound used by the echosounder. These factors must be taken into account when analyzing and interpreting acoustic survey data.

There is also a well known phenomenon known as the dead-zone where fish near the seabed (particularly over rough or sloping ground) may not be able to be detected acoustically (Mitson, 1982). The dead zone is *“the closest point to the bottom at which detection of fish is possible”* (Johannesson and Mitson, 1983). As Johannesson and Mitson (1983) explain, *“the distance of this point above the bottom is half the length of the transmitted pulse. When the distance between the fish and the bottom is equal to half the pulse length, it’s evident that, as the rear of the pulse leaves the fish, but is still moving towards the bottom, its echo starts moving towards the transducer. However the leading edge of the pulse (or wavefront) has already been to the bottom and its echo has travelled by half the pulse length, also, back towards the transducer. Therefore, at the instant we are considering, the front edge of the bottom echo is level with the rear edge of the transmitted pulse at the position the rear edge of the fish echo has just left. If the fish is any closer to the bottom than half the pulse length, the rear edge of the pulse would not have left the fish before the wavefront of the bottom echo arrived back at the fish position. The fish and the bottom echos would therefore be merged.”*

Historically, acoustic techniques have developed and been most successfully applied in temperate and pelagic or benthic-pelagic fisheries where species specific aggregations (or at least aggregations that are not very complex in species composition) are more common (Vilhjalmsson *et al.* 1982; Thorne, 1982; Koslow, 1994). Wilkins (1986) found *“the difficulty of identifying the species composition of observed schools are matters of special concern”*. Thus, for applications where a range of fish species are found in close association

with the target species, care must be taken when analyzing and interpreting the data from acoustic surveys in order to isolate scattering due to the species of interest from that of other fish species.

9.2.3 Issues in acoustic stock surveys for tropical demersal fish

Acoustic techniques are a well established method for estimating the abundance of fish (Johannesson and Mitson, 1983). The acoustic method has particular limitations when dealing with issues such as fish near the seabed, or fish over rough or sloping seabeds (Mitson, 1982; Aglen *et al.* 1999). The difficulty in these cases is due to the acoustics deadzone, where the fish is unable to be distinguished from the seabed. The level of the deadzone where fish are unable to be detected using acoustics is increased when over sloping seabeds.

The results from acoustic techniques are also confounded when the assemblages of fish are not uniform in distribution through the water column, in density through the assemblage, or in species (Alvarez and Ye, 1999). For schools of fish the total scattering strength is approximated by the sum of the scattering from each individual fish. This approximation assumes that the phase component of acoustic scattering by the fish within the school is random. While the random phase assumption has been shown to be valid (Foote, 1983), it may break down for lower frequencies and for schools with tight and regular fish spacings (Alvarez and Ye, 1999). That is, at low frequencies, the scattering by a dense school of fish can be very different from the scattering by a single fish (Alvarez and Ye, 1999). Alvarez and Ye (1999) derive a relationship for the validity of the random phase approximation relating to the frequency and inter-fish spacing. At 120 kHz, fish schools would require inter-fish distances of less than 1.5 cm for the random phase approximation to break down (Alvarez and Ye, 1999).

For multi-species assemblages the total scattering strength is then given by the total scattering from the target species as well as that from any other fish present within the assemblage. For single frequencies of interrogation, this means that acoustics has difficulty in isolating the acoustic scattering information from target species from non-target species. However as different species will have different scattering characteristics at different frequencies, multi-

frequency acoustic instruments may be able to discriminate between fish species within multi-species assemblages (Kloser *et al.* 1998).

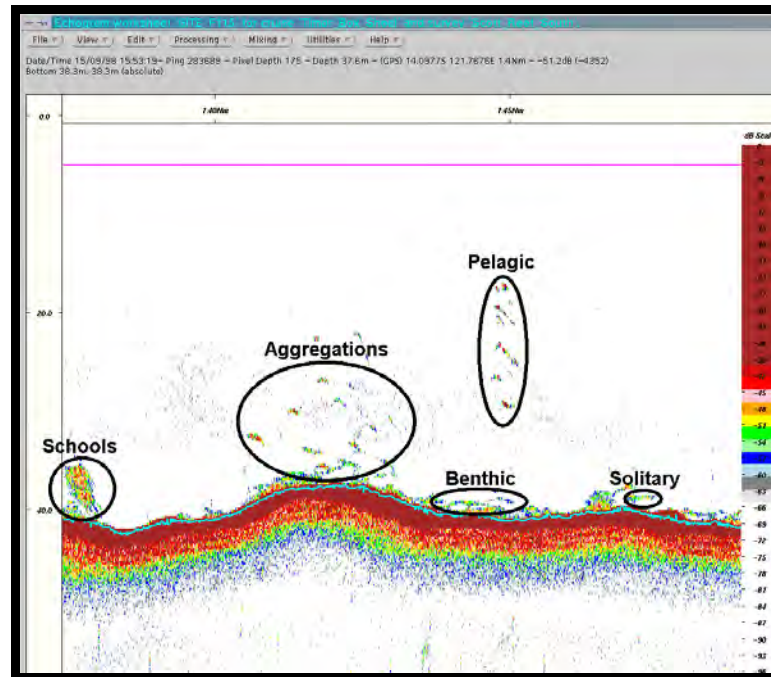


Figure 9–1: Echogram showing the complex nature of tropical inter-reefal finfish assemblage structure. This includes mixtures of both commercial (or target) species as well as non-commercial species. The assemblage ranges from solitary fish to aggregations. The habitat range is from benthic, bentho-pelagic to pelagic.

The habits of tropical demersal fish, in particular, species such as snappers (*Lutjanidae* sp.), emperors (*Lethrinidae* sp.) and coral trout (*Plectropomus* sp.), have several characteristics (as outlined in section 9.2.1) that cause issues of the type discussed above for the application of acoustic techniques in the assessment of their abundance. They may inhabit areas of rough or high relief seabed, they may occur close to the seabed, they may occur in low abundance or as solitary fish, and even when associated with larger groupings they are usually complex multi-species assemblages (Figure 9–1). In these situations, the resulting acoustic signal is complex, particularly as the target strengths of different species and sizes of fish vary in multi-species assemblages.

9.3 Field survey approach

We examined the issues raised by the desktop approach, by comparing observations by two technologies (acoustics and a ground-truth sampling device ie. video) deployed simultaneously over the same seabed under conditions like those under which actual acoustic

surveys may be carried out. This “field survey” approach was carried out through direct observation of the technique and through analysis of the results.

9.3.1 Methods

We investigated the feasibility of acoustics as a method for surveying tropical finfish resource abundance in inter-reefal areas under operational conditions. This field survey approach required two streams of measurement. They were:

1. High quality quantitative acoustic echosounder data (and the software to analyse this data).
2. Ground-truth information on the finfish species and abundance, present in the echosounder’s beam during the recording of the acoustic data.

We collected useful acoustic information during the first “megabenthos dynamics” field survey on the Great Barrier Reef in October 1997 (Chapter 5). The digital “Benthic Acoustic System” instrument developed during the FRDC Project 93/058 (Pitcher *et al.* 1999) was used to collect this acoustic data. Subsequently, CSIRO Marine Research purchased a portable digital echosounder (Simrad EY500), which is a calibrated instrument that provide high quality digital acoustic data and analysis software is available that specifically enables data processing for fish stock abundance purposes. It was considered that this instrumentation would provide a better opportunity to examine acoustic techniques for tropical demersal fish stock abundance measurement.

The EY500 echosounder was deployed during a field program conducted in the Timor Sea northwest of Broome in September 1998 (Skewes *et al.* 1999). A similar suite of tropical demersal inter-reefal finfish species to those found in the GBR were present in this area. Hence, the Timor study provided an opportunity and good quality “ground-truth” information on finfish identification and abundance collected in a similar manner to acoustic surveys. With the EY500 echosounder data, the Timor study provided adequate scope and high quality data. We used this study to examine a field survey approach to the objectives of this project in assessing acoustic techniques for surveying tropical finfish resource abundance in inter-reefal areas.

The shoal areas (15-50 m deep) of the Timor Sea MOU74 Box area were surveyed to assess the status of the stocks of sedentary and finfish resources in the area, and the habitats that supported them. Of the shoal areas contained within the Timor Box, Scott Reef South lagoon had by far the highest density of commercial species of tropical demersal reef finfishes, identified as target species for this investigation. So this area was selected to assess the capability of quantitative underwater acoustics to indicate tropical demersal finfish abundance.

At the Scott Reef South shoal, a total of 42 ground-truth sites were sampled, across a range of different reef and inter-reefal habitats, including sand, rubble, reef and high-density epibenthic gardens. At each site, we surveyed a 500 m long transect of seabed with a towed video camera to record demersal finfish abundance and species identification information as well as collecting quantitative Simrad EY500 acoustic and depth data simultaneously. Position was logged on both the video and acoustic track by differential GPS (accurate to <5 m), cross-referenced between instruments via a time-stamp and recorded in a data base.

The echosounder transducer, from which acoustic signatures were recorded, was mounted on the vessel ahead of the towed video camera system, which was deployed from the stern of the vessel. The towed drop-camera was designed to minimise the along track distance between the vessel (and corresponding vessel mounted sensor such as the echosounder transducer) and the camera system near the seabed. However the logistics of this deployment was also constrained such that towed drop-camera platform is not within the acoustic footprint of the echosounder.

9.3.1.1 Video ground truth data analysis and finfish identification

Finfish ground truth data was collected using remote video, following protocols developed previously for surveys on the Great Barrier Reef and in Torres Strait (Pitcher *et al.* 1999; Long *et al.* 1997; Skewes *et al.* 1996). The video system used was a towed drop-camera, deployed from the stern of the vessel and towed at a height of approximately one-half metre above the seabed. The towed drop-camera used a colour CCD camera mounted in a water proof housing and video images were transmitted to the vessel in real-time along an umbilical cable, into two computer-controlled SVHS video recorders and then to high-resolution video monitors.

During drop-camera deployment an operator constantly viewed the video in real time and entered data on finfish type-class (commercial or non-commercial) whenever finfish sighting events occurred. This data was tagged with a unique event identifier and recorded to a data base every 1-2 seconds along with position and time information to indicate areas where finfish were present. Also in real-time, during each transect, another observer recorded fish type-class (commercial or non-commercial), and further classifications to family or species if possible, as well as approximate abundance for each finfish sighting event. The information recorded by both observers was cross-referenced using the unique event identifiers entered into the database.

Though the data recorded by observers was entered in real time during the survey, video playback later was used to minimise uncertainties in fish identification and abundance estimates. The video playback was undertaken in the laboratory after the survey and investigated each fish sighting event to attempt identification of those fish for which identification was not possible or ambiguous in the field and to confirm the identification of those entered during the survey. We then combined the independent field and laboratory video analysis information wherever possible. This provided a georeferenced ground truth set of information on the fish type (or species) and abundance along the acoustic survey transects.

Abundance estimates made from fish events in the video provided useful quantitative information; the particular type of fish-class (commercial or non-commercial) was also important qualitative information. This qualitative and quantitative information gained from the video ground-truth transects was corrected and examined in a number of ways which are outlined in the following paragraphs. When compared with acoustic information, this qualitative and quantitative ground-truth information allowed us to assess particular aspects of the acoustic technique.

Fish abundance estimates were made at each sighting event in the video, where possible. Solitary fish occurring in the view of the video camera were straightforward. Fish abundance estimates were difficult where the number of fish sighted was large, even when examined during video playback. This difficulty in estimating events with larger fish abundances decreased the reliability by either overestimating or underestimating the abundance.

We examined the fish events in the video in order to compare video estimates with the ability of acoustics to estimate a particular class of fish abundances (e.g. commercial fish). In particular we created sets of ground-truth information that restricted finfish events to include only those from the fish class of interest (e.g. commercial finfish). Fish abundance estimates were calculated for three classes: all finfish, just commercial fish, and just non-commercial fish. The finfish event abundance estimates were then summed to give a total abundance estimate for each of the classifications (all fish, commercial, or non-commercial and included family and species where known) over the 500m transect at each site.

9.3.1.2 Acoustic data analysis

In order to evaluate the effectiveness of acoustics as a potential index of tropical benthic finfish abundance and distribution, particularly for commercial species, quantitative acoustic echogram signals from the water column at close proximity to the seabed were collected. This acoustic echogram data was recorded over the entire study area of Scott Reef South using the Simrad EY500 portable scientific echosounder. The EY500 transmitted a pulse of high frequency (120 kHz) sound that was reflected by water column and seabed targets including the target of interest “tropical commercial finfish”, non-commercial finfish (including solitary, aggregated and schooling distributions), plankton, epibenthic organisms such as coral and sponges, as well as the seabed itself. The reflected acoustic signal was converted to electrical signals by the echosounder transducer and stored digitally for later analysis. Time and position was logged from GPS for the entire acoustic transect track.

The CSIRO-developed software package ECHO (Waring *et al.* 1994; Kloser *et al.* 1998) was used to process the digitised acoustic echogram data (see Figure 9–2 and Figure 9–7). For each ground-truth site an “echogram worksheet” was created in the ECHO software to allow the registration and analysis of the acoustic data for each 500 m transect. Using the echogram worksheets, data quality assurance and post-processing was performed. These analysis stages included, editing the echograms for bad data (due to instrument malfunctions, or operator error), removing background noise (including sea state, man-made acoustic and electrical noise), and setting threshold values for the targets of interest (e.g. commercial finfish).

The data were restricted to exclude: data shallower than 5 m (due to sea-surface bubble layer effects); below bottom data (unnecessary for this analysis); and poor quality or unusable data.

The seabed layer was automatically defined from the built-in Simrad EY500 bottom detection algorithm and checked for quality. The seabed bottom pick is a key indicator of data quality, and poor quality seabed bottom pick data were edited out of the echogram, if possible (Figure 9–3).

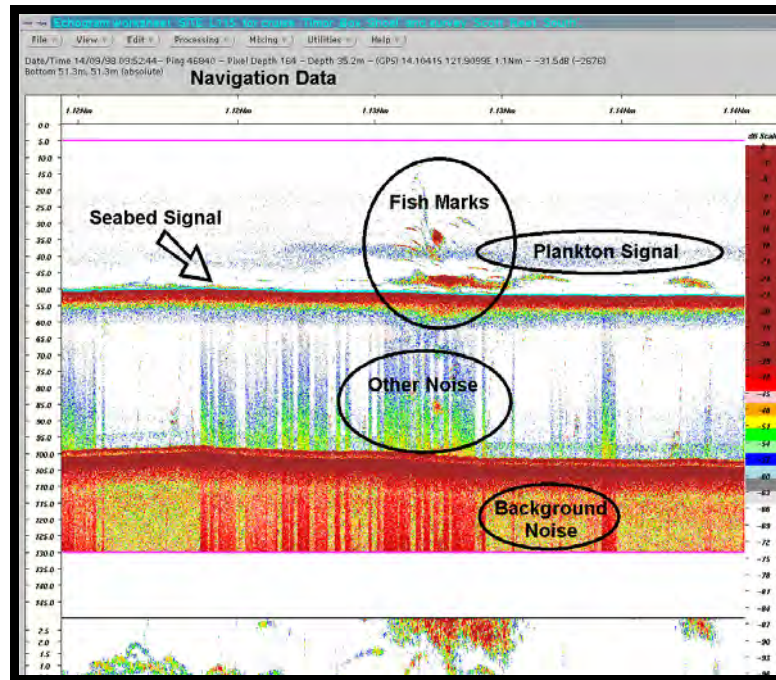


Figure 9–2: ECHO acoustics analysis software showing Simrad EY500 echogram data with fish marks and other significant components of the acoustic echogram signal.

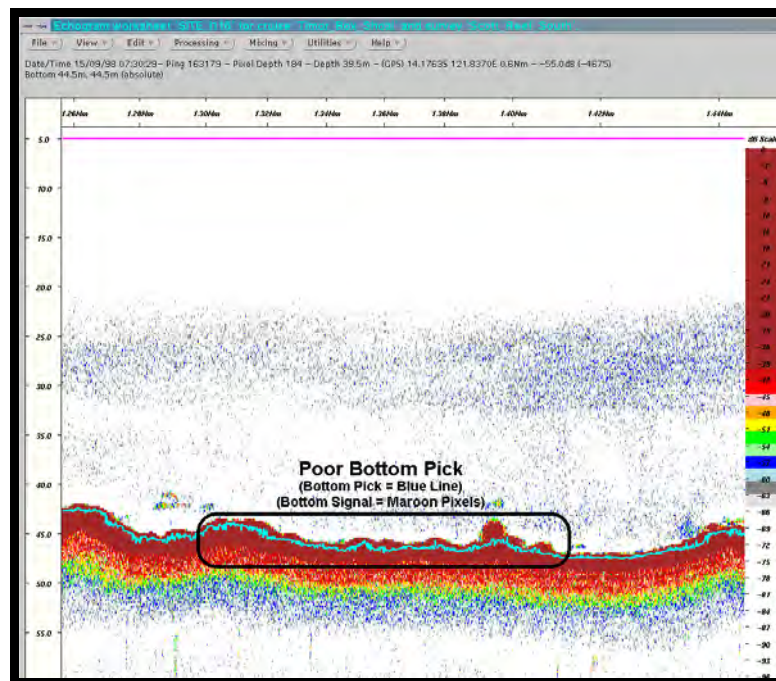


Figure 9–3: Poor Simrad EY500 bottom detection, results in erroneous echogram data. This data was edited out of the echogram worksheet, where possible.

For this project we were concerned with echogram targets occurring near (within 10 m of) the seabed. The reason for this restriction is that this is the nominal habitat range of those commercial finfish species associated with the seabed, which were the target of this study (Figure 9–4). Another restriction was the upper limit of visibility for groundtruth video available to identify finfish from the towed camera system, which was deployed within 2 m of, and tracked, the seabed.

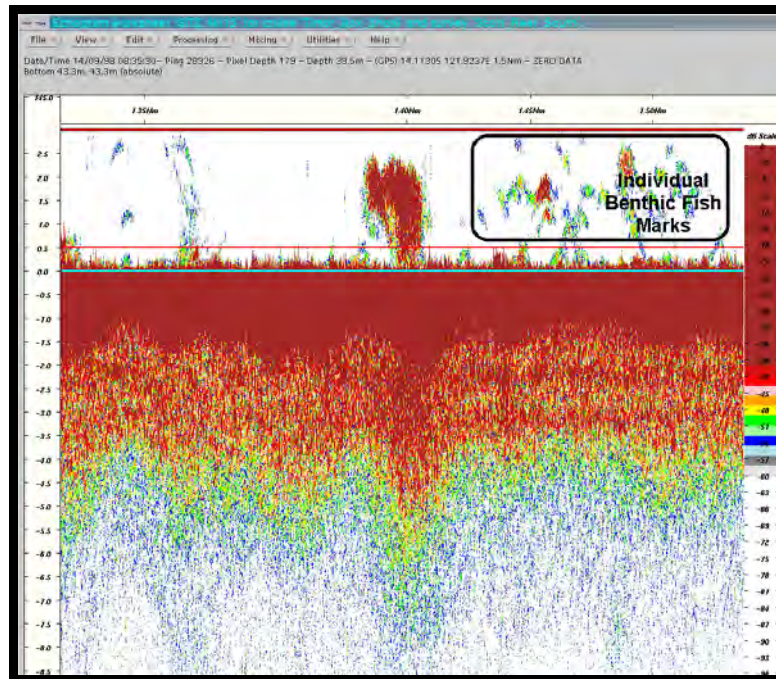


Figure 9–4: Hi-resolution bottom-locked echogram showing good benthic fish marks close to the seabed (red line shows the lower boundary of the integration layer).

The acoustic dead-zone is that area above the seabed in which a water column target is unable to be detected or discriminated from the seabed signal (see Figure 9–5). The ability of the acoustic system to detect the targets of interest is crucial (Lawson and Rose, 1999) in the application of an acoustic technique, in particular when considering targets associated with, or near the seabed, the acoustic dead zone must be taken into account. Over a sloping seabed “fish close to the seabed, but still in area where detection is possible, will be in regions of the beam containing lower transmitted energy and having lower receiving sensitivity than on axis” (Mitson, 1982). The formula for calculating the acoustic dead zone is given by (Johannesson and Mitson, 1983; Ona and Mitson, 1996):

where:

$$h = d(1 - \cos(\theta/2)) + \frac{c\tau}{2}$$

h = dead zone height in metres
 d = total depth of water from transducer to sea bottom (average 45 m)
 θ = full beam angle of transducer at half power points (9.8°)
 τ = pulse duration (0.1 ms)
 c = speed of sound (1533 m/s)

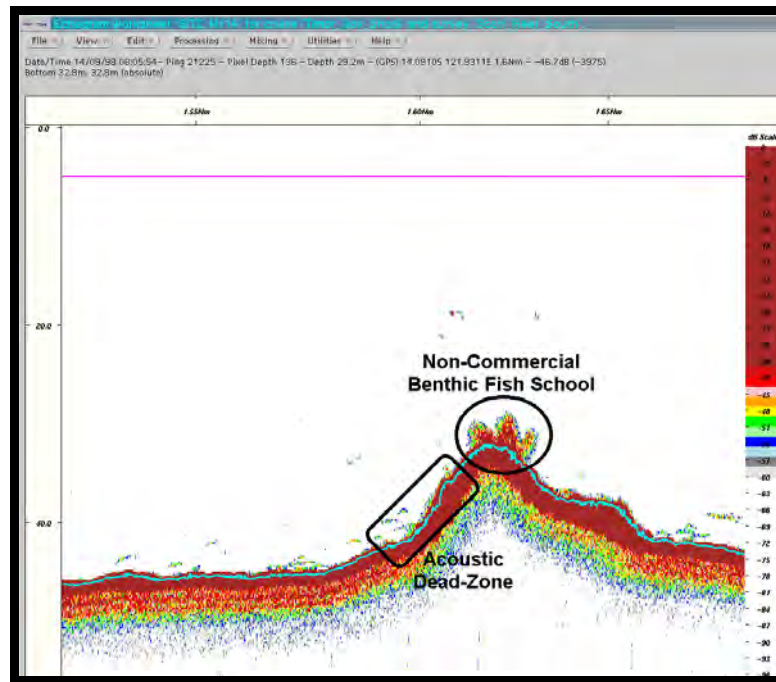


Figure 9–5: School of benthic non-commercial fish; note the close association with the seabed – it is difficult to distinguish where the school finishes and where the bottom starts. Also, note where the acoustic dead zone has an effect on ability to distinguish fish from seabed, especially on slopes.

For this study the average depth was approximately 45 m, resulting in an acoustic dead zone height of approximately 0.25 m. Given this acoustic dead zone, we also allowed a 100% margin for poor seabed bottom picks (see Figure 9–6), which would add error to echo integration. Thus, acoustic echogram data within 0.5 m of the seabed was considered unreliable and not used for this analysis. This excluded any poor quality data from the analysis; where these high-bottom signal values would confound the acoustic data. Using this method, referenced to the built-in Simrad EY500 seabed bottom pick, it was possible to set up the integration analysis layers automatically in the ECHO software. To have the defined layer closer to the seabed signal would require hundreds of hours of fine hand-editing of the echogram seabed layer. This hand editing the echogram seabed layer is not an algorithmic process and therefore would have produced results that were subjective and not easily repeatable.

Consequently given the limits due to target species habitat range, ground-truth limitations, ability to detect, acoustic dead zone and erroneous seabed bottom picks, as explained above, an analysis overlay was established that referred to the seabed from 0.5 m above bottom to 10 m into the water column from the seabed (Figure 9–7). The analysis overlay allowed the integration of finfish targets of interest (identified if possible from the video) over that seabed referenced layer, tracking the seabed regardless of depth variations. This layer was then

integrated over the echosounder ping (vertically on the echogram worksheet) and then along the ship track over intervals of 0.01 nautical mile (horizontally on the echogram worksheet) to give the area backscattering coefficient (SA). The area backscattering coefficient gives the acoustic energy reflected by targets from each echosounder ping and summed over the particular integration cell (in this case 9.5 m high by ~18.5 m along track). There were typically 27 integration cells per 500 m ground-truth transect.

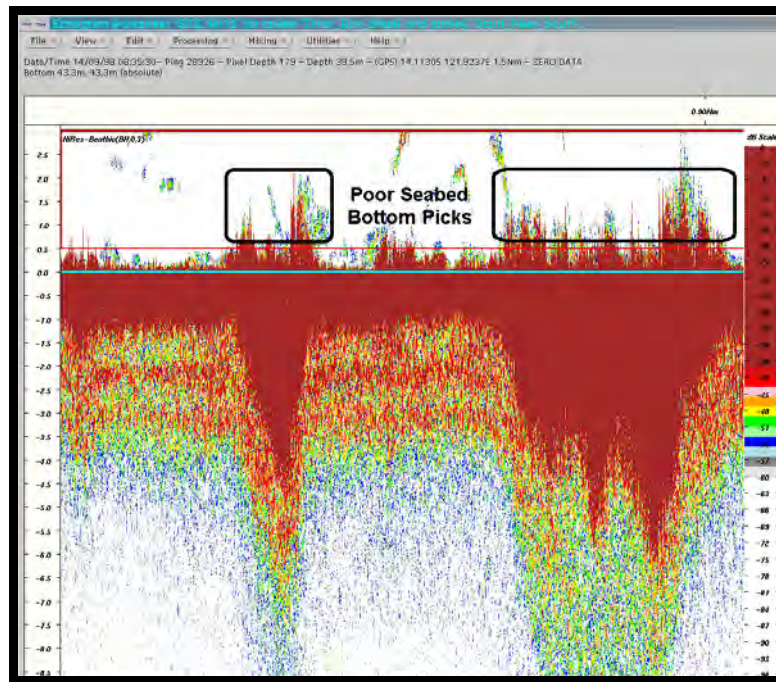


Figure 9–6: Bottom locked echogram shows the effect of poor bottom picks in defining the benthic echo integration layer.

The nature of acoustic echogram data integration analysis, which produced the area backscattering coefficient (SA), was such that integrating a ping essentially convolves together all of the acoustic energy reflected back to the transducer without discrimination of the reflectors nature. That is to say, within a ping (and consequently within a integration cell) it was difficult to discriminate the energy reflected by the individual reflectors (e.g. from the seabed, larger fish targets, small fish targets, pelagic or benthic fish targets, or from plankton reflectors, see Figure 9–8 and Figure 9–9) without significant hand editing of the echogram within ECHO, or without sophisticated analysis tools of a kind currently not available and knowledge of the characteristic target strengths for the species of interest.

For this analysis we had to consider all water column targets during echo integration, including plankton, pelagic and benthic finfish (see Figure 9–8 and Figure 9–9). Data

modifiers were set where practical to exclude as much as possible of the smaller target strength plankton signal from the analysis, by setting signal level thresholds. However it was impossible without extensive hand editing of the echograms or by having used sophisticated split-beam which allows in-situ target strength measurement or multi-frequency acoustic instrumentation (Kloser *et al.* 1998), to exclude plankton or small schooling bait fish signals from the analysis.

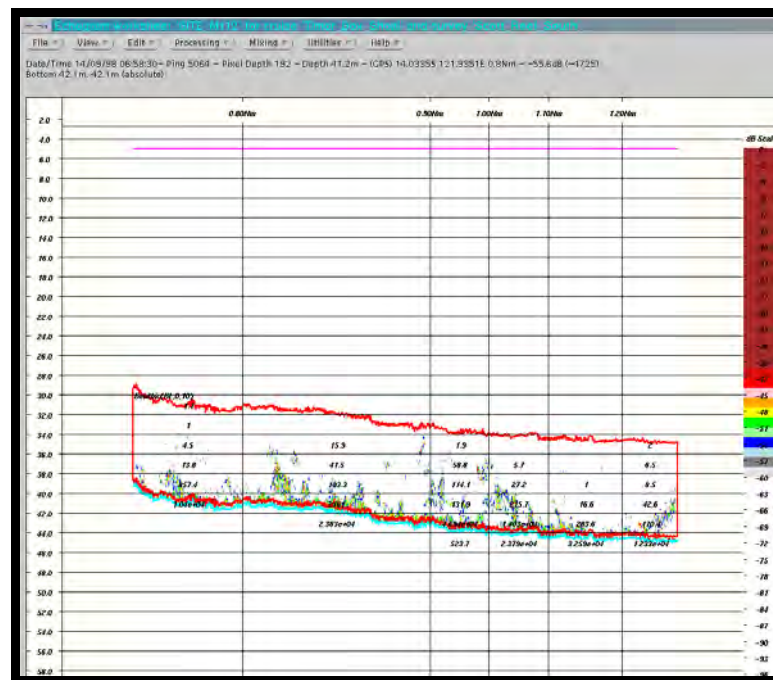


Figure 9–7: ECHO acoustics analysis software showing echogram data. This figure highlights the analysis layer used to calculate the acoustic estimate of tropical finfish. This benthic integration analysis layer (outlined in red) extends from 0.5 m above the detected seabed (light blue) to 10 m into water column. The along track analysis sections are also shown as the grid.

It is worth noting at this stage that we used absolute acoustic backscatter measures to test against fish abundance rather than converting this measure to fish biomass via target strength values. This approach is adequate to test the feasibility of the method and the extra resources required to measure actual target-strength–fish-size relationships of tropical demersal fish species was not warranted until the method is demonstrated to be practical.

The calculated area backscattering coefficient (SA) values for integration cells within a site were then filtered for outliers resulting from any remaining erroneous data which were not removed during earlier processing stages. This erroneous data was usually due to the integration layer including some seabed data due to poor bottom picks (e.g. SA values greater than $20000 \text{ m}^2/\text{nm}^2$). When the area backscattering coefficient (SA) for a cell was found to be

doubtful (i.e. above the 20000 m^2/nm^2 threshold), this cell's value was replaced by the mean integration cell SA for cells along that transect. Along each transect the backscattering coefficient (SA) values within each integration cell were added together (Nakken and Olsen, 1977) to give a total area backscattering coefficient value for the 500m transect at that site.

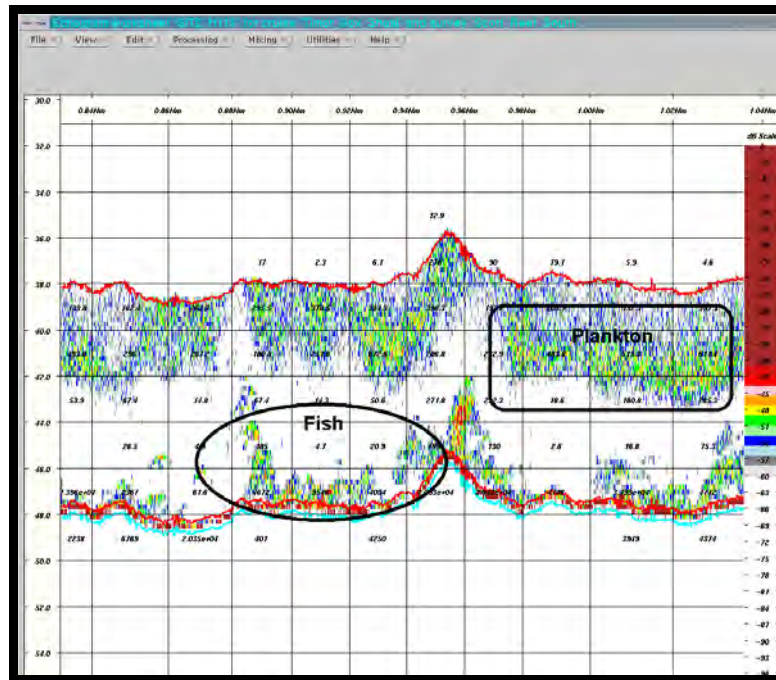


Figure 9–8: Backscatter from plankton within the integration layer — resulting backscatter coefficients were skewed by this planktonic noise signal. This signal may be significant across the entire transect.

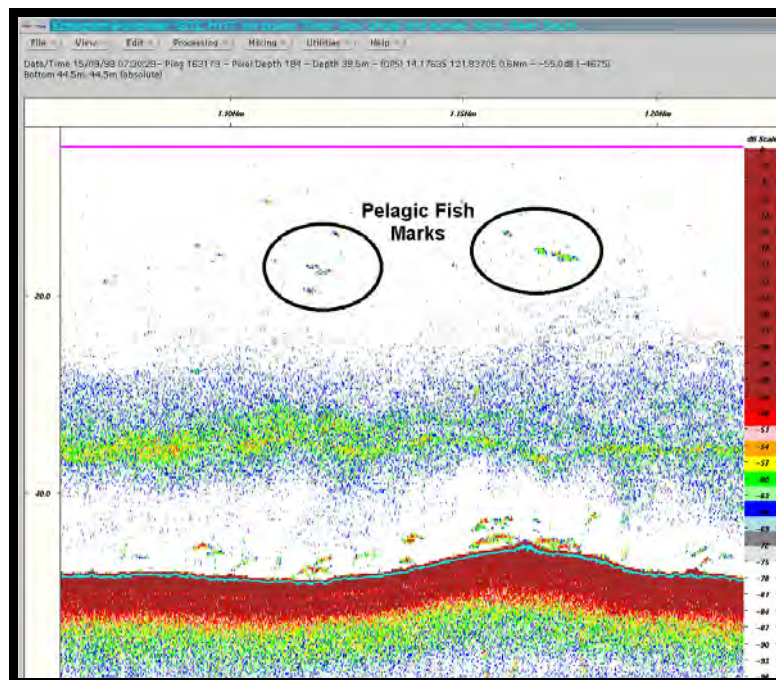


Figure 9–9: Pelagic marks not included in the integration layer for analysis, nevertheless affect the acoustic signal that was analysed.

9.3.1.3 Correlation analysis - acoustic and finfish/video

Qualitative correlation analysis

Even though the distance between the drop-camera's field of view and the vessel mounted echosounder's footprint was reduced to a minimum, there was still a significant distance between them. The resulting lag in time between the vessel and drop-camera passing over a point on the seabed depended on a number of variables, including vessel speed, currents and water depth, but was typically about 30 seconds. Therefore there was a lag between the acoustic echogram data and the ground-truth video information, such that finfish were sampled acoustically 30 seconds before the towed video camera sampled them to allow identification of fish type-class. This lag was taken into account when cross-referencing acoustic and video information. A number of examples of echogram signals where corresponding video analysis identified finfish of particular class type (commercial or non-commercial) were extracted to show these pictorially.

Quantitative correlation analysis

For underwater acoustics to be a potentially successful method in estimating tropical commercial finfish abundance the relationship between acoustically derived and actual abundance (identified from ground truth video) should be positively correlated. Thus the relationship between the total area backscattering coefficient (SA) and the total abundance of finfish for each site (also by finfish event type where possible), was investigated using correlation and linear regression analysis.

Linear regression analysis uses the method of least squares to fit a continuous linear function so as to minimize the sum of the squared residuals (S-plus Guide, Insightful Corp, 2001). The values for the fish abundance ground-truth predictor variable over a transect, were weighted in the regression. The weighting values for a transect were set such that larger fish abundance events, which were estimated with greater error (see section 9.3.1.1 above) were given less influence in the linear regression. As count data are often square-root transformed to normalise mean-variance ratios, the mean fish event abundance was used to weight each transect in the regression according to the formula:

$$w = \frac{1}{\sqrt{\bar{x}}}$$

where:

- w = transect regression weighting
- \bar{x} = mean fish event abundance within transect

The correlation between acoustic and video indicators of tropical finfish abundance were also investigated for various combinations site and acoustic filters (e.g. large SA values from poor seabed picks) outlined in section 9.3.1.2 above. For each filter, the correlation coefficient, regression R^2 and statistical significance (p) of the relationship were calculated.

9.3.1.4 Precision of absolute fish population estimates

In order to compare the precision of the video fish abundance estimates and the acoustic estimates, we stratified the transects by habitat over the Scott Reef sample area (Figure 9–10).

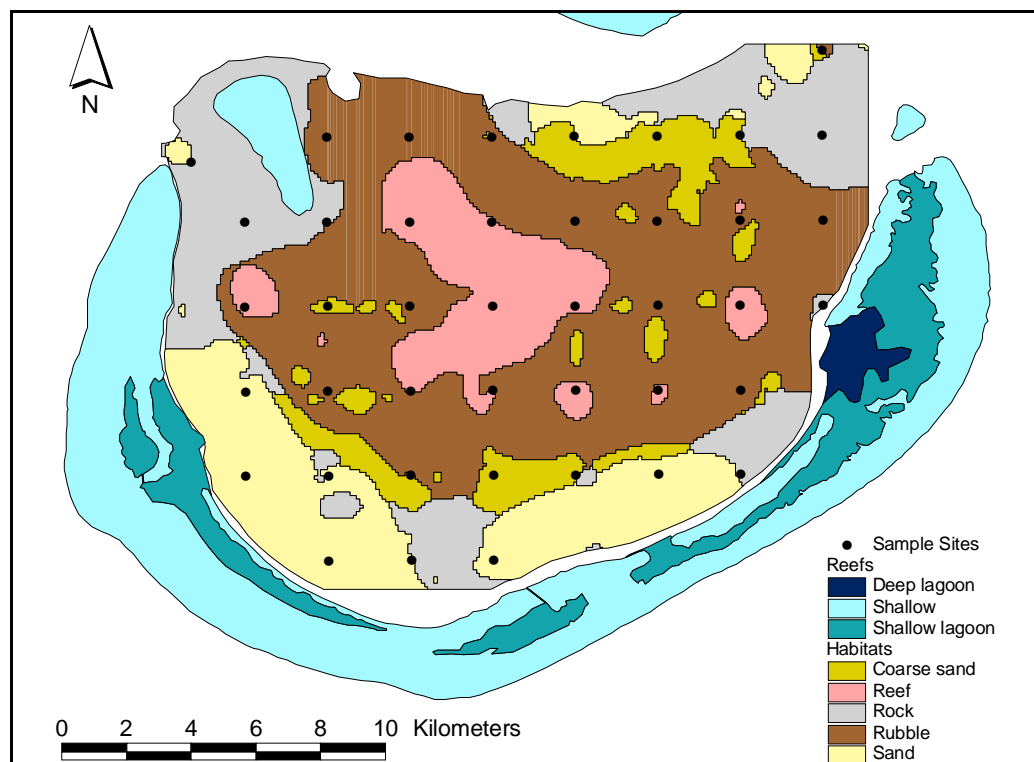


Figure 9–10: Scott Reef South sample area showing sample sites and habitat strata.

The stratified mean and variance estimates as well as 90% confidence limits were calculated for both the video and acoustic estimates of fish abundance over a transect. Using results from each sample transect we calculated a total estimated value over the entire sample area. As the acoustic system collected information wherever the vessel was transiting between ground-truth sites, there was a lot of extra information available. This information was available for locations other than the transects where video was collected as ground truth. Using this extra acoustic information we calculated a 90% confidence limit, in order to compare with other results.

With stratified sampling the total number of N transects over the sample area were divided into sub-samples of $N_1, N_2, N_3, \dots, N_L$ habitat strata units respectively. Given that each habitat stratum was homogenous in that the measurements varied little from one unit to another, a precise estimate of any stratum mean was obtained for that stratum. These estimates were then combined to give a precise estimate for the whole area. The notation of terms used for stratified sampling calculation and formulae used follow below:

N total number of sampling units (transects) over the study area;

N_h total number of sampling units (transects) in stratum h ;

n_h actual number of samples taken in stratum h ;

y_{hi} value obtained from i th unit in stratum h ;

$W_h = \frac{N_h}{N}$ stratum h weighting;

$f_h = \frac{n_h}{N_h}$ sampling fraction in stratum h ;

$\bar{y}_h = \frac{\sum_{i=1}^{n_h} y_{hi}}{n_h}$ stratum h mean;

$\bar{y}_{st} = \sum_{h=1}^L W_h \bar{y}_h$ stratified mean over all strata;

s_h^2 sample estimate of stratum h variance;

$v(\bar{y}_{st}) = \sum_{h=1}^L \left(\frac{W_h^2 s_h^2}{n_h} \right) - \sum_{h=1}^L \left(\frac{W_h s_h^2}{N} \right)$ estimated strata variance.

Using the stratified mean over all strata \bar{y}_{st} we were able to calculate a total estimator value over the entire sample area. The estimator includes a 95% confidence limit expressed as a percentage and calculated using the T-statistic and the estimated strata variance $v(\bar{y}_{st})$.

9.3.2 Results

In this section we present results and draw conclusions from the field survey approach to assessing underwater acoustics as a sampling method for assessing tropical demersal fish abundance. We compared observations by underwater acoustic and video ground-truth sampling technologies deployed simultaneously over the same seabed under typical survey conditions.

First, we present results from the video ground truth, identifying fish species and estimating abundances. Then, we present results from the simultaneous acoustic survey and subsequent data analysis. Finally, we draw together these results and compare the correlation between the two sampling techniques (acoustic and ground-truth) in order to assess the effectiveness of the acoustic technique.

9.3.2.1 Video ground truth data analysis and finfish identification

During the Timor shoals field survey we observed a similar fish suite of species to those of importance to reef-line, charter and recreational fishers (referred to as “commercial” species) elsewhere in northern Australia, including the Great Barrier Reef. We observed fish of the families *Lutjanidae* (sea perches / snappers), *Lethrinidae* (sweetlip / emperors) and *Serranidae* (coral trout, *Plectropomus* sp. and cod, *Epinephelus* sp.).

In Table 9-1, we outline those particular species and considered to be of “commercial” importance for the purposes of this study, and the target of our investigation. The table presents those species of fish in decreasing order of commercial importance with the Coral Trout (*Plectropomus leopardus*) considered the most important. In some cases we were able to identify the observed fish to species level, more often though we were only able to identify fish to genus or family level. Though in about one quarter of cases, however, we were only able to identify these fish as being of the category of “commercial (see Table 9-2).

Of those commercial fish that we observed and were able to identify to species level there were two members of the Family *Serranidae* - *Plectropomus leopardus* and *Epinephelus fuscoguttatus*, these are highlighted in Table 9-1 by dark grey shading. Of those commercial fish which we observed and were able to classify to a coarser taxonomic level we also highlighted in Table 9-1 by light grey shading. In these cases we were only able to identify the fish to Genus or Family level (e.g. we might have known the fish was of the genus *Epinephelus*, however were unable to tell which species).

Table 9-2 summarises fish sighting events with summary statistics by category or class of fish (“commercial” and “non commercial”), and fish identification (family and species) if known. We found that over 93% of the almost 1500 fish estimated were of the non-commercial category (see Table 9-2).

Table 9-1. List of the commercially important species of fish found in northern Australia, including the Great Barrier Reef. These fish were observed at sites across the shelf off Townsville in approximately decreasing order of importance (value). Shaded species are present in video ground truth observations for this project (dark shading to species, lighter shading to family level only).

Species
<i>Plectropomus leopardus</i>
<i>Lutjanus malabaricus</i>
<i>Lutjanus sebae</i>
<i>Lethrinus laticaudus</i>
<i>Choerodon schoenleinii</i>
<i>Epinephelus fasciatus</i>
<i>Epinephelus fuscoguttatus</i>
<i>Epinephelus quoyanus</i>
<i>Carangoides fulvoguttatus</i>
<i>Lethrinus</i> sp. B
<i>Lutjanus adetii</i>
<i>Lutjanus carponotatus</i>
<i>Lutjanus vittus</i>
<i>Digamma pictum</i>
<i>Lethrinus semicinctus</i>

The results for each video ground-truth sample site are listed in appendix 9.1. For all fish the mean fish abundance for a video-ground truth site was 35.2 with a standard deviation of 66.8. Figure 9–11 shows a graphical summary of fish abundances for both the commercial and non-commercial types of fish from video transects for each site. The figure highlights the high variability of fish abundance by site and confirms that most of the fish observed were non-commercial species.

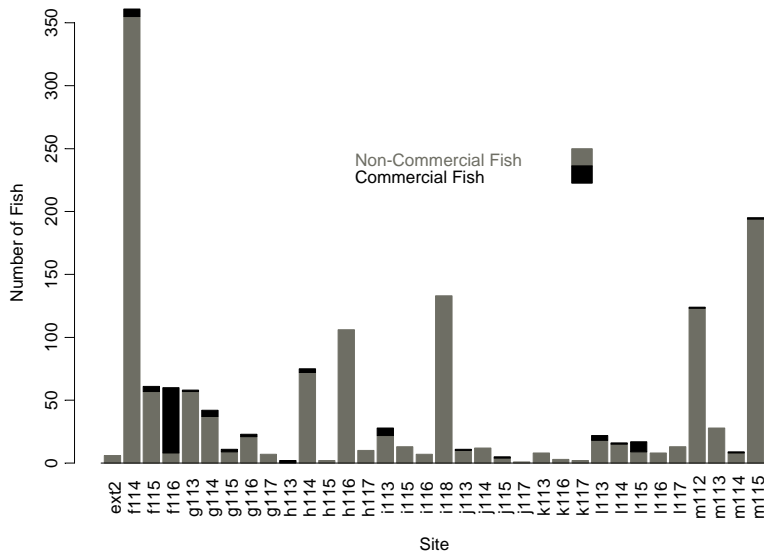


Figure 9–11: Estimated total number and class of fish observed during video transects.

Table 9-2. Finfish sighting events and summary statistics (number of sighting events, number of sites with event, total number of finfish, mean and standard deviation of fish per event, percentage of event class, and percentage of total) by class of fish (commercial and non commercial), fish identification (family and species) if known, recorded from video transects.

CLASS	FAMILY	SPECIES	# Events	# Sites	Σn	mean(n) \pm stdev(n)	% Class	% Total
Commercial	<i>Serranidae</i>	<i>Epinephelus fuscoguttatus</i>	1	1	1	1.0 \pm N.A.	1.0	0.07
Commercial	<i>Serranidae</i>	<i>Epinephelus polyphemadion</i>	2	1	2	1.0 \pm 0.0	2.0	0.14
Commercial	<i>Serranidae</i>	<i>Epinephelus</i> sp.	1	1	1	1.0 \pm N.A.	1.0	0.07
Commercial	<i>Serranidae</i>	<i>Plectropomus</i> sp.	18	10	18	1.0 \pm 0.0	17.8	1.2
Commercial	<i>Lutjanidae</i>	<i>Lutjanis gibbus?</i>	2	2	51	25.5 \pm 34.6	50.5	3.4
Commercial	<i>Lethrinidae</i>	<i>Lethrinus</i> sp.	1	1	1	1.0 \pm N.A.	1.0	0.07
Commercial	Unknown		19	13	27	1.4 \pm 1.2	26.7	1.8
TOTAL						2.3 \pm 7.4	100%	6.75%
Non Commercial	<i>Pomacentridae</i>	<i>Sexstriatus</i>	1	1	2	2.0 \pm N.A.	0.1	0.14
Non Commercial	<i>Caesio</i>	?	2	2	60	30.0 \pm 28.3	4.4	4.1
Non Commercial	<i>Acanthuridae</i>	?	1	1	20	20.0 \pm N.A.	1.5	1.4
Non Commercial	Unknown	?	341	33	1296	3.8 \pm 12.3	94.0	87.6
TOTAL						4.0 \pm 12.5	100%	93.25%

We found that the mean abundance per fish sighting event was greater for non-commercial species than it was for commercial species (see Table 9-2). There was a mean abundance per commercial fish event of 2.4 (SD = 7.4), while the mean abundance of non-commercial was 4 (SD 12.5). The high standard deviation (and consequently increased mean value) for commercial fish events may be attributed to a single event of large abundance. This single event was an estimated 50 fish of the *Lutjanidae* family schooling together. Excluding this rare occurrence the mean number of commercial fish sighted per event was approximately one. Most commercial fish events (over 90%) are of solitary fish, so we may conclude that commercial types of species are quite likely to be observed as solitary fish. Though a large proportion (approximately 60%) of the actual abundance were non-solitary fish and ~50% of the fish (perhaps also 50% of the biomass) is actually aggregated.

The number of commercial fish was not found to be strongly related to the total number of fish (Figure 9–12). There were a number of transects where large total abundance of fish did correspond to a large abundance of commercial type fish. However we did not find a large abundance of commercial fish without the presence of other fish. In fact there was only one site where two commercial fish were found in the absence of any non-commercial fish. The single commercial fish event of 50 *Lutjanidae* family schooling together to occurred on a site where the total number of fish was only 60 fish.

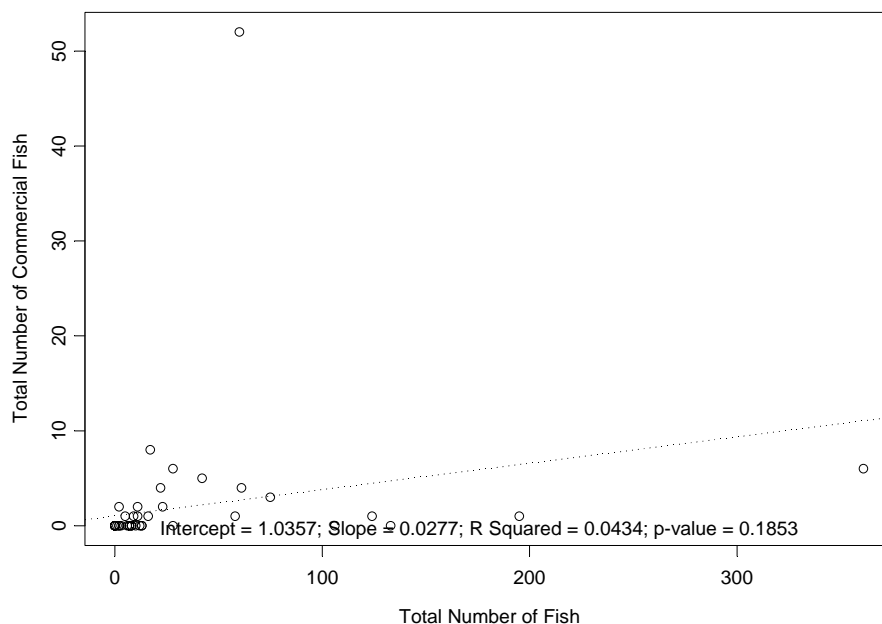


Figure 9–12: Relationship between the total number of fish (commercial and non-commercial) and the total number of commercial fish sighted on a video transect.

By far the most common fish sighting event, with 308 occurrences, was of a single fish from either commercial or non-commercial type class (see Figure 9–13). The next most common fish sighting event had fish was observed in pairs, though this occurred only 24 times (compared to over 300 solitary fish events). We also observed what seem to be “modes” of abundance estimates from the video-ground truth data, with counts of 1, 2, 5, 10, 20, 50 (see Figure 9–13) the most common. These “modes” of abundance estimate are due to observers guessing the abundance to the nearest easily recalled number when they are unable to accurately count the number of fish. This estimation error is probably in random directions (i.e. some estimates too high and some too low) so it probably doesn’t lead to sampling bias. Though of course large estimates of abundance will not be accurate. Further investigation could test whether there was a consistent tendency to over/under guess (bias) by comparing the real time entries with those from more careful post-analysis of the videos.

There may be further issues of sampling inaccuracies with the towed video camera system, which are highlighted by cross referencing with the acoustic sampling. While these issues will be dealt with in greater detail in Section 9.3.2.3, here we refer to camera avoidance and the different sampling volumes of the (video and acoustic) systems.

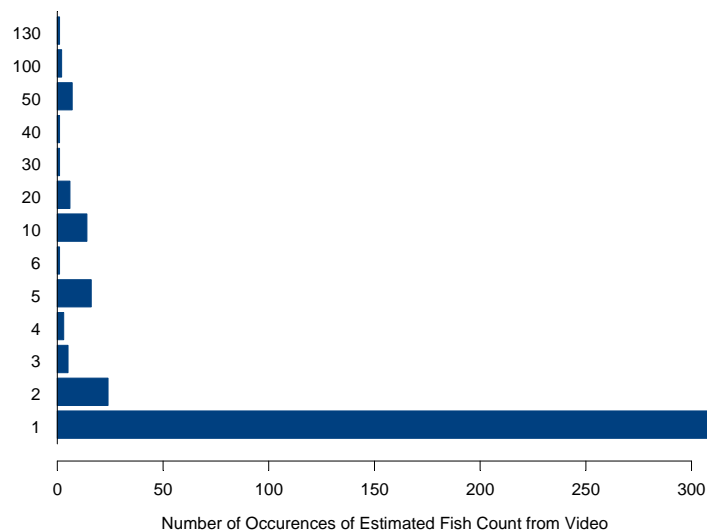


Figure 9–13: Occurrences of Fish Count ‘Levels’ Estimated from Video.

Camera avoidance by fish has been documented (Koslow *et al.* 1995) and leads to sampling bias for these techniques. For examples there are cases when the acoustic system clearly shows numerous fish marks but no fish were sampled by the video system due to either the fish moving to avoid the camera system or because the acoustics has a wider footprint than

the video (or even the echo sounder or boat noise may scare them away). We noted some examples (see Figure 9–14) where this behaviour by fish may be evident and this is confirmed by video records where fish would swim away from the camera before it got close enough to identify them.

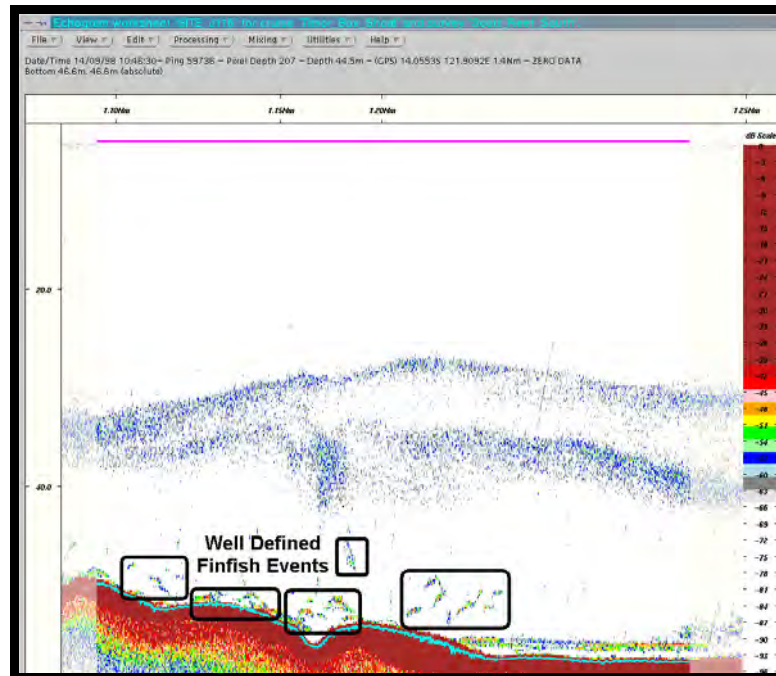


Figure 9–14: Clear fish events in the echogram data, however, no finfish were tagged in the video database.

Apart from camera avoidance there is an issue of the different sampling areas of the video and acoustic systems. The sampling area (or field of view) for the video camera depends on height above the seabed and distance at which a fish may be clearly observed. The width of this sampling field of view across the transect is of the order of 3-4 meters at a distance of about 2 meters in front of the camera and at a height of 1-2 meters above the bottom. When compared to the sampling volume of the acoustic system, which is more than twice that at 8 meters across the transect (at the transducers half power beamwidth and for a mean depth of 45m) and included targets up to 10 meters above the bottom. The difference in sampling volume may have lead to the case where fish were sampled acoustically and not by the video ground-truth system.

9.3.2.2 *Acoustic data analysis*

Initially, we present a qualitative assessment of the echogram results from acoustic sampling in the field study area. We examined whether the acoustic data has of sufficient quality and

proved information on tropical demersal fish. This is followed by a detailed examination of the quantitative results of the echo-integration analysis.

Qualitative assessment of acoustics

The information in acoustic echograms collected during the Timor study area clearly showed the presence of tropical demersal finfish. For example Figure 9–15 shows two large schools of non-commercial finfish (identified from video ground-truth). On inspection the overall quality of the echogram data was sufficient to allow further investigation using quantitative echo integration analysis.

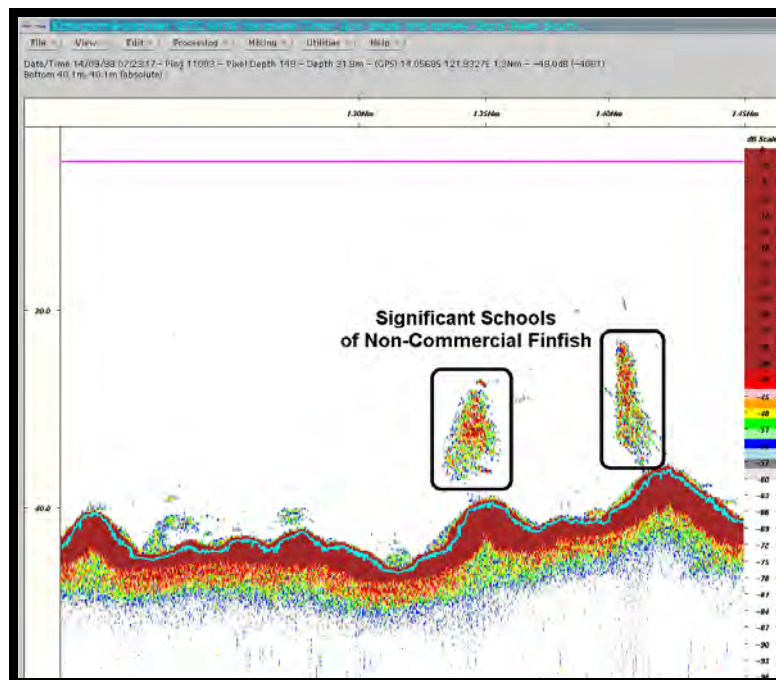


Figure 9–15: Site M113 showing two significant schools of non-commercial fish.

On some occasions individual commercial fish were very clearly observed as marks in the echogram, even close to the seabed (Figure 9–16). From this example (see Figure 9–16) you can see the characteristic “boomerang” shaped echogram signals from individual fish acoustic reflection characteristics.

Given that we are attempting to detect fish that occur close to the seabed, errors induced by poor bottom pick can be significant (see Figure 9–17). Though most of the data was high quality; poor bottom pick backscatter values can be as large as (or in some cases larger) those

produced by legitimate fish marks. In our quantitative assessment of acoustics we used filters to edit out this poor data.

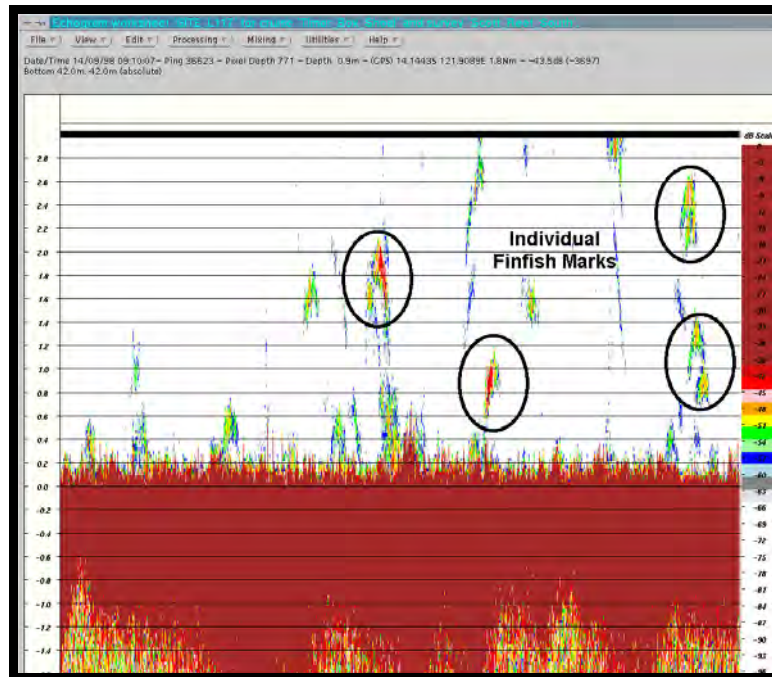


Figure 9-16: Good fish marks close to bottom (hi - res bottom locked echogram). Individual fish marks are circled.

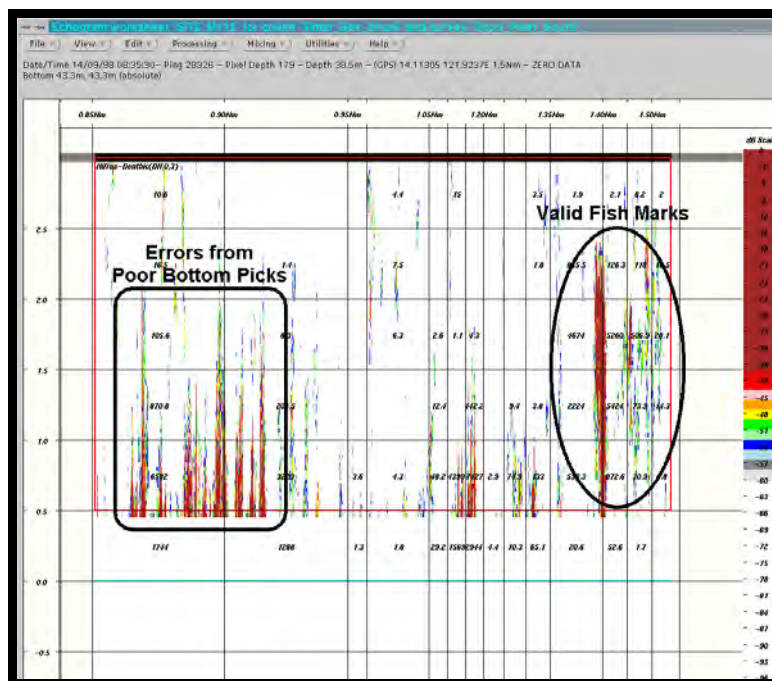


Figure 9-17: Whole transect of hi-res bottom referenced echograms, show the errors introduced by poor bottom picks at the start of the transect. Values are as large as (or in some cases larger) those produced by valid fish marks later in the transect.

Quantitative assessment of acoustics

Summary statistics by sample site for the mean area backscatter coefficients (or SA's) are shown in Table 9-3, for each video and acoustic transect site. The range of total acoustic backscatter over a sample site ranges varies markedly from 225 m^2/nm^2 to 694133 m^2/nm^2 with a mean and standard deviation of 103656 m^2/nm^2 and 138238 m^2/nm^2 respectively. The variability in acoustic backscatter between sites is clearly shown in Figure 9–18.

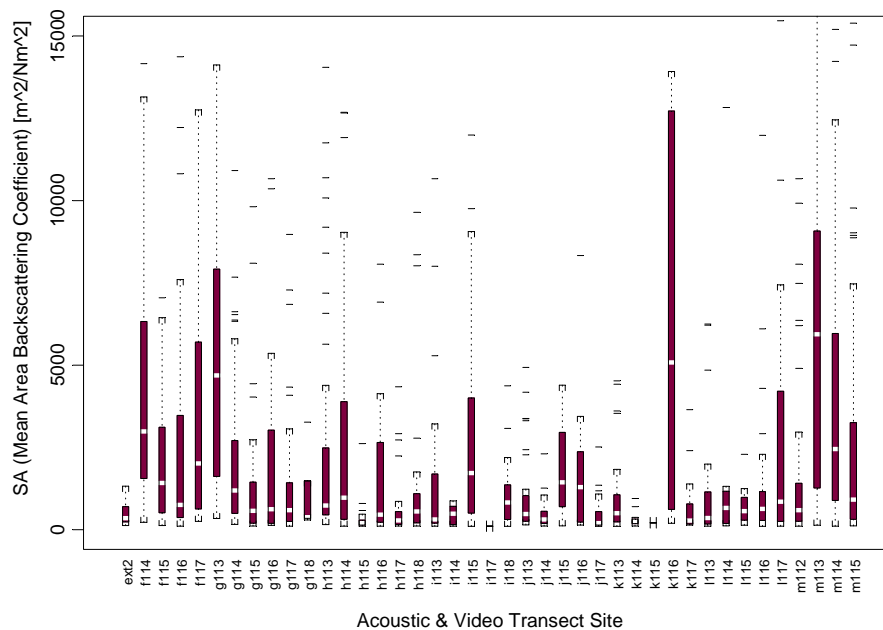


Figure 9–18: Boxplot of SA (mean area acoustic backscattering coefficients) showing range, mean, one standard deviation about the mean and outliers for each acoustic and video ground-truth transect site.

We noted the extreme variance for site i116 and suspected this was due to poor seabed bottom picks allowing seabed bottom signals to be included in the echo integration for fish backscatter. This was subsequently confirmed on further inspection of the echograms for this site. The data from site i116 was of such a poor quality over the whole transect the site was removed from further analysis.

We see that for most integration cells the area backscattering coefficient was small (Figure 9–19); corresponding to little or no backscatters such as fish sampled by the acoustic beam and present in the echo integration cell shows the histogram of area backscattering coefficients for echo integration cells over the whole study area.

Table 9-3. SA (mean area backscatter coefficient) index summary statistics (number of acoustic integration cells per site, total SA (acoustic backscatter) over site, mean and standard deviation SA), for each video and acoustic transect site.

Site	N	$\Sigma SA (m^2/Nm^2)$	mean(SA) \pm stdev(SA)
Ext2	17	6860.80	403.58 \pm 380.76
f114	66	327153.21	4956.87 \pm 5839.48
f115	58	108110.25	1863.97 \pm 1823.76
f116	60	183079.80	3051.33 \pm 6430.79
f117	31	25042.06	807.81 \pm 2500.85
g113	59	303115.90	5137.56 \pm 3831.09
g114	62	180679.50	2914.19 \pm 4532.65
g115	58	50294.39	867.14 \pm 1814.43
g116	57	82156.36	1441.34 \pm 2919.92
g117	58	82939.12	1429.98 \pm 3006.22
g118	77	6822.60	88.61 \pm 408.12
h113	62	164169.60	2647.90 \pm 4121.77
h114	60	198413.50	3306.89 \pm 5100.20
h115	35	8439.43	241.13 \pm 446.32
h116	64	49109.46	767.34 \pm 1599.83
h117	73	22114.60	302.94 \pm 717.78
h118	42	42319.30	1007.60 \pm 2230.46
i113	27	38205.61	1415.02 \pm 2624.06
i114	18	2774.79	154.15 \pm 257.29
i115	32	149455.39	4670.48 \pm 10142.10
i116	34	694133.69	20415.70 \pm 13915.08
i117	17	594.18	34.95 \pm 26.64
i118	32	23604.66	737.65 \pm 1005.68
j113	42	38442.03	915.29 \pm 1211.26
j114	32	12962.06	405.06 \pm 457.81
j115	14	25456.20	1818.30 \pm 1390.12
j116	15	19725.37	1315.02 \pm 2206.12
j117	37	9900.94	267.59 \pm 502.79
k113	56	45392.81	810.59 \pm 1016.39
k114	19	5315.49	279.76 \pm 212.56
k115	10	225.70	22.57 \pm 66.09
k116	8	76687.20	9585.90 \pm 10427.61
k117	32	11743.86	367.00 \pm 775.31
l113	32	28880.93	902.53 \pm 1670.87
l114	25	192585.21	7703.41 \pm 24108.69
l115	30	9123.65	304.12 \pm 514.50
l116	58	59763.50	1030.41 \pm 2772.87
l117	55	69143.21	1257.15 \pm 2848.15
m112	55	82219.13	1494.89 \pm 2548.46
m113	55	361206.65	6567.39 \pm 6600.47
m114	70	364993.70	5214.20 \pm 7237.28
m115	69	190198.32	2756.50 \pm 5475.13

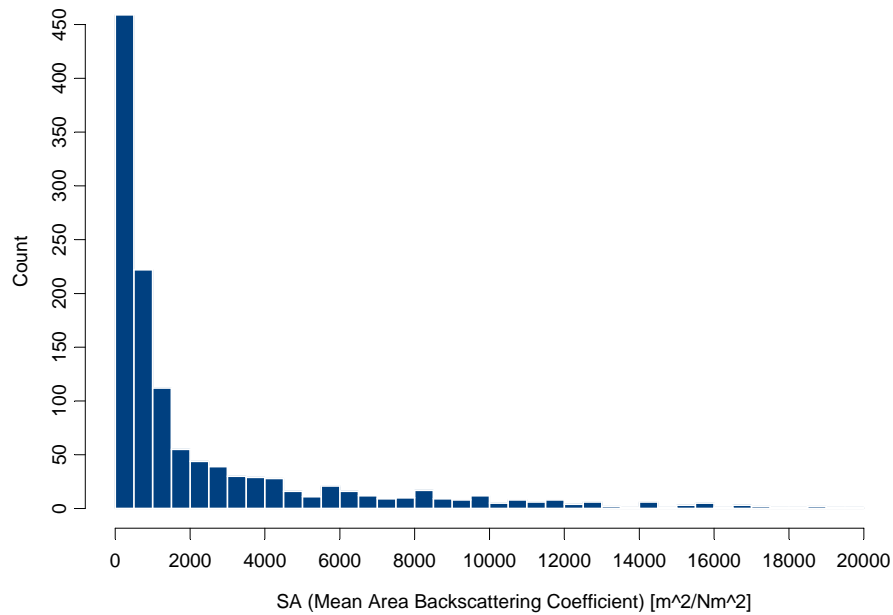


Figure 9–19: Histogram of mean area backscattering coefficient histogram for echo integration cells over the whole study area.

Erroneous data for individual integration cells was filtered for SA values greater than 20000 m^2/nm^2 removing integration cells affected by poor seabed bottom pick. The filter operated on each 18.5 m long integration cell, rather than filter out the entire 500 m long transect as was the case required for site i116. Of the 1813 integration cells over the entire study area only 34 (or approximately 2%) were affected by this filter.

9.3.2.3 Correlation analysis - acoustic and finfish/video

Initially, we present a qualitative assessment of the correspondence between acoustics and finfish sampling from the field study. This is followed by the detailed examination of results from the correlation analysis between acoustic information and fish abundance.

Qualitative correlation analysis

We compared the cross-referencing between the video ground-truth sampling of finfish and concurrent acoustic sampling. The goal was to see whether the fish we saw and identified in the video were present in the acoustic records. In some cases we found some excellent correspondence between fish events in the video and the acoustic echograms.

The complex nature of developing acoustics as an estimator for tropical commercial finfish species is highlighted in Figure 9–20. This shows the echogram of the entire transect for site F114. The transect consisted of the two large schools of non-commercial fish and a solitary Coral Trout (*Serranidae plectropomus spp.*) identified from the video.

The echogram of the first school corresponds to an unidentified school of non-commercial fish estimated to be about 100 individual fish. The echogram record of the second school (see Figure 9–20) was unambiguously resolved from the corresponding video record and identified to species. The abundance and actual species of the school was approximately 50 Fusiliers (*Caesio sp.*). This demonstrates the potential concordance between the video and acoustic data types.

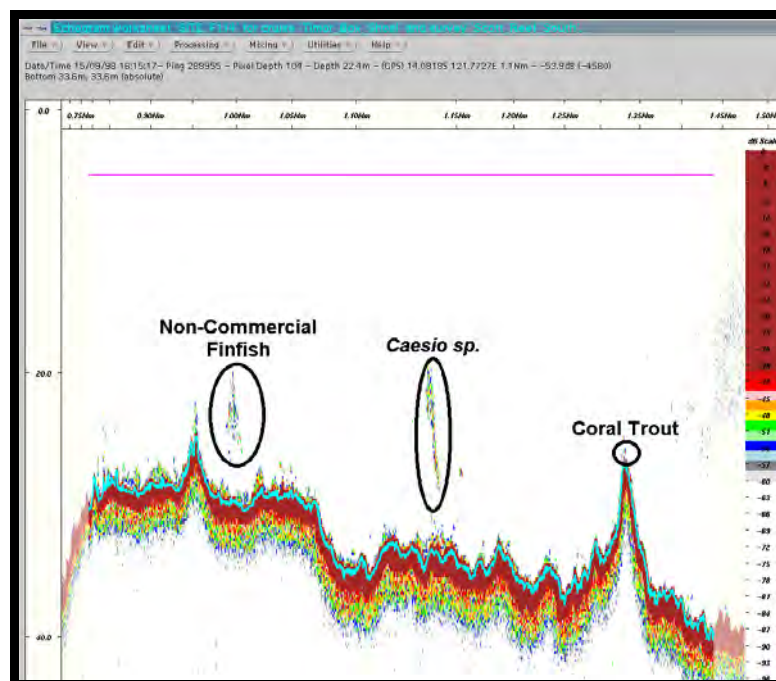


Figure 9–20: Echogram of the entire transect for site F114, showing the two significant schools of non-commercial fish (a school of unidentified fish estimated to be ~100, a school of approximately 50 *Caesio*) and a solitary Coral Trout (*Serranidae plectropomus spp.*) identified from the video.

In a third example the acoustic echogram record shows one of the target commercial species of tropical demersal finfish a solitary Coral Trout (*Serranidae plectropomus spp.*). This echogram shows that even for examples of solitary fish near the seabed, for which acoustic detection is difficult, we were able (in some cases) to find exact concordance between video and acoustic records.

Quantitative correlation analysis

The results of the correlation and regression analysis are presented in Table 9-4. We calculated the linear correlation coefficient between the total SA (mean acoustic backscatter coefficient) over a sample site and the total abundance of fish over the same site. The measure of the statistical significance of the regression relationship is shown in Table 9-4. Results are shown for groupings of all fish, commercial fish only and non-commercial fish only. The results include information for both site and integration cell filters that were applied to the acoustic estimator.

Table 9-4. Table of correlation coefficient (regression R^2 and statistical significance p) between total SA (mean area backscatter coefficient) and fish observed, for various analysis and filtering schema.

Site Filter	SA Filter	Correlation Coefficient (Regression R^2 and p)		
		Fish Class		
		All Fish	Commercial	Non-Commercial
None	None	0.29 (0.057 and 0.127)		
i116	None	0.45 (0.151 and 0.012)		
i116	20000	0.47 (0.167 and 0.008)	0.13 (0.026 and 0.312)	0.46 (0.153 and 0.012)

In Table 9-4, the site filter refers to the correlation analysis with and with out site i116 (the site found to include significant bottom pick errors, see Section 9.3.2.2) included in the analysis. With this error filled site included the correlation coefficient between acoustic and video estimated fish abundance was only 0.29 and the linear regression had a poor significance of 0.13. With site i116 removed the correlation between acoustic and video estimated fish abundance increased appreciably to 0.45 and the regression relationship was more statistically significant, with a p -value of 0.01. While still a poor correlation between the two sampling methods the relationship is still positive, as expected if the methods were sampling the same thing. The resulting improvement in correlation validates the decision to remove site i116 from the analysis and highlights the significant effect of poor seabed definition in the acoustic detection of tropical demersal fish. All further analyses did not include this site. While correlation between the two sampling methods the relationship is positive as expected, the correlation is not high.

The scatter-plot of fish abundance against SA showed that generally there are no high fish abundance estimates that correspond with low acoustic backscatter values (Figure 9-21). This result indicates that the acoustic technique is able to detect higher numbers of fish than observed in video. While there are some occurrences of high acoustic backscatter measures

corresponding with low fish abundance estimates, this is of less concern than if the converse were true. This was confirmed by checking that such values are not seabed signals or other scatterers such as plankton. This result may be attributed to the different sampling areas; where the acoustic technique samples have greater area than the video.

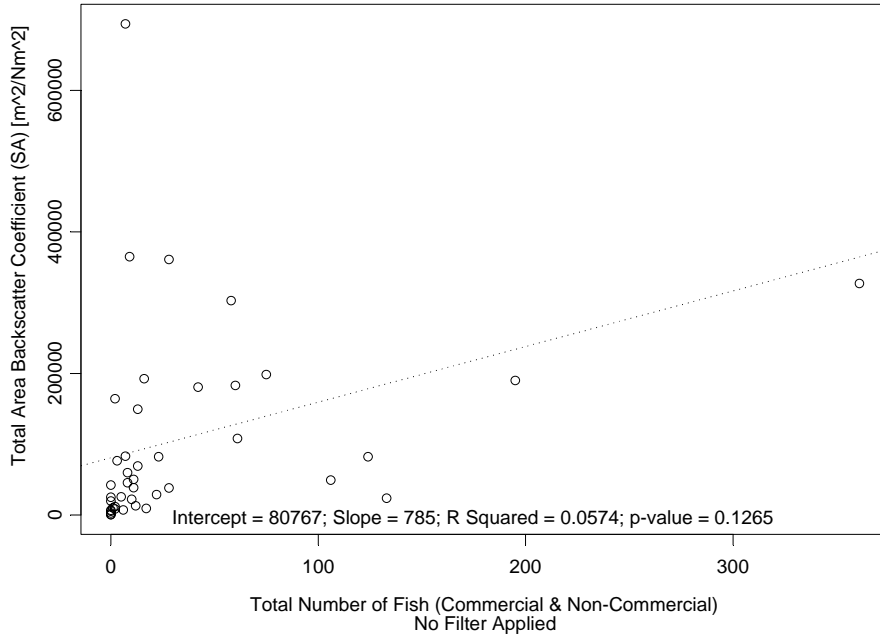


Figure 9–21: Backscatter coefficient vs fish abundance estimate for both commercial fish and non-commercial fish.

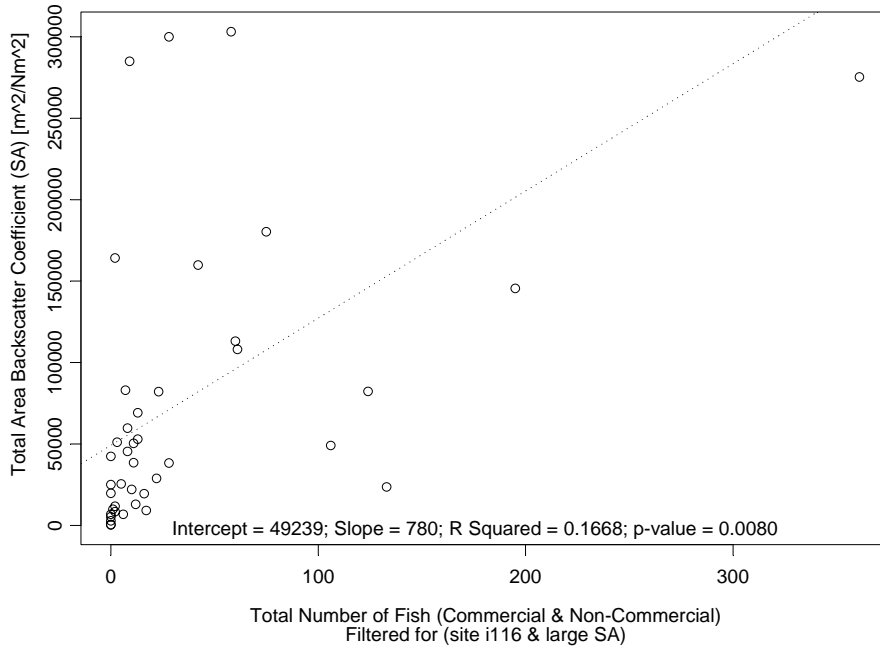


Figure 9–22: Filtered backscatter coefficient vs fish abundance estimate for both commercial fish and non-commercial fish.

The SA filter column in Table 9-4 refers to a filter of the resulting mean area backscattering coefficient for each individual integration cell within a sample site. The results, including the 20000 m^2/nm^2 SA threshold filter, showed only a slight improvement to a correlation coefficient of 0.47 (from 0.40) and the regression relationship has greater statistical significance ($p = 0.008$).

Figure 9–22 shows the relationship between the acoustic backscatter measures and fish abundance estimates where filters have been applied to data for large SA outliers (due to poor seabed detection) and uncertainty in large fish abundance estimates taken into account in weighting the regression coefficients. The figure is a scatter plot of fish abundance against SA (mean backscattering coefficient), with a line of linear regression confirming a stronger positive relationship. The correlation result was improved with the filter (Figure 9–22) compared to without the filter (Figure 9–21). The relationship is such that there are no high fish abundance estimates that correspond with low acoustic backscatter values.

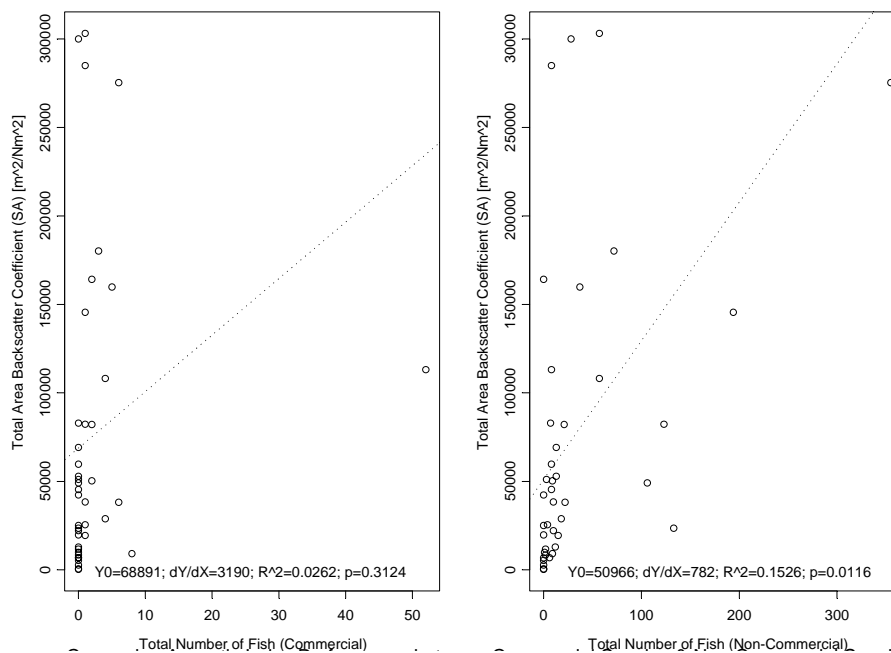


Figure 9–23: Backscatter coefficient vs fish abundance estimate for commercial fish only and for non-commercial fish only.

We compared the correlation performance of estimating fish abundance using acoustics for the different type classes of fish (commercial and non-commercial). The correlation coefficient for non-commercial types of fish was 0.46 (see Table 9-4) and the regression was significant with a p -value of 0.01. This result compares well with previous results, which take all fish into account. The correlation coefficient for commercial types of fish was poor, with a

value of 0.13 (see Table 9-4) and the regression was not statistically significant ($p=0.31$). The poor result for commercial types of fish is highlighted by the linear regression line in the scatter plot of fish abundance against SA (mean backscattering coefficient), compared with the relationship for non-commercial fish (Figure 9–23). The relationship for commercial types of fish was influenced excessively by the single schooling event of 50 *Lutjanidae* at one of the sites (see section 9.3.2.1).

9.3.2.4 Precision of absolute fish population estimates

The mean area acoustic backscatter results (SA) over the entire Scott Reef South study area are presented graphically in Figure 9–24. In this figure we compare the SA values for the ground truth sites where video and acoustic data was collected, with equivalent 500 m transects over the remainder of the Scott Reef lagoon where only acoustic data was recorded. Generally there is a high concordance between the acoustic SA measures, with the higher SA measures in the rock and rubble habitats in the north-west and north-east corners of the lagoon.

The acoustic and video methods for estimating fish abundance were analysed, using the habitats (see Figure 9–24) to stratify the results and calculate a confidence limit for the estimates. The results for these stratified analyses are presented in Table 9-5, Table 9-6, and Table 9-7.

In the stratified analysis we took into account the size of each habitat strata. The rubble habitat was by far the largest in area covering 12227 ha (or 42%) of the 293236 ha of the Scott South lagoon. The rock and sand habitats were of similar size and the two next largest in area at 6364 ha (or 22 %) and 4932 ha (or 17 %) respectively. The reef habitat strata covered 3156 ha (or 11%) and coarse sand covered 2556 ha (or 9 %) (see Table 9-5).

The number of 500 m sampling transects in each strata are also shown for the ground truth acoustic and video sites in Table 9-5 and Table 9-6. Of the 41 sample sites over the entire lagoon, there were 11 sites in the rubble strata; 9 sites in the reef strata; 8 sites in both the coarse sand and sand habitat strata; with only 5 samples sites in the rock strata. Given that the

rock strata was the second largest in terms of area, the 5 sample sites in this strata represented only a moderate density of sampling; while the reef strata was more densely sampled.

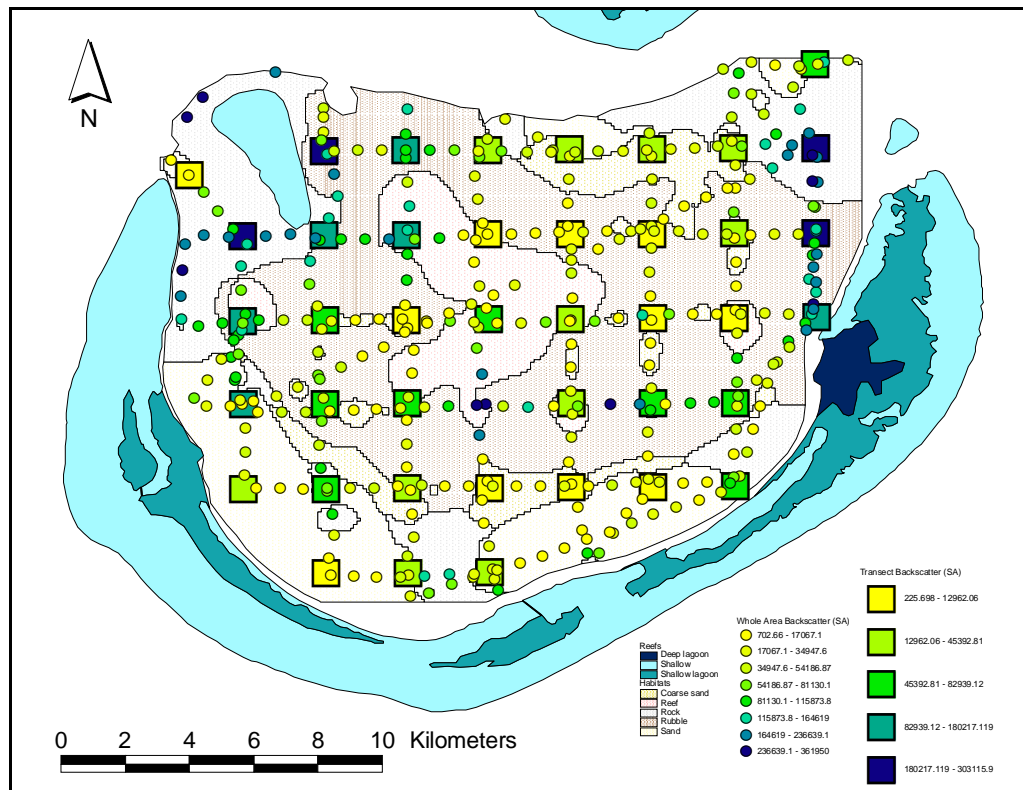


Figure 9–24: Scott Reef South sample area showing acoustic sampling results overlaying the habitat strata (refer to Figure 9–10) used in the analysis. The mean area backscatter coefficient (SA - m^2/nm^2) is shown for each of the ground-truth 500m transect sample sites (large square symbols). SA values are shown for acoustic data collected over the entire sample area (small round symbols) from equivalent 500m segments. The SA (m^2/nm^2) scale ranges from low (yellow) to medium (green) to high (blue).

The number equivalent 500 m transects over the remainder of the Scott Reef lagoon for which only acoustic data was collected are shown in Table 9-7. The total number of acoustic transects in this case is 360 sample sites. The density of sampling using the acoustics only is much higher (in fact almost 9 times higher) than where video was also deployed. In this case, for each habitat strata the density of sampling more closely follows the habitat strata area proportions shown above. There were 138 sample transects in the rubble habitat strata; 74 in the sand habitat strata; 64 in the rock habitat strata; 44 in the reef habitat strata; and 43 in the coarse sand habitat strata.

Table 9-5. Stratified video fish count analysis results: total 500 m video-transect (estimated area 0.175 Ha) fish count (all fish – commercial and non-commercial) and 90% confidence interval

Habitat Strata	Sites [N_h]	Area [ha]	Weighting [W_h]	Stratum Mean [\bar{y}_h]	Stratum Variance [s_h^2]	Stratified Mean [$\bar{y}_{st.}$]	Stratified Variance [$v(\bar{y}_{st.})$]	
Coarse Sand	8	2556	0.09	11.38	91.41	1.0	0.1	
Reef	9	3156	0.11	31.11	1545.36	3.4	2.0	
Rock	5	6364	0.22	127.80	22349.70	27.8	211.8	
Rubble	11	12227	0.42	23.09	1395.69	9.7	22.2	
Sand	8	4932	0.17	26.00	2281.43	4.4	8.1	
TOTAL	41	29236	1			46.22	244.22	
Total Fish Count		7,721,645		90% Confidence Interval				± 56.9%

Table 9-6. Stratified acoustic analysis results using mean area backscatter coefficient (SA m²/nm²) for each of the ground-truth 500 m transect sample (estimated area 0.4 Ha). Table shows total SA and 90% confidence interval

Habitat Strata	Sites [N_h]	Area [ha]	Weighting [W_h]	Stratum Mean [\bar{y}_h]	Stratum Variance [s_h^2]	Stratified Mean [$\bar{y}_{st.}$]	Stratified Variance [$v(\bar{y}_{st.})$]	
Coarse Sand	8	2556	0.09	29228.19	302105960	2555.3	288641.6	
Reef	9	3156	0.11	55386.73	3187834191	5979.0	4127576.4	
Rock	5	6364	0.22	189968.88	9219707177	41353.4	87378554.3	
Rubble	11	12227	0.42	92981.48	12265784002	38887.5	195042915.9	
Sand	8	4932	0.17	39062.58	1526515257	6590.2	5431146.4	
TOTAL	41	29236	1			95365.5	292268834.6	
Total SA m²/nm²		6,970,280,810		90% Confidence Interval				± 30.2%

Table 9-7. Stratified acoustic analysis results using mean area backscatter coefficient (SA m²/nm²) for acoustic data collected over the entire sample area from equivalent 500 m segments (estimated area 0.4 Ha each). Table shows total SA and 90% confidence interval

Habitat Strata	Sites [N_h]	Area [ha]	Weighting [W_h]	Stratum Mean [\bar{y}_h]	Stratum Variance [s_h^2]	Stratified Mean [$\bar{y}_{st.}$]	Stratified Variance [$v(\bar{y}_{st.})$]	
Coarse Sand	43	2556	0.09	20823.10	247733553	1820.5	44035.8	
Reef	44	3156	0.11	51923.04	2296411960	5605.1	608189.7	
Rock	64	6364	0.22	119927.83	6849933714	26106.5	5071823.4	
Rubble	138	12227	0.42	60850.12	4307247993	25449.3	5459443.1	
Sand	71	4932	0.17	31324.86	780249257	5284.8	312791.8	
TOTAL	360	29236	1			64266.2	11496283.8	
Total SA m²/nm²		4,697,225,620		90% Confidence Interval				± 8.7%

Table 9-5, Table 9-6, and Table 9-7 show the stratified mean and variance estimates for the each of the sampling types; video fish counts, acoustic backscatter over a video ground truth site, and acoustic backscatter over the entire Scott Reef area. The stratum mean and variance estimates using the video fish count method of sampling was highest for the rock habitat strata (see Table 9-5). The reef, rubble and sand habitats had similar median abundances, while the coarse sand habitat had the lowest abundance (see Table 9-5).

The stratified mean and variance estimates from acoustic sampling deployed concurrently with video ground truth over 500 m transects are shown in Table 9-6. The rock and rubble habitat strata exhibit the highest mean acoustic estimator values (see Table 9-6). The stratum variance for the rubble habitat was extremely high compared with other habitat strata (and also other sampling methods). The coarse sand strata had the lowest acoustic estimator values (see Table 9-6).

The stratified mean and variance estimates from acoustic sampling collected over the remaining areas of Scott South lagoon using equivalent 500 m segments are shown in Table 9-7. The rock and rubble habitat strata again exhibit the highest mean acoustic estimator values. It should be noted that stratum variance for the rubble, while still high, is comparable with the rock habitat strata for this analysis. The coarse sand strata had the lowest acoustic estimator values (see Table 9-7).

The video and acoustic data collected at sample transects along with the acoustic data collected over the entire sample area, delineate the same order of habitat preference for fish. The habitat with the largest fish abundance was rock, then in decreasing order of abundance estimator rubble, reef, sand and coarse sand.

The stratified mean estimators for the video fish counts and acoustic data collected at concurrent transects were compared for each habitat (Figure 9–25). The relationship between the two estimation techniques is significant ($p = 0.018$) with an R^2 of 0.88. The rubble habitat stratum was the most divergent between the two techniques, with the number of fish being underestimated by the video compared with the acoustics (or vice-versa). The stratified mean estimators for the two acoustic datasets (one collected at video ground truth sites and the other collected over the entire sample area) were also compared (Figure 9–26). As expected given that the two acoustic estimates use the same method (though the acoustics over the entire area

has 9 times as many samples) the relationship between the two acoustic estimates is significant ($p = 0.002$) with an R^2 of 0.97.

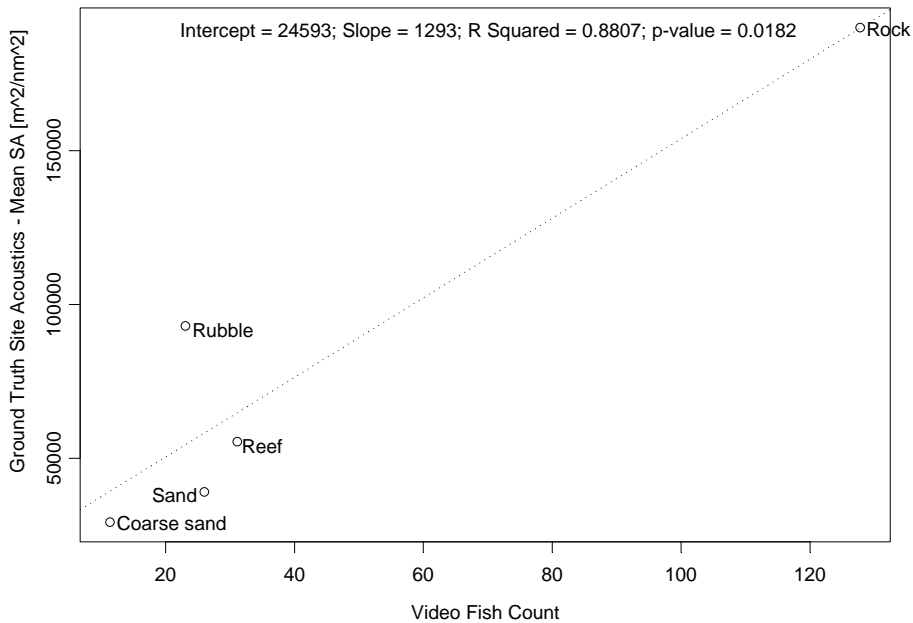


Figure 9-25: Regression of habitat stratum means for acoustic SA and video fish count estimates.

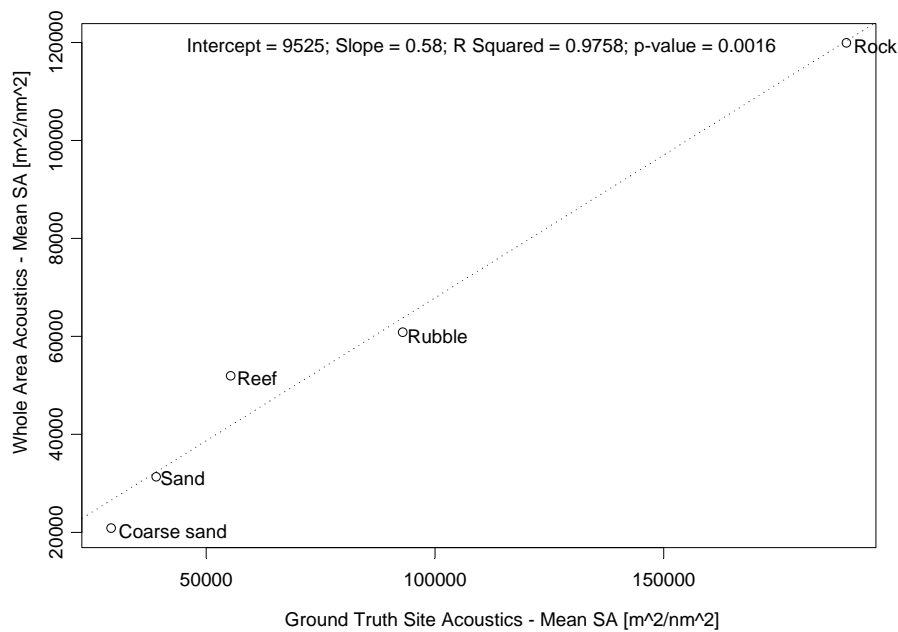


Figure 9-26: Regression of habitat stratum means for acoustic SA estimates from ground-truth sample sites against data collected over the entire area.

The total stratified abundance estimate for the video fish counts over the entire Scott Reef lagoon was 7.72 million fish, with a 90% confidence interval of $\pm 56.9\%$ (see Table 9-5). The stratified acoustic abundance estimators for the two sets of acoustic data are shown in Table 9-6 and Table 9-7. Using the data obtained only while at ground truth video sites, the total mean acoustic backscatter index (SA) for Scott Reef was $6.97 \times 10^9 \text{ m}^2/\text{nm}^2$ with a 90%

confidence interval of $\pm 30.2\%$. While using the data obtained in 500 m segments over the entire Scott Reef lagoon the total mean acoustic backscatter index (SA) for Scott Reef was $4.69 \times 10^9 \text{ m}^2/\text{nm}^2$ with a 90% confidence interval of only $\pm 8.7\%$ — a more precise result.

The regression relationship between the acoustic SA estimators (dependent) and the video fish counts (independent) — the inverse of that earlier in this section (Figure 9–22) — was used to relate acoustic SA estimates to fish counts at the 500 m transect scale. Uncertainty in both the SA estimates (Table 9-6, Table 9-7) and the regression ($s^2_{y,x}=43733.9$) was propagated through to approximate a minimum 90% confidence interval of the fish abundance estimate for the entire lagoon. The fish abundance, using acoustics from ground-truth transects, was calculated to be 4.39 million fish ($\pm 41.4\%$, including uncertainty of regression), while that from using all acoustic data from the entire vessel track was calculated to be 3.28 million fish ($\pm 26.4\%$, including uncertainty of regression). The results of the acoustic estimators (referred to fish counts) and video estimates were compared graphically (Figure 9–27).

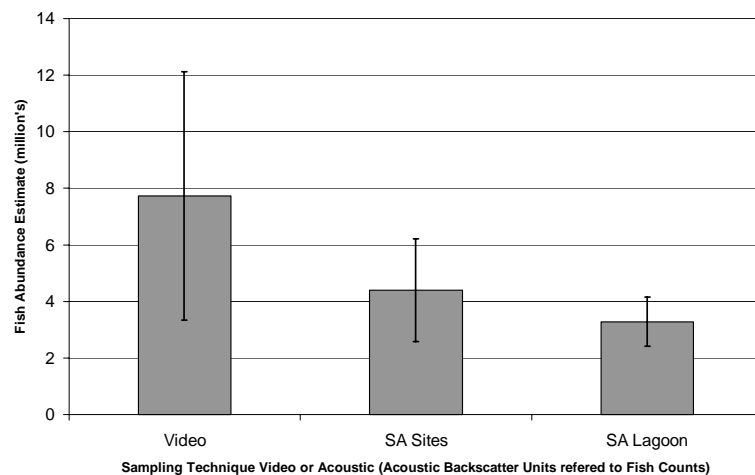


Figure 9–27: Comparison of total fish abundance estimates ($\pm 90\%$ confidence interval) for Scott Reef lagoon, for each sampling technique: fish counts from video; fish numbers derived for acoustic SA estimates from 500 m transects at sample sites; and fish numbers from acoustic SA estimates from 500 m segments over entire survey area (acoustic SA estimates converted to fish counts using regression relationship).

9.4 Discussion

We have found through our desktop investigation that the characteristics of commercial tropical demersal fish present a number of challenges for the application of acoustic techniques in the assessment of their abundance. These fish exhibit many characteristics that make acoustic assessments of their abundance difficult. They inhabit areas close to rough seabeds, they occur in low abundance, and in complex multi-species assemblages.

As commercial categories of fish only made up a very small proportion of all the fish observed, when assessing these techniques, there was proportionately less ground truth data available. The relatively high abundance of non-commercial fish masked the information on the commercial fish species of interest. As we were attempting particularly to evaluate techniques for assessing abundance of commercial categories of fish this result is important and may mean that, using single frequency acoustics, we are only able to assess the presence of all tropical demersal fish together, and not separate them into commercial or non-commercial (or target and non-target species) categories.

In most cases the acoustic echogram data were of a high quality and those errors or noise signals present were successfully dealt with in pre-processing stages of the analysis by removing that data which was obviously corrupted by aeration, hydraulic and electrical noise, ship motion, and poor bottom picks. The processing used in analysis of this acoustic data was applied using algorithmic analysis capabilities of the EY500 echosounder instrument and the ECHO software. For example the EY500's automatic detection of the seabed signal and ECHO's algorithmic definition of echo integration layers from that seabed definition. However there were times when these algorithms could not handle the complex nature of the acoustic echogram information. For instance poor detection of the seabed (e.g. due to bad weather) or distinguishing between water column scatterers of interest (e.g. discriminating plankton from fish)

Where the algorithmic analysis procedures for selection of echo integration layers give obviously erroneous results, manual interpretation and analysis using software is possible; using other sampling information as a guide. Thus more accurate indicators of finfish biomass from the acoustic echogram data may be estimated after intensive manual editing of the echogram worksheets in the ECHO software; for example, manually defining either the seabed acoustic bottom, the water column integration layer boundary, or classifications of water column scatterers to exclude or include. Manual editing of the echogram would exclude water column scatterers that are not of interest (e.g. plankton, bait fish) from the analysis. This may be achieved by classifying finfish targets of interest into or out of the echogram analysis (which may also allow limited species targeting using video data from sample sites as a cross-reference). Estimates for benthic fish species may also be improved by manual editing of the near bottom boundary of the echogram processing layer to include fish targets

that exist between the 0.5 meter data processing boundary and the dead-zone limit nearer to the actual seabed.

The correlation result for commercial fish shows that there is only a weak positive relationship between acoustic estimates of commercial fish abundance and those estimated from the video. This is not surprising given the low numbers of commercial fish detected, relative to non-commercial fish, and when they were detected they were mostly solitary — except a single schooling event of more than 50 fish (possibly *Lutjanis gibbus*) at one of the sites. Nevertheless, despite the difficulties in surveying tropical demersal fish using acoustic techniques, the results achieved in a test field survey in this project suggest that further investigation is warranted. The relationship between video fish counts and acoustic SA in this Project, compares favourably with previous experimental results combining acoustic and video techniques for assessing tropical reef fishes (Gledhill et.al., 1996).

The stratified estimates obtained, taking into account habitats, showed the highest abundance of fish over rock and rubble and reef habitats. This result confirmed our knowledge and understanding of tropical demersal fish gained through our desktop study. Also, results from the stratified analysis showed that the acoustic technique had a statistically smaller error, compared with video estimates of fish. The precision of the acoustic estimate improves again when taking into account all of the available acoustic data for the entire vessel track through the study area (not just at ground truth sites). Acoustic data collection is possible underway, when no other type of data (trawl surveys, fish trapping, baited video stations or video transects) is able to be collected. This is one of the main benefits of the acoustic technique: acoustic data may be collected continuously, thus improving the precision of the estimates.

The best results were achieved when all observed fish were considered, compared with the analysis restricted to commercial species only. The low number of commercial fish events observed made it hard to fully assess the acoustic technique in this study. However, even with further field-survey based development of acoustic techniques, it may be that this method — by itself — is not practical or cost effective for tropical demersal finfish of commercial importance, as is addressed in the following discussion.

The benefits of an acoustic technique compared with a towed camera are that the size of the sampled area is much greater and acoustic techniques can work in turbid water. Compared

with a trawl, acoustic systems are non-extractive (or environmentally friendly) and can sample over rough ground. Acoustic systems are easy to deploy, though they do require technical expertise to operate correctly.

A drawback of acoustics techniques are that they require time consuming analysis, especially for tropical demersal fish due to the potential need for extensive manual editing of echograms to extract the target fish of interest from the unwanted backscatter. Generally, issues of practicality of acoustic techniques are being addressed through technological advancements in acoustic hardware and software. Split-beam acoustic systems allow discrimination of target strengths of individual fish in the beam for estimating biomass, and multi-frequency systems can facilitate identification of species. Software development with improved algorithms allowing automatic definition of seabed and fish targets, aggregations or schools would reduce the need for manual editing of echograms.

In conclusion, using acoustic methods solely, for routine surveys of tropical demersal fish abundance may not be practical. However, when integrated with other instrumentation such as video sampling or in conjunction with other direct sampling methods such as baited traps or from other catch data, acoustics would provide useful additional information to improve precision of estimates. The question is how to integrate this information to improve the stock estimate in a cost-effective way. Acoustics may also be useful in guiding other sampling techniques through an initial acoustic survey. McClatchie (2000) found “*ground truth techniques are most effective when they are directed by the acoustic observations*”. That is, acoustic indices may be used as a basis for stratification for subsequent sampling by other devices. The success of acoustic techniques, like other remote sensing technologies, is dependent on high quality and high-density ground-truth information.

9.5 Appendix

Appendix 9.5–1: Number of finfish sighting events, type of fish, fish identification (family and species) and total number of fish, from video transects, by site.

SITE	EVENTS	TYPE	FAMILY	SPECIES	FISH
EXT2	6	Non Commercial	Unknown		6
	5	Commercial	<i>Serranidae</i>	<i>Plectropomus spp.</i>	5
F114	1	Commercial	Unknown		1
	1	Non Commercial	<i>Caesionidae</i>	?	50
	23	Non Commercial	Unknown		305
	1	Commercial	<i>Serranidae</i>	<i>Plectropomus spp.</i>	1
	1	Commercial	<i>Lutjanidae</i>	?	1
F115	2	Commercial	Unknown		2
	1	Non Commercial	<i>Acanthuridae</i>	?	20
	16	Non Commercial	Unknown		37
	1	Commercial	<i>Serranidae</i>	<i>Plectropomus spp.</i>	1
F116	1	Commercial	<i>Lutjanidae</i>	<i>gibbus?</i>	50
	1	Commercial	Unknown		1
	6	Non Commercial	Unknown		8
F117	0				0
	1	Commercial	<i>Serranidae</i>	<i>Plectropomus spp.</i>	1
G113	1	Non Commercial	<i>Caesionidae</i>	?	10
	20	Non Commercial	Unknown		47
	1	Commercial	<i>Serranidae</i>	<i>Epinephelus sp.</i>	1
G114	2	Commercial	<i>Serranidae</i>	<i>Plectropomus spp.</i>	2
	2	Commercial	Unknown		2
	16	Non Commercial	Unknown		37
G115	2	Commercial	<i>Serranidae</i>	<i>Plectropomus spp.</i>	2
	4	Non Commercial	Unknown		9
G116	1	Commercial	Unknown		2
	8	Non Commercial	Unknown		21
G117	4	Non Commercial	Unknown		7
G118	0				0
H113	1	Commercial	<i>Serranidae</i>	<i>Plectropomus spp.</i>	1
	1	Commercial	Unknown		1
H114	3	Commercial	<i>Serranidae</i>	<i>Plectropomus spp.</i>	3
	19	Non Commercial	Unknown		72
H115	2	Non Commercial	Unknown		2
H116	8	Non Commercial	Unknown		106
H117	10	Non Commercial	Unknown		10
H118	0				0
	2	Commercial	Unknown		6
I113	1	Non Commercial	<i>Pomacentridae</i>	<i>Sexstriatus</i>	2
	6	Non Commercial	Unknown		20
I114	0				0
I115	8	Non Commercial	Unknown		13
I116	6	Non Commercial	Unknown		7
I117	0				0
I118	4	Non Commercial	Unknown		133
J113	1	Commercial	Unknown		1
	10	Non Commercial	Unknown		10
J114	7	Non Commercial	Unknown		12

SITE	EVENTS	TYPE	FAMILY	SPECIES	FISH
J115	1	Commercial	<i>Serranidae</i>	<i>Plectropomus spp.</i>	1
	4	Non Commercial	Unknown		4
J116	0				0
J117	1	Non Commercial	Unknown		1
K113	8	Non Commercial	Unknown		8
K114	0				0
K115	0				0
K116	3	Non Commercial	Unknown		3
K117	2	Non Commercial	Unknown	<i>Epinephelus polyphekadion</i>	2
	2	Commercial	<i>Serranidae</i>		2
L113	2	Commercial	Unknown		2
	18	Non Commercial	Unknown		18
L114	1	Commercial	Unknown		1
	15	Non Commercial	Unknown		15
L115	1	Commercial	<i>Serranidae</i>	<i>Plectropomus spp.</i>	1
	1	Commercial	<i>Lethrinidae</i>	<i>Lethrinus sp.</i>	1
	3	Commercial	Unknown		6
	9	Non Commercial	Unknown		9
L116	8	Non Commercial	Unknown		8
L117	13	Non Commercial	Unknown		13
M112	1	Commercial	<i>Serranidae</i>	<i>Epinephelus fuscoguttatus</i>	1
	24	Non Commercial	Unknown		123
M113	28	Non Commercial	Unknown		28
M114	1	Commercial	Unknown		1
	8	Non Commercial	Unknown		8
M115	1	Commercial	Unknown		1
	17	Non Commercial	Unknown		194

10 Benefits

The outputs of this study are in the form of knowledge of the occurrence of benthos habitat in the central GBR, data and models of the dynamics of some megabenthic species that contribute to habitat structure, indications of the use of such habitats by some fish species, and methods for assessing heterogeneous seabed habitats and their associated fish stocks (BRUVS, towed-video & acoustics) for sustainable marine resource management.

These outputs can be used to examine a number of issues, including: evaluation of trawl management strategies, planning of habitat refuge areas, habitat restoration, application of knowledge to differing sectorial concerns, and legislative requirements for sustainability and conservation. Many of these issues revolve around the impact of trawling on seabed habitat and associated stocks, and the rate of recovery of habitat if areas were reserved. In prawn and fish trawl grounds, the results could be extended to the question of improving productivity by setting aside refuge areas, to allow habitats and stocks to rebuild, and trawling in specific corridors adjacent to the refuge areas. To achieve this, these results could be incorporated into a management scenario evaluation (MSE) framework.

The data obtained on the dynamics of sessile megabenthos that live on tropical shelf seabeds has contributed greatly to the previously limited scientific knowledge of these populations. The synthesis of these data into relatively simple models has contributed information needed for managing interactions between these fauna and trawling. This information will be used in a Trawl Scenario Model (Ellis and Pantus, 2001) to assist evaluation of alternative management strategies (MSE) in terms of environmental sustainability outcomes and industry outcomes, and in ecological risk assessments (ERA) of trawl fisheries (currently those managed by AFMA, and in future for others). Vulnerability of megabenthos to trawling is a combination of two factors — resilience (removal per-trawl) & recovery rates. In this project we have demonstrated that megabenthos typically would have slow to medium-slow recovery rates (*sensu* Pitcher *et al.* 2000a) in areas set aside from further impact, provided those areas are suitable for megabenthos. Further, given the available estimates for resilience (Poiner *et al.* 1998; Pitcher *et al.* 2000b), megabenthos range in vulnerability to trawling from medium-low to very high. The benefit of this knowledge is that management strategies aiming to achieve environmental sustainability can focus on assessment of a shorter list of more vulnerable species. These approaches (MSE, ERA, and vulnerability assessments) are

relevant to, and can be adopted into current and future management for environmentally sustainable development of coastal and shelf fisheries that depend on benthic habitat, as required by legislation. The benefits will be an objective balance between economic/industry objectives and environment/conservation objectives.

The potential benefits of combined towed-video and acoustic techniques for assessing tropical demersal finfish resources was demonstrated, though further work is needed. This combination takes advantage of the towed camera to count fish and identify those species of interest to an assessment and of the acoustics to cover a much larger sample area. The fact that acoustic data may be collected at all times, including in turbid water, thus improving the precision of the estimates is one of the main benefits of the technique. Compared with trawls or traps, video and acoustic systems are non-extractive (“environmentally friendly”) and can sample over rough ground. Towed-video and acoustic systems are easy and rapid to deploy, though they do require technical expertise to operate correctly.

The north Queensland fishing charter boat fleet now has an understanding of the types of habitat with which some of their target species (eg. snappers and emperors) are associated. Previously, their knowledge was derived solely from their observations of echosounder traces — now, this is supplemented by video and quantitative data on fish and megabenthos. Fishing charterers and demersal fisheries have benefited through the development of complementary, and non-extractive (BRUVS, towed-video & acoustics) techniques for assessing the abundance of stocks on which they depend.

Related projects on the effects of trawling and the effects of line fishing, in programs supported by the FRDC and the CRC-Reef, will benefit through ability to interpret their results in the wider context of benthic dynamics and reef / inter-reef trophic links. This research has also provided significant background and methodology for other large-scale / longer-term research needed to address similar issues on other open shelf areas, such as those off the NSW coast, SEF, NPF and NWS.

These benefits and beneficiaries are as identified in the original application.

11 Further development

Seabed benthic biodiversity survey:

Detailed information on benthic habitats and constituent biodiversity was obtained for a relatively small region of the central section of the Great Barrier Reef. Each additional seabed site sampled continued to add new species to the inventory and the estimated species richness was more than double that sampled and continued to increase with each additional sample. Substantially more sampling effort is required to understand the local species richness, map spatial patterns of the inter-reefal benthic assemblages, and develop bio-physical relationships for bio-regionalisations. These are being addressed by projects recently started in the GBR and in Torres Strait.

Megabenthos population dynamics:

Several environmental factors appear to limit the successful settlement of larvae. These may include the availability of suitable substratum free from sedimentation, from sand scouring, from competition by algae or predation. We had limited numbers of recruits to our study sites and still have limited understanding of the conditions or determinants of recruitment or the rates of recruitment for many of the species studied. This aspect of the natural dynamics of megabenthos requires further work.

In our study, we found little evidence of sexual reproduction in any of the sponge and octocoral samples collected. Funds and logistics prevented us from sampling the benthic animals more frequently than the twice per year proposed. The reproductive biology of Indo-Pacific gorgonians is virtually unknown. Some gorgonians are known to brood larvae, whilst others rely on releasing gametes into the water column (fertilisation is external). No reproductive structures were seen in any of the specimens examined. Whether or not these gorgonians are reproductively viable on a year-round basis is unknown. It may be worthwhile sampling the populations in the experimental area just prior to the annual spawning event typical of many scleractinian corals on the Great Barrier Reef. It is entirely possible that some octocorals also concentrate their reproductive effort in a synchronous spawning event at this time. This is a large gap in our knowledge of the ecology of megabenthos that is worthy of investigation.

Megabenthos Modelling:

This study has shown that megabenthos populations are likely to experience significant stochastic variations in recruitment, growth, survival, or other perturbations or impacts on ecological, relatively short, time-scales. This means that populations are unlikely to be in stable states and their current size distributions are a reflection of past dynamics, however, measurements are made of current dynamics. Because of these random effects, a single study such as this is not able to characterize the typical distribution of these demographic parameters and further empirical studies of megabenthos demography are required to develop a more complete understanding.

In this regard, this study appears to be only the first to attempt to understand the demographics of off-reef tropical megabenthos, and for nine species succeeded in measuring growth-rates with adequate initial precision and description of natural variation, especially considering the mixed benefit due to the impact of the cyclones. Mortality was less precisely described, primarily because relatively few deaths occurred, but also due to the impact of cyclones. However, recruitment probabilities remain the most uncertain parameter — despite this study's relatively large observation plots — they have been measured only imprecisely over a 2-year period (short relative to the long time dynamics of these populations) and further measurements are needed. This uncertainty is crucial given the long recovery times are critically dependent on rates of recruitment, and on the degree of self-recruitment of meta-populations. Further, the rates of actual recruitment that we measured were typically less than (only 20-50%) that required to maintain the resident densities observed during the study. It is possible that recruitment was atypically low during the period of the study, and/or the resident densities observed reflect an earlier period of atypically high recruitment. Alternatively, mortality may have been atypically high during the period of the study and/or atypically low prior to the study. Nevertheless, this leaves open the possibility that the recovery rates estimated herein may be optimistic and, given the sensitivity of recovery rates to recruitment, emphasizes that need for additional data on rates of recruitment for these megabenthos.

A complete assessment of the interaction between megabenthos and trawling — a spatially dynamic process — also requires information on the distribution and intensity of trawl effort, and the distribution & abundance of seabed biota that may be affected by trawling. With such information, quantitative environmental risk assessment is possible, and further, it would be possible to quantitatively evaluate which management strategies will best achieve

environmental sustainability goals (Pitcher *et al.* 2000a) while taking into account consequences for the fishery (eg. Ellis and Pantus, 2001). Rigorous assessments of this kind are needed to contribute to an objective balance between ecologically sustainable fishing and biodiversity conservation as ESD management changes are implemented in those Australian fisheries that affect seabed habitat.

Habitat use by key fish species:

Our results show that the cross-shelf location in studies of fish-habitat associations is a prime determinant in the results. Further, it is likely there are long-shore, latitudinal differences in fish-habitat associations that could not be addressed by the current study. Consequently, there are uncertainties in transferring results from this study to all situations involving disturbance of megabenthos, and further, region-specific studies are required.

We observed that of commercially important species, juvenile *L. sebae* were most commonly observed in habitats dominated by megabenthos, though sample sizes were small and it was not possible to be certain that they were restricted to such habitats due to the lack of detailed contiguous coverage habitat maps. Further work would require high resolution mapping of megabenthos habitat patches, so that observations and sampling of fish in different habitats could be conducted accurately.

The trophic studies were limited by the relatively low number of fish sampled and the smaller number that contained food other than the bait provided to attract them into the traps. These specimens have contributed to understanding of the feeding relationships of these species though none of the prey items found could be related solely to megabenthos habitats. Further trophic studies, including isotopic and chemical tracers, are required to understand the ecosystem that includes these fish species and habitats.

Fish assessment methods:

Baited Remote Video Stations were shown to out-perform un-baited stations and traps. However, species identification can be difficult and development of appropriate fish identification guides would be useful. Further, video stations and traps provide only estimates of relative abundance, not absolute abundance as both are dependent on the attraction to the bait plume and other fish behaviour. In the case of video stations, fish abundance can be extracted only as MaxN, the largest number of individuals of a given species seen on the

video at any instant, and so does not directly quantify attendance to the station. Thus it is difficult to estimate absolute abundance from video stations, and further work would be required on attraction and video statistics in order to produce absolute abundance estimates from these techniques.

The results achieved in our acoustics evaluation field survey suggest that further investigation of acoustics is warranted, despite the difficulties that tropical demersal fish present. Nevertheless, applying only acoustic methods to routine surveys of tropical demersal fish abundance may not be practical and joint development integrating with other instrumentation such as video sampling or in conjunction with other direct sampling methods such as baited traps or from other catch data, would prove useful. Stratification based on acoustics would be one straightforward method of integrating these information types to improve stock estimates in a cost-effective way.

Technological advancements in acoustic hardware and software made by manufacturers can be implemented; eg. split-beam acoustic systems allow discrimination of target strengths for individual fish for estimating biomass, and multi-frequency systems can facilitate identification of species. Software development with improved algorithms could be developed to allow automatic definition of seabed and fish targets, aggregations or schools; this would reduce the need for manual editing of echograms. Finally, data-fusion techniques need to be developed to incorporate acoustics with other data to cost-effectively achieve improved accuracy and precision.

12 Planned outcomes

The outputs from this project — including: (1) data on the bio-physical distribution and population dynamics of living structural seabed habitat organisms; (2) models of the dynamics of these species and estimates of their potential recovery rates; (3) information on the ecological usage of megabenthos habitat by key finfish species; and (4) assessment of fishery independent techniques for estimating tropical demersal finfish abundance — will contribute to a range of useful outcomes as they are adopted by management, industry and the assemblage.

The project's outputs have contributed to a high priority area for research previously identified by the FRDC, i.e. habitat dynamics and processes. There will also be outcomes and uptake by the science assemblage as the results are communicated to other habitat ecologists.

The project's estimates of recovery rates of living habitat, and information on habitat use by fish, will be useful for planning management strategies for sustainable fisheries, planning habitat protection areas, refuges, and marine protected areas, and consideration of the feasibility of habitat restoration activities. Adoption of this information by the “trawl-scenario-model” will enable managers to use MSE approaches to examine alternative management strategies that have less impact on habitat, preserve critical habitat in refuges, reduce conflict between commercial extractive activities and conservation needs, and may lead to increased productivity among commercial species. The outputs of this study have become increasingly important as fisheries, particularly tropical trawl fisheries, respond to and implement changes to meet the sustainability and ecological assessment requirements of contemporary legislation. For example, the results are now being taken up in developing ecological risk assessments of AFMA's fisheries for EA's Strategic Assessments and similarly in the Queensland Trawl Fishery whose managers are currently conducting a review of sustainable levels of effort. The scope and importance of these outcomes will increase when the CRC-Reef/FRDC Great Barrier Reef Seabed Mapping Project provide benthic distribution information and updates the trawl-scenario-model to assist Queensland managers in these matters, and when the CRC-Torres Strait Projects similarly assist AFMA managers. The ultimate outcomes of these activities are ecologically sustainable fisheries and an objective balance between commercial fishing and national biodiversity conservation goals.

The project's information on fish-habitat relationships has and will continue to contribute to the understanding of the nature and importance of deeper habitat by the north Queensland fishing charter boat fleet, and other users and managers of these areas. Further, the Project's assessment of a range of techniques for measuring finfish abundance, including fish-traps, remote (baited) video stations and acoustics, has provided managers with fishery-independent tools and options, that have little or no environmental impact, for monitoring tropical finfish resources.

13 Conclusions

The research outcomes of the project are summarized below, in the context of the original objectives, partitioned into appropriate groups of related outputs.

13.1 Objective 1. Determine the dynamics of megabenthos.

The population dynamics parameters (growth, mortality, recruitment, and reproduction) of nine species of structurally dominant large seabed habitat organisms (megabenthos), including sponges, gorgonians, and corals, were estimated in a tropical region of the Great Barrier Reef, off Townsville. It was also demonstrated that these fauna were important for demersal fish habitat and biodiversity of the seabed environment.

This objective was prefaced by an initial survey of the seabed in the central Great Barrier Reef, primarily to locate suitable study sites but also to document habitat distribution and benthic biodiversity. The seabed was sampled by a towed video camera, a small naturalist's epibenthos sled and a sediment grab. The benthic species assemblages reflected the mix of substrata, ranging from muddy sand in the lagoon stations to coarser sediments in the inter-reefal region with rock remnants of palaeo-reefs. The harder and rocky substratum areas contained most of the megabenthos assemblages (gardens) and the occurrence and abundance of these gardens correlated positively with higher current velocity and negatively with muddy and sandy substrata. The samples were bio-diverse, however, characterization of the full species richness of the area would require significant additional sampling effort. Few sites had megabenthos gardens as substantial as those observed in the northern Great Barrier Reef or in Torres Strait, except for channels between the Palm Islands where study sites for the Project were established.

Megabenthos recruitment, growth, mortality and reproduction were measured by ROV and divers during repeated visits to study sites among the Palm Islands. Relatively few (32) new recruits ($> \sim 8$ cm) were observed in quadrats totalling 48 m², and for the study species recruit-densities ranged from 0.005–0.031 m². Cyclones appeared to severely reduce recruitment (by $\sim 75\%$). The growth of individual animals within a species was highly variable, as some individuals were observed to grow and shrink in size over the study period. The average linear

growth rates of megabenthos ranged about 1 – 7 cm yr⁻¹, maximum growth increments ranged about 4 – 25 cm yr⁻¹, and shrinkage ranged about -2 – -20 cm yr⁻¹. Natural mortality was a stochastic process and varied considerably. Average mortality across all species was about 14% yr⁻¹ (typical range about 8–23% yr⁻¹) under normal conditions, and the additional mortality caused by cyclones averaged ~8–9%. Little evidence of reproduction was found among specimens collected, possibly due to the limited (bi-annual) sampling frequency possible during the study. In general, cyclones had a dramatic effect on the sessile benthic assemblages, causing damage or complete mortality to many megabenthos. However, many soft corals (Nephtheidae) appeared several months after the cyclones.

13.2 Objective 2. Model the dynamics of megabenthos.

The dynamics of nine species of seabed habitat megabenthos fauna were modeled and the potential recovery or re-establishment after trawling was estimated, indicating long time-frames for possible resumption their role as habitat for fish and other biota.

There are very few comparable modeling studies of megabenthos demographics; those available were of shallow reef corals. The project found that megabenthos populations are very unlikely to be in stable states (at equilibrium with respect to size-distribution or “carrying capacity”), because of variations in recruitment, growth, survival or other perturbations or impacts, and the time-scale of such perturbations is likely to be relatively short. Growth rates for megabenthos could be surprisingly fast and some could achieve about half maximum size in 3–9 years post-recruitment, contrasting to some extent with the expectation of slow growth. Nevertheless, growth was highly variable, with some individuals regressing on one or more occasions, demonstrating that size was a very poor indicator of age. A significantly longer time period would be needed to attain maximum dimensions — perhaps 20-50 years. Mortality rates were relatively low (compared with productive fish stocks) at 5-30% per annum and in the same range as those mortalities observed for corals. The damage by cyclones typically restructured megabenthos size-distributions and caused additional mortality in same the order as normal annual rates. The additional mortality caused by the pass of a single trawl was up to double that caused by cyclones or normal annual rates.

The modeled time for recovery after cyclones or trawling could be lengthy and was more dependent on recruitment rates, rather than growth rates — higher recruitment lead to faster

recovery. If populations were dependent on self-recruitment, rather than external sources, recovery would be slower. In mixed self-/external-recruitment scenarios, half-recovery was typically half to two decades. Establishment scenarios were also more dependent on recruitment than growth rates, with half establishment times similar to half-recovery times. Estimates of full recovery or establishment times were imprecise because of asymptotic model behaviour near 'carrying capacity'. However, the indications were that megabenthos may take several to many decades to fully recover or re-establish where they have been significantly impacted or removed.

This study appears to be the first to attempt to understand the demographics of off-reef tropical megabenthos and for nine species has succeeded in measuring growth-rates with adequate initial precision and description of natural variation, especially considering the mixed benefit due to the impact of the cyclones. Mortality was less precisely described, primarily because relatively few deaths occurred, but also due to the impact of cyclones. However, recruitment probabilities remain the most uncertain, yet critical, parameter — despite this study's relatively large observation plots — they were measured only imprecisely over a 2-year period (a short time relative to the long dynamics of these populations). This uncertainty is crucial given the long recovery times are critically dependent on rates of recruitment. Further, the rates of actual recruitment that we measured were typically less than (20-50%) that required to maintain the resident densities observed during the study, leaving open the possibility that the indicated recovery rates may be optimistic. Given the sensitivity of recovery rates to recruitment, this emphasizes the need for additional data on rates of recruitment for these megabenthos.

This project has estimated that megabenthos have slow to medium-slow recovery rates (*sensu* Pitcher *et al.* 2000a; ie. about 5%–10% of 'carrying capacity' recovered in the first year after impact), and given the wide range of resilience (high to low) of megabenthos (ie. removal rates in the range ~5%–20% per trawl), the fauna studied here represent a range of vulnerability to trawling (the combination of resilience and recovery) from medium-low to very high. The more vulnerable species especially need to be considered when evaluating management strategies aiming to achieve environmental sustainability.

13.3 Objective 3. Document the use of megabenthos by key fish species.

The use of living megabenthos habitat by fish species, particularly those of key commercial interest, was assessed. The attributes primarily examined included small scale (10s-100s m) distributions with respect to megabenthos, and evidence of trophic links from examination of fish gut contents.

The ecological usage of epibenthic habitat by key commercial finfish species:

Non-invasive methods were applied to examining the relationship between megabenthos assemblages and associated fish assemblages, as baited and unbaited video cameras proved useful tools for characterizing fish biodiversity and relative abundance. These tools, if used in conjunction with others that can produce detailed habitat maps of a study area, are also useful in studying fish-habitat associations below the limits of SCUBA. The maps of habitat are necessary to interpret the patterns of fish abundance on the videos in terms of the true mosaic of available habitat.

Cross-shelf location was a prime determinant of the observed patterns in fish assemblages, as previous studies have shown. Within the strong cross-shelf pattern, different fish assemblages were observed in areas with megabenthos compared with areas without. A number of non-commercial species were common in megabenthos areas but not elsewhere.

In terms of the fish-habitat associations of commercially important species, we observed that juvenile *L. sebae* were most commonly caught and sighted in habitats dominated by megabenthos, though their numbers were moderate. We conclude that they are an important component of the fish assemblage associated with megabenthos, but we cannot predict if they are restricted to such habitats.

In terms of adults of commercially important species, we found no indication of a dependency of adult “redfish” (*Lutjanus sebae*, *L. malabaricus*, *L. erythropterus*) on megabenthos. Trap catches and video sightings of the adults were restricted to coarse carbonate sediments and sand/*Halimeda* habitats in deep gutters.

The food chain links between epibenthic habitat and key commercial finfish species:

The stomach contents of fish sampled by traps set on and off megabenthos habitats were examined. Of the 108 stomachs analysed, few (15) contained food other than the bait provided to attract them into the traps. Ten of the 15 stomachs were *Lutjanus malabaricus*, but the numbers were too few for statistical analyses of on/off megabenthos differences. None of the prey items found could confidently be related solely to megabenthos habitats. The most prevalent items in *L. malabaricus* stomachs were small “coral prawns” *Metapenaeopsis* spp, and squid and cuttlefish.

13.4 Objective 4. Assess methods for surveying fish abundance.

Three fishery-independent and “environmentally-friendly” techniques for surveying tropical finfish resource abundance in inter-reefal areas were assessed, including: fish-traps, remote (baited) video stations and quantitative acoustics.

Fish-traps:

Fish traps were demonstrated to be poor sampling tools, because probability of capture was observed to depend not just on the probability of retention but also on the probability of entry — and the majority of species seen around the traps showed no interest in entering the traps in daytime sets. Only 14% of all fish seen as “available” around the traps actually entered the traps and only 3% of the available fish were actually retained and caught by the traps. A few species had a high probability of entry and being retained, but on the other hand, some important families of fish never entered the traps. This gave a very limited picture of biodiversity in different habitat types. Trap effectiveness was improved approximately twofold by use of galvanic timed releases to open bait canisters after dusk and shut doors before midnight, increasing the probability of retention.

Traps have the advantage of providing specimens for ageing and dietary studies, which are important for assessment purposes. In the north-west of Australia, “industry standard” traps have proven effective as fishery-independent stock assessment tools for a limited suite of commercially important species (S. Newman, pers. comm.). Traps can also be used overnight for nocturnal species.

Remote (baited) video stations:

The use of baited and unbaited video cameras, set in strings of replicates in habitat types known or unknown from complementary surveys, was demonstrated to offer a powerful tool for daytime collection of information on biodiversity and relative abundance of fishes. In the case of baited cameras, the action of the bait plume increased the accumulation of fish species compared with unbaited, and there was no evidence it deterred species from attending the video stations. The presence of the video system, the bait plume, and the behaviour and abundance of conspecifics and other species were all evidently involved in the attraction of the fish to the units.

Video stations have the advantage of being non-extractive, though species identification can sometimes be difficult. Accurate and precise measurements of fish length *in situ* is possible if paired camera systems are deployed (Harvey *et al.* 2001a, 2001b). Further, video stations, and traps, provide only estimates of relative abundance, not absolute abundance as both are dependent on the attraction to the bait plume and other fish behaviour. In the case of video stations, fish abundance can be extracted only as *MaxN*, the largest number of individuals of a given species seen on the video at any instant, and so does not directly quantify attendance to the station. Thus it is difficult to estimate absolute abundance from video stations, as is the case with traps.

In this study, video stations were used with ambient light during the daytime, although overnight trap-sets showed that a variety of important fish families are active by night. Thus lighting systems will need to be developed to allow BRUVS to be deployed at night, though this adds an additional unknown of fish behaviour to be considered (Harvey and Cappo 2001).

Acoustics:

The usefulness of acoustics as a fishery independent and environmentally friendly technique to survey tropical demersal finfish resources was assessed. These fish exhibit many characteristics which make acoustic assessments of their abundance difficult. They inhabit areas close to rough seabeds, posing problems for detection due to the acoustic dead zone, they occur in low abundance, and in complex multi-species assemblages so it is not possible to separate individual species within multi species schools.

Despite these difficulties, acoustic backscatter and tropical demersal fish abundance was positively correlated. The best results were achieved when considering all species of fish and not restricting the investigation to particular commercial species. Though the low number of commercial fish events during our survey made it difficult to assess the acoustic technique, the results achieved suggest that further investigation is warranted, particularly the use of acoustic information for stratification and more cost-effective deployment of direct sampling tools.

A demonstrated advantage of the acoustic technique was improved precision of the fish biomass estimates due to the continuous acquisition of acoustic data. That is, the acoustic estimate was more precise because acoustic data is available for the entire vessel track through a study area, not just at survey sites. Thus, the acoustic technique when compared with towed-video estimates of fish counts had a tighter confidence interval.

Other advantages of acoustic techniques include: a much larger area can be sampled, operates through turbid water, non-extractive (or environmentally friendly) and can sample over rough ground. Acoustic systems are easy to deploy, though they do require technical expertise to operate correctly.

Acoustic data may require time consuming analysis, especially for tropical demersal fish due to the potential need for extensive hand editing of echograms to extract the target fish of interest from the unwanted backscatter. Technological advancements in acoustic hardware and software (such as split-beam acoustic systems, multi-frequency systems, and improved software algorithms) have the potential to facilitate post-analysis. However, other methods have similar post-survey time demands, such as sorting trawled samples or scoring video tapes.

It is unlikely that acoustic methods alone would be successful for routine surveys of tropical demersal fish abundance. However, when integrated with other instrumentation such as video sampling or in conjunction with other direct sampling methods such as baited traps or other catch data, acoustics would provide additional information useful for improving precision and/or for guiding the deployment other sampling techniques.

14 References

- Aglen, A., Engas, A., Huse, I., Michalsen, K., Stensholt, B.K. (1999) How vertical fish distribution may affect survey results. *ICES Journal of Marine Science*, 56, 345-360.
- Alderslade, P. (1998). Revisionary systematics in the gorgonian family Isididae, with descriptions of numerous new taxa (Coelenterata: Octocorallia). Records of the Western Australian Museum Supplement No. 55. Pp.1-359, figs.1-326.
- Alvarez, A., Ye, Z. (1999) Effects of fish school structures on acoustic scattering. *ICES Journal of Marine Science*, 56, 361-369.
- Babcock, R.C. (1991) Comparative demography of three species of scleractinian corals using age- and size-dependent classifications. *Ecol. Monogr.* **61**:225–244
- Babcock, R.C., Bull, G.D., Harrison, P.L., Heyward, A.J., Oliver, J.K., Wallace, C.C. and Willis, B.L. (1986). Synchronous spawnings of 105 scleractinian coral species on the Great Barrier Reef. *Marine Biology*. 90, 379-394.
- Bellwood, D.R. (1998). What are reef fishes? Comment on the report by D.R. Robertson: Do coral reef fish faunas have a distinctive taxonomic structure? *Coral Reefs*. **17**, 187-189.
- Birtles, A. and Arnold, P. (1983) Between the Reefs: some patterns of soft substrate epibenthos on the GBR Shelf, pp. 159-163 in Baker, J.T., Carter, R.M., Sammarco, P.W., Stark, K.P. (Eds) *Proceedings of GBR Conference, Townsville, 1983*.
- Birtles, A. and Arnold, P. (1988) Distribution of trophic groups of epifaunal echinoderms and molluscs in the soft sediment areas of the central GBR Shelf, *Proceedings of the 6th. International Coral Reef Symposium, Townsville, Australia, 1988*, 3: 325-332.
- Cannon, L. R. G., Goeden, G. B. and Campbell, P. (1987). Community patterns revealed by trawling in the inter-reef regions of the Great Barrier Reef. *Memoirs of the Queensland Museum* 25(1): 45–70.
- Cappo, M., and Brown, I. (1996). Evaluation of sampling methods for reef fish populations of commercial and recreational interest. CRC Reef Research Centre, Technical Report No. 6. 72 pp. CRC Reef Research Centre, Townsville, Queensland, Australia.
- Cappo, M., and Kelley, R. (2001).Chapter 11. Connectivity in the Great Barrier Reef World Heritage Area – an overview of pathways and processes. In; “Oceanographic processes

- of coral reefs: physical and biological links in the Great Barrier Reef" (ed. E. Wolanski) CRC Press, pp 161-188.
- Cappo, M., Eden, P., Newman, S.J., and Robertson, S. (2000). A new approach to validation of the periodicity and timing of opaque zone formation in the otoliths of 11 *Lutjanus* species from the central Great Barrier Reef. *Fishery Bulletin* 98(3), 474-488.
- Caswell, H and S. Brault (1992) Life cycles and population dynamics: mathematical models for marine organisms. *Oceanus* 35:86-93
- Caswell, H. (1982a) Optimal life histories and the maximization of reproductive value: a general theorem for complex life cycles. *Ecology*, 63: 1218-1222
- Caswell, H. (1982b) Stable population structure and reproductive value for populations with complex life cycles. *Ecology*, 63: 1223-1231
- Chao, A. (1984). Non-parametric estimation of the number of classes in a population. *Scandinavian Journal of Statistics* 11, 265-270.
- Chao, A. (1987). Estimating the population size for capture-recapture data with unequal catchability. *Biometrics* 43, 783-791.
- Coffroth, M.A., Lasker, H.R., Diamond, M.E., Bruenn, J.A. and Bermingham, E. (1992). DNA fingerprints of a gorgonian coral: A method for detecting clonal structure in a vegetative species. *Marine Biology*. 114, 317-325.
- Coles, R.G., Lee Long, W.J. McKenzie, L.J. Short, M., Rasheed, M.A. and Vidler, K. (1996). Distribution of deep-water seagrass habitats between Cape Weymouth and Cape Tribulation, north-eastern Queensland, Report to the GBR Marine Park Authority. *Queensland Department of Primary Industries Report*, 33 pp.
- Colwell, R. K. (1997). Estimates: Statistical estimation of species richness and shared species from samples. Version 5. User's Guide and application published at: <http://viceroy.eeb.uconn.edu/estimates>.
- Connell, S.D., Kingsford, M.J. (1998) Spatial, temporal and habitat related variation in the abundance of large predatory fish at One Tree Reef, Australia. *Coral Reefs*. 17, 49-57.
- Crouse, D.T., Crowder, L.B., and H. Caswell (1987) A stage-based population model for loggerhead sea turtles and implications for conservation. *Ecology*, 68: 1412-1423
- Dahan, M. and Benayahu, Y. (1997). Clonal propagation by the azooxanthellate octocoral *Dendronephthya hemprichi*. *Coral Reefs*. 16, 5-12.

- Dayton P. K. (1984). Patch dynamics and stability of some California kelp assemblages. *Ecological Monographs* 54: 253-289.
- Dayton P. K., and M. J. Tegner. (1984). The importance of scale in community ecology: a kelp forest example with terrestrial analogs. Pp. 457-481 in: P. W. Price, C. N. Slobodchikoff and W. S. Gaud editors. *A New Ecology: Novel Approaches to Interactive Systems*, Wiley, New York.
- Dayton, P.K., Thrush, S.F., Agardy, M.T., Hofman, R.J., (1995). Environmental effects of marine fishing. *Aquat. Cons. Mar. and Freshw. Ecos.* 5, 205-232.
- Denny, M. W. (1988). *Biology and the mechanics of the wave-swept environment*. Princeton University Press, Princeton, New Jersey, USA.
- Folk, R.L. 1968. Petrology of sedimentary rocks. University of Texas Press, Austin. *Ecology Progress Series* 22: 153-161.
- Ellis, D.M. and DeMartini, E.E. (1995). Evaluation of a video camera technique for indexing abundances of juvenile pink snapper, *Pristipomoides filamentosus*, and other Hawaiian insular shelf fishes. *Fishery Bulletin* **93**, 67-77.
- Ellis, N. and F. Pantus (2001) Management Strategy Modelling: Tools to evaluate trawl management strategies with respect to impacts on benthic biota within the Great Barrier Reef Marine Park area. *CSIRO Marine Research Report*, Cleveland, Australia.
- Fabricius, K. and Alderslade, P. (2001). Soft corals and sea fans: a comprehensive guide to the tropical water genera of the central-west Pacific, the Indian Ocean and the Red Sea. Pp. 1-264. Australian Institute of Marine Science and the Museum and Art Gallery of the Northern Territory.
- Fabricius, K.E. (1995). Slow population turnover in the soft coral genera *Sinularia* and *Sarcophyton* on mid- and outer-shelf reefs of the Great Barrier Reef. *Marine Ecology Progress Series*. 126, 145-152.
- Fabricius, K.E. (1997). Soft coral abundance on the central Great Barrier Reef: effects of *Acanthaster planci*, space availability, and aspects of the physical environment. *Coral Reefs*. 16, 159-167.
- Fabricius, K.E. (1999). Tissue loss and mortality in soft corals following mass bleaching. *Coral Reefs*. 18, 54.

- Fabricius, K.E. (2001) Chapter 9. Biodiversity on the Great Barrier Reef: Large-scale patterns and turbidity-related local loss of soft coral taxa. In: In: Wolanski E (ed) *Oceanographic Processes of Coral Reefs: Physical and Biological Links in the Great Barrier Reef*. CRC Press LLC Boca Raton, Florida, 127-144.
- Fabricius, K.E. and De'ath, G. (1997). The effects of flow, depth and slope on cover of soft coral taxa and growth forms on Davies Reef, Great Barrier Reef. Pp. 1071-1076 in: Lessios, H.A. (Ed.) *Proceedings of the 8th International Coral Reef Symposium*, Panama, Vol. 2. Smithsonian Tropical Research Institute, Balboa, Republic of Panama.
- Fisk, D.A. and Harriott, V.J. (1990). Spatial and temporal variation in coral recruitment on the Great Barrier Reef: implications for dispersal hypotheses. *Marine Biology*. 107, 485-490.
- Folk, R.L. (1968). *Petrology of sedimentary Rocks*. The University of Texas Press, Austin.
- Foote, K.G. (1983) Linearity of fisheries acoustics, with addition theorems. *Journal of the Acoustical Society of America*, 73: 1932–1940.
- Fromont, J. and Bergquist P.R. (1994). Reproductive biology of three sponge species of the genus *Xestospongia* (Porifera: Desmospongiae: Petrosida) from the Great Barrier Reef. *Coral Reefs*. 13, 119-126.
- Gledhill, C.T., Lyczkowski-Shultz, J., Rademacher, K., Kargard, E., Crist, G., Grace, M.A. (1996) Evaluation of video and acoustic index methods for assessing reef-fish populations. *ICES Journal of Marine Science*, 53(2), 483-485.
- Gleeson, M.G. (1996). Coral recruitment in Moorea, French Polynesia: the importance of patch type and temporal variation. *Journal of Experimental Marine Biology and Ecology*. 207, 79-101.
- Goh, N.K.C. and Chou, L.M. (1995). Growth of five species of gorgonians (Sub-class Octocorallia) in the sedimented waters of Singapore. *Marine Ecology*. 16(4), 337-346.
- Gotelli, N.J. (1988). Determinants of recruitment, juvenile growth and spatial distribution of a shallow water gorgonian. *Ecology*. 69(1), 157-166.
- Grigg, R.W. (1977) Population dynamics of two gorgonian corals. *Ecology* **58**:278–290
- Gulland, J.A. (1983). *Fish Stock Assessment: a manual of basic methods*. (FAO/Wiley Inter-Science: New York).

- Hall, S.J., (1999). The effects of fishing on marine ecosystems and communities. Blackwell Science, Oxford.
- Harriott, V.J. (1999). Coral growth in subtropical eastern Australia. *Coral Reefs*. 18, 281-291.
- Harvey, E. S., Fletcher, D., and Shortis, M. (2001a). A comparison of the precision and accuracy of estimates of reef-fish length made by divers and a stereo-video system. *Fishery Bulletin* 99(1), 63-71.
- Harvey, E. S., Fletcher, D., and Shortis, M. (2001b). Improving the statistical power of visual length estimates of reef fish: A comparison of divers and stereo-video. *Fishery Bulletin* 99(1), 72-80.
- Harvey, E., and Cappo, M. (2001). "Video in Australian fisheries and mariculture – Proceedings of a National Workshop. Rottnest Island, WA, September 4-7, 2000" Draft Final Report to FRDC, Project 2000/187. <http://www.aims.gov.au/pages/research/video-sensing/index.html>
- Hill, B.J. and Wassenberg, T.J. (2000). The probable fate of discards from prawn trawlers fishing near coral reefs; A study in the northern Great Barrier Reef, Australia. *Fisheries Research* 48, 277-86.
- Hooper, J.N.A. (1996). Revision of Microcionidae (Porifera: Poecilosclerida: Demospongiae), with descriptions of Australian species. *Memoirs of the Queensland Museum* 40. Pp.1-626; figs.1-314 col. pls.1-12.
- Hooper, J.N.A., Quinn, R.J. & Murphy, P.T. (1998). Bioprospecting for marine invertebrates. Pp. 109-112. In Proceedings of the Bioprospecting, Biotechnology & Biobusiness Conference, University of Western Australia, Perth, December 1998.
- Hughes, T.P. (1984). Population dynamics based on individual size rather than age: a general model with a coral reef example. *American Naturalist* 123: 778–795.
- Hughes, T.P. and J.H. Connell (1987) Population dynamics based on size or age? A reef coral analysis. *Am. Nat.* **129**: 818–829
- Hutchings, P. (1990). Review of the effects of trawling on macrobenthic epifaunal communities. *Australian Journal of Marine and Freshwater Research*. 41:111-120.
- Insightful Corporation (2001) S-PLUS 6 for Windows Guide to Statistics, Volume 1. Seattle, Washington.

- Johannesson, K.A., Mitson, R.B. (1983) Fisheries acoustics: a practical manual for aquatic biomass estimation. FAO Fisheries Technical Paper 240.
- Jones, J.B., (1992). Environmental impact of trawling on the seabed: a review. *N. Zeal. J. Mar. Freshwat. Res.* 26, 59-67.
- Kialola, P.J., Williams, M.J., Stewart, P.C., Reichelt, R.E., McNee, A., Grieve, C. (1993) Australian Fisheries Resources, Bureau of Resource Sciences, Canberra, Australia. ISBN 0 642 18876 9.
- King, B., Wolanski, E. (1996). Tidal current variability in the Central Great Barrier Reef. *J. Marine Systems* 9, 187-202.
- Kloser, R.J., Sakov, P.V., Waring, J.R., Ryan, T.E., Gordon, S.R. (1998) Development of software for use in multi-frequency acoustic biomass assessments and ecological studies. Final Report to FRDC (Project T93/237), CSIRO Marine Research Report, 74pp, ISBN 0 643 06192 4.
- Koslow, J.A. et.al. (1994) Development and use of acoustic techniques for the assesment of deepwater commercial fish stocks. Final Report to FRDC (Project 90/25), CSIRO Marine Research Report, 131pp.
- Koslow, J.A., Kloser, R., Stanley, C.A. (1995) Avoidance of a camera system by a deepwater fish, the orange roughy (*Hoplostethus atlanticus*). *Deep Sea Research I*, 42, 233-244.
- Kovach Computing Services. (2000). Multivariate Statistical Package, MVSP, version 3.1. Copyright © 2001 Kovach Computing Services, Anglesey, Wales.
- Kulbicki, M., Labrosse, P., Letourneur, Y. (2000) Fish stock assessment of the northern New Caledonian Lagoons: 2 – Stocks of lagoon bottom and reef-associated fishes., *Aquatic Living Resources*, 13(2), 77-99.
- Leigh, E. G, R. T. Paine, J. F. Quinn, and T. H. Suchanek. (1987). Wave energy and intertidal productivity. *Proceedings of the National Academy of Science, USA* 84: 1314-1318
- Leslie, P.H. (1945) On the use of matrices in certain population mathematics. *Biometrika* **33**: 183–212.
- Levin, L.A. Caswell, H., DePatra, K.D., and E.L. Creed (1987) Demographic consequences of larval development mode: Planktotrophy vs. lecithotrophy in *Streblospio benedicti*. *Ecology*, **68**: 1877-1886.

- Lewis, J. R. (1964). *The Ecology of the Rocky Shores*. The English University Press Ltd., London.
- Leys, S.P. and Lauzon, N.R.J. (1998). . Hexactinellid sponge ecology: growth rates and seasonality in deep water sponges. *Journal of Experimental Marine Biology and Ecology*. 230, 111-129.
- Long, B. G. and Poiner, I. R. (1994). Infaunal benthic community structure and function in the Gulf of Carpentaria, northern Australia. *Australian Journal of Marine and Freshwater Research* 45: 293–316.
- Long, B.G., Poiner, I.R. and Wassenberg, T.J. (1995) Distribution, biomass and community structure of megabenthos of the Gulf of Carpentaria, Australia. *Marine Ecology Progress Series*. 129: 127-139.
- Long, B.G., Skewes, T.D., Taranto, T.J., Smith, G.P., McLeod, I., Pitcher, C.R., Poiner, I.R. (1997) Torres Strait infill and landfall survey. Part 1: Torres Strait infill survey. Report to NSR re: Papua New Guinea – Queensland gas project. CSIRO Division of Marine Research Report, July 1997, 36pp.
- Long, B.G., T.D. Skewes, T.J. Taranto, G. Smith, I. McLeod, C.R. Pitcher, I.R. Poiner (1997) Torres Strait infill and landfall survey. Part 1: Torres Strait infill survey. Report to NSR re: Papua New Guinea Queensland gas project. CSIRO Division of Marine Research Report, July 1997, 36 pp.
- MacLennan, D.N., Holliday, D.V. (1996) Fisheries and plankton acoustics: past, present, and future. *ICES Journal of Marine Science*, 53(2), 513-516.
- McCatchie, S., Thorne, R.E., Grimes, P., Hanchet, S. (2000) Ground truth and target identification for fisheries acoustics. *Fisheries Research*, 47, 173-191.
- McPherson, G. R. and Squire, L. (1992). Age and growth of three dominant *Lutjanus* species of the Great Barrier Reef inter-reef fishery. *Asian Fisheries Science* 5, 25-36.
- McQuaid, C. D., and G. M. Branch. (1985). Trophic structure of rocky intertidal communities: response to wave action and implications for energy flow. *Marine Biology*,
- Meroz, E. and Ilan, M. (1995). Life history characteristics of a coral reef sponge. *Marine Biology*. 124, 443-451.

- Misund, O.A. (1997) Underwater acoustics in marine fisheries and fisheries research. *Reviews in Fish Biology and Fisheries*, 7, 1-34
- Mitson, R.B. (1982) Acoustic Detection and Estimation of Fish Near the Sea-Bed and Surface. FAO Fisheries Report No. 300, Symposium on Fisheries Acoustics, Bergen, Norway, June 1982.
- Nakken O., Olsen, K (1977). Target strength measurements of fish. *Rapp P-v Réun Cons Int Explor Mer* 170: 52–69.
- Newman, S. J., and Williams, D. McB. (1995). Mesh size selection and diel variability in catch of fish traps on the central Great Barrier Reef, Australia: a preliminary investigation. *Fisheries Research*. 23, 237-253.
- Newman, S. J., and Williams, D. McB. (1996). Variation in reef associated assemblages of the Lutjanidae and Lethrinidae at different distances offshore in the central Great Barrier Reef. *Environmental Biology of Fishes* 46, 123-128.
- Newman, S. J., Williams, D. McB., and Russ, G. R. (1997). Patterns of zonation of assemblages of the Lutjanidae, Lethrinidae and Serranidae (Epinephelinae) within and among mid-shelf and outer-shelf reefs in the central Great Barrier Reef. *Marine and Freshwater Research*. 48, 119-128.
- Newman, S., Cappo, M., and Williams, D.McB. (2000). Age, growth, mortality rates and corresponding yield estimates using otoliths of the tropical red snappers, *Lutjanus erythropterus*, *L. malabaricus* and *L. sebae*, from the central Great Barrier Reef. *Fisheries Research*. 48(1), 1-14.
- Ona, E., Mitson, R.B. (1996) Acoustic sampling and signal processing near the seabed: the deadzone revisited. *ICES Journal of Marine Science*, 53, 677-690.
- Paine, R. T. (1974). Intertidal community structure: experimental studies on the relationship between a dominant competitor and its principal predator. *Oecologia* 15: 93-120.
- Palmer, M. W. (1993). Putting things in even better order: the advantages of canonical correspondence analysis. *Ecology*. 74: 2215-2230.
- Pascual, M. and H. Caswell (1991) The dynamics of a size-classified benthic population with reproductive subsidy. *Theor. Pop. Biol.* 39: 129-147
- Pitcher C.R., Wassenberg T.J., Smith G.P., Cappo M., Hooper J.N.A, and Doherty P.J. (1999). Innovative new methods for measuring the natural dynamics of some

- structurally dominant tropical sponges and other sessile fauna. *Memoirs of the Queensland Museum* 44, 479-84.
- Pitcher, C. R., Poiner, I. R., Hill, B. J., and C. Y. Burridge (2000a) Implications of the effects of trawling on sessile megazoobenthos on a tropical shelf in northeastern Australia. *ICES Journal of Marine Science*, **57**: 1359–1368.
- Pitcher, C.R. (1997). Status of Inter-Reefal Benthos in the GBR World Heritage Area. Pp. 323–334. In State of the GBR World Heritage Area 1995. Technical Workshop Proceedings, November 1995, GBRMPA Workshop Series #23. (Great Barrier Reef Marine Park Authority: Townsville).
- Pitcher, C.R., Burridge, C.Y., Wassenberg, T., Smith, G.P., O'Connor, R., Jones, P., Ellis, N., Fry, G. (2000b) Recovery of seabed habitat from the effects of impact of prawn trawling in the far northern section of the Great Barrier Reef: Final Report to GBRMPA on Year 1 Research. *CSIRO Division of Marine Research Report*, 180 pp.
- Pitcher, C.R., Burridge, C.Y., Wassenberg, T.J., Poiner, I.R. (1997). The effects of prawn trawl fisheries on GBR seabed habitats. Pp. 107–123. In The Great Barrier Reef, science, use and management: a national conference: proceedings. Vol. 1. (Great Barrier Reef Marine Park Authority: Townsville).
- Pitcher, C.R., Gordon, S.R., Kloser, R., Jones, P. (1999) Development of an Acoustic System for Remote Sensing of Benthic Fisheries Habitat for Mapping, Monitoring and Impact Assessment, Final Report to FRDC (Project 93/058), CSIRO Marine Research Report, 103pp. ISBN 0 643 06196 7.
- Pitcher, C.R., Skewes, T.D., Dennis, D.M. and Prescott, J.H. (1992) Distribution of seagrasses, substratum types and epibenthic macrobiota in Torres Strait, with notes on pearl oyster abundance. *Australian Journal of Marine and Freshwater Research* 43: 409-419
- Poiner, I.R., Glaister, J., Pitcher C.R., Burridge, C., Wassenberg, T., Gribble N., Hill B., Blaber, S.J.M., Milton, D.A., Brewer D., Ellis, N., (1998) *The environmental effects of prawn trawling in the far northern section of the Great Barrier Reef Marine Park: 1991–1996*. Final Report to GBRMPA and FRDC. CSIRO Division of Marine Research – Queensland Department of Primary Industries Report, 554 pp.
- Ramm, D. C., Pender, P. J., Willing, R. S., and Buckworth, R. C. (1990) Large-scale spatial patterns of abundance within the assemblage of fish caught by prawn trawlers in

- northern Australian waters. *Australian Journal of Marine and Freshwater Research* 41 (1), 79-95.
- Randall, J.E., Allen, G.R., Steene, R.C. (1990) Complete Diver's and Fishermen's Guide to the Fishes of the Great Barrier Reef and Coral Sea, Crawford House Press, Bathurst, Australia.
- Rogers, C.S. (1990). Responses of coral reefs and reef organisms to sedimentation. *Marine Ecology Progress Series*. 62, 185-202.
- Rogers, C.S. (1993). Hurricanes and coral reefs: the intermediate disturbance hypothesis revisited. *Coral Reefs*. 12, 127-137.
- Sainsbury, K.J., (1987). Assessment and management of the demersal fishery on the continental shelf of north western Australia. In: Polovina JJ and Ralston S (eds) Tropical snappers and groupers: biology and fisheries management. Westview Press. Boulder, Colorado, pp. 465-503
- Sainsbury, K.J., Campbell, R. Whitelaw, A.W., (1993). Effects of trawling on the marine habitat on the north west shelf of Australia and implications for sustainable fisheries management In: Hancock DA (ed) Sustainable fisheries through sustainable fish habitats. Australian Society for Fish Biology Workshop. AGPS, Canberra, pp. 137-145.
- Sainsbury, K.J., Campbell, R., Lindholm, R., Whitelaw, A.W., (1997). Experimental management of an Australian multispecies fishery: examining the possibility of trawl-induced habitat modification. In: Pikitch EK, Huppert DD and Sissenwine MP (eds). Global trends: fisheries management. American Fisheries Society, Bethesda, Maryland, pp. 107-112.
- Sale, P. W. ed. (1991) The ecology of fishes on coral reefs. Academic Press, San Diego, CA USA, pp 1-754.
- Scoffin, T.P. and Tudhope, A.W. (1985). Sedimentary environments of the central region of the Great Barrier Reef of Australia. *Coral Reefs*. 4, 81-93.
- SIMRAD (1993) Simrad EY500 Portable Scientific Echo Sounder - Instruction Manual. Simrad Subsea A/S P2473E. Horton, Norway.
- Skewes, T.D., Dennis, D.M., Jacobs, D.R., Gordon, S.R., Taranto, T.J., Haywood, M., Pitcher, C.R., Smith, G.P., Milton, D.A., Poiner, I.R. (1999) Survey and stock size estimates of the shallow reef (0 - 15 m deep) and shoal area (15 - 50 m deep) sedentary

- marine resources and habitat mapping within the Timor sea MOU74 box. Volume 1: Stock estimates and stock status. Final Report to FRRF, CSIRO Marine Research Report.
- Skewes, T.D., Pitcher, C.R., Long, B.G., McLeod, I., Taranto, T.J., Gordon, S.R., Smith, G.P. (1996) Torres Strait infill survey. Report to IPC re Pandora gas development project. CSIRO Division of Fisheries Report, September 1996, 64 pp.
- Sluka, R.D., Chiappone, M., Sullivan Sealey, K.M. (2001). Influence of habitat on grouper abundance in the Florida Keys, U.S.A. *Journal of Fish Biology* 58(3), 682-700.
- Smith, G.W., Ives, L.D., Nagelkerken, I.A. and Ritchie, K.B. (1996). Caribbean sea-fan mortalities. *Nature*. 383,487.
- SPSS. (1999). Statistical Package for Social Sciences, SPSS version 10.0. SPSS Inc. Chicago, Illinois.
- Tanner, J.E. (1995). Competition between scleractinian corals and macroalgae: An experimental investigation of coral growth, survival and reproduction. *Journal of Experimental Marine Biology and Ecology*. 190, 151-168.
- ter Braak, C. J. F. (1986). Canonical correspondence analysis: a new eigenvector technique for multivariate direct gradient analysis. *Ecology* 67: 1167-1179.
- ter Braak, C. J. F., and I. C. Prentice. (1988). A theory of gradient analysis. *Advances in Ecological Research*. 18: 271-317.
- Thomas, G.L., Kirsch, J. (2000) Nekton and plankton acoustics: an overview. *Fisheries Research*, 47, 107-113.
- Thorne, R.E., Trumble, R.J., Lemberg, N.A., Blankenbeckler, D. (1982) Hydroacoustic assessment and management of herring fisheries in Washington and southeastern Alaska. FAO Fisheries Report No. 300, Symposium on Fisheries Acoustics, Bergen, Norway, June 1982.
- Usher, M.B. (1972) Developments in the Leslie matrix model. Pp: 29-60 in J.N.R. Jeffers, ed. *Mathematical models in ecology*. 12th Symp. Brit. Ecol. Soc., Grange-over-sands, Lancashire, 1971. Blackwell, Oxford.
- Van Dolah, R.F., Wendt, P.H., Nicholson, N. (1987). Effects of a research trawl on a hard bottom assemblage of sponges and corals. *Fisheries Research* 5:39-54.

- Vilhjalmsson, H., Reynisson, P., Hamre, J., Rottingen, I. (1982) Acoustic abundance estimation of the Icelandic stock of Capelin 1978-1982. FAO Fisheries Report No. 300, Symposium on Fisheries Acoustics, Bergen, Norway, June 1982
- Walker, T.A. and Bull, G.B. (1983). A newly discovered method of reproduction in gorgonian coral. *Marine Ecology Progress Series*. 12, 137-143.
- Waring, J.R., Kloser, R.J., and Pauly, T. (1994). Echo – Managing Fisheries Acoustic Data. In: 'Proceedings of the International Conference on Underwater Acoustics University of New South Wales, Dec. 1994'. pp. 22-24. (Australian Acoustical Society: Darlinghurst Public School, NSW.)
- Watling, L., Norse, E.A., (1998). Disturbance of the seabed by mobile fishing gear: a comparison to forest clearcutting. *Conservation Biology* 12, 1180-1199.
- Watson, R. A. and Goeden, G. (1989). Temporal and spatial zonation of the demersal trawl fauna of the central Great Barrier Reef. *Memoirs of the Queensland Museum* 27(2): 611–620.
- Watson, R.A., Dredge, M.L., and Mayer, D.G. (1990) Spatial and seasonal variation in demersal trawl fauna associated with a prawn fishery on the central Great Barrier Reef, Australia. *Australian Journal of Marine and Freshwater Research* 41: 65-77
- Whitelaw, A.W., Sainsbury, K.J., Dews G.J., and Campbell. R.A. (1991). Catching characteristics of four fish-trap types on the North West Shelf of Australia. *Australian Journal of Marine and Freshwater Research* 42, 369-82.
- Wilkins, M.E. (1986) Development and evaluation of methodologies for assessing and monitoring the abundance of widow rockfish, *sebastes Entomelas*. *Fishery Bulletin*, 84(2), 287-310.
- Williams, D. McB. (1983) Longitudinal and latitudinal variation in the structure of reef fish communities. In "Proceedings of the inaugural Great Barrier Reef Conference", August 28 - September 2, 1983, (Eds Baker, J. T. Carter R. M. Sammarco P. W. Stark K. P.), pp 265-270.
- Williams, D. McB. and Hatcher, A. I. (1983) Structure of fish communities on outer slopes of inshore, mid-shelf and outer shelf reefs of the Great Barrier Reef. *Mar. Ecol. Prog. Ser.* 10 (3), 239-250.

- Williams, D. McB. and Russ, G. R. (1994) Review of data on fishes of commercial and recreational fishing interest in the Great Barrier Reef. *Research Publication (Great Barrier Reef Marine Park Authority) Number 33* 1, 1-103.
- Williams, D.McB., Fowler, A.J., and Newman, S.J. (1997). Development of trap and drop-line sampling techniques for reef fishes: a report to Great Barrier Reef Marine Park Authority. 54 pp. Research Publication No. 43. Great Barrier Reef Marine Park Authority, Townsville, Queensland, Australia.
- Willis, T. J., Millar, R.B. and Babcock, R.C. (2000). Detection of spatial variability in relative density of fishes: comparison of visual census, angling and baited underwater video. *Marine Ecology Progress Series* 198, 249-60.
- Wulff, J.L. (1995). Effects of a hurricane on survival and orientation of large erect coral reef sponges. *Coral Reefs*. 14, 55-61.
- Yau, C., Collins, M.A., Bagley, P.M., Everson, I., Nolan, C.P., and Priede, I.G. (2001). Estimating the abundance of Patagonian toothfish *Dissostichus eleginoides* using baited cameras: a preliminary study. *Fisheries Research* 51, 403-412.

15 Appendices

15.1 Intellectual Property

There is no intellectual property of a commercial nature arising from this Project.

15.2 Staff

List of all staff that have been engaged on the project:

CSIRO Marine Research

C.R. Pitcher

T.J. Wassenberg

G.P. Smith

M. Austin

S.R. Gordon

R.H. Bustamante

C.H. Moeseneder

S. Cheers

A. Koutsoukos

R. O'Connor

D.M. Dennis

G. Fry

Australian Institute of Marine Science

M.C. Cappel

P.J. Speare

P.J. Doherty

Queensland Museum

J.A. Kennedy

S.D. Cook

C. Adams

P. Tomkin

J.N.A. Hooper

